PROGRAM & ABSTRACTS

50th International

Arctic Workshop 2021

15-17 APRIL

Celebrating the scientific legacy of John T. Andrews

Online Meeting

Division of Polar Programs
National Science Foundation

Institute of Arctic & Alpine Research
University of Colorado Boulder

Compiled in 2021 by:

Institute of Arctic and Alpine Research (INSTAAR)

Terms of use:

This report may be cited as:

50th International Arctic Workshop, Program and Abstracts 2021. Institute of Arctic and Alpine Research (INSTAAR), University of Colorado at Boulder, 163 pp.

This report is distributed by:

Institute of Arctic and Alpine Research
University of Colorado at Boulder
4001 Discovery Drive
Campus Box 450
Boulder, CO 80309-0450
http://instaar.colorado.edu

Cover photo:

John Andrews on board the C.S.S. Hudson, Kangerlugsuaq Fjord, East Greenland, October 1993. Photo: Jaia Syvitski.

PROGRAM AND ABSTRACTS

50th ANNUAL INTERNATIONAL ARCTIC WORKSHOP

April 15th – 17th, 2021

Online via Zoom

INSTAAR
Institute of Arctic and Alpine Research
University of Colorado, Boulder

Organizing Committee:

Gifford Miller
Wendy Roth
David Lubinski
Anne Jennings

Introduction

Overview and history

The 50th Annual International Arctic Workshop will be held online 15-17 April, 2021, via the Zoom online platform. The meeting is sponsored and hosted by the Institute of Arctic and Alpine Research (INSTAAR). This workshop has grown out of a series of informal annual meetings started by John T. Andrews and sponsored by INSTAAR and other academic institutions worldwide.

Theme

"*Celebrating the scientific legacy of John T. Andrews*". Immediately following the workshop on Saturday will be an in-person/online special event honoring John, his research on Pleistocene ice sheets, and his advising of many graduate students.

Web site

http://instaar.colorado.edu/meetings/AW2021

Program

The online workshop takes place on three succeeding partial days, mostly from 9am to 3pm Mountain Time. This schedule is designed to help prevent Zoom fatigue and accommodate attendees across time zones. Attend live 3-minute lightning talks, each with 5-minute Q/A on Zoom. No posters. Each lightning talk has a more detailed 10-minute video for registrants to view anytime in the week before the Workshop or until 01 May 2021.

NSF

The National Science Foundation's Division of Polar Programs has a long tradition of being a supporter of the Arctic Workshop. *Any opinions, findings, and conclusions or recommendations expressed in this material are those of the author(s) and do not necessarily reflect the views of the National Science Foundation.*

Arctic Workshop 2021
Program Summary

All times are Mountain Time (Denver)

THURSDAY 15 APRIL

9:00	**Welcome & introduction**
9:20	**1. Terrestrial paleonenvironments I**
10:30	Break
10:40	**2. Culture/Policy/Data**
11:30	**3. Keynote – Sara Sayedi**
12:10	Optional social breakout groups
1:00	**4. Terrestrial paleonenvironments II**
2:00	Break
2:10	**5. Modern environments & proxies I**
3:10	End of day

FRIDAY 16 APRIL

9:00	**Announcements**
9:10	**6. Modern environments & proxies II**
10:30	Break
10:40	**7. Ice sheets & glaciers I**
11:30	**8. Keynote – Mark Serreze**
12:10	Optional social breakout groups
1:00	**9. Marine**
2:00	Break
2:10	**10. Ice sheets & glaciers II**
3:00	End of day

SATURDAY 17 APRIL

9:00	**Announcements**
9:20	**11. Ice sheets & glaciers III**
10:20	**12. Keynote – Andrew Christ**
10:50	**Closing comments**
11:00	End of science sessions
11:00	**John T. Andrews event**
1:00	End of Andrews event

Program Details

9:00 AM – THURSDAY 15 APRIL 2021

9:00 **Workshop welcome & introduction**
Gifford Miller, Director of Arctic Workshop
Merritt Turetsky, Director of INSTAAR

1. Terrestrial paleoenvironments I

Thursday am Chair: Anne Jennings

09:20 **Detection of a marine to terrestrial transition in lake sediment from Baffin Island, Arctic Canada, using sedimentary DNA**
Power, Matthew; Crump, Sarah E; Miller, Gifford H; Bunce, Michael; Allentoft, Morten [pg 102]

09:30 **A previously undocumented influence on H isotopes of Arctic mid-chain plant waxes through the Holocene: moss-associated methane oxidation**
McFarlin, Jamie M; Axford, Yarrow; Kusch, Stephanie; Masterson, Andrew L; Lasher, Everett; Osburn, Magdalena R [pg 85]

09:40 **Quantifying Holocene plant contributions to sedimentary leaf waxes in an Arctic lake setting**
Hollister, Kayla V; Thomas, Elizabeth K; Raberg, Jonathan; Raynolds, Martha K; Gorbey, Devon B; Crump, Sarah E; Miller, Gifford H; Sepúlveda, Julio [pg 51]

09:50 **Assessing new temperature and conductivity calibrations on a 24,000-year record of lacustrine branched glycerol dialkyl glycerol tetraethers in the Polar Ural Mountains**
Lovell, Kathryn; Thomas, Elizabeth K; Cowling, Owen C; Castañeda, Isla S; Svendsen, John Inge [pg 82]

10:00 **Extending brGDGT-based paleoclimate proxies to high latitudes**
Raberg, Jonathan H; Harning, David J; Crump, Sarah E; de Wet, Greg; Blumm, Aria; Kopf, Sebastian; Geirsdóttir, Áslaug; , et al. [pg 104]

10:10 **Multi-proxy biomarker records and forward modeling of western Greenland Holocene lake temperatures and dynamics**
Cluett, Allison A.; Thomas, Elizabeth K.; Cowling, Owen C.; Castañeda, Isla S. [pg 37]

10:20 **Human paleo-genomics and Beringian landscapes**
Hoffecker, John F.; Raff, Jennifer A.; O'Rourke, Dennis H.; Tackney, Justin C.; Potapova, Olga; Elias, Scott A.; Hlusko, Leslea J.; Scott, G. R. [pg 46]

10:30 Break

10:40 AM – THURSDAY 15 APRIL 2021

2. Culture/Policy/Data
Thursday am Chair: Julie Brigham-Grette

10:40 **Northern knowledge for resilience, environmental sustainability and adaptation in coastal communities (NORSEACC)**
King, Leslie A.; Ogilvie, Astrid E.J.; Lepore, Walter [pg 61]

10:50 **The Arctic Rivers Project: A co-produced assessment of the climate sensitivity of Alaskan & Yukon rivers, fish, and Indigenous communities**
Musselman, Keith N.; Herman-Mercer, Nicole; Newman, Andrew J.; Koch, Joshua C.; Brooks, Cassandra; Gooseff, Michael; Cozzetto, Karen; Mutter, Edda [pg 91]

11:00 **Understanding resilience and long-term environmental change in the High Arctic: Narrative-based analyses from Svalbard (SVALUR)**
Ogilvie, Astrid E.J.; Miles, Martin; van der Wal, René; Löf, Annette [pg 92]

11:10 **Arctic Spatial Data Infrastructure: A global information highway to meet the challenges of a fragile Arctic ecosystem**
Riopel, Simon [pg 112]

11:20 **Profile curated collections of data with portals on the Arctic Data Center**
McLean, Erin L; Jones, Matthew B; Budden, Amber E; Walker, Lauren; Jones, Christopher S [pg 86]

3. Keynote - Sara Sayedi
Thursday am

11:30 **Integrating terrestrial and subsea permafrost into climate policy**
Sayedi, Sayedeh Sara; Abbott, Benjamin W [pg 115]

12:00 Break

Optional social breakout groups on Zoom
Thursday am

12:10 Choose from the 6 breakout groups by hovering over a group's number and clicking the "Join" button that appears.

12:50 End breakout groups

1:00 PM – THURSDAY 15 APRIL 2021

4. Terrestrial paleoenvironments II

Thursday pm Chair: Jason Briner

01:00 **Patterns of postglacial vegetation establishment clarified by lacustrine sedaDNA from Baffin Island, Arctic Canada**
Crump, Sarah E.; Power, Matthew; Fréchette, Bianca; de Wet, Gregory; Raynolds, Martha K.; Raberg, Jonathan H.; Allentoft, Morten; , et al. [pg 38]

01:10 **Annually resolved past climate changes from South Sawtooth Lake 2900-year-long varved record**
Francus, Pierre; Lapointe, François; Bradley, Raymond S.; Abbott, Mark B. [pg 39]

01:20 **Exposing the history of volcanism and sea-level changes at the Mount Edgecumbe Volcanic Field in Southeast Alaska using cosmogenic nuclides**
Lesnek, Alia J; Licciardi, Joseph M.; Briner, Jason P; Baichtal, James F; Walcott, Caleb K [pg 77]

01:30 **Disentangling the evolution of Holocene climate, soil erosion and human impact in Iceland**
Ardenghi, Nicolò; Harning, David J; Raberg, Jonathan; Sepúlveda, Julio; Geirsdóttir, Áslaug; Miller, Gifford H; Þórðarson, Þorvaldur [pg 23]

01:40 **Coupled marine and terrestrial climate dynamics revealed by multicentury, annually resolved proxy records from Fennoscandia**
Mette, Madelyn J.; Wanamaker Jr., Alan D.; Carroll, Michael L.; Ambrose, William G.; Retelle, Michael J.; Andersson, Carin [pg 88]

01:50 **The Holocene Thermal Maximum across Greenland: Reconciling differences in the timing and magnitude of peak warmth**
Axford, Yarrow; de Vernal, Anne; Osterberg, Erich C. [pg 27]

2:00 Break

2:10 PM – THURSDAY 15 APRIL 2021

5. Modern environments & proxies I

Thursday pm Chair: Kathy Licht

02:10 **Sedimentary lipid biomarkers combined with novel hyperspectral imaging techniques: A multiproxy Holocene-length sedimentary reconstruction from Lake 578, S Greenland**
Schneider, Tobias; Castañeda, Isla S.; Zhao, Boyang; Salacup, Jeffrey M.; Makri, Stamatina; Bradley, Raymond S. [pg 120]

02:20 **Late Holocene temperature and hydroclimate reconstruction from southern Greenland: evidence from biomarkers in lake sediments**
Zhao, Boyang; Castañeda, Isla S.; Bradley, Raymond S.; Salacup, Jeff M.; Schneider, Tobias [pg 151]

02:30 **An investigation of modern eastern North American Arctic lakes reveals latitudinal patterns in lake water isotope seasonality**
Gorbey, Devon B; Thomas, Elizabeth K; Raynolds, Martha K; Miller, Gifford H [pg 44]

02:40 **Biomarker characterization of the North Water Polynya, Baffin Bay: Implications for local sea ice and temperature proxies**
Harning, David; Holman, Brooke; Woelders, Lineke; Jennings, Anne; Sepúlveda, Julio [pg 45]

02:50 **Torrent or trickle?: Tracking glacial lake evolution and flood events using composite lake records**
Pendleton, Simon; Donnelly, Jeffrey; Kurz, Mark D; Condron, Alan [pg 96]

03:00 **Arctic seabed: New detailed mappings of compositions and physical properties**
Jenkins, Chris [pg 52]

03:10 End of day

9:00 AM – FRIDAY 16 APRIL 2021

9:00 **Announcements**
Gifford Miller, Director of Arctic Workshop

6. Modern environments & proxies II

Friday am Chair: David Harning

09:10 **Navigating NNA -- from planning and vulnerability to research action**
Brigham-Grette, Julie; Kumpel , Emily; Bulter, Caitlyn; Temte, James; Weston, Bessie; Lewis , Tracy; Paul , Paul [pg 33]

09:20 **The M'Clintock Ice Shelf: last gasp of the NW Laurentide Ice Sheet**
Furze, Mark F.A.; Pienkowski, Anna J.; Corlett, Hilary; Troyer-Riel, Robert; Thiessen, Rabecca; Szidat, Sönke [pg 43]

09:30 **Comparison of early twentieth century Arctic warming and contemporary Arctic warming in the light of daily and sub-daily data**
Przybylak, Rajmund; Wyszynski, Przemyslaw; Arazny, Andrzej [pg 103]

09:40 **Creating a database of mountain soil temperature on the subarctic Kola Peninsula**
Shtabrovskaya, Irina; Zenkova, Irina [pg 124]

09:50 **On the interannual variability of spring Bering Strait water temperatures**
Lenetsky, Jed E; Serreze, Mark C [pg 76]

10:00 **Investigating climatic and ecologic controls on modern plant leaf wax production along a latitudinal transect of Baffin Island**
Lindberg, Kurt R; Thomas, Elizabeth K; Raynolds, Martha K; Hollister, Kayla V [pg 81]

10:10 **Impact of lake basin morphometry and mixing on Arctic lake water isotope composition**
Mahar, Isabelle F; Cluett, Allison; Thomas, Elizabeth [pg 83]

10:20 **Vegetation around six lakes along a climate gradient in Baffin Island**
Raynolds, Martha K; Bültmann, Helga; Kasanke, Shawnee; Raberg, Jonathan; Miller, Gifford [pg 106]

10:30 Break

10:40 AM – FRIDAY 16 APRIL 2021

7. Ice sheets & glaciers I
Friday am Chair: Giff Miller

10:40 **Revisiting the Nutrient Recovery Hypothesis: can contemporary population cycles influence ecosystem function?**
Roy, Austin; McLaren, Jennie [pg 114]

10:50 **Thermokarst pond plant communities of Prudhoe Bay, Alaska: Environmental gradients and temperature feedbacks**
Watson-Cook, Emily; Walker, Donald A.; Raynolds, Martha K.; Breen, Amy L. [pg 147]

11:00 **Mapping ice flow velocity using an interactive, cloud-based feature tracking workflow**
Zheng, Whyjay; Grigsby, Shane; Sapienza, Facundo; Taylor, Jonathan; Snow, Tasha; Pérez, Fernando; Siegfried, Matthew R [pg 153]

11:10 **Quantifying layers of refrozen melt in ice cores using bubble density**
Kindstedt, Ingalise; Winski, Dominic; Kreutz, Karl; Osterberg, Erich; Campbell, Seth; Wake, Cameron; Schild, Kristin [pg 58]

11:20 **Unprecedented recent warmth in the context of the last 2000 years in Svalbard and the imminent disappearance of the west coast valley glacier Linnébreen**
Retelle, Mike; Lapointe, Francois; Bradley, Ray; Wagner, Katrin; Farnsworth, Wes [pg 109]

8. Keynote - Mark Serreze
Friday am

11:30 **From questions of what and why to why it all matters: Evolving thoughts on the changing Arctic**
Serreze, Mark C [pg 123]

Optional social breakout groups on Zoom
Thursday am

12:10 Choose from the 6 breakout groups by hovering over a group's number and clicking the "Join" button that appears.

12:50 End breakout groups

1:00 PM – FRIDAY 16 APRIL 2021

9. Marine

Friday pm Chair: Sarah Crump

01:00 **Honoring John T Andrews: The sediment fill of fjords**
Syvitski, Jaia [pg 134]

01:10 **Changes in sediment sources in the Labrador Sea during the Late Quaternary**
Andrews, John T; Piper, David [pg 15]

01:20 **Icebergs and tropical rainfall**
Bradley, Raymond S; Diaz, Henry F [pg 30]

01:30 **Foraminiferal stratigraphy and lithofacies reveal the timing and environments of deglaciation and onset of Arctic/Atlantic throughflow in the Arctic Island Channels**
Kelleher, Robert V; Jennings, Anne; Brooks, Nicole; Feng, Cici; Andrews, John T; Brookins, Sarah; Woelders, Lineke; , et al [pg 55]

01:40 **Little Ice Age triggered by intrusion of Atlantic waters into the Nordic Seas**
Lapointe, Francois; Bradley, Raymond S; Retelle, Michael [pg 65]

01:50 **Abrupt mid-20th century onset of post Little Ice Age hydrographic instability in the Northern North Atlantic**
Lehman, Scott J; Sejrup, Hans Petter; Hjelstuen, Berit Oline; Becker, Lukas; Runarsdottir, Rebekka Hlin; Ionita-Scholz, Monica [pg 73]

2:00 Break

2:10 PM – FRIDAY 16 APRIL 2021

10. Ice sheets & glaciers II

Friday pm Chair: Mike Retelle

02:10 **Cyclic patterns in Quaternary deposits on the Northwind Ridge, western Arctic Ocean: glacial vs. marine signature**
Polyak, Leonid; Dipre, Geoffrey; Wang, Rong [pg 98]

02:20 **Changes in South Greenland's peripheral glaciers since the Little Ice Age**
Larocca, Laura J; Axford, Yarrow; Bjørk, Anders A; Brooks, Jeremy P [pg 70]

02:30 **Evidence for a more extensive Greenland Ice Sheet in southwestern Greenland during the Last Glacial Maximum**
Sbarra, Christopher; **Briner**, Jason P.; Graham, Brandon; Thomas, Elizabeth; Poinar, Kristin; Young, Nicolás [pg 117]
(**Briner** is presenter)

02:40 **Does Northeastern Cumberland Peninsula preserve a dateable pre-MIS2 moraine record – or NOT?**
Kaplan, Michael R; Miller, Gifford H; Briner, Jason P; Young, Nicolás E [pg 54]

02:50 **A revised glacial history of the Smoking Hills region, northwestern arctic Canada: evidence for late Pliocene and Quaternary continental Laurentide glaciations and the preservation of old buried glacial ice**
Smith, I. Rod; Evans, David J.A.; Gosse, John C.; Galloway, Jennifer M. [pg 128]

03:00 End of day

9:00 AM – SATURDAY 17 APRIL 2021

9:00 **Announcements**
Gifford Miller, Director of Arctic Workshop

11. Ice sheets & glaciers III
Saturday am Chair: Ray Bradley

09:20 **Evidence of palaeo-ice streaming in NE-Iceland**
Aradóttir, Nína; Benediktsson, Ívar Örn; Ingólfsson, Ólafur; Brynjólfsson, Skafti [pg 22]

09:30 **A database for submarine glacial landforms and glacimarine sediments in the High-Arctic**
Streuff, Katharina T.; Ó Cofaigh, Colm [pg 132]

09:40 **The culmination of the last glaciation in the Kenai Peninsula, Alaska based on 10Be ages from Alaska's biggest moraine boulders**
Tulenko, Joseph P.; Ash, Brendan J.; Briner, Jason P.; Reger, Richard D. [pg 136]

09:50 **The hunt for ice-free areas along the coastal Cordilleran Ice Sheet margin during the LGM continues: No dice in the northern Alexander Archipelago**
Walcott, Caleb K.; Briner, Jason P.; Baichtal, James F. [pg 139]

10:00 **The multidisciplinary story of Antarctica's history as told from blue ice moraines**
Licht, Kathy; Kaplan , Mike; Bader, Nicole; Graly, Joseph; Kassab, Christine [pg 79]

10:10 **Episodic cryosphere expansion in Arctic Canada during the Common Era reinforced by repeat dating of entombed plants and supported by climate model simulations**
Miller, Gifford; Pendleton, Simon; Lehman, Scott; Jahn, Alexandra; Zhong, Yafang; Geirsdóttir, Áslaug [pg 89]

12. Keynote - Andrew Christ
Saturday am

10:20 **Camp Century revisited: an ecosystem under the ice reveals Greenland's warmer past**
Christ, Andrew J [pg 35]

10:50 **Closing Comments from the Arctic Workshop**

11:00 End of science sessions

11:00 AM – SATURDAY 17 APRIL 2021 ANDREWS EVENT

11:00am	**Celebration of John T. Andrews**
	Subsequent time stamps are for the video recording of the event
0min	**Start of video - Introduction** Giff Miller
3.5min	**Science life before CU Boulder** John Andrews [pg 19]
29min	**Memories and poems for John & Martha** Slides from Pat & Mukta Webber
43min	**Early days of John Andrews, Canadian roots** Video memories from John England
1hr 8min	**The Andrews legacy of promoting/mentoring women** Julie Brigham-Grette
1hr 7min	**John's encounters and research around Iceland** Video memories from his Icelandic colleagues Áslaug Geirsdóttir, Gudrún Helgadóttir, Árny Sveinbjörnsdóttir, Gréta Kristjánsdóttir, Saedís Ólafsdóttir, and others. Voiceover by Helgi Atlason.
1hr 16min	**Open microphone comments**
1hr 16min	Anne Jennings
1hr 17min	Astrid Ogilvie
1hr 19min	Scott Lehman
1hr 22.5min	Scott Elias
1hr 23.5min	Ray Bradley
1hr 28.5min	Peter Clark
1hr 35min	Áslaug Geirsdóttir & Gudrún Helgadóttir
1hr 38min	Michael Kaplan
1hr 42min	Kathy Licht & Wendy Roth
1hr 43.5min	Val Sloan
1hr 46.5min	Christoph Vogt

PM – SATURDAY 17 APRIL 2021 ANDREWS EVENT

1hr 48min **Memories of John**
Giff Miller

2hr 6min **Presentation of engraved granite tribute to John**
The ~4 ft tall granite slab includes an engraved map and two plaques stating *John T. Andrews. Arctic Pioneer – 50 years, Baffin Island, Greenland, Iceland, and the seas between.*
Chance Anderson & Giff Miller

2hr 10min **End of video**

01:00pm **End of Andrews event**

Changes in sediment sources in the Labrador Sea during the Late Quaternary

Andrews, John T [1]; **Piper**, David [2]

[1] University of Colorado; andrewsj@colorado.edu
[2] Geological Survey of Canada--Atlantic; david.piper@canada.ca

Studies of the sediment history in the Labrador Sea have frequently focused on the detrital carbonate facies associated with Heinrich events sourced from the collapse of the Hudson Strait Ice Stream and linked to long-distance iceberg transport (Andrews and Tedesco 1992; Bond et al. 1992; Rashid et al. 2003) as well as the generation of turbidites that flowed toward and down the North Atlantic Mid-Ocean Channel (Chough et al. 1987; Hesse 2016; Hesse and Khodabakhsh 2016). In this presentation we use a database of 1445 sediment samples from cores and surface samples (Fig. 1) to evaluate whether we can detect spatial and temporal changes in mineral compositions during the late Quaternary and Holocene, remembering that in this glacial marine environment we must expect mixing of provenance indicators. We use a suite of 90 bedrock and IRD-clasts to understand the range of non-clay and clay mineral compositions that could be transported to the Labrador Sea by glacial erosion and transport, and then use this supervised data set to predict the origins of the 1445 samples. The supervised analysis resulted in 10 distinct compositional entities (Fig. 2) and we illustrate the application by showing the downcore variations in mineral wt% and predicted mineral facies for HU2011031-059 on northern Flemish Cap (Mao et al. 2014) (Fig. 3A). We test the robustness of the predictions by using the non-parametric Classification Decision Tree program "rpart" (Fig. 3B). This indicated that only 18% of the samples were misclassified. One of the important issues that we are currently examining is whether the four granitoid-rich facies have specific provenance value.

Acknowledgements: This project was started by Jeremy Hoffman as part of a PhD project at Oregon State University supported by NSF. We thank Kate Jarrett and other staff at GSC-Atlantic for their assistance in sampling the many cores used in this study.

Andrews, J.T., and Tedesco, K. 1992. Detrital carbonate-rich sediments, northwestern Labrador Sea: Implications for ice-sheet dynamics and iceberg rafting (Heinrich) events in the North Atlantic. Geology, 20: 1087-1090.

Bond, G., Heinrich, H., Broecker, W.S., Labeyrie, L., McManus, J., Andrews, J.T., Huon, S., Jantschik, R., Clasen, S., Simet, C., Tedesco, K., KLas, M., Bonani, G., and Ivy, S. 1992. Evidence for massive discharges of icebergs into the glacial Northern Atlantic. Nature, 360: 245-249.

Chough, S.K., Hesse, R., and Muller, J. 1987. The Northwest Atlantic Mid-Ocean Channel of the Labrador Sea. IV. Petrography and provenance of the sediments. Canadian Journal Earth Sciences, 24: 731-740.

Hesse, R. 2016. Ice-proximal Labrador Sea Heinrich layers: a sedimentological approach. Canadian Journal of Earth Sciences, 53: 71-100. doi:10.1139/cjes-2015-0033.

Hesse, R., and Khodabakhsh, S. 2016. Anatomy of Labrador Sea Heinrich layers. Marine Geology, 380: 44-66.

Mao, L., Piper, D.J.W., Saint-Ange, F., Andrews, J.T., and Kienast, M. 2014. Provenance of sediment in the Labrador Current: a record of hinterland glaciation over the past 125 ka. Journal of Quaternary Science, 29: 650-660. doi:10.1002/jqs.2736.

Rashid, H., Hesse, R., and Piper, D.J.W. 2003. Distribution, thickness and origin of Heinrich layer 3 in the Labrador Sea. Earth and Planetary Science Letters, 205: 281-293.

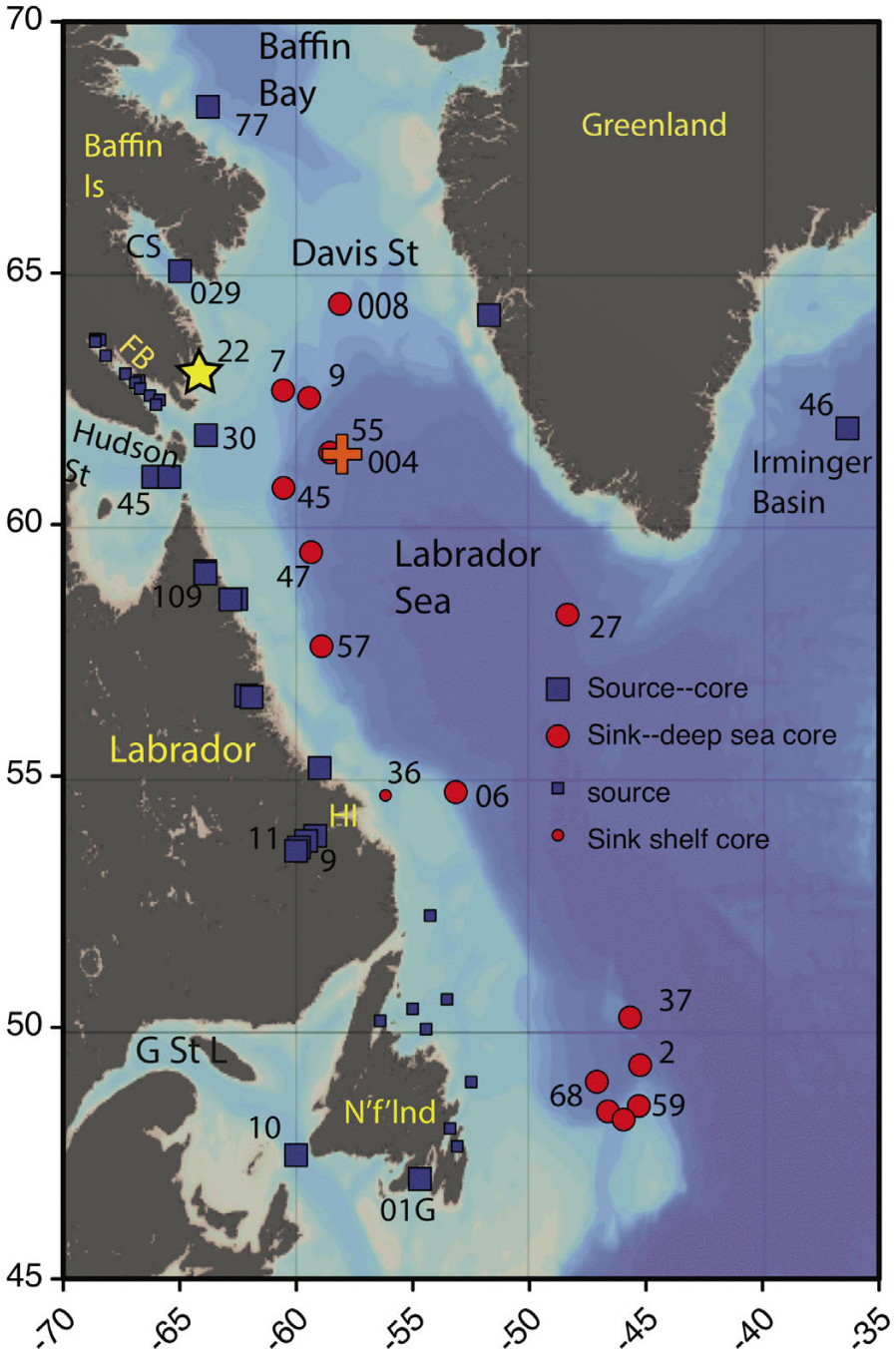

Fig 1. Map of the core and sample sites.

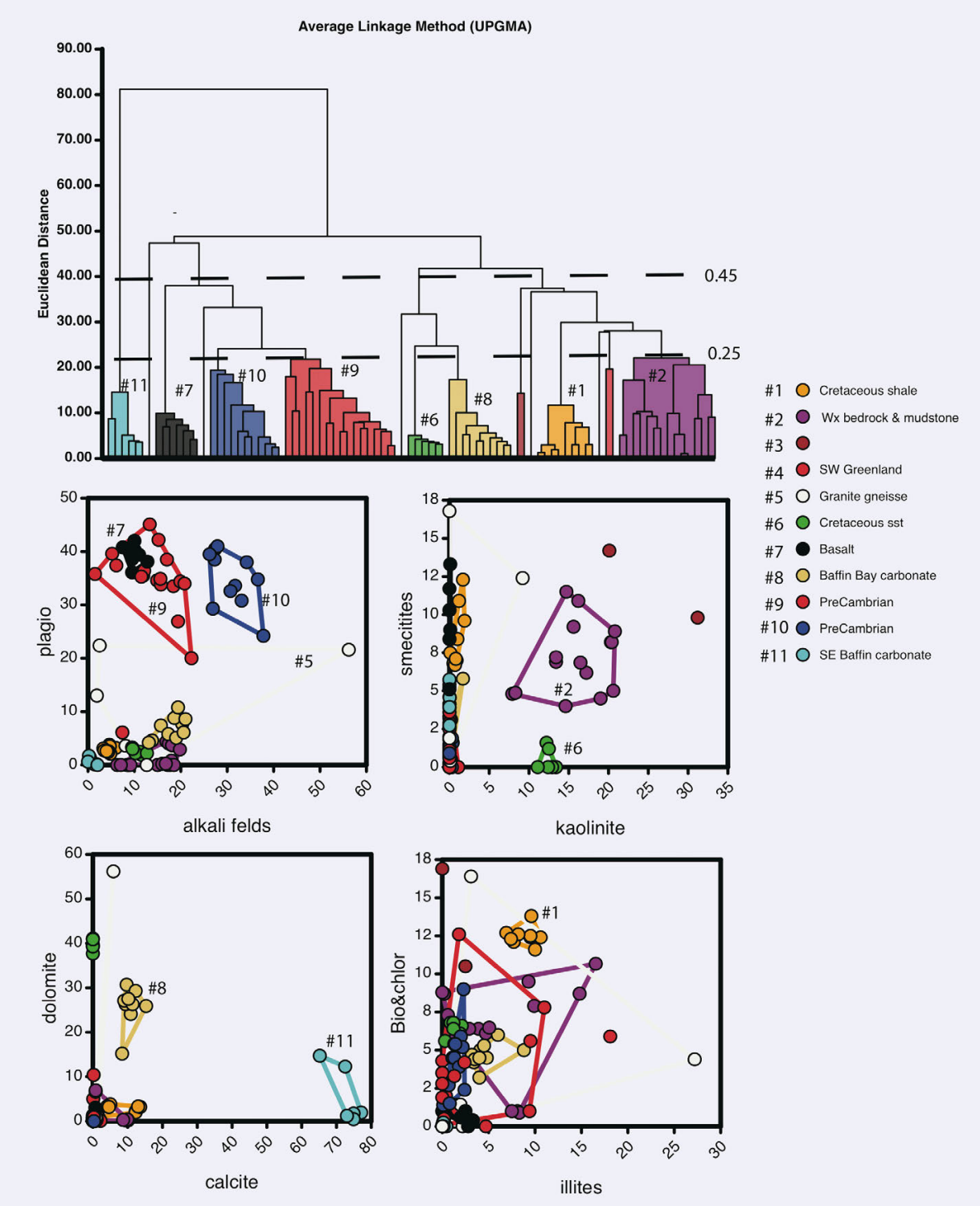

Fig 2. Hierarchical dendrogram based on 90 bedrock or IRD-clast samples.

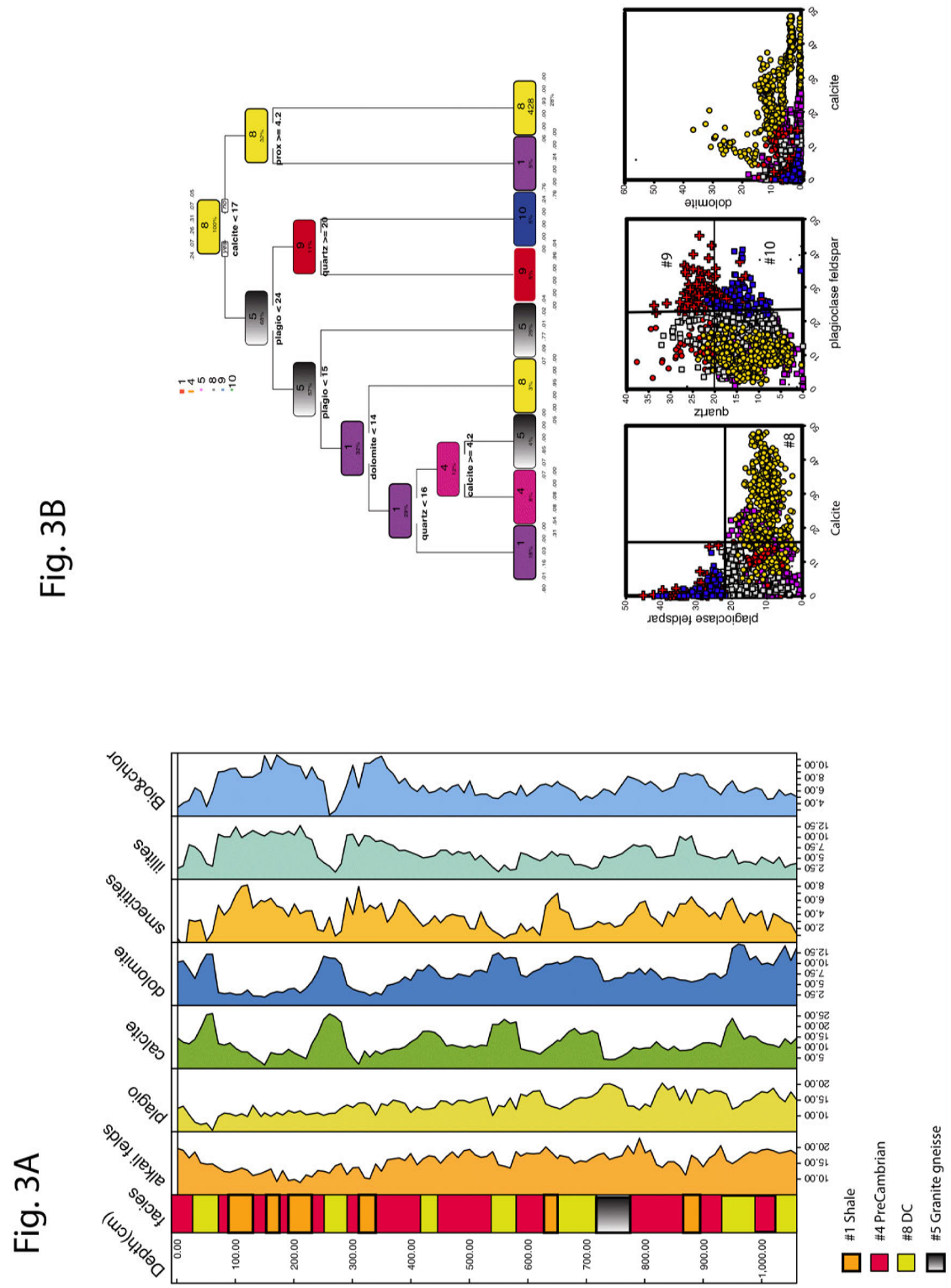

Fig 3.
A: Downcore plot of data from HU2011-059 (Mao et al., 2014) showing the predicted mineral facies.
B) Classification Decision Tree of the predicted unsupervised core data based on Fig. 2

D.M. & G. Andrews, Grocers, Purveyors of Balloon Yeast "We always rise to the occasion": The Arctic Workshop, and a brief account of life before CU

Andrews, John T [1]

[1] University of Colorado; andrewsj@colorado.edu

"We always rise to the occasion": Come to think about it, not a bad motto.

The first Arctic Workshop was intended to try and provide what was solely missing in my graduate education---that is an opportunity to learn how to present research materials to an audience; some might (truefully/cruelly) say that nothing has changed in my presentations! Martha told me that at my first presentation in 1961 I spent the entire talk with my back to the audience! Comparing the graduate and even undergraduate presentation efforts then to now is literally lettuce v oranges.

My own PhD advisor Professor Cuchlaine King, the University of Nottingham, told me during my one year PhD period at Nottingham (yes indeed---ONE Year---eat your hearts out! The University changed its rules as a result) "…it is more important (and fun) to disprove a paradigm than support it". A message I have tried to impart to graduates I have supervised and I must admit that they---many in this audience---have done an excellent job of correcting me. Infact, it is both necessary and important for me to thank my many MSc and PhD graduate students----- I learned from all of them and it has been a pleasure to keep in touch with many and watch their progression through life, frequently with a certain level of awe and amazement, and certainly with a large measure of pride. A combination of Martha, my Mother, three unmarried aunts, the girls of Millom Grammar School, and my supervisor Cuchlaine King, resulted in me understanding that women are often, usually smarter than I am, and I was my fortunate enough to have many excellent women graduate students---that does not take away any credit from their male counterparts.

I reached Boulder via: Millom, Nottingham, Montreal, Knob Lake, Montreal (1960=McGill= Martha & 60 yrs later), Ottawa, Nottingham, and Ottawa. Martha, Melissa, and I came to Boulder and CU in January 1968---Thomas arrived in 1972. My mother (Dorothy nee Black) and father's Millom Grammar School (aka High School) class included Cliff Addison , FRS, who went on to be the Professor of Inorganic Chemistry at Nottingham , and the Poet Norman Nicholson, who wrote in his autobiography "Wednesday Early Closing" "Marjorie married a Professor (Cliff Addison) and Dorothy was mother of another." We can now add "Melissa married a Professor and Martha was mother of another!"

All my graduates (and others' graduates) learned the value of library research under the guidance of Martha, a professional librarian, and she also hosted the "poster breakfast" in the Reading Room for the AWs. A feature of the early AW's was also the party that Martha and I hosted in our house; this essential activity was taken over for many years by Giff and Midra,

but at some point the size of the workshop (and/or the ages of the hosts?) relegated that high-point. I managed the AW (with the help of Wendy Roth, Anne Jennings, Bill Manley and Dave Lubinski [the web manager], and others) until I retired, at which point it was under the direction of Tad Pfeffer, who in turn relinquished control to Giff Miller, assisted by Anne Jennings, Wendy, and Dave. Of course for many years the AW has alternated between its "home" base and other Universities in the USA, Canada, Norway, Iceland, and Sweden and the local committees (many with CU connections) have played a major role in keeping the workshop relevant, interesting, and fun. Thus the AW has been under the management, in an academic sense, of "sons" and "daughters" and whether it continues in the future will depend on "granddaughters and grandsons". Whatever happens, it has been a blast!

MANY THANKS, especially to Martha, Melissa, and Thomas, to Giff, Anne, Wendy, and Dave for organizing the 50th AW, and to all of my graduate students and to you here for attending this celebration. It is also a pleasure to recognize Pat and Mukta Weber who are both old friends (from 1963) and former colleagues---Pat was a former Director of INSTAAR.

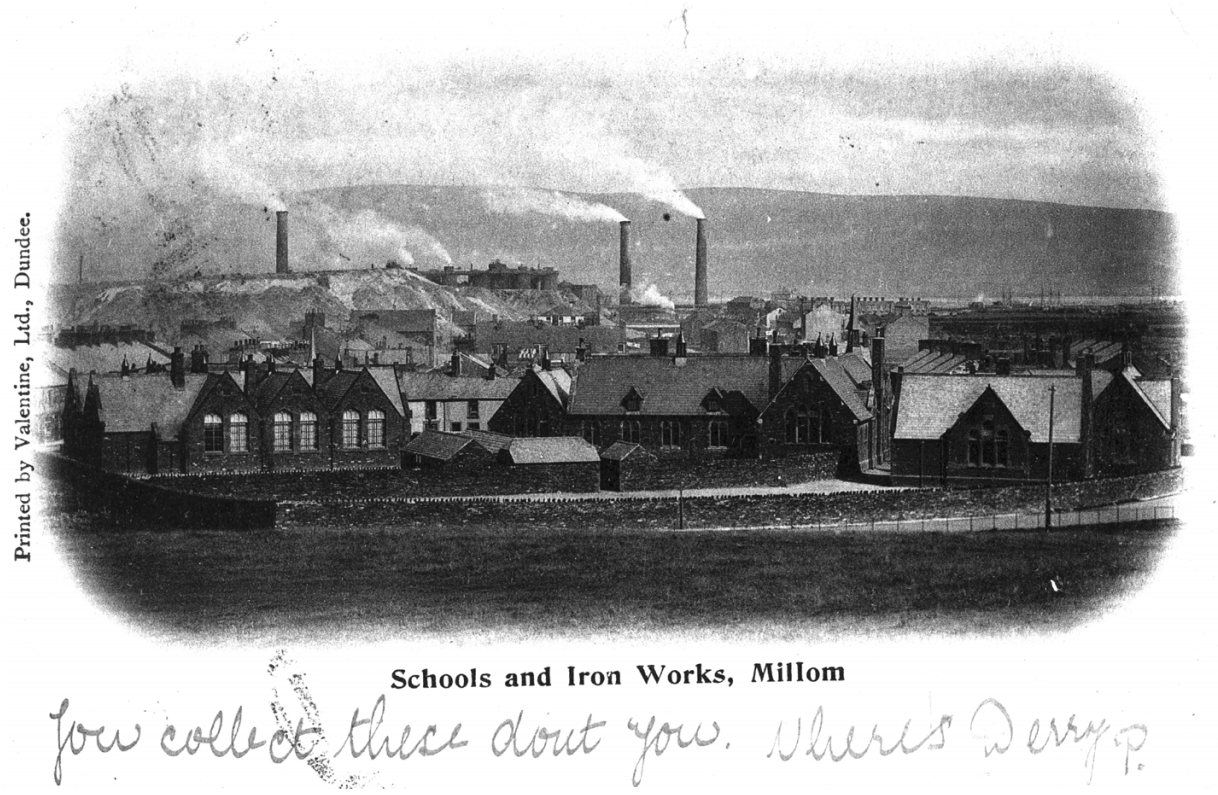

Fig 1. View from the Park looking southward across the Duddon Estuary and Furness fells, with the Elementary School in the foreground, the Company Houses are off to the left, and the Iron Works and associated slag banks are visible in the middle ground. Photograph taken sometime between 1910 and 1930 (guess).

Fig 2. John at Flitaway Lake, 1963

Evidence of palaeo-ice streaming in NE-Iceland

Aradóttir, Nína [1]; **Benediktsson**, Ívar Örn [2]; **Ingólfsson**, Ólafur [3]; **Brynjólfsson**, Skafti [4]

[1] Institute of Earth Science, University of Iceland; nia1@hi.is
[2] Institute of Earth Science, University of Iceland; ivarben@hi.is
[3] Institute of Earth Science, University of Iceland; oi@hi.is
[4] Icelandic Institute of Natural History; skafti@ni.is

The geomorphology of ice stream beds is critical for understanding the behaviour of ice streams as the formation of bedforms can be linked to the mechanism of ice streaming. Ice streams within the Icelandic Ice Sheet (IIS) have been proposed but limited studies exist on their configuration and dynamics. The aim of this project is to investigate the fingerprints of palaeo-ice streams in NE-Iceland with particular focus on streamlined subglacial bedforms (SSBs) in order to advance our understanding of the geomorphological imprint, configuration and dynamics of these palaeo-ice streams in time and space. This will be achieved by mapping and investigating glacial bedorms and sedimentary records in Þistilfjörður, Bakkaflói, Bakkaheiði, Vopnafjörður and Jökuldalsheiði areas through multiple glacial geological, geomorphological, and geophysical methods. The streamlined terrain preserves the flow sets of several cross-cutting palaeo-ice streams that were probably active during the Last Glacial Maximum (LGM) and throughout the deglaciation.

Within the Vopnafjörður flow set in NE-Iceland, the internal architecture of two drumlins from the Bustarfell drumlin field has been studied by combining ground-penetrating radar (GPR) and sedimentological data. For the GPR data collection, 16 profiles were surveyed with 50 and 100 MHz antennas that penetrated down to a maximum depth of 16 m and 9 m, respectively. Between 5 and 7 generalized radar facies and surfaces have been identified to describe and interpret the surveyed profiles. Results from the lithostratigraphic logs indicate that the drumlins are composed of massive till beds, which show deformation structures and fissility and are sometimes separated by glaciofluvial material. The logs and the GPR profiles correlate relatively well in the upper part of the drumlins (< ~4 m depth) whereas continuous to discontinuous undulating reflectors in the lower part (> ~4 m depth) are not visible in the stratigraphic logs but might represent fluvial material that has undergone deformation. Post glacial sediment (< ~4 m depth) can be seen on the lateral flanks of the drumlins and occasionally on their lee side. Based on these findings, a preliminary hypothesis is that subglacial erosion, accretion and shear deformation contributed to the development of the drumlins under fluctuating pore-water pressures.

The study can provide an insight into the dynamics of palaeo-ice streams in Iceland as well as the development of the IIS during and following the LGM. Furthermore, the results are essential to constrain models for the formation of bedforms under fast flowing ice, and further contribute to the understanding of the linkage between ice stream development and climate change.

Disentangling the evolution of Holocene climate, soil erosion and human impact in Iceland

Ardenghi, Nicolò [1]; **Harning**, David J [2]; **Raberg**, Jonathan [3]; **Sepúlveda**, Julio [4]; **Geirsdóttir**, Áslaug [5]; **Miller**, Gifford H [6]; **Þórðarson**, Þorvaldur [7]

[1] INSTAAR; nicolo.ardenghi@gmail.com
[2] INSTAAR; david.harning@colorado.edu
[3] INSTAAR; jonathan.raberg@colorado.edu
[4] INSTAAR; jsepulveda@colorado.edu
[5] University of Iceland; age@hi.is
[6] INSTAAR; gmiller@colorado.edu
[7] University of Iceland; torvth@hi.is

The Arctic is warming twice as fast as the global average, with mean summer temperatures predicted to be 4–6°C higher than in the late 20th century by year 2100. In order to inform policy, predictive models rely on the understanding of climatic factors and feedback mechanisms. However, while large uncertainties remain, they can be reduced through the study of past climate evolution.

Soil erosion has been severe across Iceland for centuries and it is commonly thought to have been initiated at settlement (~870 CE; Dugmore et al., 2009). However, the roles of time (soil development), climate (mainly summer temperature), volcanism, and human impact (mostly settlement along with pastoral activity) as the cause of the widespread soil erosion, remains debated.

Twenty thousand years ago, Iceland and its shallow continental shelf lay beneath an independent ice sheet. As Iceland deglaciated (after 15 ka BP), plants colonised from distant sources and soil formed and developed (e.g., Geirsdóttir et al., 2020). By ~5 ka BP, the cooling caused by the decreasing northern hemisphere summer insolation (Fig. 1 A-B) resulted in the decline of birch woodlands, increased catchment soil erosion during colder summers, and regrowth or expansion of Iceland's cryosphere (Neo-glaciation), with ice caps reaching maximum dimensions during the Little Ice Age (~1250-1850 CE). Though the primary forcing for Northern Hemisphere Holocene cooling is thought to be the monotonic decline in summer insolation, high-resolution records of environmental change indicate that Iceland's landscape response was non-linear (Fig. 1 B; Geirsdóttir et al., 2019, 2020).

Our ongoing project at INSTAAR aims to accurately reconstruct a continuous history of climate across Iceland since the last glacial period (~11.5 ka BP), and determine to what extent climate, volcanism and/or humans (Norse settlement) led to the widespread soil erosion, a pervasive feature of the contemporary Icelandic landscape.

We will rely on a novel integration of a rich archive of lipid biomarker proxies and sedimentary DNA (Fig. 2) obtained through downcore analysis of a series (3-5) lacustrine sediment cores. These are securely dated, high-resolution records spanning the entire Holocene and covering (Fig. 3) the western (A), the northern (B), and the south-eastern (C) coastal sectors of Iceland. The proxies we plan to use are brGDGTs (bacterial membrane lipids) for paleo-temperature; algae/plant waxes *n*-alkyl compounds, with their stable isotopic composition (delta^{2}H, delta^{13}C) for paleo-hydrology; and faecal sterols/bile acids and fire markers (polycyclic aromatic hydrocarbons, levoglucosan, and possibly charcoal) for human presence/agency. *Seda*DNA analysis will provide information on the evolution of the vegetation cover in the Icelandic landscape throughout the Holocene, with a focus on the deglaciation process, avoiding the shortcomings of pollen aeolian transport from more southern regions.

Additionally, interpretation of these proxies will be bolstered by the results of a parallel analysis of tephra layers (providing secure chronology, along with radiocarbon) and other organic/inorganic proxies (e.g., biogenic silica) tracing the evolution of volcanism and primary productivity.

Arnalds, O., Thorarinsdottir, E.F., Metusalemsson, S., Jonsson, A., Gretarsson, E., Arnason, A., 2001. Soil Erosion in Iceland. Soil Conservation Service. Agricultural Research Institute, Reykjavik, Iceland.

Berger, A., Loutre, M.-F., 1999. Parameters of the Earths orbit for the last 5 Million years in 1 kyr resolution. Supplement to: Quat Sci Rev 10.4: 297–317. doi:10.1594/PANGAEA.56040

Cabedo-Sanz, P., Belt, S.T., Jennings, A.E., Andrews, J.T., Geirsdóttir, Á., 2016. Variability in drift ice export from the Arctic Ocean to the North Icelandic Shelf over the last 8000 years: A multi-proxy evaluation. Quaternary Science Reviews 146, 99–115. doi:10.1016/j.quascirev.2016.06.012

Dugmore, A.J., Gisladóttir, G., Simpson, I.A., Newton, A., 2009. Conceptual Models of 1200 Years of Icelandic Soil Erosion Reconstructed Using Tephrochronology. Journal of the North Atlantic 2, 1–18. doi:10.3721/037.002.0103

Geirsdóttir, Á., Harning, D.J., Miller, G.H., Andrews, J.T., Zhong, Y., Caseldine, C., 2020. Holocene history of landscape instability in Iceland: Can we deconvolve the impacts of climate, volcanism and human activity? Quaternary Science Reviews 249. doi:10.1016/j.quascirev.2020.106633

Geirsdóttir, Á., Miller, G.H., Andrews, J.T., Harning, D.J., Anderson, L.S., Florian, C., Larsen, D.J., Thordarson, T., 2019. The onset of neoglaciation in Iceland and the 4.2 ka event. Climate of the Past 15, 25–40. doi:10.5194/cp-15-25-2019

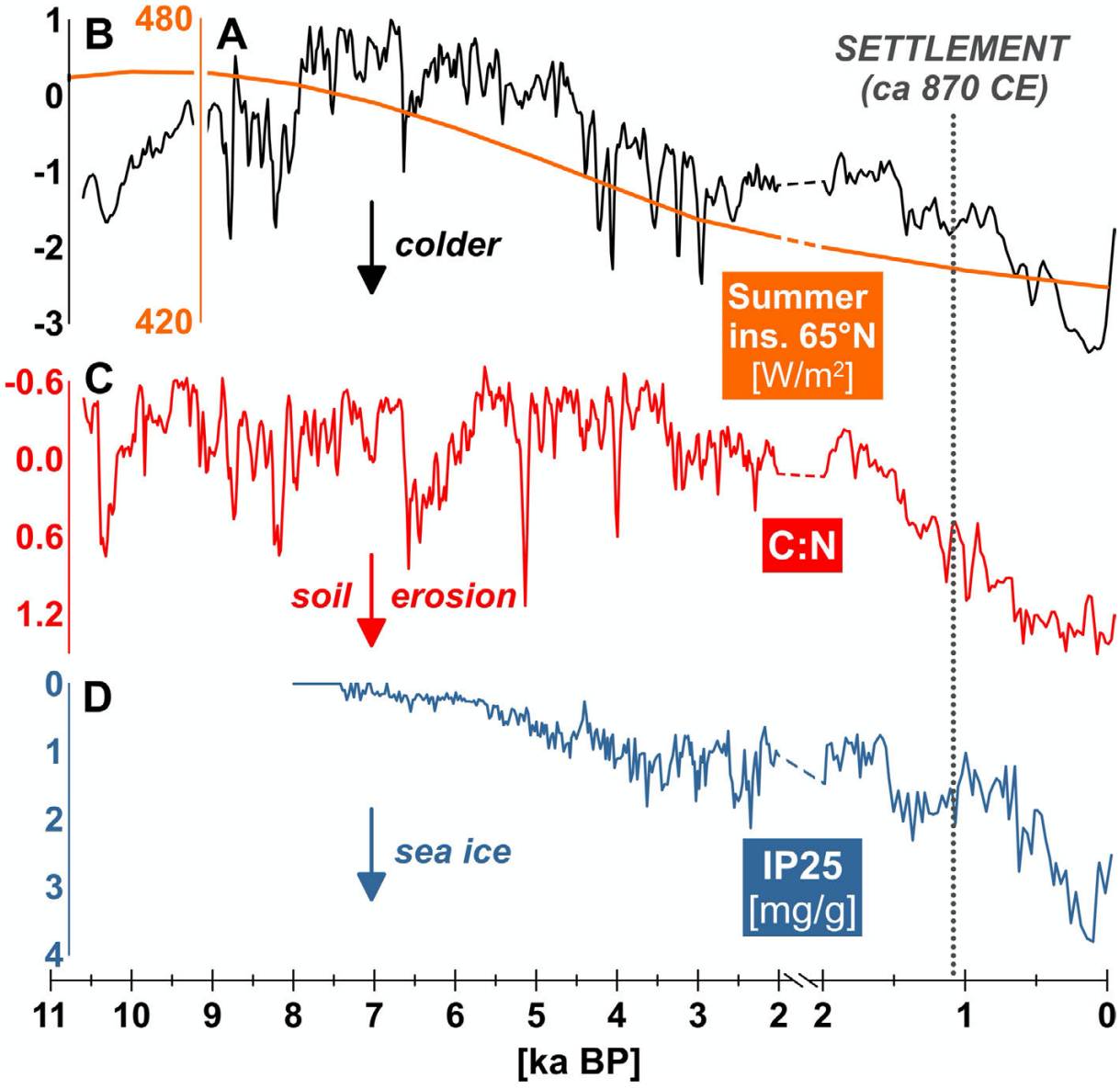

Fig 1. (A) Summer insolation at 65°N (Berger and Loutre, 1999). Iceland 7-lake composite records: (B) Holocene relative summer temperature, (C) C:N (Geirsdóttir et al., 2019). (D) IP25 (sea ice) on the north shelf of Iceland (MD99-2269) (Cabedo-Sanz et al., 2016).

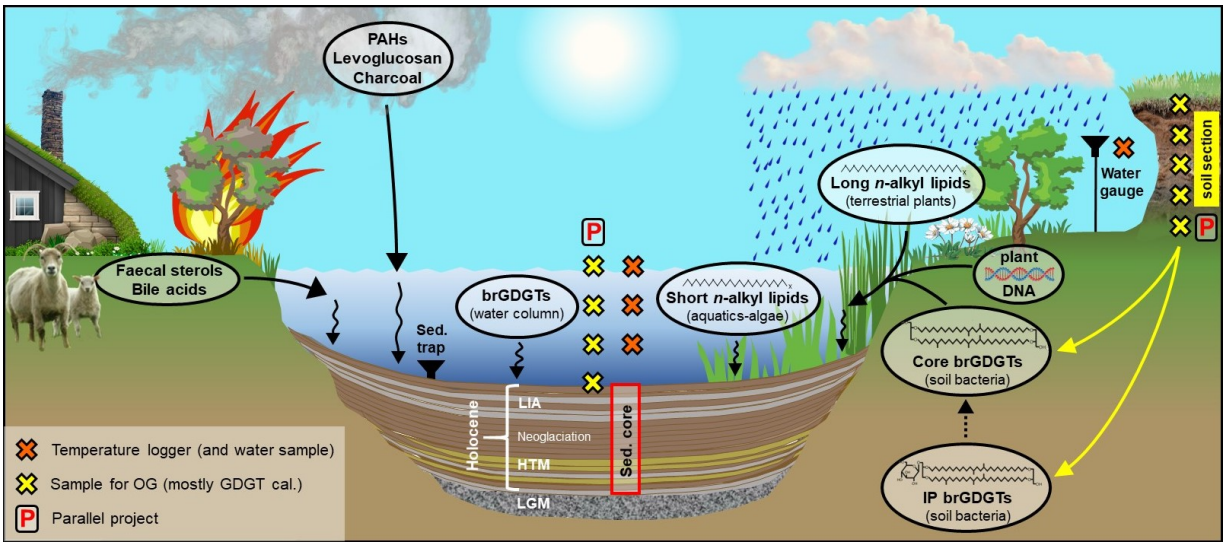

Fig 2. Schematic illustration of our field sampling-instrumentation strategies.

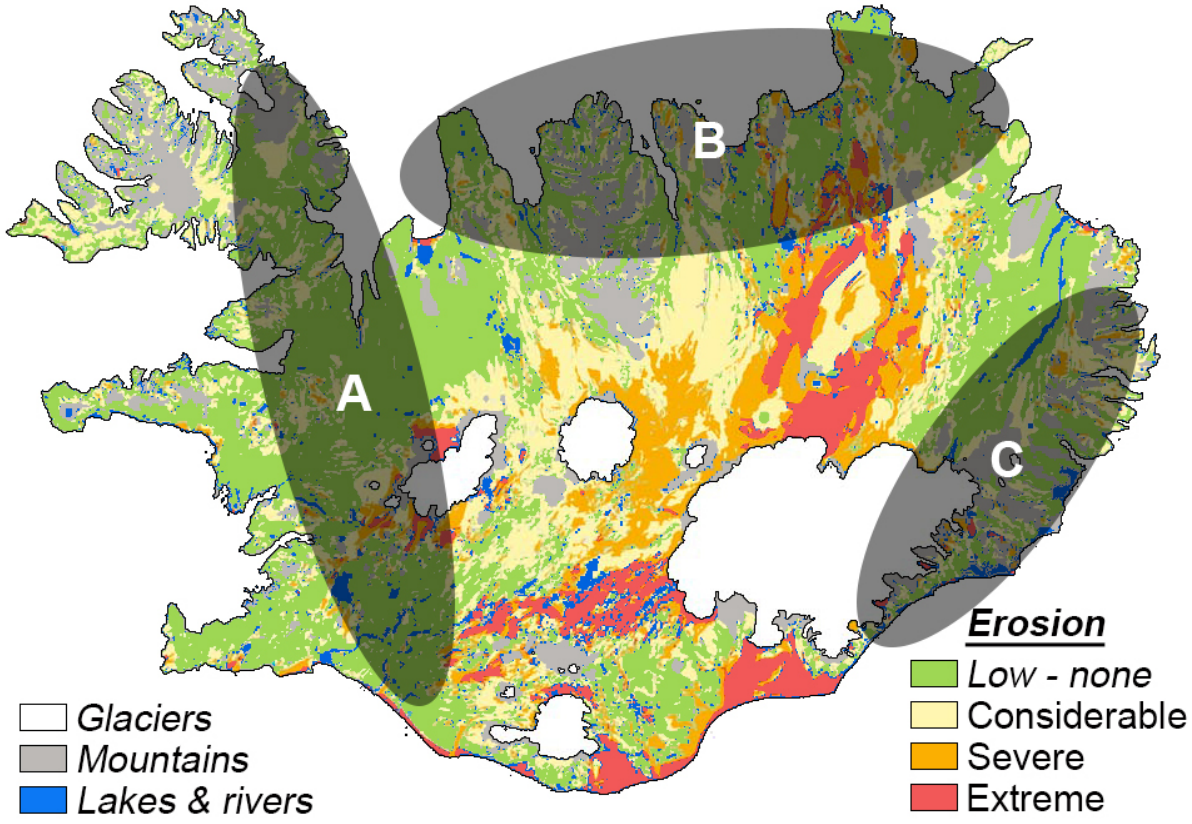

Fig 3. Modern soil erosion in Iceland (modified from Arnalds et al., 2001). Black shaded areas indicate the three main regions (A-western, B-northern, and C-south-eastern coasts) covered by our lacustrine archives.

The Holocene Thermal Maximum across Greenland: Reconciling differences in the timing and magnitude of peak warmth

Axford, Yarrow [1]; **de Vernal**, Anne [2]; **Osterberg**, Erich C. [3]

[1] Northwestern University; axford@northwestern.edu
[2] Université du Québec à Montréal; devernal.anne@uqam.ca
[3] Dartmouth College; erich.c.osterberg@dartmouth.edu

In the early to middle Holocene, higher boreal summer insolation drove thousands of years of elevated temperatures across much of the Arctic including Greenland. In Greenland, the timing, magnitude and seasonality of Holocene warmth have remained ambiguous despite decades of research. For example, a subset of temperature reconstructions (mostly based upon pollen, ice cores from the Greenland Ice Sheet, and nearshore marine sediments) suggest modest peak warmth in the middle Holocene – lagging long after peak summer insolation forcing, and supporting the hypothesis that decaying ice sheets suppressed early Holocene temperatures across a large part of the North Atlantic region. In contrast, the other subset of temperature reconstructions (mostly derived from marginal ice caps, midges in lakes, and offshore marine records) record dramatic peak warmth during the early Holocene. The latter records support the primacy of insolation forcing over Greenland, and may also imply that strong feedbacks amplified warming in the region. These alternate temperature histories have very different implications for understanding how ice sheet decay modulates climate change in this sensitive region, and how the ice sheet itself responds to warming.

To more confidently characterize Greenland's Holocene temperature history, we compiled published long-term (>7000-year long) quantitative air and sea surface temperature reconstructions from ice, lake sediment and marine sediment cores. We also compiled qualitative evidence for warmer-than-present local conditions from extralimital terrestrial fauna and the past disappearance or reduced size of numerous modern-day mountain glaciers and ice caps. Some key findings include:

• There is compelling evidence that summer air temperatures rose above those of the mid-20th Century in the early Holocene around much of Greenland, indeed by 10 ka in many regions including over the central ice sheet. Maximum summer temperature anomalies in the east, northwest and over the central ice sheet occurred in the early Holocene and were as large as 3 to 5 °C above mid-20th Century summer temperatures.

• The far south and southwest (adjacent to the Labrador Sea) may be exceptions where early Holocene warming was muted and peak summer air temperatures occurred in the middle Holocene. However, more records are needed to confirm this pattern.

• The notion of middle Holocene peak warmth across much of Greenland arose from a combination of (1) proxy-specific issues, namely proxy seasonality (winter trends may oppose or mute summer signals in annual proxies like stable isotopes of ice), changes in ice sheet

surface elevation (with higher elevations of core sites in the early Holocene masking regional summer warmth in ice core proxies), and lagged vegetation migration and/or no-analog vegetation in the early Holocene, and (2) the effects of ice sheet meltwater on sea-surface conditions. Along Greenland's coasts in the early Holocene, freshwater discharge from the rapidly shrinking Greenland Ice Sheet led to strong stratification of near-shore surface waters and thus increased winter sea ice and cold winters – while offshore sites strongly influenced by the North Atlantic Current experienced very warm sea surface conditions.

• Overall, our compilation points to higher early Holocene summer air temperatures over the ice sheet than are often presumed, including in studies designed to test ice sheet models. Our results confirm the primacy of summer insolation in driving summer temperature trends around Greenland. They also reinforce that the early Holocene was a period of competing strong and complex influences on Greenland climate, leading to significant spatial and seasonal heterogeneity of temperature trends. In comparison, temperature reconstructions in the middle and late Holocene are characterized by more widespread agreement between proxies and settings and the vast majority of middle to late Holocene temperature-sensitive proxy records mirror insolation forcing on a multi-millennial timescale.

Acknowledgements

We thank the many colleagues whose research contributed to this compilation, and the people of Kalaallit Nunaat for welcoming scientists to their homeland. This review was supported by US NSF CAREER grant OPP-1454734, the Natural Sciences and Engineering Research Council of Canada, and the Fonds de Recherche du Québec-Nature et Technologies. An advance proof of the corresponding article is available from Annual Review of Earth and Planetary Sciences, doi:10.1146/annurev-earth-081420-063858.

On this occasion of the 50th Arctic Workshop, we also thank John T. Andrews for inspiring and supporting decades of investigations into the paleoclimate history of northeastern North America.

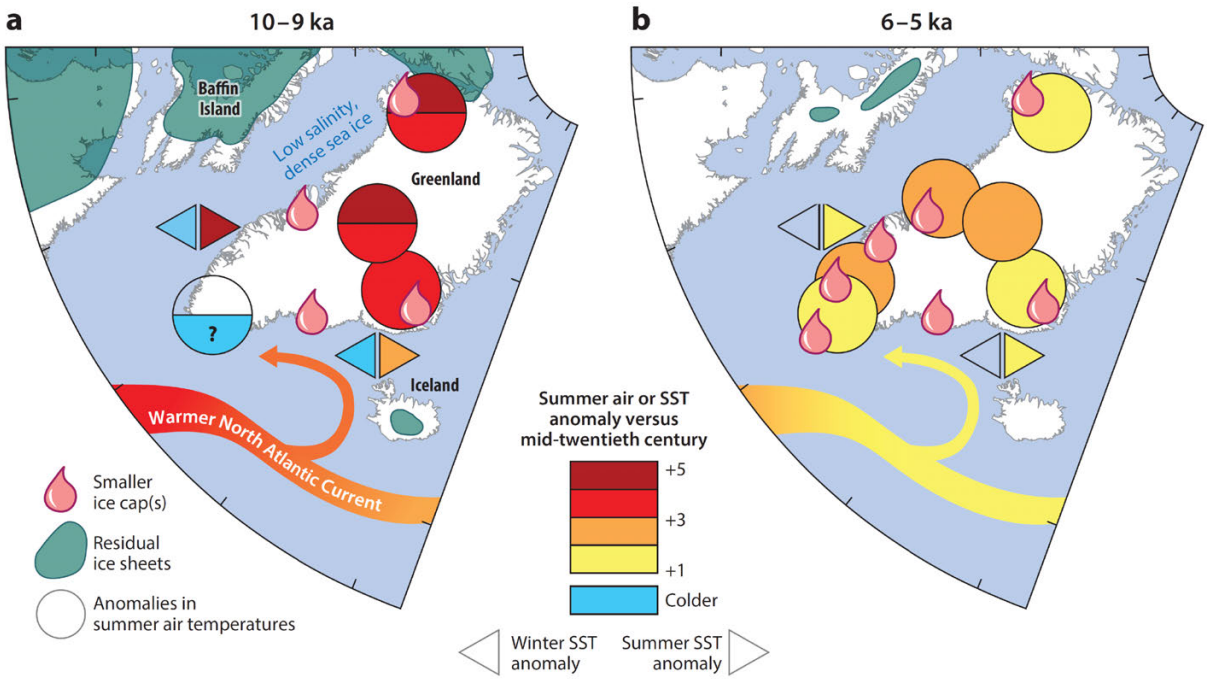

Fig 1. Summary of major climatic differences around Greenland from (a) 10-9 ka versus modern and (b) 6-5 ka versus modern, including: Anomalies in summer air temperature (circles; estimates for Summit reflect elevation correction of reconstructions from Buizert et al 2018), winter SST (left triangles) and summer SST (right triangles) compared to the mid-20th century AD; large differences in sea-surface salinity and sea ice (italicized text); regions with ice caps and mountain glaciers smaller than today (droplets); and major residual Pleistocene ice sheets that are now absent (gray shading). From 10-9 ka the Greenland Ice Sheet was thicker at Summit than today (Vinther et al 2009) but similar in area; from 6-5 ka the ice sheet was smaller than today, with its minimum size poorly constrained (Larsen et al 2015, Young & Briner 2015). Half circles reflect larger uncertainties or ranges between air temperature proxies. Gray triangles indicate SSTs similar to the mid-20th century. Note enhanced SST seasonality in the early Holocene, with lower winter and higher summer SSTs. This figure appears in the corresponding article in Annual Review of Earth and Planetary Sciences, doi:10.1146/annurev-earth-081420-063858.

Icebergs and tropical rainfall

Bradley, Raymond S [1]; **Diaz**, Henry F [2]

[1] University of Massachusetts; rbradley@geo.umass.edu
[2] University of Hawaii; hfdiaz@hawaii.edu

Tropical hydrological events, characterized by extreme regional rainfall anomalies, were a recurrent feature of marine isotope stages (MIS) 2-4 and involved some of the most abrupt and dramatic climatic changes in the late Quaternary. These anomalies were pervasive throughout the Tropics and resulted from the southward displacement of the Hadley circulation and the Intertropical Convergence Zone and its associated convective rainfall.

Lake sediments, stalagmites and offshore marine sediments that integrate inland continental conditions provide a comprehensive record of changes over the past~70,000 years. Within the uncertainties of dating, tropical rainfall anomalies occurred very close in time (±102-103 years) to the deposition of North Atlantic ice-rafted debris (IRD) that defines Heinrich events. Even though there may have been considerable amounts of freshwater entering the North Atlantic --without any associated sediment-- prior to the release of sediment-loaded icebergs from calving glaciers, the IRD record is in fact a good proxy for the amount and distribution of additional freshwater forcing which was necessary to bring about a drastic reduction in the Atlantic Meridional Overturning Circulation strength during each HE.

As a consequence of this reduction in AMOC and an abrupt expansion in the area of sea-ice, cooling of the North Atlantic and adjacent continents took place, with a rapid atmospheric response involving the southward displacement of the ITCZ and associated rainfall belts. The climatic consequences of this large-scale change in the Hadley circulation, modulated by regional factors, is clearly recorded throughout the Tropics as a series of abrupt and anomalous hydrological events.

Bradley, R.S. and Diaz, H.F. 2021. Late Quaternary abrupt climate change in the Tropics and Sub-Tropics: the continental signal of Tropical Hydrological Events (THEs). (in review)

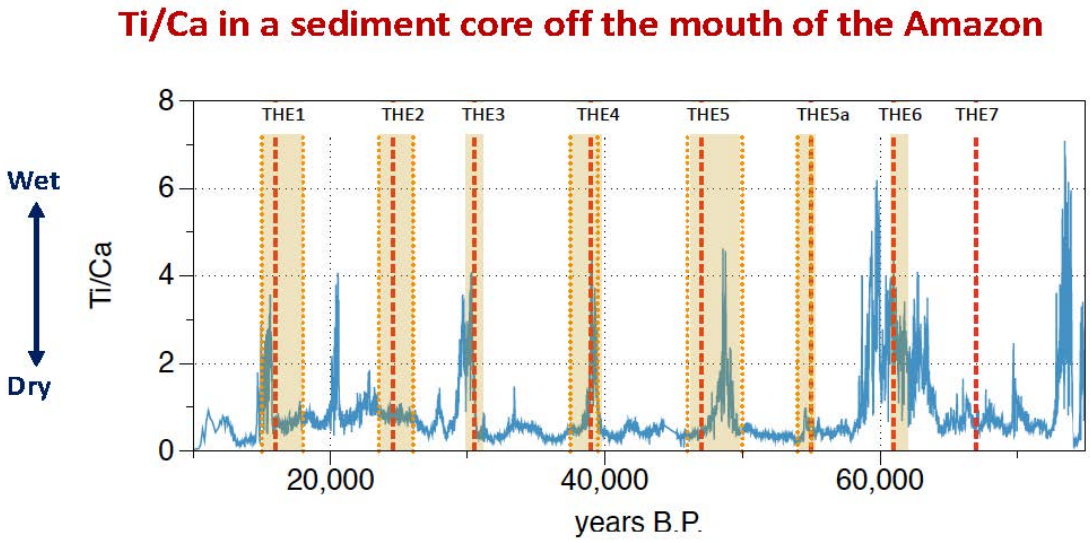

Fig 1. Ti/Ca ratio for marine sediment core CDH 86, off the mouth of the Amazon River (0.3°N, 44° 12.2°W). The Ca is derived from biogenic CaCO3(mostly from pteropods, foraminifera, and calcareous nannoplankton)whichis assumed to have been relatively constant over time.High ratios thus indicate that higher amounts of clastic material were delivered to the ocean during times of relatively dry conditions in the continental interior(adaptedfrom Nace et al., 2014). Red lines denote peak times of IRD

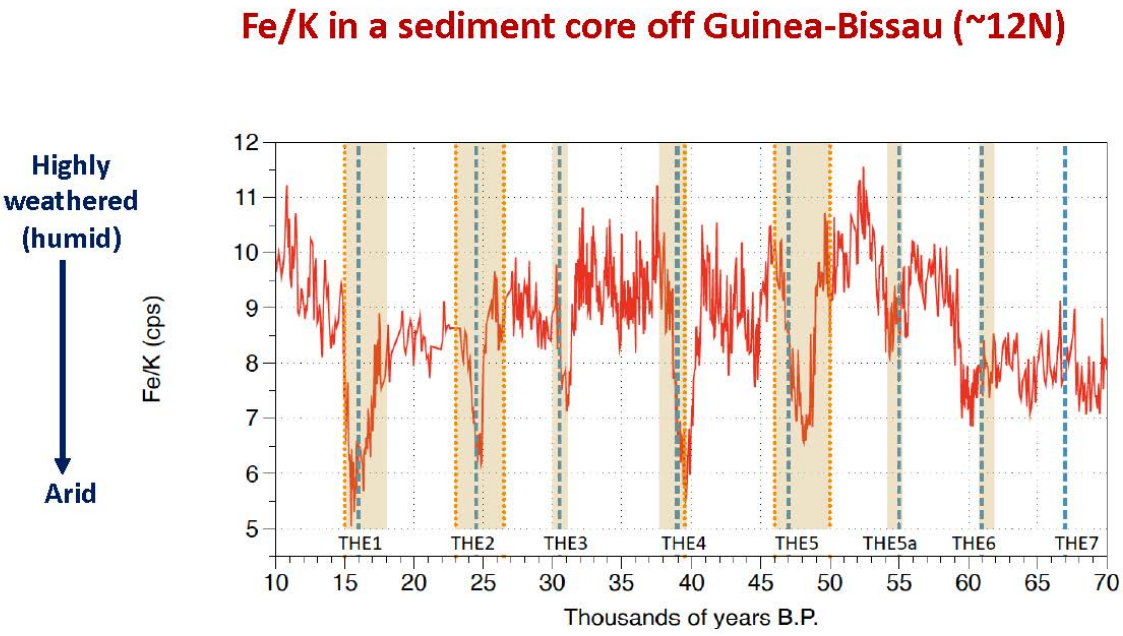

Fig 2. Ratios of Fe/K in a sediment core from off the coast of Guinea-Bissau (~12.5°N). Higher values of Fe/K indicate wetter conditions as the more weathered rocks in humid tropical regions contain more Fe relative to the more mobile potassium. The low values that punctuate this record thus indicate much drier conditions in the continental interior as the ITCZ and associated rain belt shifted southward and Trade winds delivered dust from the arid interior of the western Sahara. Grey shading denotes the timing of Heinrich events in the North Atlantic (modified, from Zarriess et al., 2011).

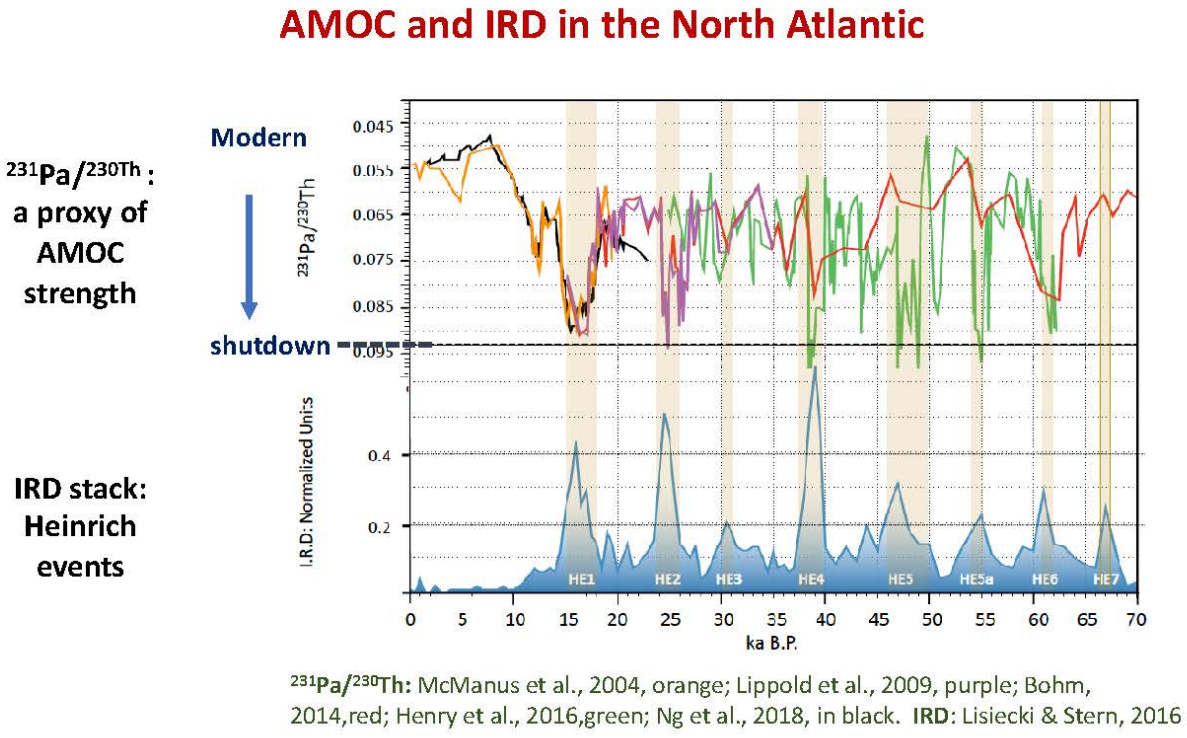

Fig 3. 231Pa/230Th in several North Atlantic sediment cores; values of >0.093 (dashed black line)represent a complete cessation of North Atlantic deepwater formation(note dataare plotted inversely; from McManus et al., 2004, in orange; Lippold et al., 2009, in purple; Bohm, 2014, in red; Henry et al., 2016, in green; Ng et al., 2018, in black, 9-point running mean). Lower blue line is the stacked record of IRD based on 15 North Atlantic cores (normalized values, from Lisiecki and Stern, 2016). Shaded brown intervals indicate times when IRD exceeded median values for MIS2-4.

Navigating NNA -- from planning and vulnerability to research action

Brigham-Grette, Julie [1]; **Kumpel** , Emily [2]; **Bulter**, Caitlyn [3]; **Temte**, James [4]; **Weston**, Bessie [5]; **Lewis** , Tracy [6]; **Paul** , Paul [7]

[1] University of Massachusetts Amherst; juliebg@geo.umass.edu
[2] University of Massachusetts Amherst; ekumpel@umass.edu
[3] University of Massachusetts Amherst; csbutler@engin.umass.edu
[4] Alaska Pacific University; jtemte@alaskapacific.edu
[5] Mekoryuk Grant Writer; buzymee@yahoo.com
[6] Kongiganak EPA-IGAP Director; kong.igap@gmail.com
[7] Kongiganak Environmental Office; kongiganak.igap2@gmail.com

Sea level rise, associated coastal erosion, river flooding, and permafrost thaw are contemporary threats to the infrastructure and sustainability of villages and tribes throughout Alaska and many parts of the Arctic. State and Federal agencies already work with villages to develop plans that involve the collection of data to determine rates and risks to ways of life. The NSF Navigating the New Arctic (NNA) program (among 10 Big Ideas) aims to increase the co-production of knowledge to accelerate the development of sustainable planning trajectories for villages. Yet bringing academic science to address contemporary and future challenges must involve partnering village educational and vocational needs for sustainability along with process, engineering, and climate change studies to fill data gaps leading to social and engineering solutions. COVID travel restrictions made building collaboration and partnerships more challenging for NNA, but we scientists must also embrace the exposure of racism and colonialism this past year across society and use it as an opportunity for science and indigenous communities to create open dialog leading, hopefully toward genuine solution-based science.

As we navigate forward in this changing Arctic, we have attempted to chart a course that holistically considers both the physical world and human dimensions of these new realities. Accordingly, any rigorous study of the changing Arctic must be grounded in the lived experience and self-determination of its inhabitants and provide opportunity for people to take ownership over their own short- and long-term response to these grand challenges. Therefore, we developed a proposal to embrace the Yupik and Cup'ig cultural relationship with the changing phases of water ("meq") in the Arctic environment of the outer Yukon-Kuskokwim Delta, including the impact of rising sea level, coastal erosion, river flooding, permafrost collapse and its impact on traditional ecosystem services as well as safe and sustainable water and sanitation infrastructure. Following on from an NNA planning grant, we deepened existing partnerships with Arctic people in Mekoryuk and Kongiganak, through collaboration with the Alaska Pacific University/Alaska Native Tribal Health Council (ANTHC). We have coproduced new dialogues with communities at risk to emerging environmental threats caused by climate change. This was a collective journey to join traditional knowledge systems with western science tools to quantify the rate of landscape change in an uncertain Arctic future and

evaluate how this change impacts long range planning to meet regional needs for sustainable livelihoods and infrastructure. We also plan to use these data in partnership with the Alaskan regulatory ecosystem and other NNA projects to suggest changes in structural barriers faced by underserved communities in Alaska. Our approach is intellectually linked to both formal and informal education in the villages of Mekoryuk and Kongiganak, but also builds and integrates new scholars from the Alaska Pacific University (a Tribal university) in careers in environmental sustainability, community engagement, and climate communication. Our work sharing Indigenous knowledge through an Indigenous educational philosophy and the newest scientific approaches will provide a means of forecasting the outcome or rates of landscape change that will not only inform our partner communities planning for future water/sanitation infrastructure but also provide a predictive framework for similar communities over the coming decades in contrasting deltaic mud and bedrock foundation systems.

Our resulting science proposal emerged as a collaboration between the villages of Mekoryuk and Kongiganak, UMass, APU, and UAF. It was a journey of collaboration and vulnerability to create a vision.

Camp Century revisited: an ecosystem under the ice reveals Greenland's warmer past

Christ, Andrew J [1]

[1] University of Vermont; Andrew.Christ@uvm.edu

The fate of the Greenland Ice Sheet (GrIS) and Arctic ecosystems in response to climate warming remain uncertain. Terrestrial records of a GrIS smaller than today and the ecosystems that emerged in formerly ice-free areas are crucial for understanding ice-sheet and ecosystem sensitivity to warming, yet rare due to present ice cover. Basal materials from ice cores can be a critical archive of past ice-free periods. Collected in 1966 from northwestern Greenland, the Camp Century ice core was the first ice core drilled to the bed of an ice sheet and retrieved 3.5 m of sub-glacial sediment (Hansen and Langway, 1966). However, the subglacial sediment was incompletely studied and then misplaced for decades – until it was re-discovered in 2017. Now, we can apply many analytical techniques to the sediment that were unimaginable at the time of its collection nearly 60 years ago.

Here, we show that the upper- and lower-most sub-glacial sediment from Camp Century contains a multi-million-year record of vegetation and glacial history in northwestern Greenland (Christ et al., 2021). The sediment preserves lipid biomarkers and frozen plant macrofossils, including Arctic willow, twigs, moss leaves and stems, and fungal spores, that resemble tundra vegetation from modern ice-free areas of Greenland. Enriched ?^{18}O values from sediment pore ice require precipitation at lower elevations and warmer temperatures that imply ice-sheet absence. Multiple geochronometric analyses suggest the upper sediment contains reworked material similar to the lower sediment. Cosmogenic ^{26}Al/^{10}Be and infrared stimulated luminescence (IRSL) data bracket the burial of the lower-most sediment between <3.2 ± 0.4 Ma and >0.7 to 1.4 Ma. In the upper most sediment, multiple IRSL dating methods indicate that the last exposure to sunlight was soon after the peak warmth of the Marine Isotope Stage (MIS) 11 interglacial. The luminescence data are consistent with the cosmogenic ^{26}Al/^{10}Be burial age of <1.0 ± 0.1 Ma, which together mandate no more than 13 kyr of exposure during the last ice-free event.

The subglacial sedimentary record from Camp Century documents at least two episodes of ice-free, vegetated conditions, each followed by glaciation. The lower sediment derives from an Early Pleistocene GrIS advance and contains the oldest record of Greenland vegetation recovered from beneath the ice sheet. The upper sediment provides direct terrestrial evidence for a smaller GrIS during MIS 11 and requires at least 1.8 m of sea level contribution from Greenland. At a wider scale, the ^{26}Al/^{10}Be in the Camp Century upper sediment match those in GISP2 subglacial bedrock from central Greenland (Schaefer et al., 2016), which suggests a similar history of ice cover across Greenland. The GrIS survived most Pleistocene interglacials, but much of it melted at least once in the last million years. The loss of the

northwestern GrIS and emergence of a tundra ecosystem during MIS 11 underscores ice-sheet sensitivity to prolonged interglacial warmth (Robinson et al., 2017; Irvali et al., 2020).

Christ, A.J., Bierman, P. R., Schaefer, J. M., Dahl-Jensen, D., Steffensen, J. P., Corbett, L. B., Peteet, D., Thomas, E. K., Steig, E. J., Rittenour, T. M., Tison, J.-L., Blard, P. H., Perdrial, N., Dethier, D., Lini, A., Hidy, A. J., Caffee, M. W. and Southon, J. R., 2021, A multi-million-year-old record of Greenland vegetation and glacial history preserved in sediment beneath 1.4 km of ice at Camp Century: Proceedings of the National Academy of Sciences, v. 118, p. e2021442118.

Hansen, B.L., and Langway, C., 1966, Deep core drilling in ice and core analysis at Camp Century, Greenland, 1961-66: Antarctic Journal of the United States, v. Sept-Oct, p. 207–208.

Irvali, N., Galaasen, E. V., Ninnemann, U.S., Rosenthal, Y., Born, A., and Kleiven, H.F., 2020, A low climate threshold for south Greenland Ice Sheet demise during the Late Pleistocene: Proceedings of the National Academy of Sciences of the United States of America, v. 117, p. 190–195.

Robinson, A., Alvarez-Solas, J., Calov, R., Ganopolski, A., and Montoya, M., 2017, MIS-11 duration key to disappearance of the Greenland ice sheet: Nature Communications, v. 8, p. 1–7.

Schaefer, J.M., Finkel, R.C., Balco, G., Alley, R.B., Caffee, M.W., Briner, J.P., Young, N.E., Gow, A.J., and Schwartz, R., 2016, Greenland was nearly ice-free for extended periods during the Pleistocene: Nature, v. 540, p. 252–255.

Multi-proxy biomarker records and forward modeling of western Greenland Holocene lake temperatures and dynamics

Cluett, Allison A. [1]; **Thomas**, Elizabeth K. [2]; **Cowling**, Owen C. [3]; **Castañeda**, Isla S. [4]

[1] University at Buffalo; aacluett@buffalo.edu
[2] University at Buffalo; ekthomas@buffalo.edu
[3] University at Buffalo; owencowl@buffalo.edu
[4] University of Massachusetts Amherst; isla@geo.umass.edu

Long-term quantitative seasonal temperature reconstructions from the Arctic provide necessary context to evaluate long-term climate-cryosphere sensitivity and climate-carbon cycle feedbacks. Here, we analyze two quantitative molecular paleotemperature proxies, glycerol dialkyl glycerol tetraethers (GDGTs) and long-chain alkenones (LCAs), in the sediments of a small lake in the Kangerlussuaq region of western Greenland which span the past c. 9.5 thousand years (ka) following local deglaciation. Branched GDGT (brGDGT)-inferred summer water column temperature anomalies relative to the uppermost sample (representing roughly the last decade) based on the methylation of branched tetraethers (MBT'5Me) decrease through the mid-to-late Holocene from 3.96 to 0.95°C. However, the co-occurrence of high ratios of the isoprenoid GDGTs caldarchaeol to crenarchaeol and distinct brGDGT distributions suggest hypoxic conditions influenced brGDGT production prior to 4.5 ka (thousand years before present), preventing the application of the MBT'5Me paleothermometer in these samples. LCAs, which we do not detect in sediments older than 5.5 ka, record stronger temperature variability than brGDGTs, with spring water temperature anomalies ranging from –2.1°C to +6.4°C. We reconcile changes in the magnitude and seasonality of LCA and brGDGT temperatures using a thermodynamic lake model forced by simulations under modern and perturbed climatologies. Summer water column temperatures, which are indistinguishable from summer surface water temperatures, and likely recorded by brGDGTs, increase linearly with summer air temperatures. In contrast, surface water temperatures in the two weeks following ice-out, when haptophyte algae bloom and synthesize LCAs, demonstrate substantially stronger interannual variability. However, multi-decadal mean surface water temperatures following ice-out increase linearly with temperature forcing, suggesting LCA-inferred spring water temperatures are biased towards specific years with favorable conditions for haptophyte communities.

Patterns of postglacial vegetation establishment clarified by lacustrine sedaDNA from Baffin Island, Arctic Canada

Crump, Sarah E. [1]; **Power**, Matthew [2]; **Fréchette**, Bianca [3]; **de Wet**, Gregory [4]; **Raynolds**, Martha K. [5]; **Raberg**, Jonathan H. [6]; **Allentoft**, Morten [7]; , et al. [8]

[1] Department of Ecology and Evolutionary Biology, University of California Santa Cruz; secrump@ucsc.edu
[2] Curtin University;
[3] Geotop, Université du Québec à Montréal;
[4] Smith College;
[5] Institute of Arctic Biology, University of Alaska Fairbanks;
[6] INSTAAR, University of Colorado Boulder;
[7] Curtin University;
[8];

Postglacial colonization of high-latitude landscapes by tundra vegetation during the early Holocene is an important case study for understanding possible rates and patterns of plant migration in a rapidly warming world. Fossil pollen in lake sediment has been used for many decades to yield insights into Arctic paleovegetation and postglacial biogeography. However, because pollen can be wind-transported long distances and, in some cases, reworked from older deposits on the landscape, pollen-based vegetation histories can sometimes obscure the true history of plant colonization, particularly in treeless landscapes. In contrast, lacustrine sedimentary ancient DNA (sedaDNA) is sourced locally and is less likely to be adequately preserved through reworking events, thus making it more reliable for determining the precise timing of plant colonization. Here, we present three sedaDNA records from Holocene lake sediment across southern Baffin Island, Arctic Canada, that clarify the timing of postglacial vegetation changes. In particular, DNA from the subarctic shrub Betula (dwarf birch) first appears thousands of years after deglaciation in all three lake catchments, suggesting delayed colonization, in contrast to its strong pollen signal in early postglacial sediments. Although moderate levels of Alnus (alder) pollen characterize early to mid-Holocene lake sediments from the region, sedaDNA suggests that Alnus was probably not present in any of the three lake catchments during the Holocene. In addition, aquatic plant community changes indicated by sedaDNA generally correspond to the timing of early Holocene warmth in the region, highlighting the potential utility of aquatic plant DNA as a qualitative temperature proxy. These records highlight the utility of ancient plant DNA in lake sediment for providing complementary information to traditional proxy records, particularly during periods of relatively rapid ecological or climatic change.

Annually resolved past climate changes from South Sawtooth Lake 2900-year-long varved record

Francus, Pierre [1]; **Lapointe**, François [2]; **Bradley**, Raymond S. [3]; **Abbott**, Mark B. [4]

[1] Institut national de la recherche scientifique, Centre Eau Terre Environnement, Québec, Canada; pierre.francus@ete.inrs.ca
[2] University of Massachusetts Amherst, Department of geosciences, Amherst, MA, USA; flapointe@umass.edu
[3] University of Massachusetts Amherst, Department of geosciences, Amherst, MA, USA; rbradley@geo.umass.edu
[4] University of Pittsburgh, Geology and Planetary Science, Pittsburgh, PA, USA; mabbott1@pitt.edu

Few annually laminated (varved) lacustrine records exist in the Arctic and elsewhere (Zolitschka et al. 2015). These sedimentary sequences are excellent high-resolution climate archives because they are continuous, undisturbed, and contain their own annually resolved chronology (Zolitschka et al. 2015). Therefore, they can inform about abrupt changes and high frequency climate variability. Over the last 25 years, we have investigated the exceptional South Sawtooth Lake (SSL) 2900-year-long varved record located on Fosheim Peninsula, Ellesmere Island.

Watershed and lake processes monitoring, as well as many short and long cores obtained in several places in the lake basin over the years allowed to understand how these sediments are deposited and to establish the main climate factors driving the sedimentation (Francus et al. 2008). A single tributary from a currently not glacierized watershed feeds the lake that consists in a proximal and distal basin separated by a sill. Finely laminated sediments are only deposited in the distal basin and are mainly formed by the settling of overflows and interflows.

The annual nature of these laminations is confirmed by multiple cores retrieved over 25 years, as well as by 137Cs and 210Pb dating. About 100 thin-sections covering the entire composite sequence were made and examined at the SEM. About 8000 high-resolution backscattered images were used to precisely delineate varves and to obtain grain size for each year of sedimentation. The 5.25-meter long record was also analyzed using a medical CT-Scanner and Itrax Core scanner with a 100 microns resolution, for paleomagnetic variations, and optically stimulated luminescence dating.

The properties of each varve from the uppermost core section was compared to a set of instrumental data (on-site meteorological data, linked to hydrological monitoring, and the closest Meteorological Service of Canada station at Eureka). Coarse grain size, reflected in PC1 of a Principal Component Analysis, is significantly and positively correlated with May to August temperature from 2011 to AD 1948. PC1 also displays a significant correlation ($r = 0.65$, $p < 0.001$) over the last 2900 years with the nearby Agassiz Ice Cap δ18O record, including lower values during the Little Ice Age cold period (Lapointe et al. 2019) (Fig 1).

PC2 is indicative of Ti and finer particle size (% < 20 mm). Colder conditions preserve snow in the area, and tend to favour fine to medium silt deposition in the lake and represents nival melt (Francus et al. 2002). Ti and PC2 show a negative correlation to instrumental temperature ($r = 0.49$, $p < 0.001$) at Eureka. SSL record was also compared to major natural

climate oscillations (Fig. 2A and 2B). We found that Ti was correlated ($r = 0.57$, $P < 0.0001$) to instrumental Atlantic Multidecadal Variability (AMV) (Enfield et al. 2001) (Fig. 2C). The maximum Ti concentration coincides with the coldest SSTs in the North Atlantic from 1900–1925 CE, while lowest Ti values were found when SSTs were warmest, after 2005 CE.

We used this relationship to project past AMV changes over the last 2900 years (Fig. 3A). Amongst several significant correlation, the strongest was found with DYE-3 δ18O record from southern Greenland (Vinther et al. 2009), 2,000 km SE of SSL (Fig. 3B). The overall strong covariability between the AMVSSL and this ice core archive shows that southern Greenland and the Canadian High Arctic shared a common climate pattern over the past 3 millennia, driven by Atlantic SSTs.

Enfield, D., Mestas-Nunez. M., Trimble. P., 2001, The Atlantic multidecadal oscillation and its relation to rainfall and river flows in the continental U.S. Geophys. Res. Lett. 28, p. 2077–2080.

Francus, P., Bradley, R.S., Abbott, M.B., Patridge, W., Keimig, F., 2002. Paleoclimate studies of minerogenic sediments using annually resolved textural parameters. Geophys. Res. Lett. 29, 20, p. 5951-5954.

Francus, P., Bradley, R.S., Lewis, T., Abbott, M., Retelle, M., Stoner, J.S., 2008, Limnological and sedimentary processes at Sawtooth Lake, Canadian High Arctic, and their influence on varve formation. J Paleolimnol 40, 3, p. 963-985.

Lapointe, F., Bradley, R.S., Francus, P., Balascio, N.L., Abbott, M.B., Stoner, J.S., St-Onge, G., De Coninck, A., Labarre, T., 2020, Annually resolved Atlantic sea surface temperature variability over the past 2,900 y. Proc Natl Acad Sci U S A 117, 44, p. 27171-27178.

Lapointe, F., Francus, P., Stoner, J.S., Abbott, M.B., Balascio, N.L., Cook, T.L., Bradley, R.S., Forman, S.L., Besonen, M., St-Onge, G., 2019, Chronology and sedimentology of a new 2.9 ka annually laminated record from South Sawtooth Lake, Ellesmere Island. Quatern Sci Rev 222. p.

Vinther, B. et al. 2009, Holocene thinning of the Greenland ice sheet. Nature 461, p. 385–388.

Zolitschka, B., Francus, P., Ojala, A.E.K., Schimmelmann, A., 2015, Varves in lake sediments – a review. Quat Sci Rev 117, p. 1-41.

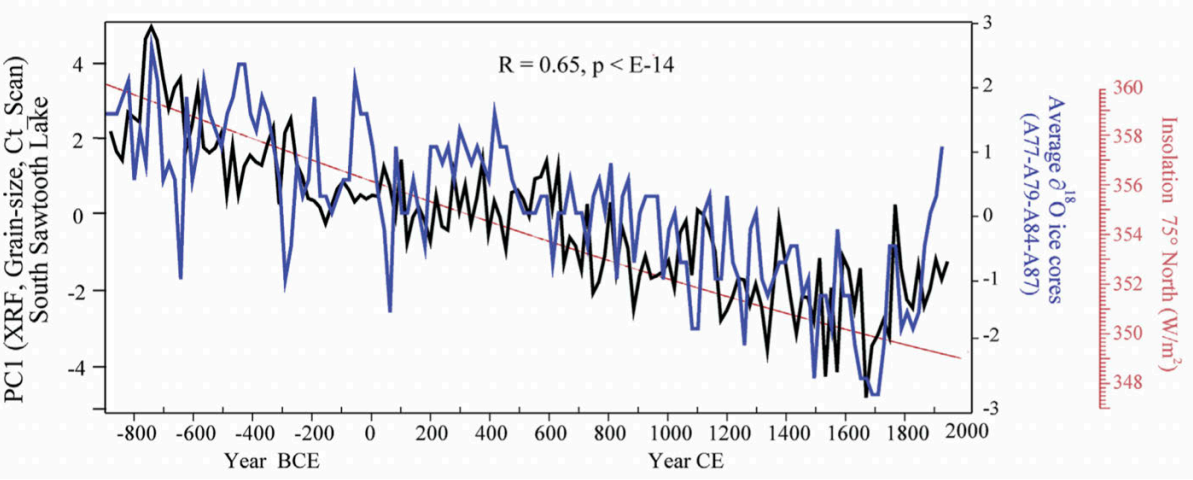

Fig 1. Comparison between South Sawtooth Lake PC1 (micro-XRF, HU, maxDo, D50 and D99) with Agassiz δ18O (mean of A77-A79-A84-A89 ice cores; Fisher et al., 1995).

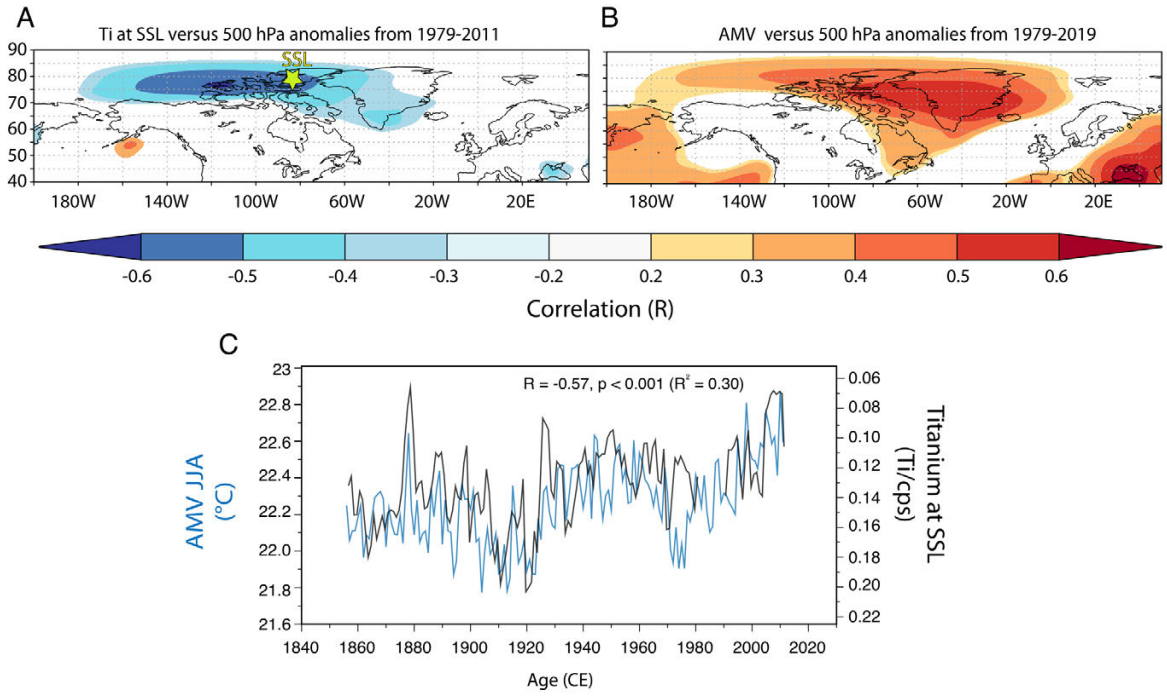

Fig 2. Ti variability at SSL and its relationship with instrumental AMV. (A) Map correlation between Ti variability and atmospheric pressure at 500 hPa from ERA-Interim during summer (JJA) from 1979 to 2011. (B) Same as A but for the instrumental AMV during summer (JJA) from 1979 to 2019 (Enfield et al. 2001). (C) Comparison between Ti at SSL (inverted values) and the instrumental summer (JJA) AMV over the instrumental period 1856–2011. Yellow star (A) denotes the location of SSL record. (modified from Lapointe et al. 2020).

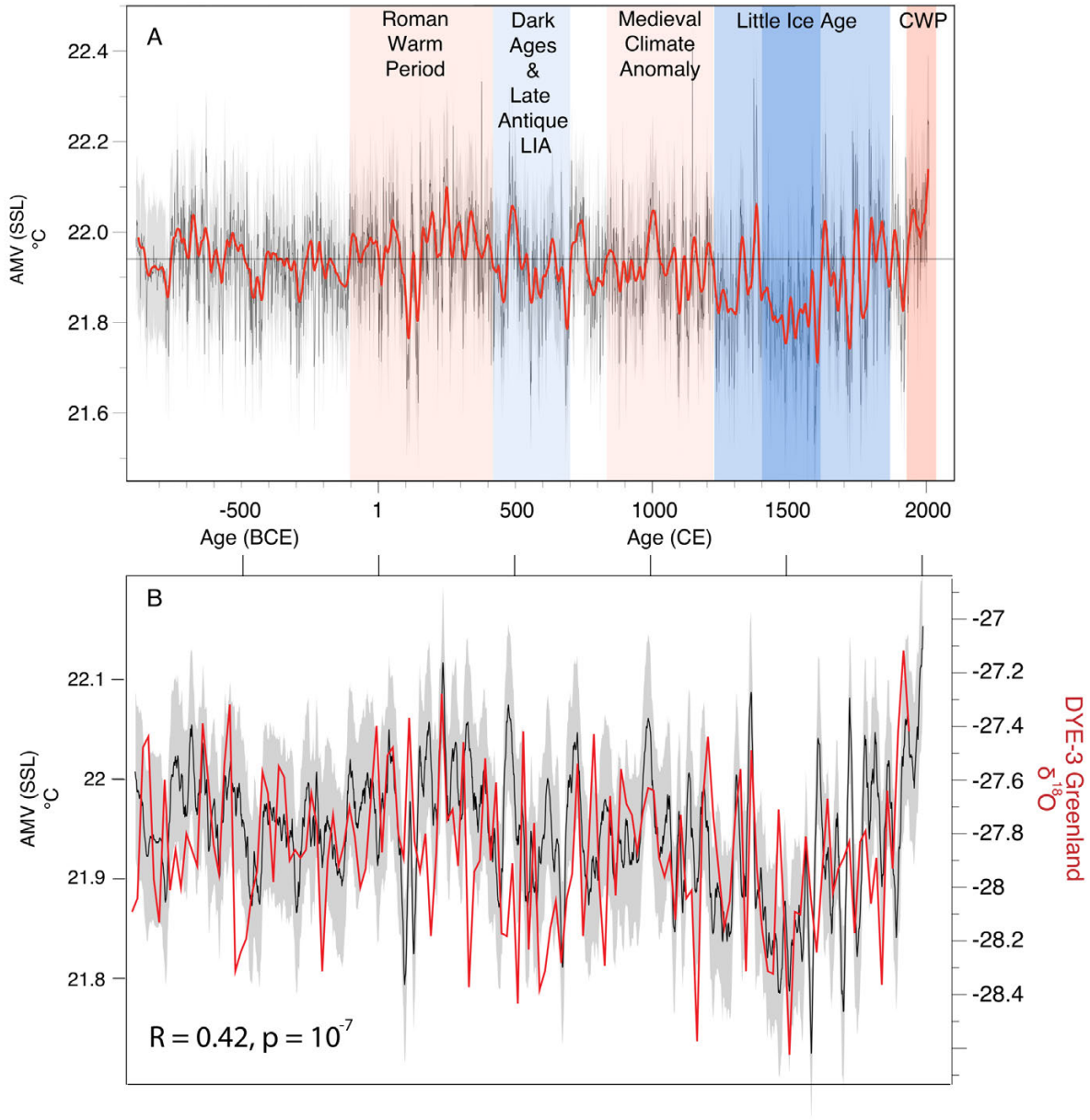

Fig 3. (A) Annual AMV changes over the past 2,900 years with a 30-y loess first- order low-pass filter (red). The gray horizontal line is the estimated average SST over the past 2,900 years (22.19°C). CWP denotes Current Warm Period. Shaded gray regions represent the 95% confidence intervals on the annual reconstructed AMVSSL, based on uncertainty estimates. (B) Comparison between DYE-3 Greenland δ18O record and the AMVSSL (modified from Lapointe et al. 2020).

The M'Clintock Ice Shelf: last gasp of the NW Laurentide Ice Sheet

Furze, Mark F.A. [1]; **Pienkowski**, Anna J. [2]; **Corlett**, Hilary [3]; **Troyer-Riel**, Robert [4]; **Thiessen**, Rabecca [5]; **Szidat**, Sönke [6]

[1] UNIS - The University Centre in Svalbard; markf@unis.no
[2] Norwegian Polar Institute & UNIS - The University Centre in Svalbard; anna.pienkowski@npolar.no
[3] MacEwan University; corletth@macewan.ca
[4] MacEwan University; troyerrielr@mymacewan.ca
[5] University of Lethbridge; thiessen.rabecca@uleth.ca
[6] Universität Bern; soenke.szidat@dcb.unibe.ch

Sediment core records, recovered by the CCGS Amundsen as part of a 2016 ArcticNet cruise in M'Clintock Channel in the central Canadian Arctic Archipelago (CAA), provide a unique sedimentary history of large-scale Early Holocene ice shelf occupation and collapse. Well-constrained by foraminiferal radiocarbon dates and taken together with detailed flow-set mapping and chronologies on adjacent Victoria and Prince of Wales islands, the record illustrates a late-stage floating ice advance of over 375 km (equating to an ice shelf area >55,000 km2) from the M'Clintock Ice Stream draining the southward retreating margin of the deglaciating northwestern sector of the Laurentide Ice Sheet (NW LIS). Ice shelf advance occurred after 10.5 cal BP followed by sequential retreat from its north maximum, some one hundred cal. years later. By 9.6 cal ka BP the ice shelf had completely collapsed and ice retreated rapidly back on to mainland Canada.

Ice rafted debris and foraminiferal assemblages from calving margin and post-ice shelf glacimarine facies in the core record confirm that the formation and subsequent demise of the M'Clintock Ice Shelf resulted in the irreparable draw-down and destabilisation of the NW LIS and permitted the commencement of marine throughflow from Amundsen Gulf and the Arctic Ocean into the central CAA and the final establishment of similar-to-modern oceanic circulation by 8.8 cal ka BP. Those same foraminiferal assemblages further implicate warm Arctic Ocean Intermediate Water of re-circulated Atlantic origin, penetrating southwards from Viscount Melville Sound, as the primary driver of ice shelf retreat and collapse.

This record adds to the growing inventory of extensive and often catastrophic deglacial ice shelves identified from the Late Pleistocene and Early Holocene of the CAA and suggests that not only were short-lived large-scale ice shelves common during deglaciation, but that they may have been ubiquitous in this complex archipelago setting. This geological record of widespread ice retreat and ice shelf instability at the end of the Last Glaciation serves as a source of vital analogues for ongoing and future human-induced high latitude climate change and can provide important constraints on modelled forecasts of Antarctic ice shelf behaviour under rising sea levels and warming ocean conditions.

An investigation of modern eastern North American Arctic lakes reveals latitudinal patterns in lake water isotope seasonality

Gorbey, Devon B [1]; **Thomas**, Elizabeth K [2]; **Raynolds**, Martha K [3]; **Miller**, Gifford H [4]

[1] University at Buffalo; devongor@buffalo.edu [2] University at Buffalo; ekthomas@buffalo.edu
[3] University of Alaska Fairbanks; mkraynolds@alaska.edu
[4] University of Colorado Boulder; gmiller@colorado.edu

Precipitation in the Arctic is projected to increase dramatically over the next century. However, uncertainties surrounding precipitation seasonality remain. Lacustrine water isotope proxies are a powerful tool for reconstructing precipitation seasonality, but due to field accessibility limitations, little is known about seasonal variations in modern lake water isotope systematics in the eastern North American Arctic. We use modern lake water isotopes (d18O, d2H) measured on samples collected across a latitudinal gradient from northern Labrador to Ellesmere Island in the eastern North American Arctic, to evaluate precipitation isotope seasonality and evaporative enrichment in lakes through the ice-free season. We divided water isotope samples from 159 lakes into five latitudinal regions and find that lake water isotope values generally fall along their local meteoric water line. The few lakes that are evaporatively enriched outside the range of meteoric water are small and non-throughflowing. Although we observe some variability within each region, we generally find a latitudinal gradient in the isotopic composition of lakes along the transect: southern lakes tend to reflect amount-weighted mean annual precipitation isotopes, whereas northern lakes tend to reflect amount-weighted summer precipitation isotopes. We investigated this intra-regional variability by evaluating four lakes near Iqaluit, Nunavut that were sampled approximately biweekly through the ice-free seasons of 1994-1996 CE (Sauer, 1997). These lakes reflect mean annual precipitation and become slightly evaporatively enriched throughout the ice-free season, but remain within the range of meteoric water isotopic variability. We created a box model for these four lakes and found that the isotopic composition of lake water is most sensitive to changes in the annual runoff to precipitation ratio (R/P). Therefore, we infer that the latitudinal gradient we observe in lake water isotope seasonality is driven by a northward proportional increase in the amount of precipitation that falls during the ice-free season as well as a poleward increase in R/P, resulting from reduced vegetation cover. Accordingly, most lakes in the eastern North American Arctic are good targets to study variations in precipitation isotopes over time because they are not strongly impacted by evaporative enrichment. However, we reaffirm that a strong understanding of lake water isotope and proxy systematics for a target lake is critical to know which season will be reconstructed by a given proxy.

Sauer, P. E. (1997). Record of climate and late quaternary paleoclimate from stable isotopes in lakes and lake sediments, eastern Canadian Arctic. 5303.

Biomarker characterization of the North Water Polynya, Baffin Bay: Implications for local sea ice and temperature proxies

Harning, David [1]; **Holman**, Brooke [2]; **Woelders**, Lineke [3]; **Jennings**, Anne [4]; **Sepúlveda**, Julio [5]

[1] University of Colorado Boulder; david.harning@colorado.edu
[2, 3, 4, 5] University of Colorado Boulder;

The North Water Polynya (NOW, Greenlandic Inuit: Pikialasorsuaq), Baffin Bay, is the largest freshwater polynya and one of the most productive regions in the Arctic. This area of thin to absent sea ice is a critical moisture source for local ice sheet sustenance, and coupled with the inflow of nutrient-rich Arctic Water, supports a diverse community of Arctic fauna and indigenous people. However, as anthropogenic warming continues, formation of the ice arches in Nares Strait that block ice flow from the Arctic Ocean are forming less reliably, jeopardizing the formation of the NOW with uncertain consequences for the local cryosphere and biosphere. Looking to the past, previous studies assume that the NOW only developed following regional deglaciation and the opening of Nares Strait. However, the limited paleoceanographic records that exist from in and around the NOW, and scarcity of diagnostic biological records for the NOW's associated high pelagic productivity, hinder this assumption. In this study, we aim to characterize the NOW environment via the analysis of surface sediment samples that encompass its modern limits. Our toolkit relies on a variety of lipid biomarkers, including algal highly-branched isoprenoids and sterols for sea ice extent and pelagic productivity, and algal alkenones and archaeal GDGTs for ocean temperature, as well as modern instrumental datasets. All highly-branched isoprenoids exhibit strong correlations with each other and show highest concentrations within the NOW, which suggests a sole spring/autumn sea ice diatom source for these biomarkers rather than a combination of sea ice and open water diatoms as seen elsewhere in the Arctic. Sterols are also highly concentrated in the NOW and exhibit an order of magnitude higher concentration here compared to sites south of the NOW, consistent with the order of magnitude higher primary productivity observed within the NOW relative to surrounding waters in spring/summer months. Finally, our temperature calibrations for alkenones and GDGTs reduce the uncertainty present in global temperature calibrations, but also identify some additional variables that may be important in controlling the distribution of these lipids here, such as salinity, nutrients, and dissolved oxygen. In conclusion, our datasets provide new insight into the utility of these lipid biomarker proxies in high-latitude settings and will help provide a refined perspective on the Holocene development of the NOW with their application in downcore reconstructions currently underway.

Human paleo-genomics and Beringian landscapes

Hoffecker, John F. [1]; **Raff**, Jennifer A. [2]; **O'Rourke**, Dennis H. [3]; **Tackney**, Justin C. [4]; **Potapova**, Olga [5]; **Elias**, Scott A. [6]; **Hlusko**, Leslea J. [7]; **Scott**, G. R. [8]

[1] INSTAAR; john.hoffecker@colorado.edu
[2] University of Kansas; jennifer.raff@ku.edu
[3] University of Kansas; orourke@ku.edu
[4] University of Kansas; justin.tackney@ku.edu
[5] The Mammoth Site; olgap@mammothsite.org
[6] INSTAAR; scottelias59@gmail.com
[7] University of California-Berkeley; lesleahlusko@gmail.com
[8] University of Nevada-Reno; grscott@unr.edu

Paleo-genomics has fundamentally altered the study of the human past, including the global dispersal of modern humans and the peopling of Eurasia, Australia, and the Western Hemisphere. This is due in large measure to methodological advances, such as high-throughput sequencing, which moved the field beyond the mtDNA and Y-DNA studies of the 1990s to whole-genome analyses, as well as successful extraction of ancient DNA (aDNA) from dated human remains throughout much of the Northern Hemisphere (i.e., where conditions permit long-term preservation of DNA).

In Northeast Asia and Beringia, aDNA analyses of human remains excavated in earlier decades have been supplemented with analyses of spectacular recent finds in Siberia and Alaska (e.g., Raghavan et al. 2014; Tackney et al. 2015; Sikora et al. 2019), where a number of ancient lineages now have been identified. Among these lineages are several that contributed significantly to the genome of the First Peoples of the Western Hemisphere and have potential to shed light on the process by which it was settled—and the role of Beringia in this process (see Figure 1).

Siberia was alternately settled by people derived from western Eurasia (beginning with the initial dispersal of modern humans >45 ka) and East Asia (i.e., from the south). Beringia, in turn, was alternately settled by people in Siberia derived from western Eurasia and mainland East Asia. It was initially occupied by a west Eurasian lineage (labelled Ancient North Siberians) before the Last Glacial Maximum (LGM), but, by the end of the LGM, both Siberia and Beringia were occupied by peoples who were primarily descended from an East Asian lineage (e.g., Sikora et al. 2019; Yang et al. 2020; Yu et al. 2020).

Both the west Eurasian and East Asian groups appear to have arrived in Beringia via the "Great Arctic Plain" (exposed East Siberian Arctic Shelf) rather than the Northeast Asian maritime zone (i.e., North Pacific coast). The former was largely exposed during later MIS 3 and supported a diverse steppe-tundra large mammal community before and during the LGM (e.g., Schirrmeister et al. 2005; Sher et al. 2005; Pitulko et al. 2017). South of the Great Arctic Plain, access to Beringia from Siberia was mostly blocked by local glaciation, including the Verkhoyansk Mountains, during the LGM (Batchelor et al. 2019).

By the end of the LGM, the ancestral First Peoples were present in Beringia (they dispersed widely in the Western Hemisphere during 15–13 ka). Analysis of aDNA from dated human

remains indicates that at least two other lineages (labelled Ancient Paleo-Siberians [APS] and Ancient Beringians [AB]) were present in Beringia by the early Holocene. All three lineages are descended from an East Asian population, although two (APS and AB) received gene flow from a west Eurasian group. The APS and AB lineages diverged ~24 ka, and the First Peoples diverged from the AB population ~20 ka (Moreno-Mayar et al. 2018a, 2018b; Flegontov et al. 2019; Sikora et al. 2019).

If there is broad agreement among the paleo-genomic models with respect to the lineages and their relationships, there is a debate about where the divergence of the APS and AB lineages took place, and where the ancestral First Peoples split from the latter. Some researchers (e.g., Sikora et al. 2019) concluded that these groups were located in Beringia during the LGM, while others (e.g., Yu et al. 2020) argued that none of these lineages occupied Beringia until after the LGM.

The debate is central to the larger question of the role of Beringia in the peopling of the Western Hemisphere. Currently, there are no human remains in Beringia dating to the LGM (27–15 ka) and although there is some evidence for humans in Beringia during this interval (e.g., Vachula et al. 2020), it is widely regarded as problematic.

Here, we address the question of Beringia's role in the peopling of the Western Hemisphere by mapping lineages identified in the paleo-genomic models for the post-LGM and early Holocene (15–9 ka) on an LGM landscape (see Figure 2). It is a heuristic exercise, designed to illustrate the spatial or geographic aspect of the problem of where the First Peoples and closely related lineages (especially APS and AB) were located during the LGM and, more generally, to help integrate the paleo-genomics with the environmental setting.

The map reflects the effects of lower sea level on coastlines (glaciation is not shown). Northern Japan is joined to Sakhalin and the Russian Far East ("Paleo-Sakhalin-Hokkaido-Peninsula"), while the exposed East Siberian Arctic Shelf represented an immense plain ("Great Arctic Plain") adjoining the modern arctic coast of Siberia mentioned earlier. During the LGM, the southern Bering Land Bridge (BLB) expanded significantly in response to sea levels 60–70 meters below their late MIS 3 levels (Lambeck et al. 2002).

The post-LGM location of the Ancient First Peoples shown in Figure 2 is not based on dated human remains, but rather is deduced from the glacial chronology and dated remains in other parts of the Western Hemisphere. The lack of an available interior migration route between Beringia and mid-latitude North America until after 13 ka (e.g., Heintzman et al. 2016) indicates that this population was located on the unglaciated southern coast of the BLB no later than 15 ka (in order to account for the initial dispersal via the Pacific coast of First Peoples in North and South America during 15–13 ka). The AB lineage is represented by human remains from Trail Creek Caves, Seward Peninsula (~9.0 ka) and the Tanana Valley (USR1 [~11.4 ka]) (Moreno-Mayar 2018a, 2018b).

The APS lineage is represented by specimen (Kolyma1) from the Kolyma Basin (~9.8 ka). A closely related individual (UKY [~13.9 ka]) is reported from the Lake Baikal area (Yu et al. 2020). It is unclear if UKY represents APS people who moved from the Great Arctic Plain into

southern Siberia after the LGM or reflects an earlier APS presence in southern Siberia that preceded their movement into Beringia. It also is unclear if the Ancient North Eurasian (ANE) lineage, which is represented by human remains in southern Siberia dating to the LGM (~24 ka [MA1] & ~17 ka [AG3]), co-existed with APS after the LGM (Raghavan et al. 2014; Moreno-Mayar 2018a, 2018b; Sikora et al. 2019).

We offer the following observations with reference to Figure 2:

First, the map underscores the relationship between East Asians and the lineages in Beringia ~15–9 ka, including ancestral Native Americans. Although the ANE population, associated with mid/late Upper Paleolithic industries in southern Siberia, contributed to the genomes of the APS and AB groups—and indirectly to the Native American genome—the latter three are descended primarily from the direct ancestors of the modern Han population (Sikora et al. 2019; Yang et al. 2020; Yu et al. 2020). The latter also are the parent lineage for other modern Siberian peoples (e.g., Evenki) (e.g., Flegontov et al. 2019).

At the same time, Figure 2 illustrates the arctic route followed by the people who settled in Beringia by the end of the LGM. Regardless of when these peoples first occupied Beringia—and where they came from—they probably arrived via the "Great Arctic Plain" (i.e., exposed East Siberian Arctic Shelf). An arctic route is supported by the lack of a genetic connection between the people who occupied the Northeast Asian maritime region (Early Jomon) and the three lineages (e.g., Gakuhari et al. 2020).

During the LGM, especially after 23 ka (when a brief warm interval [GI 2] was followed by somewhat milder temperatures [22–15 ka]), the Great Arctic Plain probably offered a refugium for human groups (see above). An additional clue may be provided by the EDAR V370A allele, which underwent strong positive selection during the LGM in a population ancestral to both living Asians and Native Americans (e.g., APS). Hlusko et al. (2018) suggested that EDAR V370A represented a high-latitude adaptation to low UV radiation, which is consistent with occupation of the Great Arctic Plain during the LGM (and also with the early Holocene location of APS).

Figure 2 also illustrates the principal weakness of the hypothesis that the ANE, APS, AB, and Ancient First Peoples all were located in southern Siberia during the later LGM. How likely is it that all four populations—one of which was genetically isolated from the others—occupied the same region at this time? The problem is compounded by archaeological evidence for a significant contraction of the human population in the region during the LGM (e.g., Buvit et al. 2015).

As Figure 2 shows, the post-LGM geographic distribution of lineages in Beringia corresponds to three major regions: Great Arctic Plain (APS), eastern Beringia (AB), and the southern BLB (Ancient First Peoples) (e.g., Guthrie 2001; Crocker and Elias 2008; Rae et al. 2020). The pattern suggests that environmental variation played a role in the differentiation of the three populations.

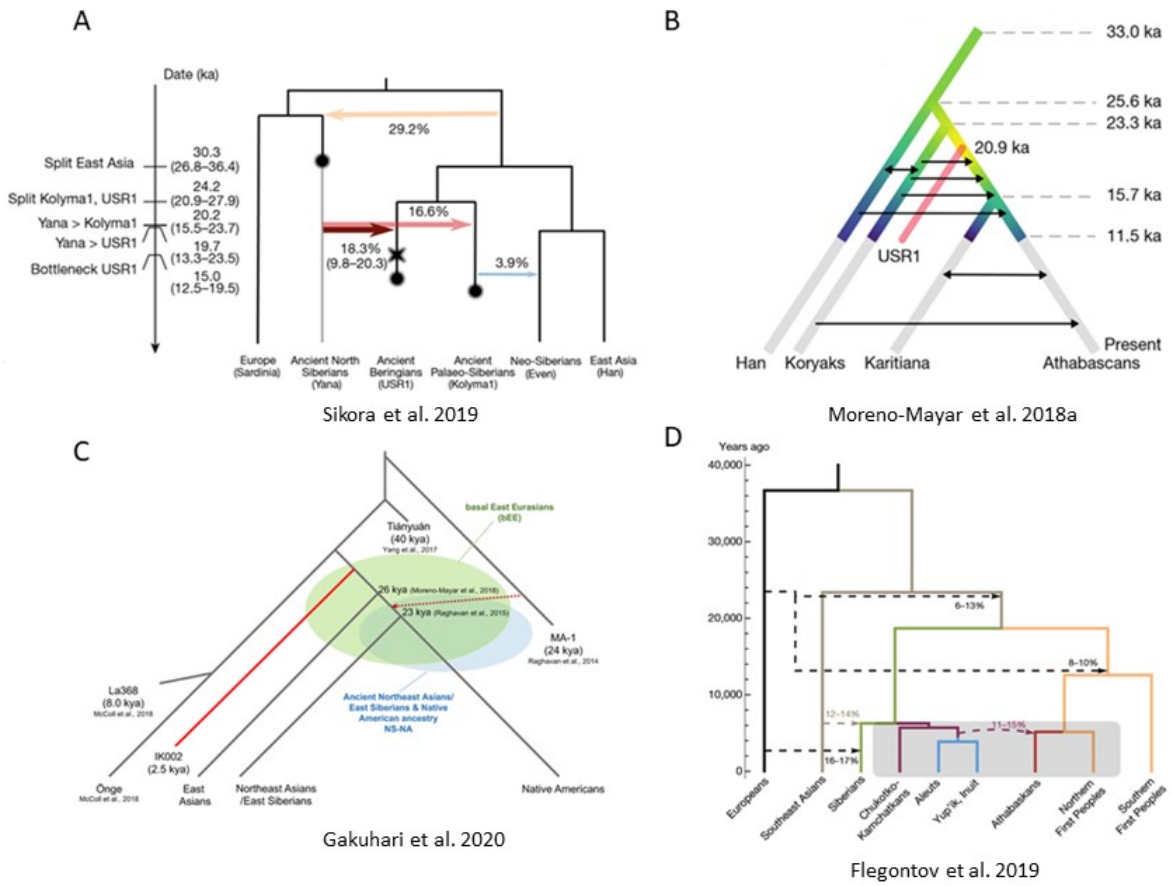

Fig 1. Human paleo-genomic models for Northeast Asia and Beringia for the last 40,000 years, based in part on the analysis of aDNA from dated human remains.

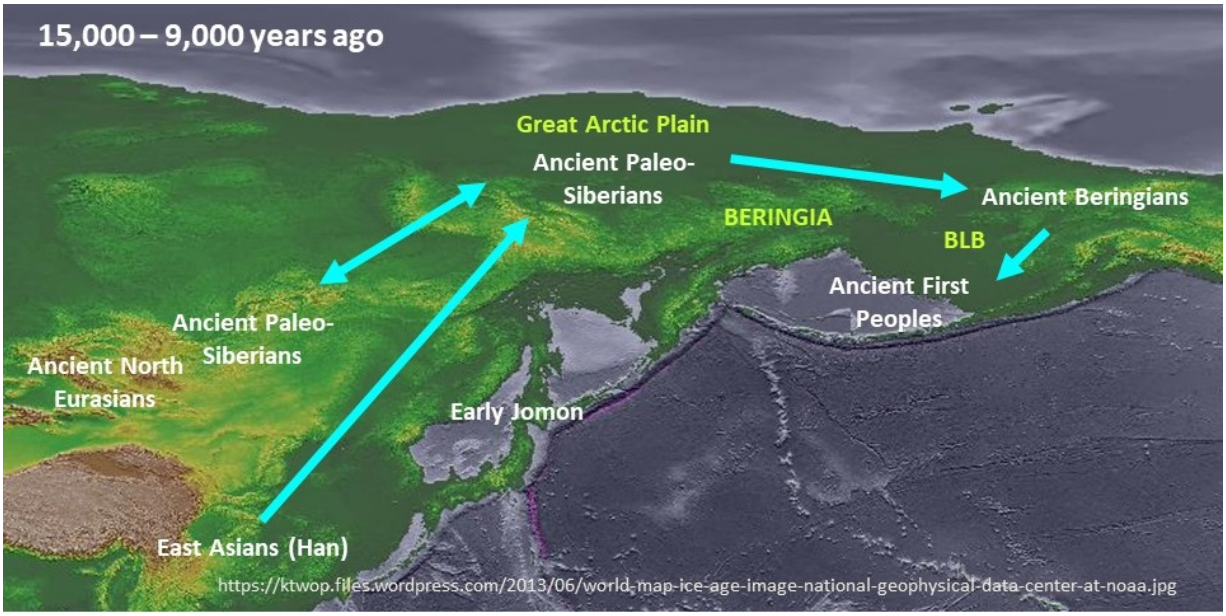

Fig 2. Geographic locations of lineages after the LGM (15–9 kcal BP) imposed on a map of LGM coastlines. The three lineages in Beringia during this period are descended primarily from a mainland East Asian population (blue arrows). The western boundary of Beringia is defined here as the Verkhoyansk Mountains.

Quantifying Holocene plant contributions to sedimentary leaf waxes in an Arctic lake setting

Hollister, Kayla V [1]; **Thomas**, Elizabeth K [2]; **Raberg**, Jonathan [3]; **Raynolds**, Martha K [4]; **Gorbey**, Devon B [5]; **Crump**, Sarah E [6]; **Miller**, Gifford H [7]; **Sepúlveda**, Julio [8]

[1] SUNY at Buffalo; kvhollis@buffalo.edu
[2] SUNY at Buffalo; ekthomas@buffalo.edu
[3] University of Colorado Boulder; jonathan.raberg@colorado.edu
[4] University of Alaska Fairbanks; mkraynolds@alaska.edu
[5] SUNY at Buffalo; devongor@buffalo.edu
[6] University of California Santa Cruz; secrump@ucsc.edu
[7] University of Colorado Boulder; gmiller@colorado.edu
[8] University of Colorado Boulder; jsepulveda@colorado.edu

The Arctic is the fastest-warming region on Earth, causing vegetation to expand into areas previously dominated by snow and ice, exacerbating warming further. The need for accurate paleoclimate reconstructions in the Arctic is thus crucial, and aquatic and terrestrial plant leaf wax hydrogen isotope values are valuable proxies for past climate. However, it can be difficult to distinguish aquatic from terrestrial waxes in lake sediments, which can lead to uncertainty surrounding interpretations of past climate. We quantify the leaf wax n-alkanoic acid chain length distributions (C20, C22, C24, …, C32) of n = 8 modern lake sediments and n = 30 species of modern plants from Lake Qaupat (QPT) on southern Baffin Island to track leaf wax production and deposition in a modern Arctic lake setting. We assess variability among modern plant chain length distributions using principal component analysis (PCA), and passively plot the sediments along these axes. We find that submerged aquatic plants, including four mosses and one graminoid, and lake sediments plot closely on the PCA biplot, indicating submerged aquatic plants contribute large portions of waxes to modern lake sediments. We adapt the Stable Isotope Mixing Models in R (simmr) package to use relative plant wax distributions as variables, and input distributions for the most abundant modern and Holocene plants, determined using vegetation mapping and sedimentary ancient DNA, respectively. We apply the model to QPT's downcore leaf wax distribution record to estimate plant contributions to lake sediment waxes during the mid- to late-Holocene. Model results indicate that Arctic shrub Salix arctica is the primary wax source (0.73 ± 0.06) to lake sediments until ~1.3 ka, after which submerged moss becomes the primary wax source (0.57 ± 0.23) to lake sediments until present. However, d2H analysis on modern Salix spp. (n = 3 S. arctica and 1 S. reticulata), submerged aquatic plant samples (n = 3 Eleocharis acicularis), and lake surface sediments (n = 4) all indicate it is unlikely that Salix spp. is the primary wax source to sedimentary mid-chain waxes: the most depleted C22 d2H value measured on Salix spp. samples is -200‰, while the most enriched C22 d2H value measured on modern lake sediments is -240‰. Furthermore, lake sedimentary C22 d2H does not exceed -230‰ throughout the entire QPT leaf wax record. E. acicularis samples collected from the edges of the main QPT basin have C22 d2H values between -231 and -234‰, suggesting that submerged aquatic plants are a more likely source of mid-chain waxes in QPT lake sediments.

For sedimentary long-chain waxes in QPT, on the other hand, it remains unclear if they are primarily sourced from terrestrial plants, or reflect an integrated aquatic and terrestrial signal, and future studies should focus on quantifying wax transport to lake sediments.

Arctic seabed: New detailed mappings of compositions and physical properties

Jenkins, Chris [1]

[1] INSTAAR CU;

The sediment textures, rock areas, carbon and carbonate contents, seafloor colors, and porosities and shear strengths are described in new mappings now released through INSTAAR CSDMS (see fig). They will be useful for research in diverse fields: marine ecology, stratigraphy, biogeochemistry, geoacoustics.

They were constructed using dbSEABED methods (tinyurl.com/dbSEABED) to over 2,300 datasets. The foundational data were obtained from multitudes of individual published papers and unpublished reports, published maps, and large data structures such as PANGAEA (pangaea.de, Germany) and the Expedition Database (ed.gdr.nrcan.gc.ca, Canada). Data from direct sampling as well as visual and probe observations are held, but not bathymetry or backscatter results (exception: rock areas).

From the foundational data, application software extracts useable data on defined parameters and their close synonyms (e.g., mean, median and graphic mean grainsizes), having regard to target uncertainty bounds (+-10% 1-sigma).

The first results are gridded at 0.1 degree, which is appropriate given that data densities vary greatly, but are thin over wide areas (see figure). The grids are presented in the equal-area IBCAO polar stereographic projection. The gridding method for the present data release was a '2.5D' (grid x,y, water depth z) Inverse Distance Weighted method, with data selection on a graph that is restricted to marine inundated areas. This had many advantages in this setting: is a transparent (not black-box) method; is faithful to the depth-related ecological zonations; deals correctly with physiographic features (such as seamounts and canyons); computes results locally (not from a map-wide model); and is able to provide spatially explicit uncertainty statistics.

dbSEABED is a globally-extensive data resource but in the Arctic context a set of special technical problems with databasing had to be solved including how to treat: allochthonous IRD (e.g., dropstones); very large grain sizes (such as IRD boulders); ice and permafrost materials; layerings in cores some of which will be disturbed (turbated); challenges for interpolation inside the Canadian Archipelago.

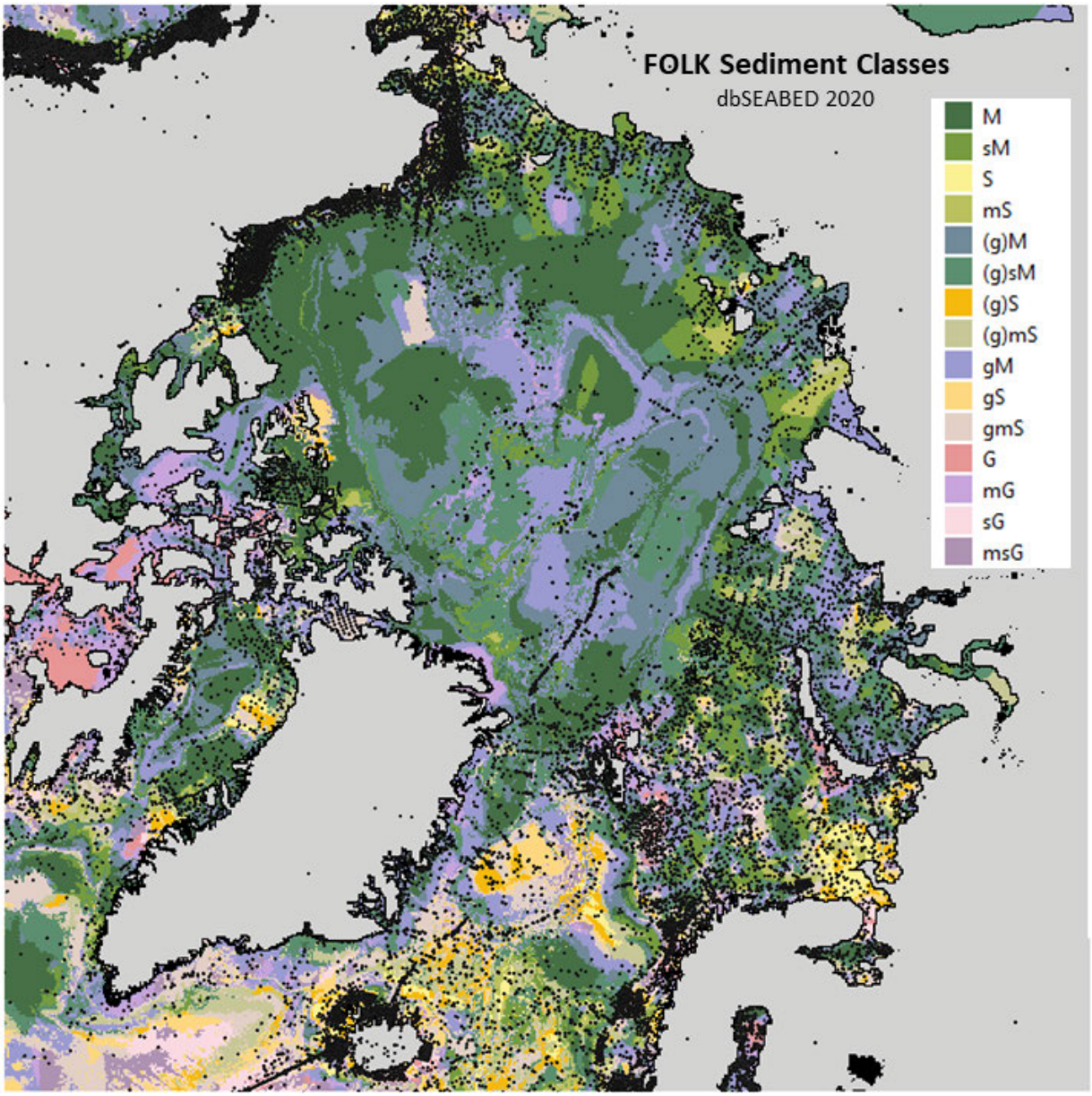

Fig 1. FOLK sediment classes from dbSEABED 2020.

Does Northeastern Cumberland Peninsula preserve a dateable pre-MIS2 moraine record – or NOT?

Kaplan, Michael R [1]; **Miller**, Gifford H [2]; **Briner**, Jason P [3]; **Young**, Nicolás E [4]

[1] LDEO; mkaplan@ldeo.columbia.edu
[2] University of Colorado; gmiller@colorado.edu
[3] University at Buffalo; jbriner@buffalo.edu
[4] LDEO; nicolasy@ldeo.columbia.edu

Easternmost Cumberland Peninsula, especially the northeastern corner, is beyond or around the 0 m isobase, which is a distinguishing attribute given its location on southern Baffin Island. Hence, at least during the last glaciation, thick Laurentide ice did not cover the easternmost peninsula (Kaplan and Miller, 2003). Three other aspects are noteworthy of the easternmost Cumberland Peninsula's glacier history, which likely relate to the area being beyond the 0 m isobase. First, the area contains, as expected, weathered upland landscapes long studied by researchers, which of course included John Andrews; this was a typical region of focus for the minimum ice sheet model, but now is revealing insights into past ice sheet dynamics and paleoenvironments. Near mouths of fjords, deltas exist with shells that provide infinite 14-C ages. Second, the southeast corner of Cumberland Peninsula contains well-developed glacial cirques partially submerged below sea level that contain no ice at present, which John also studied. The cirques reveal that the southeast corner of the peninsula exhibited long-term or persistent alpine glaciation when sea level is below present. Third, and most important perhaps, a handful of 10-Be and 26-Al ages specifically on moraine boulders have been obtained that apparently date to before MIS2 (Steig et al., 1998; Miller et al. 2002).

A hypothesis is that exposure ages on moraine boulders around northeast Cumberland Peninsula that pre-date the earliest Holocene are not accurate, contain inheritance, and that ice overran the entire area during the LGM. And, ice overran the deltas that contain infinite 14C ages on shells. On the other hand, at two different sites, existing cosmogenic ages (albeit only a few) could be considered relatively coherent, and fall between ~50 and 40 ka, or they are MIS 2 in age. Moreover, at both sites, the pre-LGM dated moraines are outside the MIS2 and 1 dated moraines and no morphostratigraphy is inconsistent. Regardless of the answer to the hypothesis, easternmost Cumberland Peninsula has potential for pre-MIS2 glacier moraine records and can continue to be a site of future investigation.

Steig, E. J., Wolfe, A. P., and Miller, G. H., 1998, Wisconsinan refugia and the glacial history of eastern Baffin Island, Arctic Canada: Coupled evidence from cosmogenic isotopes and lake sediments: Geology, v. 26, p. 835–838.

Miller, G. H., Wolfe, A. W., Steig, E. J., Kaplan, M. R., and Briner, J. P., 2002, The Goldilocks Dilemma: Big Ice, Little Ice, or "Just-Right" Ice in the Eastern Canadian Arctic: Quaternary Science Reviews, v. 21, p. 33-48.

Kaplan, M. R. and Miller, G. H., 2003, Early Holocene delevelling and deglaciation of the Cumberland Sound region, Baffin Island, Arctic Canada: Geological Society of America Bulletin, v. 115, p. 445–462.

Foraminiferal stratigraphy and lithofacies reveal the timing and environments of deglaciation and onset of Arctic/Atlantic throughflow in the Arctic Island Channels

Kelleher, Robert V [1]; **Jennings**, Anne [2]; **Brooks**, Nicole [3]; **Feng**, Cici [4]; **Andrews**, John T [5]; **Brookins**, Sarah [6]; **Woelders**, Lineke [7]; , et al [8]

[1] INSTAAR; roke6465@colorado.edu
[2] INSTAAR; Anne.Jennings@colorado.edu
[3] INSTAAR; nicoleksbrooks@gmail.com
[4] CU Boulder; cicifst@gmail.com
[5] INSTAAR; andrewsj@colorado.edu
[6] CU Boulder; Sarah.Brookins@Colorado.edu
[7] CU Boulder; Lineke.Woelders@Colorado.edu
[8];

The Arctic Island Channels (AIC) usher low-salinity, nutrient-rich Arctic surface water (ASW) and sea ice into the North Atlantic with consequences for the Atlantic Meridional Overturning Circulation (AMOC). The largest of these channels are Nares Strait and Parry Channel (Figure 1). The channels were blocked to Arctic/Atlantic throughflow by confluent ice sheets until the early Holocene. However, the timing of opening of the channels is poorly constrained as is the ensuing development of the North Water polynya that occupies northern Baffin Bay today, with productivity fueled by nutrient rich ASW. Sediment cores from Lancaster Sound, at the southeastern end of Parry Channel, capture sediment sequences that record retreat of confluent Innuitian and Laurentide ice-sheets through to modern marine conditions. We present data from three sites: 2008029-59CC (composite trigger core and piston core), inside Lancaster Sound; 2008029-49CC (composite box core, trigger core and piston core) at the mouth of Lancaster Sound and 2013029-64PC off Buchan Trough on the northern Baffin Island slope (Figure 1). Analyses of lithofacies, including counts of >2mm clasts (ice-rafted detritus (IRD)), biogenic silica, sediment mineralogy and foraminiferal assemblage data from these cores provide insight into the changing environmental conditions during deglaciation and establishment of the Arctic/Atlantic throughflows. Radiocarbon dates on foraminifera and marine algae macrofossils constrain the timing of events. A pair of 14C dates on benthic and planktic foraminifers from the same sample in 64PC (875 m water depth) provides a local marine reservoir correction $\Delta R = 600$ years to calibrate early Holocene dates on calcareous benthic organisms in the deep shelf trough sites of our cores (>580 m). Three additional benthic/planktic paired dates from the Lancaster Sound cores have been submitted to further define the early Holocene marine reservoir age.

In Lancaster Sound, glaciomarine conditions as defined by pebbly mud lithofacies overlying till begin by 11.1 cal ka BP and end at about 10.5 cal ka BP based on lack of IRD. The overlying mud unit with pyritized burrows and highly abundant calcareous benthic and planktic foraminifers and increased biogenic silica suggests that Lancaster Sound may have been open to the Arctic Ocean by 10.5 cal ka BP. An agglutinated faunal zone with >80% agglutinated foraminifers coincides with a change to increased bioturbation and lower

sedimentation rates. This zone begins soon after 8.7 cal ka BP, similar in timing to the opening of Nares Strait to ASW throughflow.

There are three foraminiferal zones defined by cluster analysis in each of the 3 cores. The zones are similar in faunal characteristics and timing. The deepest zone occurs in the detrital carbonate rich pebbly mud units overlying the till. It comprises low abundance, benthic foraminiferal faunas dominated by glaciomarine species and *Stainforthia feylingi*, reflecting glacial meltwater input and sea-ice cover while glacier ice was grounded in Lancaster Sound. Faunal zone 2 is characterized by high abundance of calcareous benthic fauna reflecting marine productivity with dominant *Islandiella norcrossi* and increasing planktic foram abundance. The opening of Parry Channel occurs in this zone coinciding with the end of IRD-rich sediment and deposition of bioturbated mud. It is marked by an abrupt increase in planktic foraminifera c. 10.5 cal ka BP in all three cores. Faunal zone 2 marks establishment of a regional marine optimum with reduced summer sea ice and increased flux of nutrient rich Arctic Surface Water fueling marine productivity. Faunal zone 3 is defined by >80% agglutinated foraminifers and greatly decreased foraminiferal abundance. It coincides with increased bioturbation, increased biogenic silica and presumed lower sedimentation rates. This zone begins soon after 8.7 cal ka BP based on 14C dates on seaweed macrofossils in all 3 cores and is similar in timing to the opening of Nares Strait to ASW throughflow. The low abundance of foraminifera likely is due to carbonate dissolution related to undersaturation of calcite by increased inflow of Arctic Surface Water, diminished input of detrital carbonate and increased biogenic carbon flux as reflected by bioturbation and the high diatom abundance.

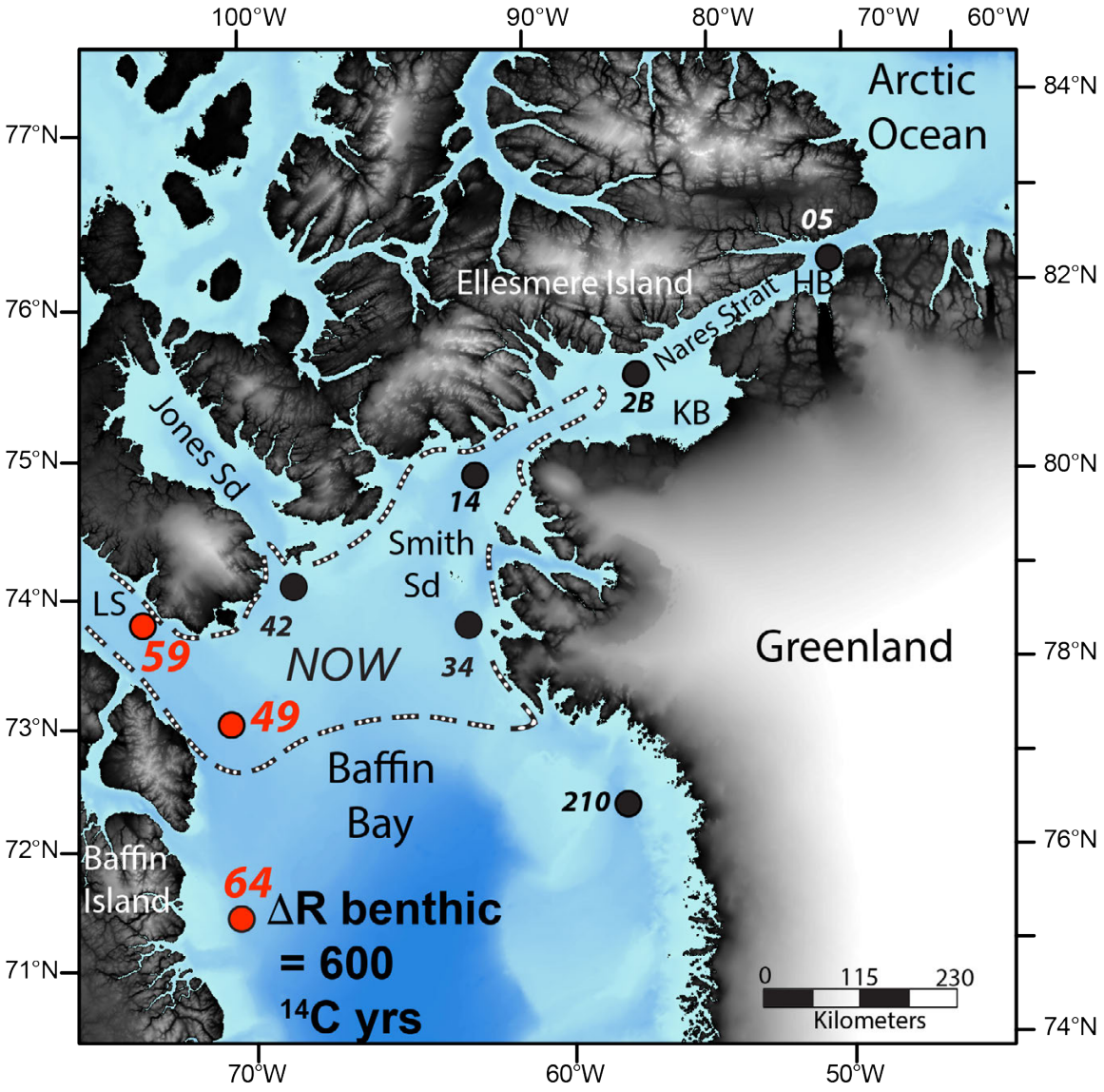

Fig 1. Map of study area in northern Baffin Bay showing locations of cores in this study (red dots) 2008029-59, 2008029-49 and 2013029-64 taken by the Geological Survey of Canada. The North Water Polyna (NOW) typical extent in June is shown by hatched line. LS = Lancaster Sound, KB = Kane Basin, HB = Hall Basin. Black dots are other cores in this project. This research is funded by National Science Foundation OPP-1804504. We acknowledge the contributions by Robbie Bennett and Kimberley Jenner of the GSC and Benoit Lecavalier of Memorial University.

Quantifying layers of refrozen melt in ice cores using bubble density

Kindstedt, Ingalise [1]; **Winski**, Dominic [2]; **Kreutz**, Karl [3]; **Osterberg**, Erich [4]; **Campbell**, Seth [5]; **Wake**, Cameron [6]; **Schild**, Kristin [7]

[1] University of Maine; ingalise.kindstedt@maine.edu
[2] University of Maine; dominic.winski@maine.edu
[3] University of Maine; karl.kreutz@maine.edu
[4] Dartmouth College; erich.c.osterberg@dartmouth.edu
[5] University of Maine; scampb64@maine.edu
[6] University of New Hampshire; Cameron.Wake@unh.edu
[7] University of Maine; kristin.schild@maine.edu

Ice cores provide some of the highest resolution records available of past climate, in particular past temperature, which can be derived through stable isotope concentrations or through melt layers. Melt layers present an especially robust way to reconstruct past temperatures due to the direct physical link between surface temperatures and their production. Despite the robustness of ice core melt layers as a quantitative summer temperature proxy, there are only two melt records contained in the PAGES2K database, and a handful of others that have been published, mostly restricted to the eastern Arctic. The one published melt record used for paleoclimatic interpretation in the North Pacific region (Winski et al. 2018) is from Mt. Hunter (Alaska Range) and spans the last 400 years. The Hunter core extends throughout the Holocene (basal 14C date of >8 kyr), with an annual layer chronology to 800 CE. Preliminary observations suggest intense melt production during the Medieval Climate Anomaly (MCA); however, melt features at this depth have not been quantified because of uncertainties related to vertical thinning, possible flow-related effects, and challenges in identifying melt layers after they have undergone a high degree of strain. We use bubble density to quantitatively distinguish refrozen melt from unaltered ice at depth in the Hunter core. Bubble density is lower in melt layers than in the surrounding ice; however, numerically quantifying bubble density has not been applied as a melt identification method.

To quantify bubble density in the Hunter core, we cut twenty-nine thin sections lengthwise (3-7 cm each) ranging from 100 to 200 m in depth (approximately 1950 back to 350 CE): 8 for control segments (unaltered ice), 3 for segments containing melt layers identified using established techniques, and 18 for segments containing ambiguous features. Thin sections were photographed with and without crossed polarized lenses, at varying brightness levels and polarizer angles. Bubbles were digitized as black ellipses in the two best polarized photos, and in the unpolarized photo taken at highest bulb brightness, resulting in three bubble maps for each thin section. The average pixel brightness within each column of pixels in each map was calculated as a measure of the bubble fraction of that pixel column. Pixel columns were then converted to depth in core using sample top and bottom depths. Lastly, the bubble fraction data from both polarized maps were combined to mitigate any error arising from differences in bubble contrast among grains due to birefringence, resulting in two final bubble fraction

datasets for each sample. Melt layers identified using established techniques, as well as some ambiguous melt features do appear in the bubble fraction data; however, their boundaries are poorly constrained, so calculating the amount of melt contained in these layers is not yet possible. Results validate established visual identification techniques with numerical quantification of bubble density (Fig. 1). Additionally, results are consistent with the existence of melt layers at depth (including during the MCA), suggesting that modern warming is not outside of the range of expected variability for this region. Further work to constrain the boundaries of melt layers at depth is necessary to derive temperatures from this preliminary melt record, and we will discuss our ideas to address this issue. However, this study is an important first step in filling a marked gap in the spatial distribution of available ice core melt records.

Winski, D., Osterberg, E., Kreutz, K., Wake, C., Ferris, D., Campbell, S., Baum, Bailey, A., Birkel, S., Introne, D., Handley, M., 2018, A 400-Year Ice Core Melt Layer Record of Summertime Warming in the Alaska Range: Journal of Geophysical Research, v. 123, p. 3594-3611.

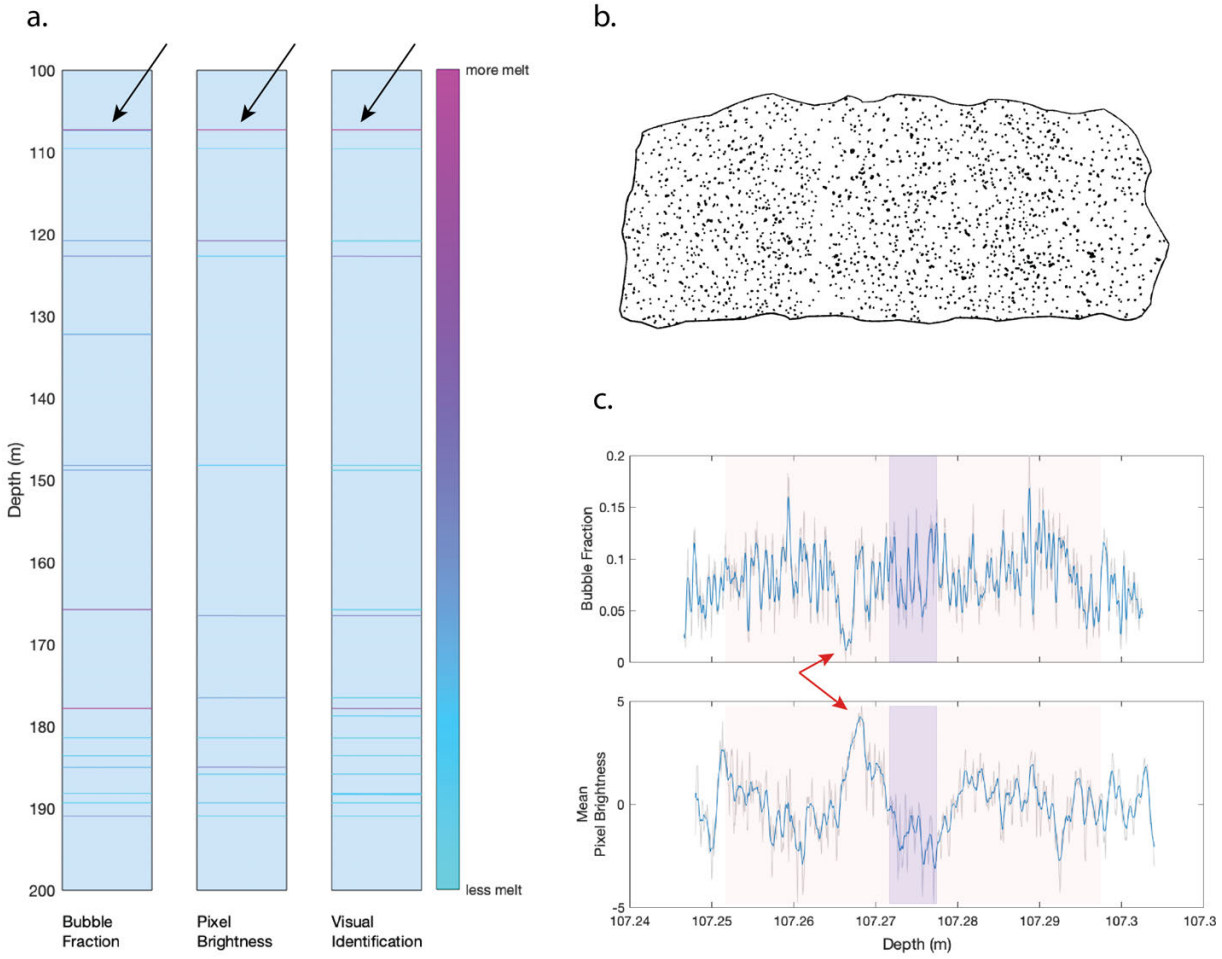

Fig 1. Relative magnitude of melt layers at 100-200 m depth from three analytical techniques (a), digitized bubble map of thin section 115a (b), and bubble fraction and detrended mean pixel brightness along thin section 115a (c). Melt layers in panel (a) are quantified based on bubble fraction, pixel brightness, and visual identification in full core photos. The location of thin section 115a (shown in panels (b) and (c)) is indicated by black arrows on core diagrams in panel (a). Red arrows indicate melt layer position identified in thin sections. Transparent Purple bars indicate depth of optically identified melt layer in full core photographs. Transparent red shading indicates uncertainty in melt layer depth in thin section arising from error introduced during thin section production. Melt layers identified in thin section are offset, but within error, from those identified in full core photographs.

Northern knowledge for resilience, environmental sustainability and adaptation in coastal communities (NORSEACC)

King, Leslie A. [1]; **Ogilvie**, Astrid E.J. [2]; **Lepore**, Walter [3]

[1] Royal Roads University, Canada; leslie.king@royalroads.ca
[2] INSTAAR, CU-Boulder and Stefansson Arctic Institute, Akureyri, Iceland; astrid.ogilvie@colorado.edu
[3] Royal Roads University; walter.lepore@royalroads.ca

NORSEACC is an interdisciplinary, international research project that investigates the role of knowledge (local, Indigenous/traditional, scientific) and governance in promoting resilience and adaptation to rapid environmental and social change in northern coastal communities. The project focuses on in-depth case studies of northern communities in their regional context, in Arctic and sub-Arctic locations in Canada, Iceland, Norway and Orkney, Scotland. Research partners in these countries are working with Indigenous and non-Indigenous coastal peoples to identify and communicate promising practices to respond to rapid environmental and social change. The NORSEACC project is documenting the ways in which Arctic processes and changes create significant impacts also beyond the Arctic, including northern coastal communities in lower latitudes and societies globally. NORSEACC is thus set in the context of global and Arctic change. The overarching goal of NORSEACC is to increase knowledge concerning the consequences of climatic, social, economic, and other related changes and implications for governance of northern coastal societies. A further research goal is to understand present and potential future linkages between climate processes and social adaptations in coupled social-ecological systems.

The primary research question is: How can governance systems and strategies be designed and implemented to incorporate local, Indigenous/traditional and scientific knowledge in order to promote resilience in the face of rapid social and ecological change in northern coastal communities? Further questions include: i) What past environmental, social and economic changes have northern coastal communities experienced? ii) How have they adapted to these changes? iii) How is knowledge (local, Indigenous/traditional, scientific) both present and past, incorporated into governance systems and policy? iv) How does knowledge concerning past change inform and influence (if not determine) present and future strategies for adaptation and sustainability? v) In northern coastal communities, what factors, including institutional and governance factors, influence resilience and successful adaptation to rapid environmental and social changes?

To answer these questions we are drawing on social ecological systems (SES) theoretical perspectives that focus on drivers of, and responses to, changes in such systems (Berkes et al., 2003; Ostrom, 2009; Moore et al., 2014). NORSEACC also makes use of the concepts and methods of panarchy to explore transformations in human-ecological systems. Panarchy provides a theoretical framework for understanding sustainability that integrates SES with

economic, ecological and social aspects at various time scales (Gunderson and Holling, 2002). Thus our theoretical framework links and integrates perspectives on knowledge, governance, resilience, adaptation, and sustainability through an historical as well as a future-oriented lens. NORSEACC is designed to address a specific knowledge gap: a paucity of assessments regarding the extent to which co-management governance innovations incorporate different forms of knowledge to promote community capacity, resilience, and sustainability. This will be achieved by addressing interdependent dynamics of those systems in a comprehensive way and then identifying the relevant knowledge systems (King, 2004; Murray and King, 2012; Cruikshank, 2005) that form the basis for governance.

NORSEACC uses a case-study methodology, encompassing both qualitative and quantitative approaches. The project case studies include information from inter alia, climate records, socio-economic data, environmental and social histories of settlement encompassing human eco-dynamics, major ecological and social events and trends, evidence of adaptations or failure to adapt to past change, local and traditional ecological knowledge, perceptions of residents and policy-makers, governance institutions at local through international levels and assessments of best potential practices for capacity building for sustainability. Primary data are collected through interviews and focus groups with local residents and decision-makers in the areas of sustainability, disaster management, planning, environment, and economic development. Collected data are used to illustrate the changes and responses experienced by case-study communities over time, and to identify elements that either promote or discourage sustainability.

Preliminary findings indicate that the success of adaptation initiatives depends in large part on alignment with community values and beliefs as well as incorporating those values and knowledge systems into governance at local and regional levels. Examples include, Haida Gwaii, Canada where the Haida are particularly notable for reinforcing and incorporating ancient laws and values into current responses to climate and biodiversity challenges. In the Orkney Islands, northern Scotland, recognition of past knowledge has led to innovative and unique climate solutions. Iceland has a unique environment dominated by ice (glaciers and, especially in the past, sea ice) and fire (volcanoes) and is renowned for its literary traditions, in particular the magnificent Icelandic sagas. The research investigates the influence of this physical and social history on current environmental practices and policies.

NORSEACC is filling a knowledge gap by identifying best potential practices for adaptation to climate change and other rapid changes in northern coastal communities. The focus on knowledge for governance is innovative, and the in-depth analysis of community responses is contributing to a deeper understanding of social-ecological systems under stress. In particular, the project is integrating a number of different community dynamics and factors that will provide a comprehensive view of past and present change and effective responses. NORSEACC is engaging communities in reflection and discovery concerning strategies that promote sustainability, resilience and successful adaptation to rapid social-ecological changes. By understanding environmental causes and impacts of change, communities will be better

prepared to address those changes in ways that lead to environmental and social sustainability. Environmental outcomes may include improved infrastructure sustainability and community planning, enhanced disaster response capacity, improved forecasting of anomalous weather events, and new strategies for adaptation and mitigation of climate-change impacts. Innovative policies will be enhanced through collaborative processes to improve decision-making and socio-ecological governance. Policy and decision makers will interact, share successful and unsuccessful strategies, and learn about potential governance and livelihood opportunities. Such social learning will enhance the capacity to respond to present and future changes and challenges.

Berkes, F., Colding, J. and Folke, C. (eds.), 2003, Navigating Social-Ecological Systems: Building Resilience for Complexity and Change, Cambridge, UK, Cambridge University Press.

Cruikshank, J., 2005, Do Glaciers Listen? Local Knowledge, Colonial Encounters and Social Imagination, Vancouver: UBC Press.

Gunderson, L. H. and Holling, C.S., 2002, Panarchy: understanding transformations in human and natural systems, Washington DC, Island Press.

King, L., 2004, Conflicting Knowledge Systems in the management of Fish and Forests in the Pacific Northwest: International Environmental Agreements: Politics, Law, and Economics, 4, 161-177.

Moore, M.L., Tjornbo, O., Enfors, E., Knapp, C., Hodbod, J., Baggio, J.A., Norström, A., Olsson, P. and Biggs, D., 2014, Studying the complexity of change: Toward an analytical framework for understanding deliberate social-ecological transformations: Ecology and Society, 19(4): 54. http://dx.doi.org/10.5751/ES-06966-190454

Murray, G. and King, L., 2012, First Nation Values and Protected Area Governance.Tla-o-qui-aht Tribal Parks and Pacific Rim National Park Reserve: Human Ecology, 40(3), 385-395.

Ostrom, E., 2009, A General Framework for Analyzing Sustainability of Social-Ecological Systems: Science, 325(5939), 419-422.

Fig 1. Sea Lion Town Haida Gwaii

Fig 2. Orkneyinga Saga Trail, Rousay, Orkney

Fig 3. Clam Garden and students

Little Ice Age triggered by intrusion of Atlantic waters into the Nordic Seas

Lapointe, Francois [1]; **Bradley**, Raymond S [2]; **Retelle**, Michael [3]

[1] University of Massachusetts-Amherst; flapointe@umass.edu
[2] University of Massachusetts-Amherst;
[3] Bates College/The University Centre in Svalbard; mretelle@bates.edu

The Little Ice Age was one of the coldest periods of the last ~10,000 years in the Northern-Hemisphere. Although there is increasing evidence that this cooling was associated with a weakening of the Atlantic Meridional Overturning Circulation (AMOC), the sequence of events that led to a significant reduction in deep convection has yet to be explained. A recent reconstruction of Atlantic multidecadal variability (AMV) reveals that sea surface temperatures (SST) in the North-Atlantic were lowest in the interval from ~1400-1600CE (Lapointe et al. 2020), a period that was preceded by anomalously high SSTs in the late 1300s as revealed by a number of highly resolved paleoceanographic proxies (Figure 1). Here, we show that the reconstructed AMV co-varies with periods of increased Atlantic blocking frequency stretching from Greenland to Western Europe over the past ~200 years, consistent with the instrumental record (Häkkinen et al. 2011). Anomalously high blocking activity occurred between 1960-1968 (Ionita et al. 2016), when SST anomalies were warmer in the Labrador Sea (Figure 2a). We argue that this SST pattern may have prevailed during the late 1300s as revealed by many palaeoceanographic proxies in the subpolar gyre (Figure 1). In addition, cooler SSTs, as indicated in a unique annually resolved bivalve shell record from the Gulf of Maine, is coherent with the notion of Atlantic high latitude blocking in the late 1300s (Figure 3b). This pattern is reminiscent of the AMOC SST fingerprint (Yan et al. 2018) in which warmer (cooler) conditions are observed in the subpolar gyre (Gulf Stream region) (Figure 2a).

On a larger scale, precipitation anomalies reveal drier conditions in S. America and extremely wet conditions in W. Africa during the increased blocking activity of the 1960s (Figure 2b), which is also consistent with drier and extremely wet conditions in the late 14th century seen in paleo records from Peru and Ghana, respectively (Figure 3 c,d). These lines of evidence support our assertion that the late 1300s was a period of enhanced atmospheric blocking in the North-Atlantic. Upon the weakening of the 1960s blocking event, increased sea ice export from Fram Strait triggered the Great Salinity Anomaly (1970s) and the subsequent weakening of the AMOC in ~1976-1985 (Ionita et al. 2016). Taken together, this is strongly suggestive that the late 1300s was a period of strengthening of the AMOC (strong blocking) that was followed by an extreme flushout of arctic sea ice, now termed the 'great sea ice anomaly' (Miles et al. 2020), that culminated in the late 14th century. We conclude that the advection of warm Atlantic waters into the Arctic led to the export of sea-ice and weakening of the AMOC in the early 1400s (Figure 3a), setting the stage for the subsequent Little Ice Age.

Alonso-Garcia, M. et al., 2017, Freshening of the Labrador Sea as a trigger for Little Ice Age development. Climate Past 13, 317-331.
Häkkinen, S. et al, 2011, Atmospheric blocking and Atlantic multidecadal ocean variability. Science 334, 655-659.
Ionita, M. et al, 2016, Linkages between atmospheric blocking, sea ice export through Fram Strait and the AMOC. Scientific reports 6, 1-10.
Kanner, L. C. et al, 2013, High-resolution variability of the South American summer monsoon over the last seven millennia. QSR 75, 1-10.
Lapointe, F. et al, 2020, Annually resolved Atlantic sea surface temperature variability over the past 2,900 y. PNAS 117, 27171-27178.
Moffa-Sánchez, P. & Hall, I. R., 2017, North Atlantic variability and its links to European climate over the last 3000 years. Nature communications 8, 1-9.
Moffa-Sánchez, P. et al, 2014, Surface changes in the eastern Labrador Sea around the onset of the Little Ice Age. Paleoceanography 29, 160-175.
Perner, K. et al, 2015, Mid to late Holocene strengthening of the East Greenland Current linked to warm subsurface Atlantic water. QSR 129, 296-307.
Shanahan, T. M. et al, 2009, Atlantic forcing of persistent drought in West Africa. Science 324, 377-380.
Wanamaker Jr, A. D. et al, 2011, Gulf of Maine shells reveal changes in seawater temperature seasonality during the MC and the LIA. PPP 302, 43-51.
Yan, X. et al, 2018, Underestimated AMOC variability and implications for AMV. GRL 45, 4319-4328.

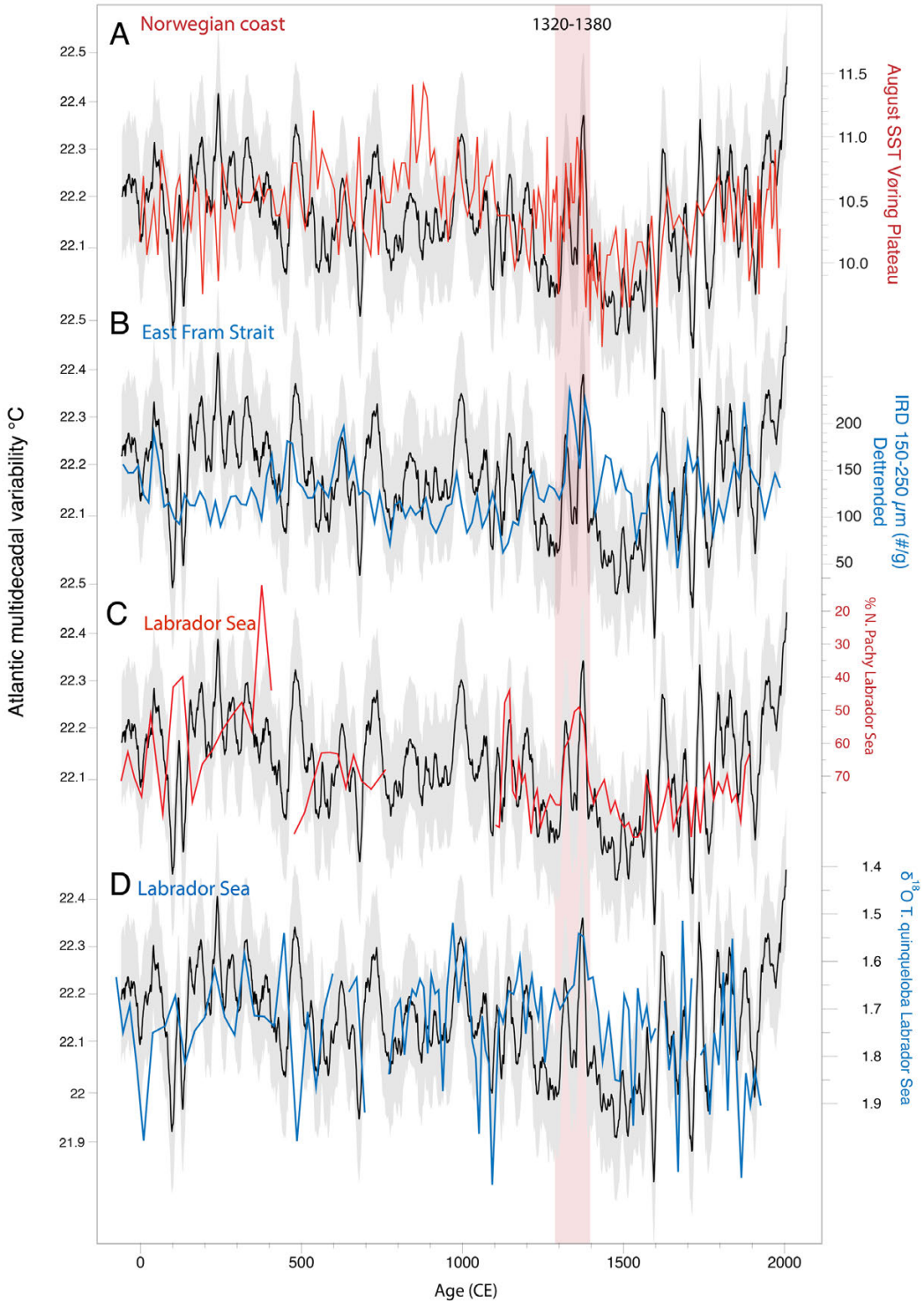

Fig 1. Selected highly resolved proxies from the Nordic Seas showing the transition from the 14th to the 15th century along with the reconstructed AMV. A) SST from the Voring Plateau, off Norway (Berner et a. 2011); B) Ice rafted debris (IRD) in East Fram Strait (Perner et al. 2015). C) % of planktonic foraminifera (N. Pachyderma) (Moffa-Sanchez et al. 2017) and D) d18O T. quinqueloba (Alonso-Garcia et al. 2017, Moffa-Sanchez et al. 2014) in the Labrador Sea.

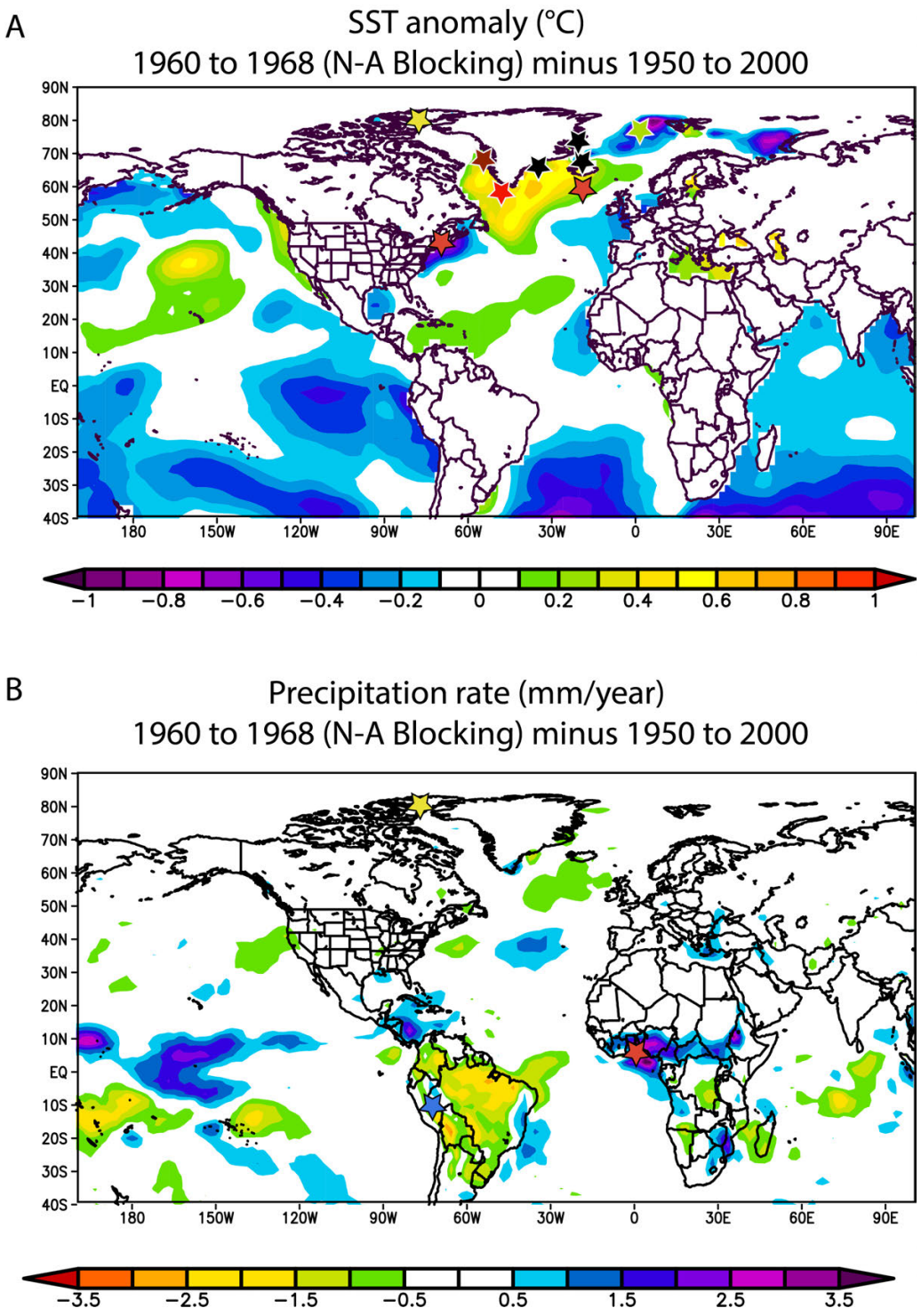

Fig 2. A: SST anomalies during period of increased blocking (1960-1968) compared to 1950-2000. B, same as A, but for precipitation rate (mm/year). Yellow star is the location of Sawtooth Lake (reconstructed AMV), colored stars are selected sites shown in Figures 1 and 3, while black stars are other sites depicting the 14/15th century anomaly not shown here. Blue and red stars in B denote the location of the Huagapo Cave and Bosumtwi Lake, respectively.

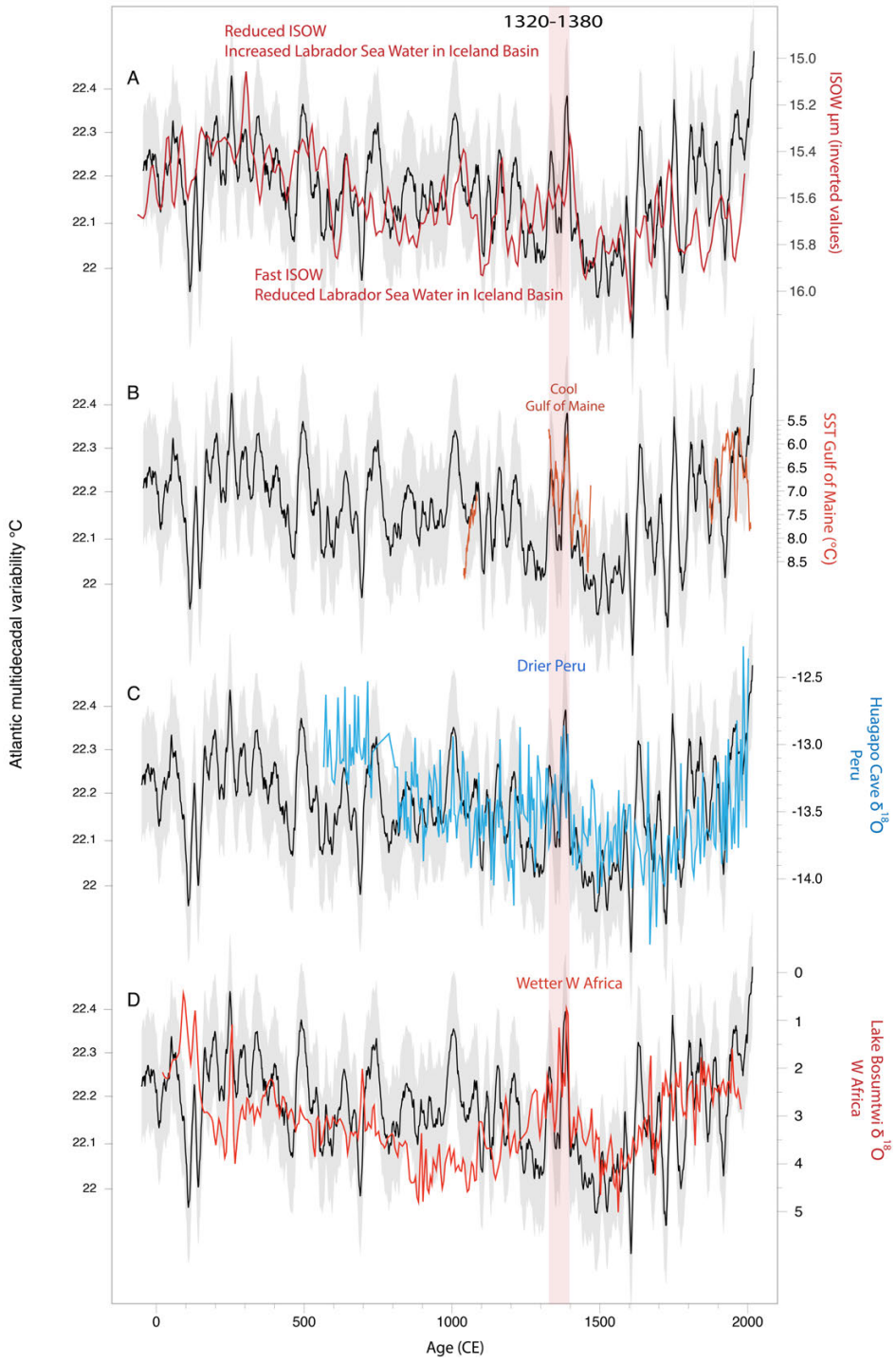

Fig 3. AMOC fingerprint during the transition from the 14th to the 15th century. a) Iceland Scotland Overturning Water (ISOW) sortable silt (Moffa-Sanchez et al. 2017) compared to reconstructed AMV. B, same as A) but for the reconstructed SST in the Gulf of Maine from bivalve shells (Wanamaker et al. 2011) (red). The ISOW record is filtered by a 3 point gaussian filter (A), and the bivalve shell record is smoothed by a 5 year gaussian filter (B). C and D, same as A and B, but AMV compared with Huagapo Cave d18O in Peru (Kanner et al. 2013) (C), and d18O at Lake Bosumtwi (Shahanan et al. 2009) (D).

Changes in South Greenland's peripheral glaciers since the Little Ice Age

Larocca, Laura J [1]; **Axford**, Yarrow [2]; **Bjørk**, Anders A [3]; **Brooks**, Jeremy P [4]

[1] Northwestern University; Laura@earth.northwestern.edu
[2] Northwestern University; axford@northwestern.edu
[3] University of Copenhagen; aab@ign.ku.dk
[4] University of Wisconsin Madison; JeremyBrooks2020@u.northwestern.edu

Glaciers and ice caps peripheral to the Greenland Ice Sheet have contributed substantially to sea-level rise this century [1]. However, multi-decadal, quantitative measurements of their fluctuations remain rare, especially prior to the satellite era. This limitation hinders our understanding of glacier response to atmospheric climate variability, and in particular to sustained warming as anticipated for the future. Here, we investigate fluctuations in South Greenland's mountain glaciers since the Little Ice Age (LIA), a cold period between ~1250 and 1900 C.E. when most glaciers across Greenland reached their historical maximum extents [2]. We map changes in the position of 62 glacier fronts over the past ~120 years using a combination of 20th century historical aerial photographs and modern satellite imagery. To extend our record to the beginning of the 20th century, we also use a high resolution orthophotograph [3] to map the positions of moraines and trimlines—geomorphic evidence that mark the glacier's historical maximum extent. In addition, we use two recently developed geospatial tools [4,5] to model LIA glacier surfaces and their equilibrium-line altitudes (ELAs) for an additional ~50 glaciers to investigate the magnitude of the LIA summer temperature depression relative to present.

Preliminary results suggest that South Greenland's peripheral glaciers have responded synchronously with changes in air temperature over the past ~120 years. We find the highest rates of retreat post LIA deglaciation in the early-to-mid 20th century: -9.5 ± 5.4 m yr-1 between ~1900 and 1954 C.E. In the mid-to-late 20th century, retreat slowed, and frontal change rates averaged -3.2 ± 0.6 m yr-1 between 1954 and 1985 C.E., and -1.6 ± 2.1 m yr-1 between 1985 and 2000/1 C.E. At the turn of the 21st century, the rate of retreat more than quadrupled from the previous time interval and averaged -7.3 ± 3.3 m yr-1 between 2000/1 and 2013/14 C.E. Retreat rates remained relatively high in the most recent time interval, averaging -5.6 ± 6.3 m yr-1 between 2013/14 and 2018/19 C.E. In comparison to similar glacier length change studies in other regions of Greenland [6-8], glaciers in the south followed the same overall trends but differed in the magnitude of change. Of particular interest, South Greenland's glaciers showed the lowest rate of retreat in the 21st century. Regional comparisons also show that glacier retreat has accelerated since (roughly) the turn of the 21st century across Greenland, which suggests a largely homogenous response to increased air temperatures. Finally, results of the LIA paleoglacier modeling show an average ELA lowering of ~90 ± 45 m, suggesting that summer air temperatures were ~0.7-0.9°C cooler than present during the coldest period of the LIA, assuming no change in precipitation.

Overall, this work extends the observational record from an understudied region of Greenland and provides pre-satellite era observations of glacier extents during a time period when quantitative measurements are rare. The work also places recent retreat into a ~100+ year perspective and will help to improve understanding of glacier sensitivity to atmospheric climate variability.

1. Bolch, T., et al. "Mass loss of Greenland's glaciers and ice caps 2003–2008 revealed from ICESat laser altimetry data." Geophysical Research Letters 40.5 (2013): 875-881.
2. Kelly, Meredith A., and Thomas V. Lowell. "Fluctuations of local glaciers in Greenland during latest Pleistocene and Holocene time." Quaternary Science Reviews 28.21-22 (2009): 2088-2106.
3. Korsgaard, N. J., et al. "Digital elevation model and orthophotographs of Greenland based on aerial photographs from 1978–1987." Scientific Data 3.1 (2016): 1-15.
4. Pellitero, R., et al. "GlaRe, a GIS tool to reconstruct the 3D surface of palaeoglaciers." Computers & Geosciences 94 (2016): 77-85.
5. Pellitero, R., et al. "A GIS tool for automatic calculation of glacier equilibrium-line altitudes." Computers & Geosciences82 (2015): 55-62.
6. Bjørk, A. A., et al. "Changes in Greenland's peripheral glaciers linked to the North Atlantic Oscillation." Nature Climate Change 8.1 (2018): 48-52.
7. Bjørk, A. A., et al. "An aerial view of 80 years of climate-related glacier fluctuations in southeast Greenland." Nature Geoscience 5.6 (2012): 427-432.
8. Leclercq, P. W., et al. "Brief communication" Historical glacier length changes in West Greenland"." The Cryosphere 6.6 (2012): 1339-1343.

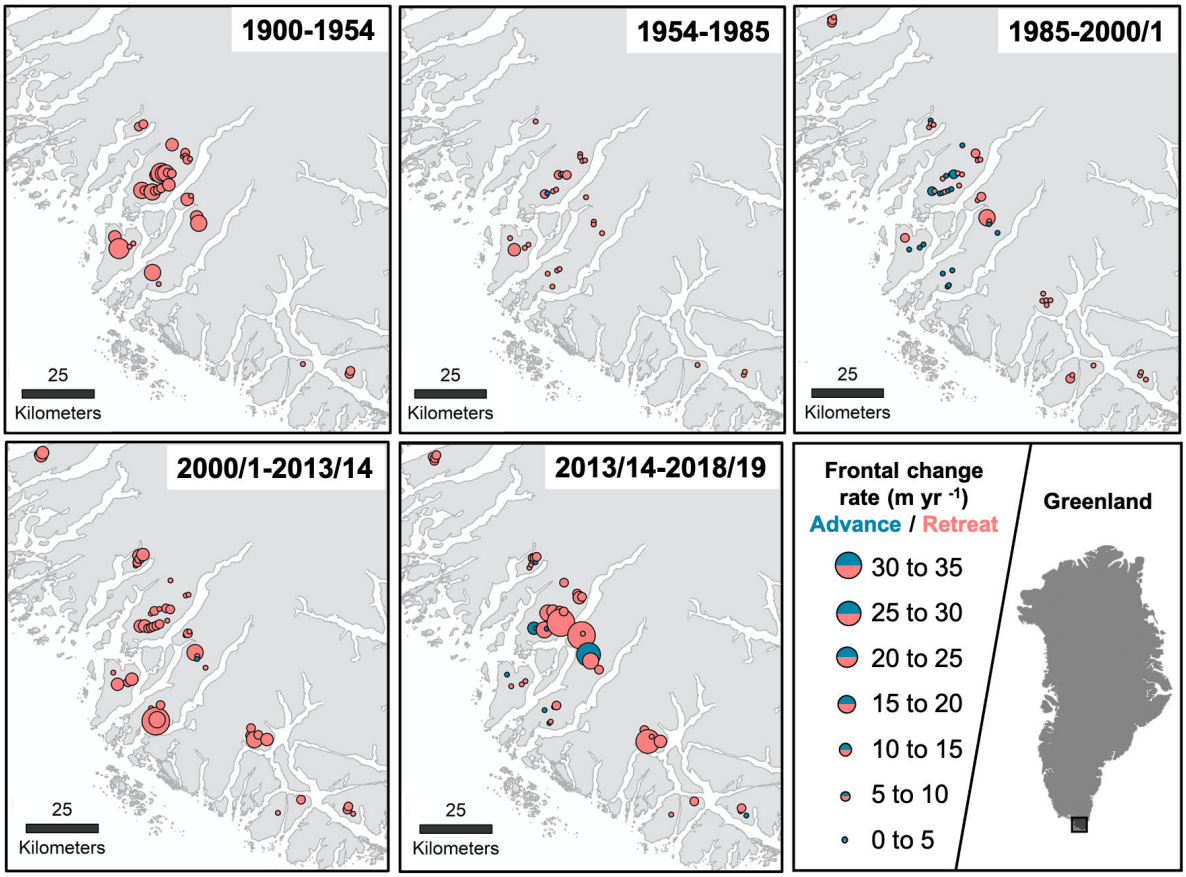

Fig 1. Frontal change rates for 62 glaciers in South Greenland over five observational periods between ~1900-2019 C.E.

Abrupt mid-20th century onset of post Little Ice Age hydrographic instability in the Northern North Atlantic

Lehman, Scott J [1]; **Sejrup**, Hans Petter [2]; **Hjelstuen**, Berit Oline [3]; **Becker**, Lukas [4]; **Runarsdottir**, Rebekka Hlin [5]; **Ionita-Scholz**, Monica [6]

[1] INSTAAR, Univ. Colorado Boulder;
[2] University of Bergen, Norway;
[3] University of Bergen, Norway;
[4] University of Bergen, Norway;
[5] University of Bergen, Norway;
[6] AWI, Bremerhaven, Germany;

A recent compilation of instrumental and proxy indicators suggests that, following more than a millennium of relative stability, the Atlantic Meridional Overturning Circulation (AMOC) began to weaken in the mid-1800s and then again around the 1960s [Caesar et al., 2012]. The linkage between many of the paleoceanographic proxies and AMOC strength relies on the strong relationship between observed and simulated patterns of North Atlantic surface and subsurface temperature variation over the past ~150 yr - which in the models is associated with changes in AMOC strength arising from simulated variation of open-ocean convection in the Labrador Sea [Caesar et al., 2018; Rhamstorf et al., 2015; Thornalley et al., 2018]. However, the connection between convection in the Labrador Sea and AMOC strength is now challenged by an extensive network of hydrographic observations suggesting that the meridional mass transports that define AMOC strength are driven largely by surface to deep water conversion in and around the Nordic Sea Basin - at least for the period of comprehensive observation since 2014 [Lozier et al., 2019]. Furthermore, the resolution of purported AMOC proxy records is typically such that they must be subjected to multi-decadal smoothing before they can been meaningfully inter-compared and/or related to the instrumental record.

Here, we provide an annually- to sub-annually- resolved marine sediment record of near-surface hydrography in the eastern branch of warm, salty Atlantic water inflow to the Nordic Seas for the period ~ AD 1750 to ~AD 1992 (core top age), with an estimated absolute chronological uncertainty of 1-15 years (1 sigma, 1-6 years after AD 1870) based on 210Pb and Cs dating, chemical identification of historic tephra and wiggle-match 14C dating. Planktonic d180 results indicate stable near-surface hydrographic conditions from ~AD 1770 to ~AD 1900, at which time we detect low amplitude variability toward higher d18O values (lower calcification temperatures) followed by the abrupt onset of much larger transient dO18 increases in AD 1950 (±1-2 yr) that appear to persist until to end of the record ~AD 1990 (see Figure). Correlation of the isotopic time series to the instrumental record of Sea Surface Temperature (SST) in the North Atlantic reveals the same spatial pattern as the so-called subpolar North Atlantic “warming hole” that (in large part) defines the AMOC SST Index [Rhamstorf et al., 2015; Caesar et al., 2018; Osman et al., 2019]. The most recent part of isotopic record is also well correlated with the temperature of the densest Nordic Sea overflow waters leaving the basin through Denmark Strait (available since AD 1950), indicating that the

near-surface inflow characteristics recorded at the study site are imparted to deep overflow waters by recirculation and deep convection within the basin in just a few years, consistent with regional hydrographic analyses [Eldevik et al., 2009]. Overall, our analysis suggests that large d180 anomalies recorded at the core site are associated with i) cooling, freshening and expansion of the North Atlantic Sub-Polar Gyre (SPG), ii) increased transport of cold, fresh SPG waters through bathymetrically-steered currents into the eastern branch of the Atlantic water entering the Nordic Seas where they may iii) influence surface buoyancy and deep water formation within the Nordic Sea Basin [Hatun et al., 2005]. Although not conclusive, this is consistent with the possibility that changes in temperature and salinity of the SPG and Labrador Sea may influence AMOC via a downstream response in and around the Nordic Sea Basin rather than via open ocean convection in the Labrador Sea itself.

Although the proximate forcing of the SPG is not entirely clear, the downstream response to changes in the SPG appears to have increased substantially around AD 1950. We briefly examine the roles of atmospheric blocking events, associated changes in sea ice and freshwater transport, and of increased Greenland Ice Sheet run off in contributing to the sudden change in response at that time.

Caesar, L., McCarthy , G.D., Thornalley, D,J.R., Cahill, N. and S. Rahmstorf, 2021. Current Atlantic Meridional Overturning Circulation weakest in last millennium. Nature Geoscience, https://doi.org/10.1038/s41561-021-00699-z

Caesar, L., Rahmstorf, S., Robinson, A., Feulner, G., Saba, V., 2018. Observed fingerprint of a weakening Atlantic Ocean overturning circulation. Nature 556, 191-196.

Eldevik, T., Nilsen, J-E Ø, Doroteaciro, I., K. Olsson, A., Sandø, Drange, H., 2009. Observed sources and variability of Nordic seas overflow. Nature Geoscience 2, 405-10.

Hatun, H., Sando, A.B., Drange, H., Hansen, B., Valdimarsson, H., 2005. Influence of the Atlantic subpolar gyre on the thermohaline circulation. Science 309, 1841-1844.

Lozier, M. S., Li, F., Bacon, S., Bahr, F., Bower, A. S., Cunningham, S. A., et al. 2019. A sea change in our view of overturning in the subpolar North Atlantic. Science, 363, 516–521. https://doi.org/10.1126/science.aau6592?

Osman, M.B., Das, S.B., Trusel, L.D., Evans, M. J., Fischer, H., Grieman, M.M., Kipfstuhl, S., McConnell, J.R., E.S. Saltzman, 2019. Industrial-era decline in subarctic Atlantic productivity. Nature 569, 551-555. Rahmstorf, S., Box, J.E., Feulner, G., Mann, M.E., Robinson, A., Rutherford, S., Schaffernicht, E.J., 2015. Exceptional twentieth-century slowdown in Atlantic Ocean overturning circulation. Nature Climate Change 5, 475-480.

Thornalley, D. J. R. et al. Anomalously weak Labrador Sea convection and Atlantic overturning during the past 150 years. Nature 556, 227–230 (2018).

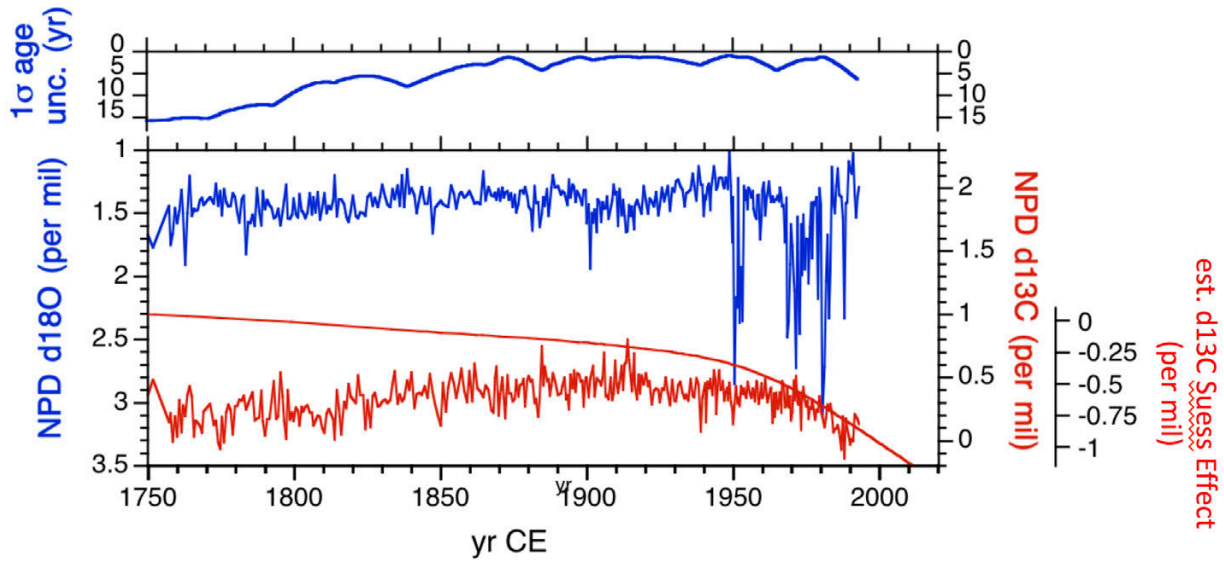

Fig 1. Isotopic record of the planktonic foraminifer *Neogloboquadrina pachyderma* dex. in core GS13-182-01CC from the Norwegian Continental Slope, beneath the eastern limb of warm Atlantic water inflow to the Nordic Sea Basin. A) Estimated age model uncertainty. B) Isotopic results along with an estimate of historic d13C change in seawater at 50 mwd (i.e., the assumed depth habitat of *N. pachyderma* dex.) in the SE Norwegian Sea due to the Suess Effect.

On the interannual variability of spring Bering Strait water temperatures

Lenetsky, Jed E [1]; **Serreze**, Mark C [2]

[1] National Snow and Ice Data Center, Cooperative Institute for Research in Environmental Sciences, University of Colorado – Boulder, Boulder, Colorado, USA; Jed.Lenetsky@colorado.edu
[2] National Snow and Ice Data Center, Cooperative Institute for Research in Environmental Sciences, University of Colorado – Boulder, Boulder, Colorado, USA; mark.serreze@colorado.edu

We find that June Bering Strait water temperatures, an important predictor of the timing of seasonal sea ice retreat in the economically important Chukchi Sea and surrounding region, are set upstream the preceding autumn and winter by ocean temperatures in the southwestern Bering Sea shelf. Positive ocean heat anomalies in autumn lead to delayed winter formation of sea ice in the western Bering sea and early ice retreat the following spring. These autumn heat anomalies exist from the surface to 65 meters depth and are preserved in the thermocline after winter freezing of surface waters. Heat anomalies move towards the Bering Strait via the Anadyr current and are magnified by shortwave radiation fluxes to the ocean surface in April and May. We show that the heat content of the Anadyr current, and not the atmospheric circulation, is the primary driver of Bering Strait water temperature variability. Water temperatures at depth in the Bering Sea Shelf are more closely linked to June Bering Strait water temperatures than are temperatures at the surface; December water temperature anomalies at 45 meters depth correlate with June Bering Strait water temperatures at $r = 0.85$. These findings highlight the importance of real time monitoring of temperatures at depth in the western Bering Sea for seasonal sea ice forecasting in the Chukchi Sea and surrounding areas and for understanding ice-associated ecological changes.

Danielson, S. L., Ahkinga, O., Ashjian, C., Basyuk, E., Cooper, L. W., Eisner, L., Farley, E., Iken, K. B., Grebmeier, J. M., Juranek, L., Khen, G., Jayne, S. R., Kikuchi, T., Ladd, C., Lu, K., McCabe, R. M., Moore, G. W. K., Nishino, S., Ozenna, F., … Weingartner, T. J. (2020). Manifestation and consequences of warming and altered heat fluxes over the Bering and Chukchi Sea continental shelves. Deep Sea Research Part II: Topical Studies in Oceanography, 177, 104781. https://doi.org/10.1016/j.dsr2.2020.104781

Luo, X., Wang, Y., Lu, Y., Wei, H., Zhao, W., Nie, H., & Hu, X. (2020). A 4-Month Lead Predictor of Open-Water Onset in Bering Strait. Geophysical Research Letters, 47(17), e2020GL089573. https://doi.org/10.1029/2020GL089573

Overland, J. E., Stabeno, P. J., & Salo, S. (1996). Direct evidence for northward flow on the northwestern Bering Sea shelf. Journal of Geophysical Research: Oceans, 101(C4), 8971–8976. https://doi.org/10.1029/96JC00205

Woodgate, R. A. (2018). Increases in the Pacific inflow to the Arctic from 1990 to 2015, and insights into seasonal trends and driving mechanisms from year-round Bering Strait mooring data. Progress in Oceanography, 160, 124–154. https://doi.org/10.1016/j.pocean.2017.12.007

Zhang, W., Wang, Q., Wang, X., & Danilov, S. (2020). Mechanisms Driving the Interannual Variability of the Bering Strait Throughflow. Journal of Geophysical Research: Oceans, 125(2). https://doi.org/10.1029/2019JC015308

Exposing the history of volcanism and sea-level changes at the Mount Edgecumbe Volcanic Field in Southeast Alaska using cosmogenic nuclides

Lesnek, Alia J [1]; **Licciardi**, Joseph M. [2]; **Briner**, Jason P [3]; **Baichtal**, James F [4]; **Walcott**, Caleb K [5]

[1] University of New Hampshire; alia.lesnek@unh.edu
[2] University of New Hampshire;
[3] University at Buffalo;
[4] Tongass National Forest;
[5] University at Buffalo;

Southeast Alaska's Mount Edgecumbe Volcanic Field (MEVF) lies along the transform boundary that separates the North American and Pacific plates. The MEVF is situated approximately 20 km from Sitka, a town with more than 8,000 residents, and understanding the history of MEVF volcanism is therefore critical for regional geohazard assessments. Reconstructions of MEVF activity can also aid in determining when humans first arrived to the northwest Pacific coast of North America (Potter et al., 2017; Braje et al., 2020). For example, the Tlingit name for Mt. Edgecumbe, L'úx, translates to "flash" or "blinking," suggesting that the volcano was active when humans settled in the region (Bunten, 2015). Moreover, areas of Southeast Alaska, including portions of the MEVF, have been identified as potential ice-free refugia during the Last Glacial Maximum (LGM; Carrara et al., 2007). Unraveling the eruptive history of the MEVF can thus play a role in assessing both the extent and timing of ice-free terrain available for human occupation during the late Pleistocene. Studies of Quaternary MEVF activity indicate that eruptions began as early as ~600 ka and continued until the mid-Holocene (Riehle et al., 1989). Tephrochronological evidence from deposits in the volcanic field reveals a period of intense explosive volcanism between ~14.6 and 13.1 ka (Riehle et al., 1992b; Begét and Motyka, 1998; Addison et al., 2010; Praetorius et al., 2016), possibly related to crustal flexure caused by retreat of the Cordilleran Ice Sheet following the LGM (Praetorius et al., 2016). The chronology of effusive activity in the MEVF, particularly during the postglacial period, is less well understood (Riehle et al., 1989).

In this presentation, we will focus on a basalt flow exposed on the eastern shores of the MEVF. This flow was mapped by Riehle et al. (1989) as potentially postglacial in age, but K-Ar ages derived from this unit are inconclusive. The basalt flow is overlain by wave-eroded pyroclastic flow deposits and a ~13.2 ka dacitic tephra (Riehle et al., 1989; Begét and Motyka, 1998). Surface features of the eastern MEVF lava flow such as tumuli and ropy structures are indicative of subaerial emplacement and cooling, and appear to rule out overriding by warm-based, erosive glacier ice. It has also been reported that in some locations the basalt encases erratics deposited during the most recent glaciation (Riehle, 1996). These lines of evidence may suggest that the basalt erupted during the late Pleistocene, sometime between deglaciation at ~15 ka (Walcott et al., 2021) and the deposition of the dacite tephra at ~13.2 ka.

Alternatively, a pre- or syn-LGM eruption and subsequent exposure in an unglaciated area could also explain preservation of the delicate flow surface features that we observed in the field, and would indicate that effusive basaltic volcanism was confined to earlier stages of the MEVF's activity (Riehle et al., 1992a). K-Ar dates on other MEVF basalt flows range from ~600-300 ka (Riehle et al., 1989), but the stratigraphic relationship between these units and the eastern MEVF basalt is unclear. Thus, both the emplacement age of the eastern MEVF basalt and the duration of surface exposure before ~13.2 ka remain an open question.

To determine the duration of eastern MEVF basalt exposure and assess if this region was ice-free during the LGM, we collected two surface samples for ^{36}Cl dating in summer 2019. Apparent exposure ages for these samples, which lie at 3 and 8 m asl, respectively, are 7.0 ± 0.6 and 7.1 ± 0.6 ka. To help explain these apparent ages, we turn to a new, locally-constrained relative sea-level curve for the MEVF and surrounding region (Baichtal et al., in review). The curve suggests sea-level was below our sampling sites before ~8.3 ka and reached a maximum elevation of 10 m asl at ~7.9 ka. This rise in relative sea-level is attributed to the migration and collapse of a peripheral crustal forebulge associated with the retreating Cordilleran Ice Sheet (Lesnek et al., 2020; Baichtal et al., in review). Between ~7.9 ka and the present, relative sea-level has fallen steadily at a rate of ~0.1 cm a^{-1}. Given this relative sea-level history, we therefore might expect both submergence/burial and exposure of our sampling sites during the Holocene. In the simplest scenario, the eastern MEVF basalt was emplaced sometime after regional deglaciation, immediately before the deposition of pyroclastic material and dacite tephra at ~13.2 ka. These deposits would have shielded the surface from cosmic radiation. Wave action during the sea-level transgression then eroded the overlying deposits, exposing the basalt flow at ~7 ka. This postglacial eruption scenario accounts for the fresh appearance of the flow surfaces, the short duration of apparent exposure, and the inclusion of glacial erratics in the flow. However, our ^{36}Cl ages alone do not rule out an earlier eruption of the eastern MEVF basalt. For example, a scenario where the basalt was emplaced in an ice-free refugium during the local LGM at ~17 ka, exposed for ~3 kyr before burial by pyroclastic deposits and tephra, and then re-exposed due to erosion of the overlying material at ~4 ka is also consistent with our results given the uncertainty in our ^{36}Cl ages and the relative sea-level curve. A mapping and ^{36}Cl dating campaign planned for summer 2021 should allow us to determine which of these two scenarios is more likely, and to better reconstruct the dynamic late Pleistocene environment of coastal Southeast Alaska.

The multidisciplinary story of Antarctica's history as told from blue ice moraines

Licht, Kathy [1]; **Kaplan** , Mike [2]; **Bader**, Nicole [3]; **Graly**, Joseph [4]; **Kassab**, Christine [5]

[1] Indiana University Purdue University Indianapolis; klicht@iupui.edu
[2] Lamont Doherty Earth Observatory; mkaplan@ldeo.columbia.edu
[3] Indiana University Purdue University Indianapolis; nicoleabader@gmail.com
[4] Northumbria University; joseph.graly@northumbria.ac.uk
[5] Indiana University Purdue University Indianapolis; ckassab@iupui.edu

Till in an extensive blue ice moraine in the central Transantarctic Mountains shows relatively continuous deposition by East Antarctic derived ice throughout the last several glacial cycles. Our datasets show that Antarctic blue ice moraines may be repositories of sediment from the warm-based portions of ice on the polar plateau and provide valuable archives of ice sheet and geologic history around the continent. The well-preserved Mt. Achernar moraine consists of quasi-continuous, hummocky sediment ridges that form on top of sublimating ice. Ground-penetrating radar (GPR) imaging of the internal structure beneath the moraine's debris cover shows that the moraine formed through the lateral accretion of basal debris-rich ice layers thrust upward over time. Pebble lithology and detrital zircon geochronology reveal distinct spatial changes between dominant sedimentary (Beacon) and igneous (Ferrar) composition at both meter and kilometer scales. The provenance changes observed in the pebble fraction are interpreted to indicate relative stability of the East Antarctic ice sheet, as the Law Glacier tapped into and eroded successively lower stratigraphic units of the Beacon Supergroup.

*Graly, J., Licht, K., *Bader, N., and Bish, D.L., 2020. Chemical weathering signatures from Mt. Achernar Moraine, Central Transantarctic Mountains I: Subglacial sediments compared with underlying rock. https://doi.org/10.1016/j.gca.2020.06.005

*Kassab, C., Licht, K., Petersson, R., Lindbäck, K., Graly, J., and Kaplan, M., 2019. Formation and Evolution of an extensive blue ice moraine in central Transantarctic Mountains, Antarctica. https://doi.org/10.1017/jog.2019.83

*Graly, J.A., Licht, K.J., *Kassab, C.M., Bird, B.W., and Kaplan, M.R., 2018. Sediment entrainment mechanisms and ice origin in an Antarctic blue ice moraine assessed through stable isotope analysis and internal structures of shallow ice cores. doi: 10.1017/jog.2018.4

*Graly, J.A, Licht, K.J., Druschel, G.K., and Kaplan, M.R., 2018. Polar desert chronologies through quantitative measurements of salt accumulation. Geology 26, 351-354.

*Bader, N.A., Licht, K.J., Kaplan, M.R., *Kassab, C., and Winckler, G., 2017. East Antarctic ice sheet stability since the mid-Pleistocene recorded in a high-elevation ice-cored moraine. Quaternary Science Reviews 159, p.88-102.

Kaplan, M.R., Licht, K., Winckler, G., Schaefer, J.M., *Bader, N., Mathieson, C., Roberts, M., *Kassab, C.M., Schwartz, R., and *Graly, J.G., 2017. Late Pleistocene stability of the East Antarctic ice sheet, as seen from the Transantarctic Mountains. doi:10.1130/G39189.1

*the geologic 'Grandmentees' of John Andrews

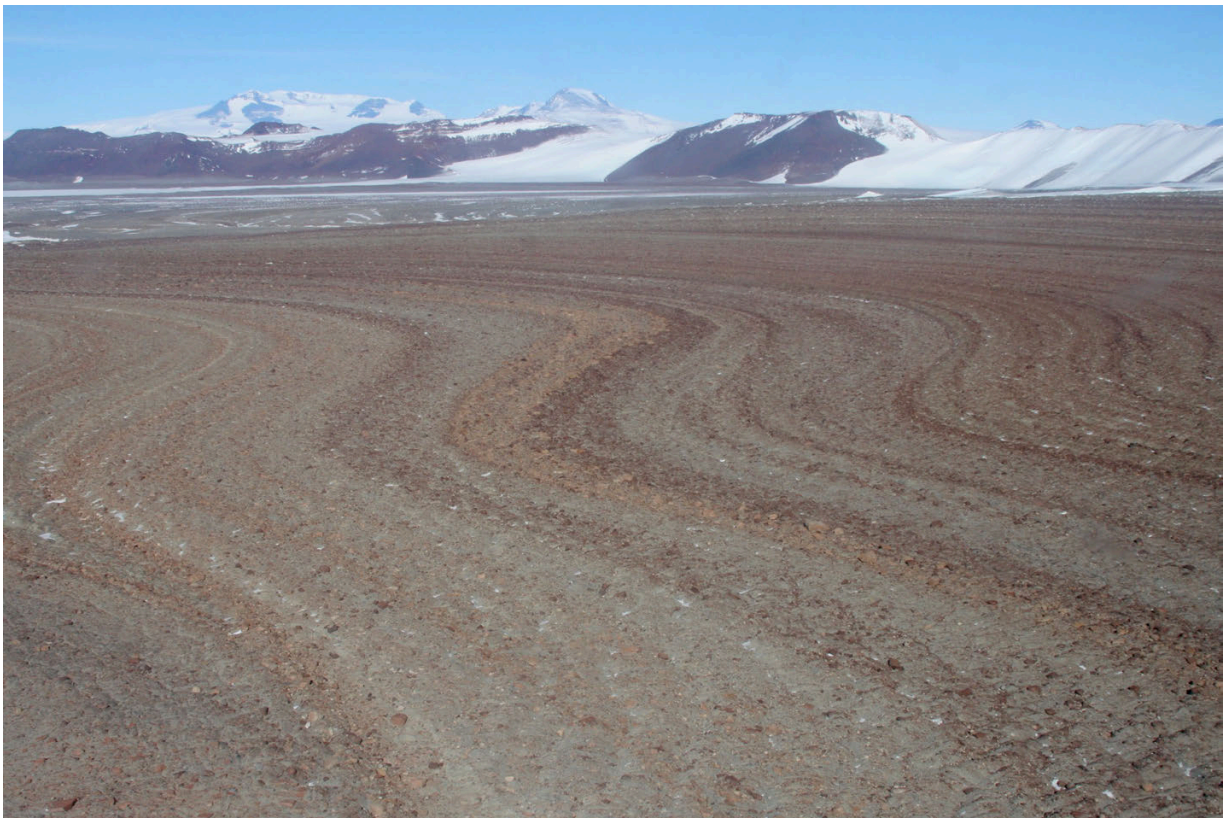

Fig 1. Photograph of the Mt. Achernar moraine highlighting continuity of compositional changes.

Investigating climatic and ecologic controls on modern plant leaf wax production along a latitudinal transect of Baffin Island

Lindberg, Kurt R [1]; **Thomas**, Elizabeth K [2]; **Raynolds**, Martha K [3]; **Hollister**, Kayla V [4]

[1] University at Buffalo; kurtlind@buffalo.edu
[2] University at Buffalo; ekthomas@buffalo.edu
[3] University of Alaska Fairbanks; mkraynolds@alaska.edu
[4] University at Buffalo; kvhollis@buffalo.edu

Paleoclimate reconstructions using plant leaf waxes often assume that long-chain waxes (≥C26/C27) are primarily produced by terrestrial vegetation and short to mid-chain waxes (≤C24/C25) by aquatic communities. However, modern leaf wax distributions at low- and mid-latitudes are sensitive to environmental conditions, including temperature and annual precipitation amount. In this study, we assess whether terrestrial plant wax Average Chain Length (ACL) changes along a climate gradient in northern Québec and Baffin Island, Nunavut, Canada. Further, we examine whether ACL within individual species varies along the gradient, or whether changes in ACL are caused by differences in plant community along the transect. We analyzed chain length distributions from leaf wax n-alkanoic acids and n-alkanes in 70 plant samples from four lake catchments along a latitudinal temperature gradient of 0.6 to 7.2 ºC mean temperature of the Months-Above-Freezing (MAF). When comparing the entire plant communities between catchments, we find that terrestrial plants produce an increasingly greater percentage of short and mid-chain waxes moving north along the transect, as the dominant growth forms transition from trees and shrubs to liverworts and mosses. These northern communities produce a greater percentage of short to mid-chain waxes (84%) than the representative submerged aquatic mosses in the catchments (57%), challenging assumptions about the division of terrestrial and aquatic leaf wax production.

We also compare ACLs of single plant species that are found in multiple catchments to infer direct relationships between wax production and MAF. These plants display high variability in ACL change along the transect, -2.0-2.7/ºC in n-alkanoic acids and -2.7-0.8/ ºC in n-alkanes with some exhibiting no change, but we find no clear relationship to the MAF temperature gradient. Our findings suggest that the apparent trend of catchment-average ACL decreasing northward is due to different species within the catchments, rather than individual species changing their wax chain length production in response to climate. If Arctic lake sediment archives record past changes in ACL, our results suggest that these variations may be interpreted to reflect changes in plant taxa present through time, rather than due to climate-induced changes in wax production by individual plant species.

Assessing new temperature and conductivity calibrations on a 24,000-year record of lacustrine branched glycerol dialkyl glycerol tetraethers in the Polar Ural Mountains

Lovell, Kathryn [1]; **Thomas**, Elizabeth K [2]; **Cowling**, Owen C [3]; **Castañeda**, Isla S [4]; **Svendsen**, John Inge [5]

[1] Department of Geology, University at Buffalo; klovell@buffalo.edu
[2] Department of Geology, University at Buffalo; ekthomas@buffalo.edu
[3] Department of Geology, University at Buffalo; owencowl@buffalo.edu
[4] Department of Geosciences, University of Massachusetts Amherst; isla@geo.umass.edu
[5] Department of Earth Science, University of Bergen, Bjerknes Centre for Climate Research; John.Svendsen@uib.no

Siberia contains relatively few records of past terrestrial climate, especially when compared to North America, Greenland, and Europe. Yet, this region was last glaciated well before the Last Glacial Maximum (LGM), and therefore contains longer lake sediment records than in much of North America and Europe. Branched glycerol dialkyl glycerol tetraethers (brGDGTs) are an emerging proxy for past temperature, pH, and conductivity in lacustrine settings. We apply several new lacustrine brGDGT temperature and conductivity calibrations to a 24,000-year-long record from Bolshoye Shchuchye, a lake in the Polar Ural Mountains, Siberia, and assess the effectiveness of brGDGT-based temperature reconstructions in this lake. The distribution of brGDGTs is similar to that of other Arctic lakes, suggesting a lacustrine source of brGDGTs. The MBT'5Me and Bayesian temperature calibrations result in higher temperatures during the LGM than during the Holocene, which is contradictory to other climate proxies, including glacier extent and pollen, which indicate the LGM was colder than the Holocene in this region. A recently developed calibration that empirically fit fractional abundances of structural subsets of brGDGTs to temperature yields a record with entirely different trends, with the LGM cooler than the Holocene, but the highest inferred temperature in the record from 15 to 10 ka. Pollen, sedimentary ancient DNA, and leaf wax abundance records, show that the Polar Ural Mountains experienced temperature changes between 15 to 10 ka generally in step with those in the North Atlantic region, suggesting that this temperature record inferred using the new brGDGT-based calibration is also not correct. However, we also applied a new brGDGT-conductivity calibration to this record, and find that conductivity was highest from about 11 to 6 ka. Seasonal lake ice cover at Bolshoye Shchuchye was likely at a minimum during this interval, as inferred from elemental ratios and the isotopic difference between long- and mid-chain leaf waxes. Lake water conductivity may have been higher from 11 to 6 ka than the rest of the record due to greater seasonal evaporation of lake water. The varying degrees of success of existing brGDGT-temperature and –conductivity calibrations suggest that brGDGTs distributions are being mainly influenced by other non-thermal factors in this record. We plan to further examine more factors causing brGDGT variability in this record, with the goal of better understanding brGDGTs in Arctic lakes.

Raberg, J. H. et al., 2021, Revised fractional abundances and warm-season temperatures substantially improve brGDGT calibrations in lake sediments: Biogeosciences, preprint.
Regnell, C. et al., 2019, Glacial and climate history of the last 24,000 years in the Polar Ural Mountains, inferred from partly carved lake sediments: BOREAS, v. 48, p. 432-443.
Zhao, B. et al., 2021, Development of an in situ branched GDGT calibration in Lake 578, southern Greenland: Organic Geochemistry, v. 152, p. 1-13.
Russell, J. M. et al., 2018, Distributions of 5- and 6-methyl branched glycerol dialkyl glycerol tetraethers (brGDGTs) in East African lake sediment: Effects of temperature, pH, and new lacustrine paleotemperature calibrations: Organic Geochemistry, v. 117, p.56-69.

Impact of lake basin morphometry and mixing on Arctic lake water isotope composition

Mahar, Isabelle F [1]; **Cluett**, Allison [2]; **Thomas**, Elizabeth [3]

[1] Barnard College, Columbia University; ifm2109@barnard.edu
[2] University at Buffalo; aacluett@buffalo.edu
[3] University at Buffalo; ekthomas@buffalo.edu

Lake water isotope proxies are used to infer past climate changes. However, among modern lakes within a single region experiencing the same climate, summer lake water isotope compositions vary strongly. We previously hypothesized that this difference in isotope composition was due to differences in lake summer residence time, which, in lakes with similar catchment sizes, is controlled largely by lake volume (Cluett & Thomas, 2020). We use sensitivity tests of idealized lake basins in the PRYSM lake water environment model (Dee, et al., 2018; Morrill et al., 2019) to test this hypothesis. Furthermore, we assess whether changing morphological parameters of a lake basin, including volume, surface area, and geometry, changes the average summer isotope composition, the signal recorded by many proxies.

We ran 19 simulations of the PRYSM model, holding climate and precipitation isotope forcings constant between runs. We used 39 years of climate data at daily resolution from the ERA-Interim Reanalysis dataset, and tuned the model parameters to match observations in a small lake on western Greenland. The only parameters that we changed between simulations were lake volume, surface area, and geometry. We focused simulations on two simplified lake geometries: rectangular prisms and cones. For the rectangular prisms, we held the volume constant but changed surface area and depth. Then, we ran several sensitivity tests with cones, in which we held one variable (e.g., volume) constant, but changed other variables (e.g., surface area and depth). Using the constant-volume simulations with rectangular prisms and the full suite of simulations with cones, we can assess whether summer lake water isotope composition changes with any individual morphometric parameter.

We find that surface area impacts average summer surface water isotope composition more strongly than volume. Lakes with the same surface area but different volumes have very similar summer isotope compositions. On the other hand, lakes with the same volume but different surface area have different summer isotope compositions: lakes with large surface areas tend to be depleted compared to lakes with small surface areas. We then examine the processes causing these observed differences in our simulations. Prior to isothermal mixing, large-surface-area lakes retain more isotopically depleted runoff during the spring melt period in the surface layer than the small-surface-area lakes. This is significant because when the large-surface-area lakes mix vertically following the spring melt period, the depleted surface water mixes through the entire lake. Consequently, these lakes more effectively incorporate spring melt into the water column and the lake water remains relatively depleted throughout the rest of the ice-free season. Small-surface-area lakes retain a smaller volume of spring runoff in the surface layer, and a greater proportion of the spring melt is flushed out of the lake basin. When these lakes then mix vertically, only a small amount of depleted surface water is mixed through the entire lake, and the lake water remains relatively enriched throughout the rest of the ice-free season.

In our sensitivity test results, it is clear that lake volume does not explain seasonal lake water isotope variability, rather, the lake surface area is the most important variable controlling lake water summer isotope composition. The summer isotope composition in lakes with large surface area tends to reflect mean annual precipitation, whereas lakes with small surface area are biased towards summer precipitation.

Cluett, A. A., & Thomas, E. K. (2020). Resolving combined influences of inflow and evaporation on western Greenland lake water isotopes to inform paleoclimate inferences. Journal of Paleolimnology, 1–18.

Dee, S. G., Russell, J. M., Morrill, C., Chen, Z., & Neary, A. (2018). PRYSM v2. 0: A proxy system model for lacustrine archives. Paleoceanography and Paleoclimatology, 33(11), 1250–1269.

Morrill, C., Meador, E., Livneh, B., Liefert, D. T., & Shuman, B. N. (2019). Quantitative model-data comparison of mid-Holocene lake-level change in the central Rocky Mountains. Climate Dynamics, 53(1/2), 1077–1094 https://doi.org/10.1007/s00382-019-04633-3

A previously undocumented influence on H isotopes of Arctic mid-chain plant waxes through the Holocene: moss-associated methane oxidation

McFarlin, Jamie M [1]; **Axford**, Yarrow [2]; **Kusch**, Stephanie [3]; **Masterson**, Andrew L [4]; **Lasher**, Everett [5]; **Osburn**, Magdalena R [6]

[1] INSTAAR; jamie.mcfarlin@colorado.edu
[2] Northwestern University; axford@northwestern.edu
[3] University of Cologne; stephanie.kusch@uni-koeln.de
[4] Northwestern University; andrew.masterson@northwestern.edu
[5] University of Pittsburgh; everett.lasher@pitt.edu
[6] Northwestern University; maggie@northwestern.edu

Ongoing warming of Arctic lakes is predicted to drive physical and biologic changes, including longer ice-free seasons, higher summer water temperatures, and heightened primary productivity. In lakes with geometries prone to thermal stratification, these changes could drive increasing methanogenesis and methane storage in the water column. However, evidence for changes in lake redox conditions and methane storage during prior warm periods is limited, inhibiting observations of long-term changes to carbon cycling in lakes that result from Arctic warming.

Although methane is a known influence on C isotopes of lacustrine organic materials, the influence of methane on H isotopes of plant biomarkers has not been documented. H isotopes of mid-chain plant waxes in lacustrine settings are conventionally interpreted as recording lake water H isotopes. Here, we present the first evidence, to our knowledge, that methane cycling can act as an influence on the H isotopes of these materials. More specifically, we present evidence from three Greenland lakes that insolation-driven warming during the early-middle Holocene led to summer stratification, low oxygen, and higher seasonal methane production. We posit that these conditions promoted a symbiotic relationship between aquatic mosses and methanotrophic bacteria and that this symbiosis contributed exceptionally depleted H to aquatic mosses, resulting in depleted H isotopes of sedimentary mid-chain waxes. In contrast, the isotopic composition of lake water and precipitation, inferred using the isotopic composition of chironomid and terrestrial plant waxes respectively, track multi-millennial cooling through the Holocene at all sites. This data supports that Arctic lakes were a potentially major source of atmospheric methane in the early-middle Holocene, although the role of aquatic mosses as a compensating C-sink has yet to be quantified.

Profile curated collections of data with portals on the Arctic Data Center

McLean, Erin L [1]; **Jones**, Matthew B [2]; **Budden**, Amber E [3]; **Walker**, Lauren [4]; **Jones**, Christopher S [5]

[1] Arctic Data Center/UC Santa Barbara; mclean@nceas.ucsb.edu
[2] Arctic Data Center/UC Santa Barbara; jones@nceas.ucsb.edu
[3] Arctic Data Center/UC Santa Barbara; aebudden@nceas.ucsb.edu
[4] Arctic Data Center/UC Santa Barbara; walker@nceas.ucsb.edu
[5] Arctic Data Center/UC Santa Barbara; cjones@nceas.ucsb.edu

The COVID-19 pandemic has made it even more difficult for Arctic researchers to do their work; instead of facing the usual obstacles associated with field work in remote locations, researchers have had to cancel field seasons due to global restrictions around limiting the spread of COVID-19. However, research can continue through the reuse of existing datasets that have been archived in repositories like the Arctic Data Center, where all data is available for download and reuse. Comprehensive metadata make discovery of relevant datasets easy, enabling new synthesis research or analysis. Now, the Arctic Data Center has made it even simpler to navigate the catalog and customize the datasets shown through portals.

With portals, researchers create an environment where a collection of datasets and project information is available in a single location. Typically, a research project's website won't be maintained beyond the life of the project and all the information on the website that provides context for the data collection is lost. By creating a portal through the Arctic Data Center, researchers can both increase discovery of a curated set of related project data and preserve information on the project's objectives, scopes, and organization. Coupled with the data files, these portals will support data use and interpretation for years to come. Since researchers are typically interested in a subset of the Arctic Data Center's 6000+ datasets, portals help them see all relevant datasets in one convenient webpage (Figure 1).

Using the portals service carries a number of benefits for research projects or distributed teams:

-The discovery interface works like the main search catalog on the Arctic Data Center and includes an interactive map that scrolls and zooms to focus the data search to a particular region

-Customized search fields can be created that help narrow down the data search to specific metadata fields like Research Vessel or Field Site

-Portals can be branded with logos and colors and has a customizable URL

-Additional information on team members, associated publications, and essential details about the project or lab can be added using a user-friendly interface and customized using Markdown

-Collating metrics all in one place

Portals make highlighting and sharing related datasets easy for researchers, projects, and

labs. 35+ groups have already taken advantage of the portals, with subjects ranging from oceanography to social science to field stations. Researchers can start creating portals today by logging in with their ORCiD even if they have not yet submitted data to the Arctic Data Center.

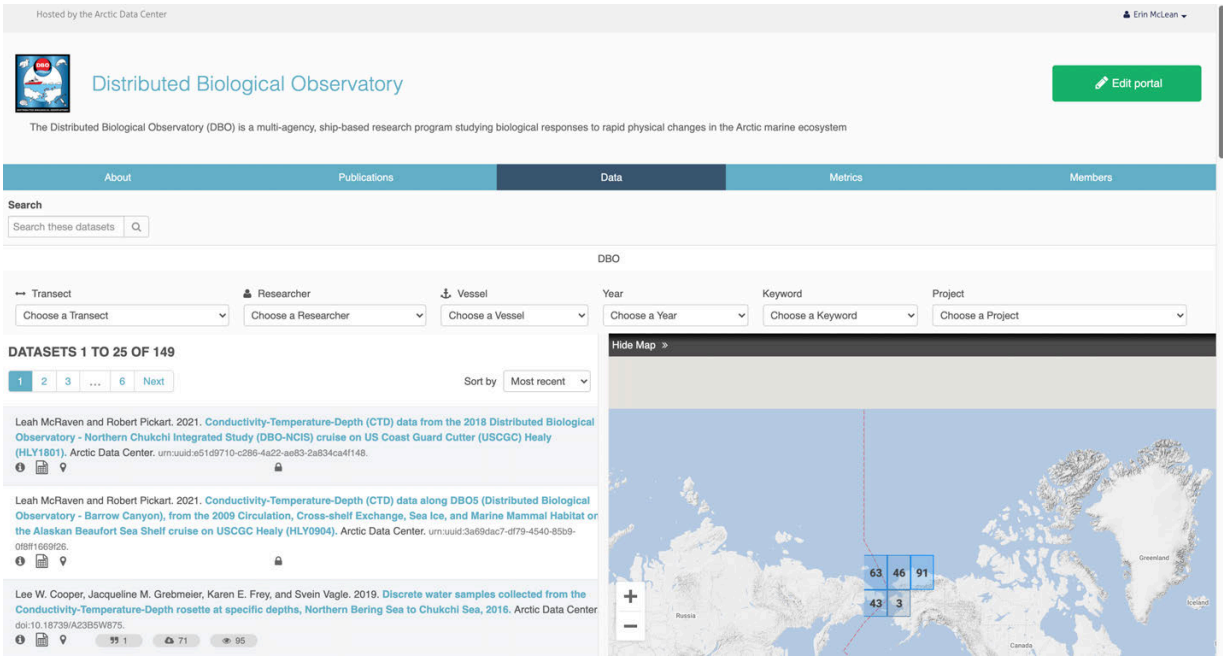

Fig 1. The data page of the portal created by the Distributed Biological Observatory, collecting all the datasets relevant to their work as a ship-based research program studying biological responses to rapid physical changes in the Arctic marine ecosystem.

Distributed Biological Observatory Data Portal. 2021. http://arcticdata.io/catalog/portals/dbo
Toolik Field Station Data Portal. 2021. https://arcticdata.io/catalog/portals/toolik

Coupled marine and terrestrial climate dynamics revealed by multicentury, annually resolved proxy records from Fennoscandia

Mette, Madelyn J. [1]; **Wanamaker Jr.**, Alan D. [2]; **Carroll**, Michael L. [3]; **Ambrose**, William G. [4]; **Retelle**, Michael J. [5]; **Andersson**, Carin [6]

[1] USGS St. Petersburg Coastal and Marine Science Center, St. Petersburg, Florida; mmette@usgs.gov
[2] Iowa State University, Department of Geological and Atmospheric Sciences, Ames, Iowa; adw@iastate.edu
[3] Akvaplan-niva, FRAM – High North Research Centre for Climate and the Environment, Tromsø, Norway;
[4] School of the Coastal Environment, Coastal Carolina University, South Carolina, USA; wambrose@coastal.edu
[5] University Centre in Svalbard (UNIS), Longyearbyen, Norway; Bates College, Department of Geology, Lewiston, Maine, USA; mretelle@bates.edu
[6] NORCE Norwegian Research Centre, Bjerknes Centre for Climate Research, Bergen, Norway; caan@norceresearch.no

The mild climate of northern Europe and Scandinavia relative to other regions at similar latitudes is partly attributed to the northward transport of warm ocean water from the Gulf Stream and North Atlantic Current and resulting ocean-atmospheric heat exchange. The past behavior of this marine variability at high-frequency timescales (i.e., annual), however, is often inferred through terrestrial proxy records, most notably, tree rings. Recent development of annually resolved proxy records from bivalve shells provides a marine counterpart to tree-ring records, and an opportunity to assess the coupling between marine and terrestrial climate in coastal regions. This study presents a newly produced, annually resolved, multicentury sea-surface temperature reconstruction using d18Oshell of the marine bivalve, Arctica islandica, from coastal northern Norway. The record is positively correlated with a Fennoscandian summer temperature reconstruction using a composite of tree ring records (1539-2005; Pearson rannual = 0.33; $p < 0.001$). A combined record of d18Oshell and shell growth also captures the decadal-scale variability at lower latitudes as characterized by the Atlantic Multidecadal Variability index (1880-2012; rannual = -0.44; rsmoothed_7yr = 0.71; $p < 0.001$; increasing correlations up to a six-year lag). These results enable insight into Arctic-Atlantic marine and terrestrial coupling through time and highlight the potential to strengthen regional marine climate syntheses using shell-based records.

Episodic cryosphere expansion in Arctic Canada during the Common Era reinforced by repeat dating of entombed plants and supported by climate model simulations

Miller, Gifford [1]; **Pendleton**, Simon [2]; **Lehman**, Scott [3]; **Jahn**, Alexandra [4]; **Zhong**, Yafang [5]; **Geirsdóttir**, Áslaug [6]

[1] University of Colorado; gmiller@colorado.edu
[2] WHOI; spendleton@whoi.edu
[3] INSTAAR; scott.lehman@colorado.edu
[4] INSTAAR; alexandra.jahn@colorado.edu
[5] University Wisconsin Madison; yafangzhong@wisc.edu
[6] University of Iceland; age@hi.is

Portions of most small ice caps in low-relief Arctic landscapes remained cold-based since their inception during the Holocene. As a result, they preserve *in situ* tundra plants that were killed as ice expanded across vegetated landscapes. As summers warmed in recent decades, ice caps in the Eastern Canadian Arctic have receded rapidly, typically 10 to 20 m a^{-1}, exposing entombed plants.

In an earlier study we reported 37 radiocarbon dates on *in situ* dead moss collected at the ice edge in 2005 from two plateau ice complexes on northern Baffin Island. Tight clustering of those ages indicated an abrupt onset of the Little Ice Age around 1280 and 1450 CE, coincident with episodes of major explosive volcanism.

We resampled those ice complexes in 2018 and 2019, by which time they had receded 150 to 250 m. We obtained 59 new radiocarbon dates on ice-edge *in situ* moss collected at the current ice margins. The new dates cluster in the same time windows as the earlier age clusters, but contain more ages from early in the Common Era. Relict ice from earlier Neoglacial ice expansions preserved beneath younger ice growth is apparent in imagery and in the ages of entombed plants, indicating incomplete past ice recession and subsequent reglaciation.

The composite probability density function of those 105 calibrated ages on entombed plants are restricted to three time windows: 335 ± 95 yr CE, 885 ± 110 yr CE, and a large cluster between 1215 and 1485 CE with peaks ~1285 and ~1440 CE. These three time windows define times of widespread cryosphere expansion coincide with the three most significant decreases in mean summer surface air temperature for the Baffin-Greenland region in a 2000-year CESM-2 simulation, enhanced by explosive volcanism, suggesting primary forcing from both declining summer insolation and positive feedbacks on cooling resulting from explosive volcanism.

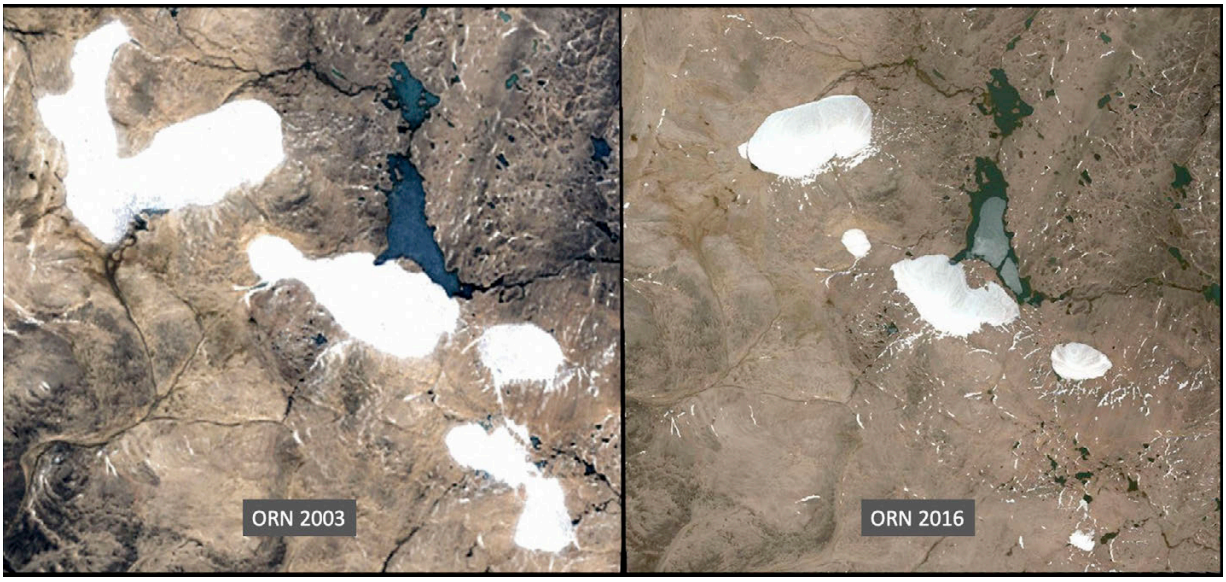

Fig 1. The Orion Ice Complex (unofficial name) at about 800 m asl on northernmost Baffin Island, Arctic Canada; ice caps occupy about 15 km length in the 2003 image. Ice-entombed plants were collected around all but the southernmost ice caps in 2005; 2018 collections were located as close to orthogonal to the 2005 ice margin as possible. Digital Globe imagery.

The Arctic Rivers Project: A co-produced assessment of the climate sensitivity of Alaskan & Yukon rivers, fish, and Indigenous communities

Musselman, Keith N. [1]; **Herman-Mercer**, Nicole [2]; **Newman**, Andrew J. [3]; **Koch**, Joshua C. [4]; **Brooks**, Cassandra [5]; **Gooseff**, Michael [6]; **Cozzetto**, Karen [7]; **Mutter**, Edda [8]

[1] INSTAAR, CU Boulder; keith.musselman@colorado.edu
[2] US Geological Survey;
[3] National Center for Atmospheric Research;
[4] US Geological Survey;
[5] CU Boulder;
[6] INSTAAR, CU Boulder;
[7] Institute for Tribal Environmental Professionals;
[8] Yukon River Inter-tribal Watershed Council;

We present ongoing efforts of the Arctic Rivers Project, an exciting collaboration among the Institute of Arctic and Alpine Research (INSTAAR) at the University of Colorado Boulder (CU), the US Geological Survey (USGS), the National Center for Atmospheric Research (NCAR), the Yukon River Inter-Tribal Watershed Council (YRITWC), the Institute for Tribal Environmental Professionals (ITEP) at Northern Arizona University (NAU), University of Saskatchewan, and University of Waterloo. The project goal is to increase collective understanding of the impacts of climate change on rivers, fish, and Indigenous communities across Northern Alaska and the Yukon River Watershed in Alaska and Canada. This is accomplished through water-quality monitoring, multidisciplinary modeling activities, and the development of narratives of change from community members themselves. Combined, our methods are being used to craft storylines of climate change in the arctic. Storylines combine experiential narrative information with diverse model output to make the predicated future more tangible regarding potential impacts. The project team is comprised of researchers from the natural and social sciences as well as the modeling community and two Indigenous organizations focused on science, outreach, and engagement. To increase the research team's ability to co-produce knowledge with Indigenous communities across a large study domain, we have formed and work closely with an Indigenous Advisory Council (IAC) comprised of 11 Indigenous community members, leaders, elders and students representing diverse communities across our study domain. Strong collaboration with Tribal and First Nation communities, community-based science networks, and environmental professionals guide the science and facilitate monitoring and modeling as part of this project. As the Arctic and its rivers continue to warm, the impacts on people, their fisheries, and winter travel routes are unknown. Better understanding of the possible future changes requires close partnership among Native communities and scientists from diverse fields of study.

Understanding resilience and long-term environmental change in the High Arctic: Narrative-based analyses from Svalbard (SVALUR)

Ogilvie, Astrid E.J. [1]; **Miles**, Martin [2]; **van der Wal**, René [3]; **Löf**, Annette [4]

[1] INSTAAR, CU-Boulder and Stefansson Arctic Institute, Akureyri, Iceland; astrid.ogilvie@colorado.edu
[2] NORCE Norwegian Research Centre, Bjerknes Centre for Climate Research, Bergen, Norway and INSTAAR, CU-Boulder; Martin.Miles@colorado.edu
[3] Swedish University of Agricultural Sciences (SLU), Uppsala, Sweden; rene.van.der.wal@slu.se
[4] Swedish University of Agricultural Sciences (SLU), Uppsala, Sweden; annette.lof@slu.se

The project "Understanding Resilience and Long-Term Environmental Change in the High Arctic: Narrative-Based Analyses from Svalbard (SVALUR)" focuses on the Norwegian archipelago of Svalbard in the Arctic Ocean as an ideal site for learning what resilience may mean when short-term residency, compromising place-based knowledge generation, is the norm. SVALUR means "cool" or "cold" in Icelandic and the project may be seen in the context of the profound changes taking place in the world's most northern biome. Because of these changes, environmental monitoring in the Arctic is more urgent than ever. Investments made to capture both current state and changes in the natural environment are extensive; however, the locations at which such monitoring takes place are few, and, with the exception of monitoring of weather and climate conditions, cover relatively short periods of time (1–2 decades). More importantly, environmental monitoring typically concerns highly specific parameters and thus fails to generate the holistic understanding needed for interpreting and responding to change. Environmental understanding held by people living, working in, and exploring extreme environments in the Arctic is, by contrast, multifaceted and relational, and can relate to shorter as well as longer periods of time (Berkes and Berkes, 2009). In order to contribute to such issues, the SVALUR project was submitted to the Belmont Forum call of 2019 (in association with other funding bodies including the National Science Foundation of the USA) which emphasised the Exploration and Explanation of Resilience in Rapidly Changing Arctic Systems (https://www.belmontforum.org/news/arctic-announcement).

Svalbard's history of human use and habitation began in the 18th and 19th centuries when it was an important focus of the whaling industry. Subsequently, coal mining settlements were established. In 1925, the "Svalbard Treaty" came into effect and granted Norway sovereignty of the archipelago. In more recent times, there has been an increased focus on scientific endeavours. In 2016, Svalbard had a population of 2,667, primarily Norwegians, but of the total there were 423 Russians and Ukrainians, 10 Polish and 322 other non-Norwegian residents. Svalbard thus lacks Indigenous communities steeped in traditions and rich in the knowledge of human-nature relationships built up over many generations. Instead, current society is mostly fluid, with people living on Svalbard for several years to then return to their respective home countries, to continue their former lives. SVALUR is innovative in that it aims to draw upon the environmental understanding of people currently living, working and

exploring in the region. Compared with scientific monitoring, such knowledge is rarely utilized, thus hindering knowledge generation and use in Arctic areas subject to rapid environmental change. SVALUR aims for transdisciplinarity through the inclusion of stakeholders and societal actors and by using co-production of knowledge to directly share understanding of environmental and other changes with both local inhabitants and visitors (tourists and scientists). Emphasis is on the three permanent settlements on Svalbard, all located on the west coast of the island of Spitsbergen: Longyearbyen, Barentsburg and Ny-Ålesund. The surroundings of these localities, together with Hornsund, are where monitoring efforts are focused. Here we are mapping out the results of long-term monitoring of climate (atmosphere, land and ocean) and marine and terrestrial ecosystems, to be compared with narratives of environmental changes from scientists and other residents.

The overarching research approach of SVALUR is thus to generate a holistic understanding of environmental change based on a variety of tools and methods and to develop these through a complementary partnership of project team members and stakeholders. This will be achieved through: i) employing methods including in-depth interviews, document analysis and web-based story mapping; ii) comparison of resultant information with environmental monitoring data in terms of overlap and potential synergies; iii) engaging in two-way communication between the project team and inhabitants and visitors to Svalbard regarding shared understanding of what resilience may mean when short-term residency, compromising place-based knowledge generation, is the norm; and iv) facilitating the mobilization of such knowledge in order that stakeholders have the opportunity to become more active agents for change. Because of the Covid-19 pandemic it has not been possible to make planned research visits to Svalbard so the project focus has shifted to concentration on meetings and consultations that can take place virtually.

SVALUR findings will provide valuable, holistic insights into long-term environmental change based on 'living memory', whilst at the same time pinpointing how current monitoring programmes can become more relevant to people's experiences and optimize their importance to people living in and visiting the High Arctic. Bringing together perceptions of environmental change derived from monitoring and narratives is pertinent to any part of the Arctic (Moezzi et al, 2017; Paschen and Ison, 2014). However, it is essential to focus on local conditions in order to contribute more meaningfully to the global whole. The increasing levels of transience throughout the Arctic make developing ways in which narrative-based understanding can complement scientific monitoring even more pressing. SVALUR will derive research methods that are holistic and co-owned, and vital for the wellbeing of both current and future generations, as well as for policy and decision-making. In short, SVALUR will: i) advance the understanding of Arctic resilience and long-term environmental change; ii) inform decision making; and iii) translate the understanding that is gained into solutions for resilience. The project team is highly interdisciplinary, and covers a wide range of focus areas, including: Arctic ecology; climatology and sea-ice studies; environmental history; resilience studies; regional environmental change; environmental governance studies; environmental

communication; and environmental humanities. SVALUR is led by René van der Wal, Arctic ecologist, of the Swedish University of Agricultural Sciences (SLU) with Astrid Ogilvie and Martin Miles representing the Instititute of Arctic and Alpine Research (INSTAAR) at the University of Colorado, Boulder, USA. For more information on the project and details of the other team members see https://www.slu.se/svalur. The project also cooperates closely with the Svalbard Social Science Initiative (SSSI) see https://svalbardsocialscience.com/.

Berks, F. and Berks, M.K., 2009, Ecological complexity, fuzzy logic, and holism in indigenous knowledge: Futures, v. 41, p. 6-12.

Moezzi, M. Janda, K.B. and Rotmann, S., 2017, Using stories, narratives, and storytelling in energy and climate change research: Energy Research and Social Science, v.31, p.1-10.

Paschen, J.-A. and Ison, R., 2014, Narrative research in climate change adaptation—Exploring a complementary paradigm for research and governance: Research Policy, v.43, p.1083-1092.

Fig 1. Svalbard sea ice. Photograph courtesy of Zdenka Sokolícková and Jakub Zarsky.

Fig 2. Longyearbyen, Svalbard. Photograph courtesy of Zdenka Sokolícková and Jakub Zarsky.

Fig 3. Coal harbour, Svalbard. Photograph courtesy of Zdenka Sokolícková and Jakub Zarsky.

Torrent or trickle?: Tracking glacial lake evolution and flood events using composite lake records

Pendleton, Simon [1]; **Donnelly**, Jeffrey [2]; **Kurz**, Mark D [3]; **Condron**, Alan [4]

[1] Woods Hole Oceanographic Institution; spendleton@whoi.edu
[2] Woods Hole Oceanographic Institution; jdonnelly@whoi.edu
[3] Woods Hole Oceanographic Institution; mkurz@whoi.edu
[4] Woods Hole Oceanographic Institution; acondron@whoi.edu

Glacial meltwater inputs have long been hypothesized to weaken Atlantic Meridional Overturning Circulation (AMOC) leading to Northern Hemisphere cooling, particularly during deglaciation from the last glacial period. While much work has been done to constrain the timing and magnitude of meltwater inputs during deglaciation as well as their potential impacts on AMOC, less is known regarding the effect of meltwater input event duration and/or frequency. For example, recent numerical modeling by our group that performed a large suite of simulations to examine a variety of potential drainage scenarios for Lake Iroquois (e.g., high flux short-duration, low discharge long-duration, multiple floods) showed that with existing constraints on the total volumes of meltwater, the drainage of this lake was unlikely (without significant additional climatic forcings) to have been the main driver of the Intra-Allerød Cold Period. However, the impact of Lake Iroquois flood duration and frequency, particularly in combination with contemporaneous meltwater inputs or other circulation mechanisms remains unknown. As a step toward filling this knowledge gap, here we report on new efforts to constrain the timing, duration, and frequency of glacial meltwater flood events originating from glacial Lake Iroquois, which entered the North Atlantic through the paleo-Hudson Valley sometime around ~13.2 ka.

Initial seismic surveys of modern lakes across Lake Iroquois paleo-shorelines in northwestern New York State indicate higher density, laminated sediments overlain by lower density, more homogenous sediments, separated by an abrupt transition (Fig. 1). Pilot cores from several lakes confirm this stratigraphy with higher density silt and clay sequences overlain by lower density gyttja. This stratigraphy supports glacial lake sedimentation when the modern lake was part of the larger Lake Iroquois, transitioning to lower density gyttja deposited after the modern lake was isolated by lake level lowering associated with Lake Iroquois drainage. This transition from glacial lake to non-glacial lake sedimentation is seen in pilot cores from additional lakes in a transect to the northwest, in each case marked by a sharp increase in organic content as well as changes in multiple geochemical proxies. In Lake Bonaparte (Fig. 1) radiocarbon dating of preserved macrofossils provides age control for the younger, non-glacial lake sequence. However, the lack of macrofossils in the older glacial lake sequence and scatter in bulk sediment ^{14}C ages prevents precise ^{14}C constraint of the transition from glacial lake to non-glacial lake sedimentation. However, varves in the glacial lake sequence were correlated to established varve chronologies in New England providing age control below the glacial lake to non-glacial lake transition. A composite age model of ^{14}C and

varve chronology constrains the transition to 13.2 ± 0.4 ka, within the range of existing age control on the initial flood event from Lake Iroquois.

Short pilot cores from additional lakes contain limited glacial lake sequences with no identifiable varves. Upon retrieval of cores capturing longer glacial lake sequences from all lakes, we aim to cross-correlate individual varve sequences (present in the seismic data) to compile a composite chronology across the Lake Iroquois paleoshoreline features, capturing the evolution of Lake Iroquois from its largest phase up to the marine incursion in the St. Lawrence Valley that followed the demise of the Lake (Fig. 1). Correlation of the varve sequences between lakes and the annual nature of varve deposition provides the best opportunity to generate a high-resolution chronology of lake-level lowerings associated with Lake Iroquois meltwater flood events. This approach will provide new constraints on the absolute timing as well as the frequency and range of possible durations of these flood events.

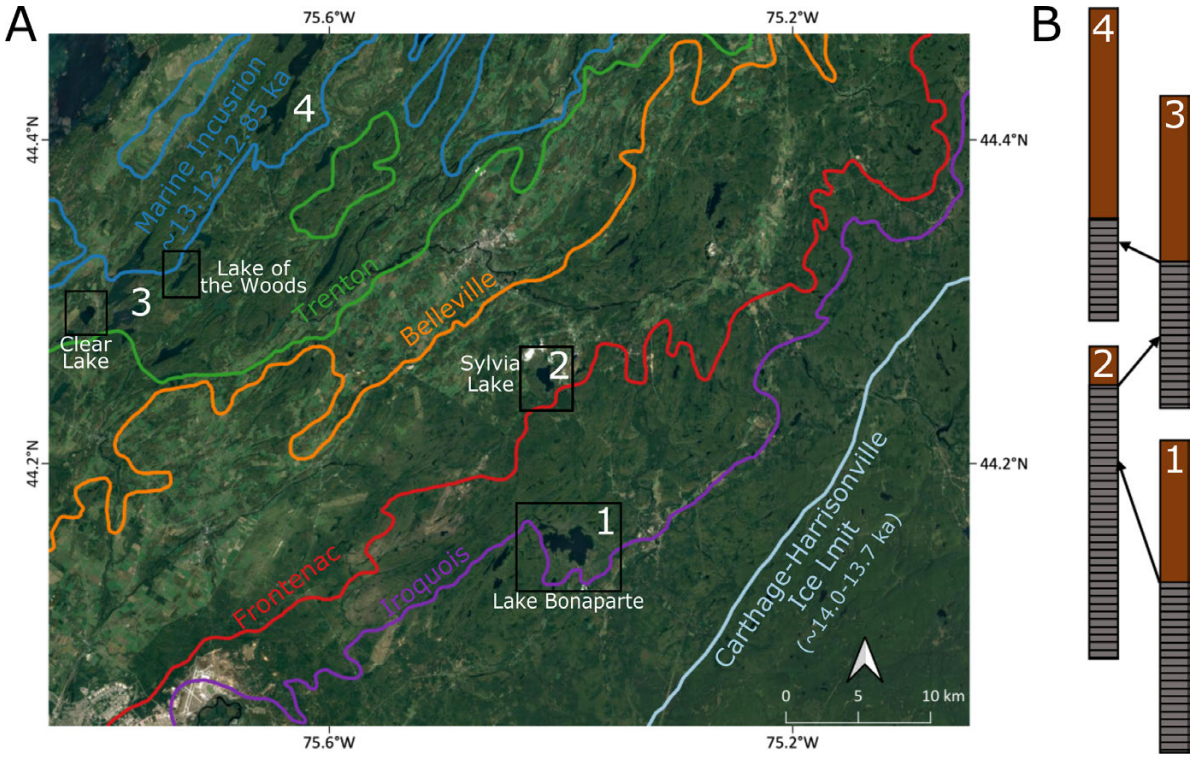

Fig 1. Map of target lakes in northwestern New York state. A) shows the pre-lake Iroquois Laurentide Ice Sheet margin (light blue line) as well as the limit of the marine incursion (dark blue line) following the final drainage of Lake Iroquois. Other colored lines denote the location of identified paleoshoreline features. Pilot cores already retrieved from four lakes (black boxes) each contain the transition from glacial lake to non-glacial lake sedimentation. B) A schematic illustrating the proposed cross-correlation between target lakes (white numbers) to generate a composite varve chronology of the evolution of Lake Iroquois and its drainage events.

Cyclic patterns in Quaternary deposits on the Northwind Ridge, western Arctic Ocean: glacial vs. marine signature

Polyak, Leonid [1]; **Dipre**, Geoffrey [2]; **Wang**, Rong [3]

[1] Ohio State University; polyak.1@osu.edu
[2] Ohio State University; geoffdipre@gmail.com
[3] Second Institute of Oceanography, China; rongwang@sio.org.cn

Despite the amplified reaction of the Arctic to climate changes, paleoclimatic cyclicity in sediment records from the Arctic Ocean is poorly understood. Identification of cyclic patterns is complicated by overall low sedimentation rates and poor age constraints, especially in sediments preceding the onset of major Arctic glaciations. We investigate paleoceanographic proxies in sediment cores from the Northwind Ridge, western Arctic Ocean north of Alaska, to identify the dominant long-term cyclicities that affected this part of the Earth during the Quaternary. Based on their proximity to the Laurentide Ice Sheet (LIS) and the depth range encompassing the Atlantic Intermediate Water (AIW) (Fig. 1), these cores are well suited for investigating major paleoclimatic changes. Some of the northernmost cores contain uniquely abundant calcareous microfossils providing material for better age constraints extending to the Early Quaternary and possibly Pliocene, although with large hiatuses (Dipre et al., 2018).

Due to the improved age framework, we recognize for the first time long-eccentricity (~400-kyr) cycles in the Arctic Ocean sedimentary proxies, expressed notably in the visually homogenous pre-glacial deposits (Early Quaternary, ca. 0.8 ? 2.6 Ma) (Fig. 2). After tuning the strongest signal identified in benthic ?13C data to the global records, we attribute these cycles to pulses of intensified AIW circulation, which presumably occurred in pre-glacial times during periods of sea level lowstand and closed Bering Strait. These intervals are characterized by sandier sediment, lower manganese content, and higher ?13C. This cyclicity pattern is consistent with intense ~400-kyr cycles in the monsoonal activity and global ice volume phase-locked to eccentricity forcing in the Pliocene to Early Quaternary (Nie, 2018). The onset of this cyclicity has been related to a change in the ocean circulation due to the Early Pliocene closure of the Panama Seaway. Our data indicate that this change affected the Arctic Ocean, probably by way of an intensified North Atlantic current continuing into the Arctic at mid-depths. At the Mid-Pleistocene Transition this circulation was presumably suppressed by the outflow of meltwater from the expanding Arctic ice sheets.

In contrast to the pre-glacial pattern outlined above, the Middle to Late Quaternary sediments on the Northwind Ridge are predominated by a distinct interlamination of glacial and interglacial-type facies (Dipre et al., 2018; Wang et al., 2021). Furthermore, the variability of proxies changes dramatically with the onset of glacial conditions, e.g., ?13C values get higher in the interglacial intervals corresponding to higher sea levels. This change indicates different paleoclimatic controls on the proxy distribution in the pre-glacial vs. glacially-dominated environments. Preliminary estimates suggest that the leading cyclicities in the

Middle-Late Quaternary sediments are in the ~20-100-kyr range, consistent with other Arctic records interpreted to indicate glacial and, possibly, sea-ice controls (e.g., Xiao et al., 2020). However, the obliquity-leaning signal on the Northwind Ridge is more pronounced than in other cores, suggesting a potentially stronger obliquity control on the Arctic LIS margin drained by very large, marine-based ice streams (Fig. 1). Cores with relatively higher sedimentation rates closer to the shelf also show signs of sub-Milankovich variability, possibly reflecting millennial-scale cyclicity in the LIS ice streaming. This pattern, however, could have been asynchronous as indicated by a complex record of glacial provenance proxies (Wang et al., 2021).

Dipre, G.R., Polyak, L., Kuznetsov, A.B., et al., 2018, Plio-Pleistocene sedimentary record from the Northwind Ridge: new insights into paleoclimatic evolution of the western Arctic Ocean for the last 5 Ma: Arktos, v. 4, 24.

Nie J., 2018, The Plio-Pleistocene 405-kyr climate cycles: Palaeogeogaphy., Palaeoclimatology, Palaeoecoogy., v. 510, p. 26–30.

Wang, R., Polyak, L., Zhang, W., 2021, Glacial-interglacial sedimentation and paleocirculation at the Northwind Ridge, western Arctic Ocean: Quaternary Science Reviews, v. 258, 106882.

Xiao, W., Polyak, L., Wang, R., et al., 2020, Middle to late Pleistocene Arctic paleoceanographic changes based on sedimentary records from Mendeleev Ridge and Makarov Basin: Quaternary Science Reviews, v. 228, 106105.

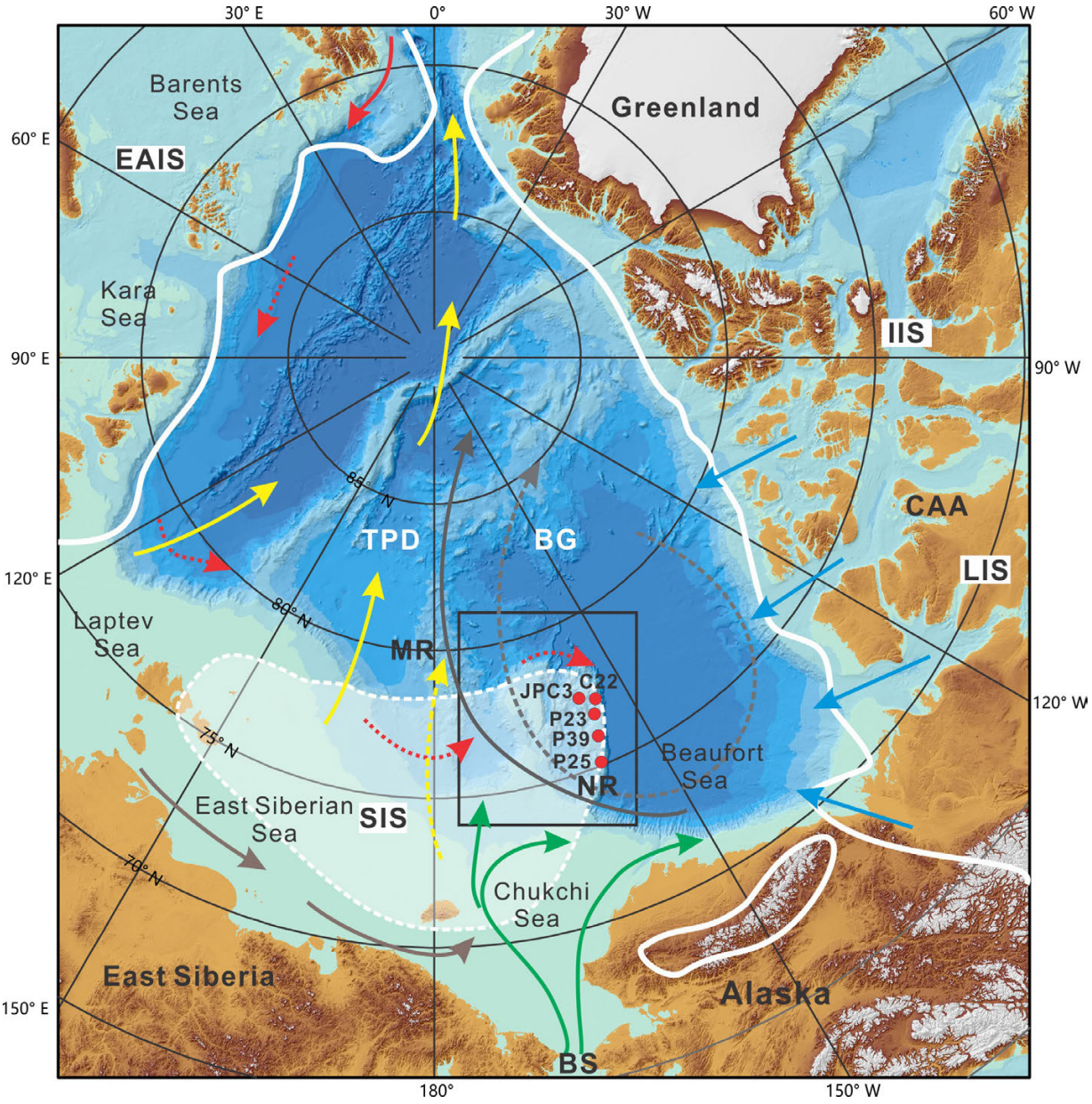

Fig 1. Index map. Yellow and gray arrows - major surface circulation features: Transpolar Drift (TPD) and Beaufort Gyre (BG) shown in two Arctic Oscillation modes. Red, green, and brown arrows - Atlantic, Pacific, and Siberian Coastal currents. Dotted red arrows - Atlantic Intermediate Water. White outlines show inferred maximum Pleistocene extent of Eurasian (EAIS), Siberian (SIS), Laurentide (LIS), and Innuitian (IIS) ice sheets. Blue arrows - major LIS/IIS ice streams. NR, MR - Northwind and Mendeleev ridges; BS - Bering Strait; CAA - Canadian Arctic Archipelago.

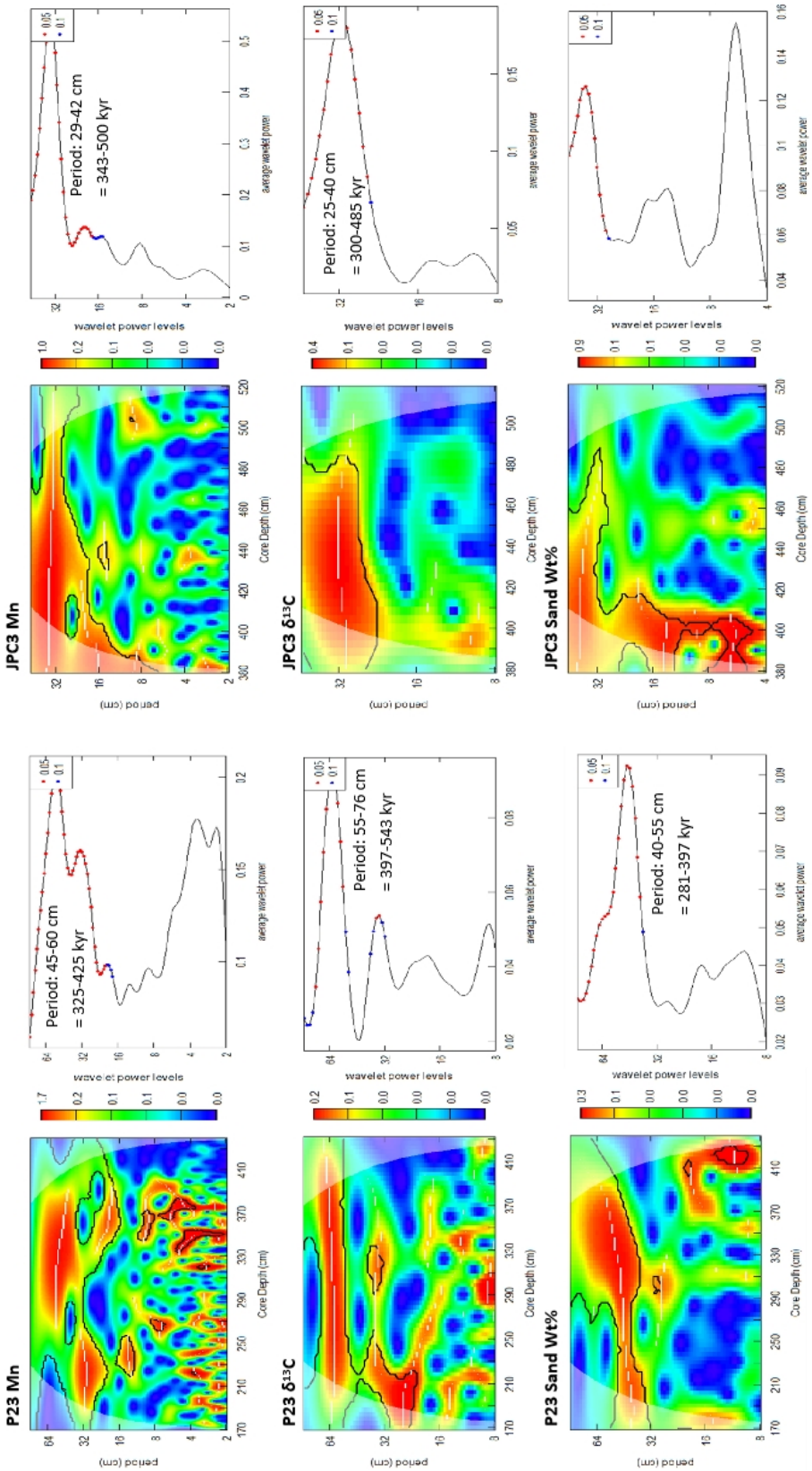

Fig 2. Wavelet analysis identifies dominant ~400-kyr cycles in the Early Quaternary (ca. 0.8-2.6 Ma) in cores P23 and JPC3: Mn, benthic foraminiferal d13C, and sand content. Cone of Influence is identified by white shading; black contours represent 10% significance level; white lines represent wave ridge. Right panels show the average wavelet power and the periods that are statistically significant at the 0.05 (red dots) and 0.1 (blue dots) levels.

Detection of a marine to terrestrial transition in lake sediment from Baffin Island, Arctic Canada, using sedimentary DNA

Power, Matthew [1]; **Crump**, Sarah E [2]; **Miller**, Gifford H [3]; **Bunce**, Michael [4]; **Allentoft**, Morten [5]

[1] Trend Laboratory, School of Molecular and Life Sciences, Curtin University, Australia; matthew.w.power@curtin.edu.au
[2] Paleogenomics Lab, University of California Santa Cruz, USA; Sarah.Crump@Colorado.EDU
[3] Institute of Arctic & Alpine Research, University of Colorado Boulder, USA; gmiller@colorado.edu
[4] Environmental Protection Authority, New Zealand; Michael.Bunce@epa.govt.nz
[5] Trend Laboratory, School of Molecular and Life Sciences, Curtin University, Australia; morten.allentoft@curtin.edu.au

The recent development and refinement of the molecular toolkit to detect ancient DNA in sediment samples (sedaDNA) has allowed the high-resolution reconstruction of ancient ecological communities dating back thousands of years. Specifically, DNA from lake sediment has been used to derive continuous records of ecological community changes through variable paleoenvironmental conditions. These paleoecological reconstructions can be an important tool for understanding how ecosystems may respond to current and future warming, but reliable methods for taxonomic detection are needed in order make optimal use of these bioarchives. In this study, metabarcoding assays targeting vertebrates, bird, and marine fauna have been carried out across a sediment core collected from Lake Qaupat, Baffin Island, Arctic Canada. While Lake Qaupat is currently ~30 m above sea level, it is located below the local marine limit related to isostatic adjustment after deglaciation. Consequently, initial sediment accumulation is in a marine environment. Combined results from the DNA assays indicate a transitional period over which marine-based fauna are systematically replaced by more terrestrial-based fauna. This transition occurs at a predicted age of 7.4 ± 0.2 ka. Ultimately, these data showcase the power of sedaDNA to document dramatic ecosystem changes through a major relative sea level change in the past, with implications for ecological responses to future sea level change.

Comparison of early twentieth century Arctic warming and contemporary Arctic warming in the light of daily and sub-daily data

Przybylak, Rajmund [1]; **Wyszynski**, Przemyslaw [2]; **Arazny**, Andrzej [3]

[1] Nicolaus Copernicus University, Faculty of Earth Sciences and Spatial Management and Centre for Climate Change Research; rp11@umk.pl
[2] Nicolaus Copernicus University, Faculty of Earth Sciences and Spatial Management and Centre for Climate Change Research; Przemyslaw.Wyszynski@umk.pl
[3] Nicolaus Copernicus University, Faculty of Earth Sciences and Spatial Management and Centre for Climate Change Research; andy@umk.pl

A summary of a large number of studies conducted since the late 1920s reveals that there is still no definite explanation of the main driving mechanisms responsible for the Early Twentieth Century Arctic Warming (ETCAW). Limited knowledge about the climate of this period, and about some forcings, seems to be the main obstacle to reaching the goal. What is required is better knowledge based on data of resolution that is greater than monthly, i.e. daily and sub-daily. The main objective of this article is to provide a comprehensive description of surface air temperature (SAT) conditions in the Arctic during the ETCAW using available long-term series of daily and sub-daily data taken from five meteorological stations representing main climatic regions in the Arctic. Four thermal parameters from 10 years were used for this purpose: mean daily air temperature, maximum and minimum daily temperature, and diurnal temperature range. Analysis of rarely investigated aspects of SAT characteristics (e.g.: number of characteristic days; day-to-day temperature variability; and onset, end and duration of thermal seasons) was also conducted. The results were compared with analogical calculations done for data taken from the Contemporary Arctic Warming (CAW) period (2007–16). The Arctic showed an increase in mean annual SAT between the ETCAW and the CAW with the greatest magnitude in the Pacific (2.7 °C) and Canadian Arctic (1.9 °C) regions and the smallest (0.2 °C) in the Baffin Bay region. Climate continentality in the Arctic was usually 1–4% greater during the ETCAW than during the CAW, except in the Siberian region.

The study was carried out as a part of the scientific project entitled “Causes of the early 20th century Arctic warming”, funded by the National Science Centre, Poland (Grant No. 2015/19/B/ST10/02933), and the Research University – Initiative of Excellence: the Emerging Field “Global Environmental Changes”, "Climate Change Research Unit" at Nicolaus Copernicus University in Toru?. 20th Century Reanalysis V3 data was provided by the NOAA/OAR/ESRL PSL, Boulder, Colorado, USA, from their website https://psl.noaa.gov/data/gridded/data.20thC_ReanV3.html. Support for the Twentieth Century Reanalysis Project version 3 dataset is provided by the U.S. Department of Energy, Office of Science Biological and Environmental Research (BER), by the National Oceanic and Atmospheric Administration Climate Program Office, and by the NOAA Physical Sciences Laboratory.

Extending brGDGT-based paleoclimate proxies to high latitudes

Raberg, Jonathan H [1]; **Harning**, David J [2]; **Crump**, Sarah E [3]; **de Wet**, Greg [4]; **Blumm**, Aria [5]; **Kopf**, Sebastian [6]; **Geirsdóttir**, Áslaug [7]; , et al. [8]

[1] University of Colorado Boulder and INSTAAR, University of Iceland; jonathan.raberg@colorado.edu
[2] University of Colorado Boulder and INSTAAR, University of Iceland; david.harning@colorado.edu
[3] University of Colorado Boulder and INSTAAR; secrump@ucsc.edu
[4] University of Colorado Boulder and INSTAAR; gdewet@smith.edu
[5] University of Colorado Boulder and INSTAAR; blumm@email.arizona.edu
[6] University of Colorado Boulder and INSTAAR; Sebastian.Kopf@colorado.edu
[7] University of Iceland; age@hi.is
[8];

Paleotemperature records from lake sediment archives are highly sought after in studies of high latitude terrestrial paleoclimate. Branched glycerol dialkyl glycerol tetraether (brGDGT) lipids have solidified themselves as an important tool in this pursuit. Although brGDGTs are globally ubiquitous, the bacterial producers of these membrane lipids remain poorly identified, precluding a full understanding of the ways in which a range of environmental parameters control their production and distribution.

Mean annual air temperature (MAT) has been the traditional target of brGDGT calibrations in lake sediments. However, it was recognized early on that brGDGT-derived temperatures in cold regions may more accurately reflect warm-season temperatures, an hypothesis that was strongly supported in high-latitude lake sediments (e.g. Shanahan et al., 2013). Since the methodological advances that allowed for the separation of brGDGT isomers and the development of new calibrations, both modern and paleo studies have continued to support a warm-season bias. Additionally, a recent Bayesian calibration found the mean temperature of Months Above Freezing (MAF, which is increasingly close to MAT at lower latitudes) to be the only mode to significantly correlate with brGDGT distributions in a global lake sediment dataset (Martínez-Sosa et al., 2020). However, this warm-season bias has yet to be tested thoroughly in the regions in which it is most pronounced – namely, those with low MAT and high seasonality. As these are the regions that are currently experiencing the most rapid climate change, their temperature histories are of high interest and the quantification of the brGDGT warm-season bias is an important target of study.

Here, we outline the results of new work (Raberg et al., 2021) that advances brGDGT paleoclimate proxies in three ways. First, we present 43 new high-latitude lake sites from the Eastern Canadian Arctic and Iceland that are characterized by low mean annual air temperatures (MATs) and high seasonality, filling an important gap in the global dataset. Second, we introduce a new approach for analyzing brGDGT data in which compound fractional abundances (FAs) are calculated within structural groups based on methylation number, methylation position, and cyclization number. Finally, we perform linear and nonlinear regressions of the resulting FAs against a suite of environmental parameters in a compiled global lake sediment dataset (n = 182). We find that our approach deconvolves

temperature, lake water conductivity, and pH trends in brGDGTs without increasing calibration errors from the standard approach. We also find that it reveals novel patterns in brGDGT distributions and provides a methodology for investigating the biological underpinnings of their structural diversity. Warm-season temperature indices outperformed MAT in our regressions, with MAF yielding the highest-performing model (adjusted R2 = 0.91, RMSE = 1.97°C, n = 182). The natural logarithm of conductivity had the second-strongest relationship to brGDGT distributions (adjusted R2 = 0.83, RMSE = 0.66, n = 143), notably outperforming pH in our dataset (adjusted R2 = 0.73, RMSE = 0.57, n = 154) and providing a potential new proxy for paleohydrology applications. We recommend these calibrations for use in lake sediments globally, including at high latitudes, and detail the advantages and disadvantages of each.

Martínez-Sosa, P., Tierney, J.E., Stefanescu, I.C., Dearing Crampton-Flood, E., Shuman, B.N., Routson, C., 2020. A global Bayesian temperature calibration for lacustrine brGDGTs. EarthArXiv [preprint]. doi:https://doi.org/10.31223/X5PS3P

Raberg, J., Harning, D., Crump, S., de Wet, G., Blumm, A., Kopf, S., Geirsdóttir, Á., Miller, G., Sepúlveda, J., 2021. Revised fractional abundances and warm-season temperatures substantially improve brGDGT calibrations in lake sediments. Biogeosciences Discussions 1–36. doi:https://doi.org/10.5194/bg-2021-16

Shanahan, T.M., Hughen, K.A., Van Mooy, B.A.S., 2013. Temperature sensitivity of branched and isoprenoid GDGTs in Arctic lakes. Organic Geochemistry 64, 119–128.

Vegetation around six lakes along a climate gradient in Baffin Island

Raynolds, Martha K [1]; **Bültmann**, Helga [2]; **Kasanke**, Shawnee [3]; **Raberg**, Jonathan [4]; **Miller**, Gifford [5]

[1] Institute of Arctic Biology, University of Alaska Fairbanks; mkraynolds@alaska.edu
[2] University of Münster, Germany; bultman@uni-muenster.de
[3] Washington State University Tri-Cities; shawnee.kasanke@wsu.edu
[4] INSTAAR, University of Colorado Boulder; jonathan.raberg@colorado.edu
[5] INSTAAR, University of Colorado Boulder; gmiller@colorado.edu

The eastern Canadian Arctic encompasses the entire Arctic bioclimate gradient, from treeline to ice caps. We sampled and mapped the vegetation around a series of lakes along this gradient. Vegetation plots were sampled around the lakes, and cover values were recorded by species for lichens, bryophytes and vascular plants, and plant communities were identified for mapping. The maps show a 1-km^2 area around the lakes, using a consistent legend, so that vegetation units can be compared between lakes. The lakes include one near Pond Inlet, Baffin Island, Nunavut (next to an ice cap, 72.4 °N), one near Clyde River, two in the Merchant's Bay area, one near Iqaluit, and one near Kuujjuaq, Nunavik, Quebec (at treeline 58.1°N) (Fig. 1).

The vegetation types ranged from rocky barrens with lichens to open spruce forest with low shrub and moss understory. The northernmost lake, AFR, has only recently become ice-free in the summer time. Summer warmth index, the sum of monthly average temperatures above 0 °C is only 0.6 °C (Fig. 2), with July the only month averaging above 0.0 °C. This is in the coldest bioclimate subzone in the Arctic, Bioclimate Subzone A (CAVM Team, 2003). One of the findings of this study was the importance of aquatic mosses in these arctic areas - at AFR they far outweigh the biomass of the terrestrial vegetation.

The next two lakes, BRO and CF8, had SWIs between 10 and 15 °C, Bioclimate Subzone C. BRO is in a mostly barren, steep landscape, with some prostrate dwarf-shrubs. The landscape around CF8 also had large barren areas, but also had patches of moist graminoid, cryptogam tundra, dominated by *Luzula* spp. (rushes) and liverworts.

The warmer arctic lakes, BIR and QPT, had SWI values around 25 °C, putting them in Bioclimate Subzone E. These temperatures are warm enough to support birch shrubs > 40 cm in height. Most of the landscape was vegetated, with a mix of moist erect dwarf-shrub tundra on rocky substrates, and moist graminoid, dwarf-shrub tundra on finer substrates.

The lake south of treeline (in the Boreal bioclimate zone, not Arctic), 3LN, had an SWI of 36.2 °C and a mean July temperature of 11.9 °C. Both of these values are warmer than the expected arctic maxima (35 °C SWI and 10 °C MJT (CAVM Team, 2003)), confirming these southern bioclimate limits for the Arctic. The landscape around this lake included glaciated ridges with vegetation between the bedrock outcrops, open spruce-larch forest with low shrubs and moss understory, and even some peat palsas.

These maps will be used to compare current vegetation with evidence of past vegetation found in cores from the lakes, which include times both warmer and colder than present (Crump et al. 2021). The differences along the climate gradient will also be helpful in predicting the response of vegetation to current climate warming. Other mapping that is being done as part of this project includes bathymetry mapping and lake catchment mapping (Fig. 3).

CAVM Team, 2003, Circumpolar Arctic Vegetation Map, scale 1:7 500 000, Conservation of Arctic Flora and Fauna (CAFF) Map No. 1, U.S. Fish and Wildlife Service, Anchorage, Alaska.

Crump, S. E., B. Fréchette, M. Power, S. Cutler, G. de Wet, M. K. Raynolds, J. Raberg, J. P. Briner, E. K. Thomas, J. Sepúlveda, B. Shapiro, M. Bunce, and G. H. Miller, 2021, Ancient plant DNA reveals High Arctic greening during the Last Interglacial: Proceedings of the National Academy of Sciences, v. 118, n. 13.

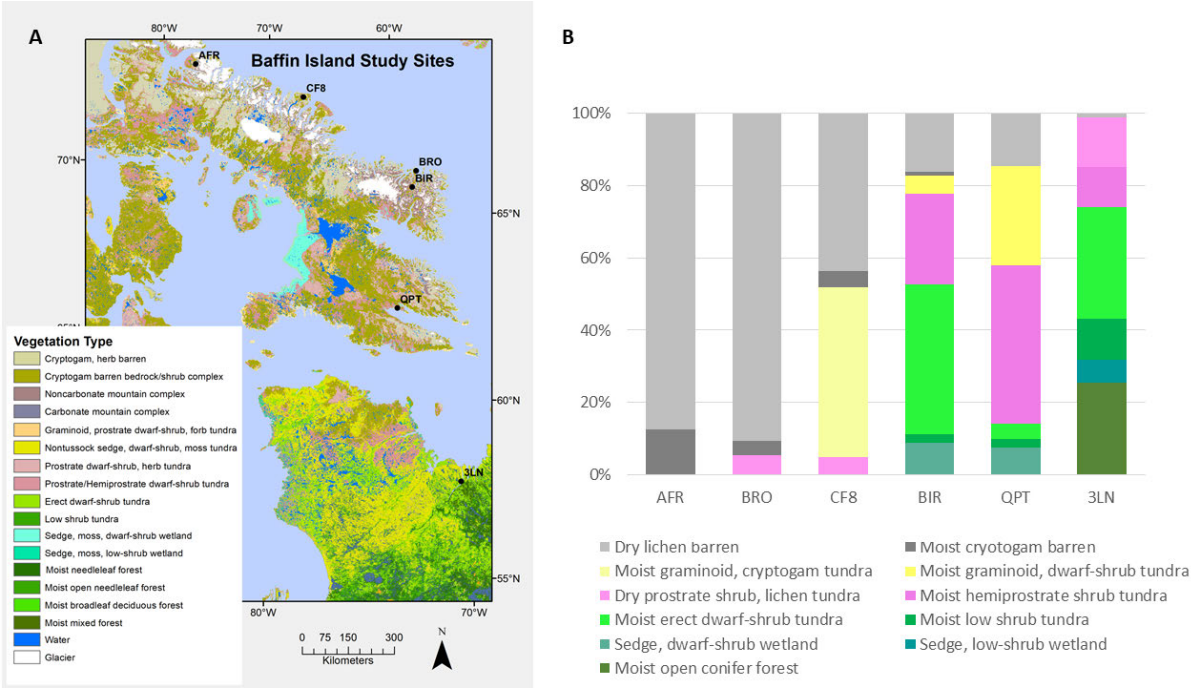

Fig 1. A. Location of six lakes that are part of a study of lake cores and vegetation along a climate gradient in the eastern Canadian Arctic. Five of the lakes are on Baffin Island, Nunavut, and one is near Kuujjuaq, Nunavik, in northern Quebec. B. Proportions of different terrestrial vegetation types in 1-km^2 maps around the lakes.

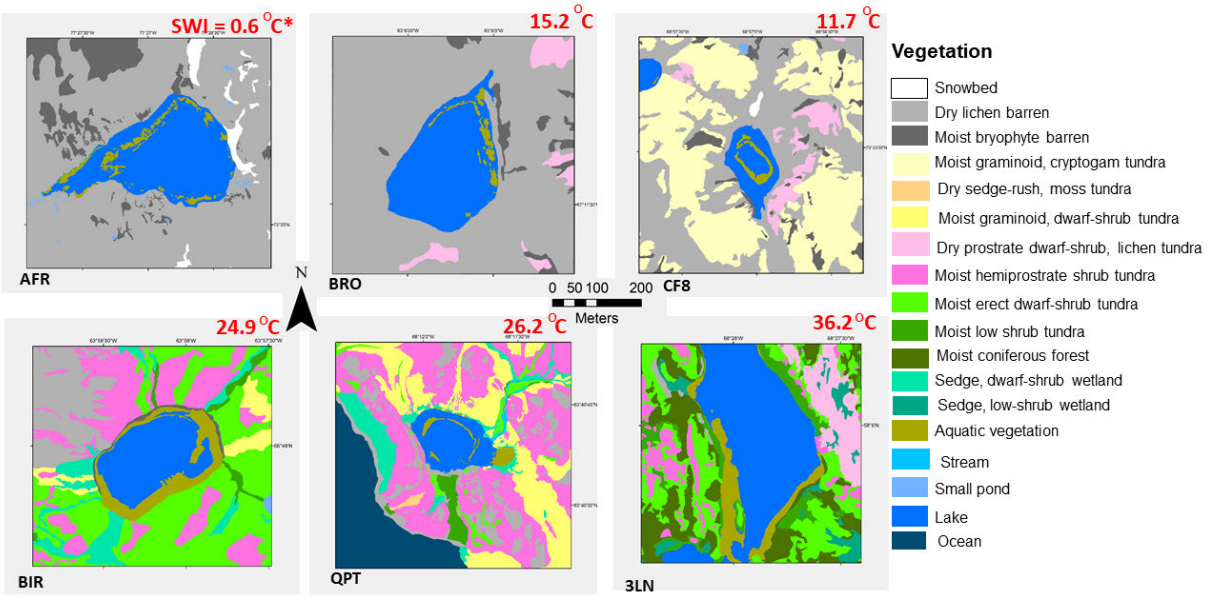

*Summer Warmth Index (SWI) 1971-2000, sum of monthly means > 0 C, courtesy Jonathan Raberg, Univ. Colorado Boulder

Fig 2. Maps of 1-km² around six lakes along a climate gradient in the eastern Canadian Arctic. Note the mapping of aquatic vegetation, dominated by aquatic mosses in the five arctic lakes. Aquatic vegetation at QPT and especially at the boreal lake, 3LN, included several vascular species.

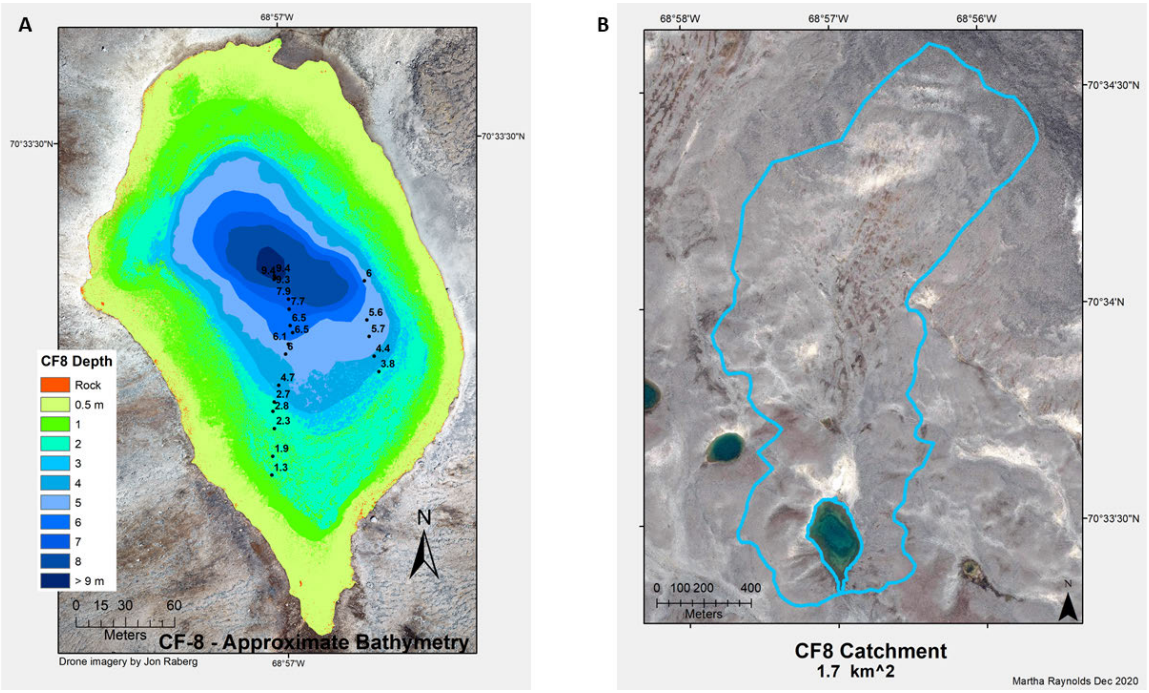

Fig 3. Example of bathymetry mapping and lake catchment mapping for lake CF8, near Clyde River, Nunavut.

Unprecedented recent warmth in the context of the last 2000 years in Svalbard and the imminent disappearance of the west coast valley glacier Linnébreen

Retelle, Mike [1]; **Lapointe**, Francois [2]; **Bradley**, Ray [3]; **Wagner**, Katrin [4]; **Farnsworth**, Wes [5]

[1] Bates College/University Centre in Svalbard; mretelle@bates.edu
[2] University of Massachusetts; flapointe@umass.edu
[3] University of Massachusetts; rbradley@geo.umass.edu
[4] Goethe-University Frankfurt am Main; Katrin60@gmx.de
[5] University of Iceland; wesleyf@hi.is

Nearly 25 years ago, Svendsen and Mangerud (1997) described Holocene glacial variations in western Spitsbergen, Svalbard. Capitalizing on the Linnébreen glacier underlain by coal-bearing sandstones, they measured total organic carbon (TOC) changes on bulk sediment from nearby Linnévatnet to infer periods of glacial activity. Periods of higher TOC (glacial activity) prevailed at ~400-500AD, ~1200-1300AD and after ~1500AD-present compared to the past ~2000 years.

In Spring 2019, we collected a transect of sediment cores from Linnévatnet including a 5m sediment core on which over 100 thin sections were made to build a chronology spanning the last 2000 years. Around 7000 images were acquired at the Scanning Electron Microscope (SEM) along with μ-XRF data to obtain annual physical and geochemical variability. To explore if variations in organic matter content (through LOI) may track changes in Linnébreen glacial activity, over 300 discrete samples at 1cm resolution were also collected for loss on ignition (organic matter [%]). Results indicate that periods of elevated organic matter content broadly agree with increased glacial activity previously defined by Svendsen and Mangerud, that is around 400-500CE, 1200-1300CE and after ~1570CE.

Calcium variations from μ-XRF reveals an overall anti-phased relationship with the organic matter content, also consistent with the findings of Svendsen and Mangerud showing that higher coal content is characterized by low carbonates content. This is because when the dominant source is glacial, the meltwater carries more coal particles in the lake while weaker glacial influence leads to increased detrital carbonates from alluvial fans draining the eastern slopes of the watershed through snowmelt and/or periods of increased rainfall. Reconstruction reveals that Linnébreen glacier activity was in general stable from 700CE until 1570CE, when an abrupt increase and unprecedented glacial growth started and persisted through the 1800s. However, at the turn of the last decade, results suggest that inferred glacial activity reached unprecedented low values in the context of the last 2000 years.

Continued warming will likely result in a further weakening of the Atlantic Meridional Overturning Circulation (AMOC). Atmospheric pattern anomalies during periods of lower AMOC underscore increased southerly winds reaching more promptly Svalbard. Recent monitoring has shown that a shift in seasonal precipitation patterns has occurred with

increased shoulder season rainfall and in the future will be predominantly in the form of rain, thereby preventing glacial (re)growth of low elevation glaciers such as Linnébreen, whose precocious disappearance appears imminent.

Svendsen, J.I. and Mangerud, J., 1997. Holocene glacial and climatic variations on Spitsbergen, Svalbard. The Holocene, 7(1), pp.45-57.

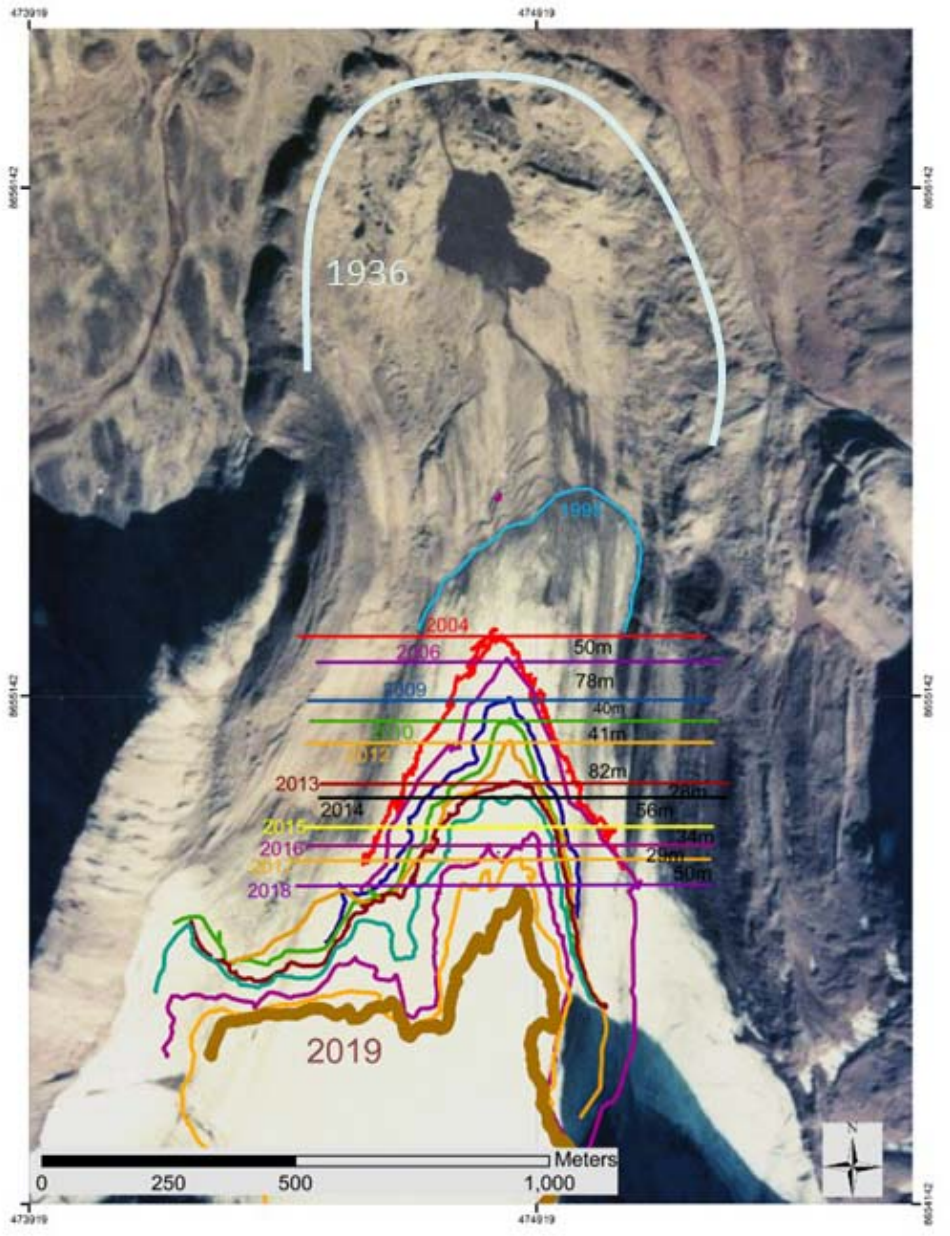

Fig 1. Retreat of Linnébreen since 1936 (S. Roof, unpublished).

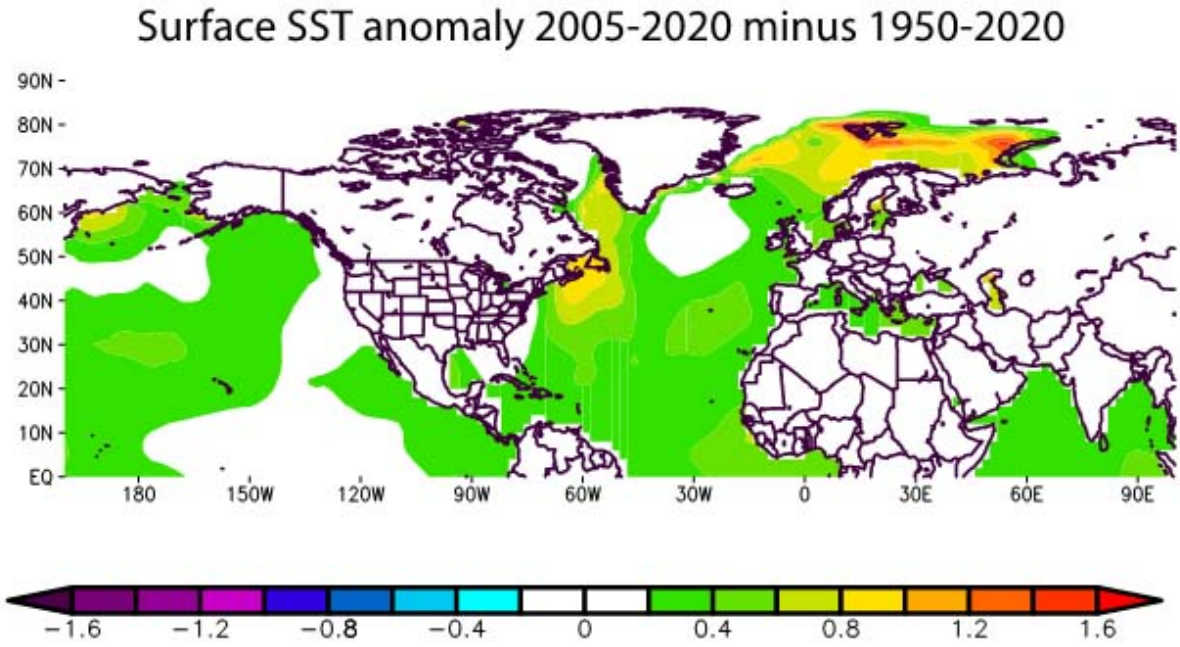

Fig 2. Sea surface temperature anomaly (°C) during the rapid global warming period (since 2005) compared to 1950-2020. Note the "cold blob" in the North Atlantic, a "fingerprint" of the weakening of the AMOC. The region of Svalbard is the one warming the fastest.

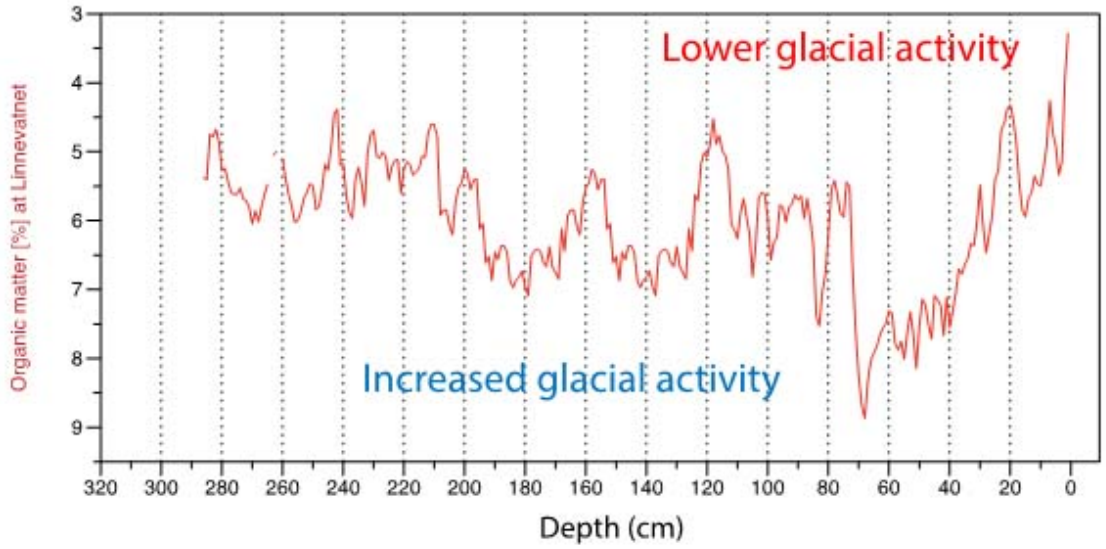

Fig 3. Organic matter [%] changes at Linnévatnet on the first 3m sediment sequence. The past decade (last ~5 cm) has seen unprecedented low values indicative of less glacial influence from Linnébreen on the sediment flux at nearby Linnévatnet.

Arctic Spatial Data Infrastructure: A global information highway to meet the challenges of a fragile Arctic ecosystem

Riopel, Simon [1]

[1] Natural Resources Canada / Ressources naturelles Canada; simon.riopel@canada.ca

Climate change affects the Arctic in different ways. Regional impacts include coastal erosion, evolving ocean currents and temperatures, shifting migration patterns over land and sea, and melting permafrost that heaves buildings and roads. These changes lead to other effects as well; for example, melting permafrost releases stores of methane gas that have been locked up for thousands of years, a greenhouse gas "25 times more potent than carbon dioxide" when released. The consequences are global.

Nations are responding to the complex challenges of climate change by setting carbon reduction targets, enhancing sustainable development goals and assessing cumulative effects. The challenge is great but straightforward: how to best access and combine these large volumes of data to help scientists, resource managers, decision-makers and citizens predict changes to our environment, society and economy. In the case of the Arctic, researchers and decision-makers can now rely on a digital infrastructure called the Arctic Spatial Data Infrastructure (Arctic SDI).

The Arctic SDI is a collaborative initiative of the National Mapping Agencies of the eight Arctic nations with a goal to promote partner-based development of an Arctic Spatial Data Infrastructure (SDI). The aim of the Arctic SDI is to provide politicians, governments, policy makers, scientists, private enterprises and citizens in the Arctic with access to geographically related Arctic data, digital maps, analytics, change detection, predictive modeling and tools for northern and remote communities to facilitate monitoring and decision making. NRCan provides "boots on the ground" for Arctic scientific diplomacy and sovereignty.

This initiative supports Arctic Council (AC) priorities, where joint projects and engagement activities were initiated with Working Groups and Permanent Participants, representing the six circumpolarIndigenous organizations. Arctic SDI is recognized by Senior Arctic Officials for improving data integration, sharing and analysis across the Arctic.

The Arctic SDI community is based on the "system of systems" or "network of networks" concept and, as such, has a nested suite of architectures based on web services and emerging back office suites of application programming interfaces based on international open standards. Arctic SDI is actively collaborating with Arctic stakeholders to create a seamless multidimensional "Digital Arctic" that will link the land, atmosphere, and marine Arctic domains within an integrated platform. The dimensions will comprise location (X, Y, or other coordinates), elevation/bathymetry/altitude, time, and flows to measure pathways and directions (e.g., currents, migration, icebergs, ice flows, etc.).

The Arctic SDI provides the behind-the-scenes connectivity needed to power and deliver

data and maps via an online geoportal, similar to the electrical networks that we rely on daily. The Arctic SDI Geoportal is the access point that allows users to combine data from many different sources, create customized thematic and statistical maps and share these on their own websites as digital, interactive and embedded maps. The Geoportal also provides access to a place name search tool with three million Arctic place names, available in Latin, Cyrillic (Russian) and Syllabic (Inuit) character sets.

This collaboration between nations, in turn, supports the development of Canada's data ecosystem that is needed to report on and realize the United Nations Sustainable Development Goals (UN SDGs) as well as federal/NRCan priorities related to Indigenous reconciliation, climate change adaptation and mitigation, and Arctic sovereignty.

Revisiting the Nutrient Recovery Hypothesis: can contemporary population cycles influence ecosystem function?

Roy, Austin [1]; **McLaren**, Jennie [2]

[1] University of Texas at El Paso; aroy3@miners.utep.edu
[2] University of Texas at El Paso; jrmclaren@utep.edu

Small mammals are widely recognized for their impacts on ecosystem properties, but little is known on how their population dynamics influence biogeochemical cycling and ecosystem function. The Nutrient Recovery Hypothesis (NRH) describes the effects of lemming population cycles on arctic vegetation and soils and provides a framework of how population cycles may influence ecosystem function. The hypothesis predicts for the high phase of the lemming cycle to shift tundra towards a carbon source and for the low phase to shift the system towards a carbon sink. Support for this hypothesis has mainly been supplied through the above-ground effects of historic lemming populations, such as changes in vegetation cover and primary productivity, while below-ground effects and contemporary population cycles have been relatively unexamined. We tested if the NRH is still supported under a contemporary population cycle by examining the effects of simulated population changes on above-ground (vegetation % cover and NDVI) and below-ground variables (soil temperature, thaw depth, total soil carbon (C), nitrogen (N), and phosphorus (P), inorganic and organic forms of CNP, microbial biomass CNP, and CNP-acquiring enzyme activity) over three years near Utqia?vik, Alaska.

Here we present our preliminary results. We observed effects of lemming population peaks on above-ground factors, such as decreasing graminoid (sedge) cover and a pattern for increasing primary productivity (NDVI). However, we found no below-ground effects except on soil temperatures, which were higher following a population crash, and microbial biomass C, which was higher when lemmings were present than when they were absent. We conclude that our data provide limited support for the NRH under contemporary conditions and that future lemming populations may provide feedbacks for shifts towards stronger carbon sink processes in the Arctic.

Integrating terrestrial and subsea permafrost into climate policy

Sayedi, Sayedeh Sara [1]; **Abbott**, Benjamin W [2]

[1] Brigham Young University; sarasayedi91@gmail.com
[2] Brigham Young University; benabbott@byu.edu

Permafrost at high latitudes and altitudes is potentially one of the largest Earth system feedbacks to climate change. Over thousands of years, these vast regions have accumulated trillions of tons of organic carbon in soils and vegetation, far exceeding the carbon stocks in the atmosphere and all living things . Though permafrost has been a persistent carbon sink for millennia, human-caused climate change, which is unprecedented in the Earth's history, could trigger widespread permafrost thaw and greenhouse gas release. Permafrost degradation has acute effects on local human communities and permafrost ecosystems, which are some of the last remaining wilderness on Earth. At its coarsest level, the permafrost zone can be split into terrestrial and subsea components. On the terrestrial side, there remains disagreement about whether vegetation will accelerate or offset greenhouse gas release from soils (McGuire et al 2018, Abbott et al 2016). Likewise, the role of disturbances such as permafrost collapse, drought, nutrient limitation, pests, and wildfire remain poorly understood (Turetsky et al 2020, Abbott et al 2021). There are even more severe knowledge gaps about the response of subsea permafrost to climate change. While there is increasing consideration of the terrestrial permafrost feedback, subsea permafrost remains virtually absent from the policy sphere (Sayedi et al 2020).

In this talk, we will describe the current understanding of the terrestrial and subsea permafrost climate feedbacks. Drawing on the rapidly expanding body of literature on the permafrost zone, we will discuss the research and policy challenges of improving understanding and reducing human emissions to decrease the severity of these feedbacks. We will pay particular attention to the subsea permafrost feedback, which has received much less coverage. Because the subsea permafrost system is unfamiliar to many, we provide some background below.

During the last ice age, the unglaciated continental shelves of the Arctic ocean and surrounding seas accumulated significant amounts of organic carbon in their soil profiles (Osterkamp and Harrison 1982). As ice sheets and glaciers melted after the last glacial maximum, sea level rose more than 130 m, inundating millions of square kilometers of tundra and taiga (Lindgren et al 2016). The submerged permafrost began thawing immediately, but because of the immense thermal inertia of this system, it is still degrading today (Shakhova et al 2009). In a recent study, we used expert assessment—a method that has been long used for making decisions under uncertainty and limited knowledge—to generate first-order estimates about carbon stocks and sensitivity in the subsea permafrost domain (Sayedi et al 2020). Drawing on published and unpublished observations and simulations, the 25 experts in our

study estimated that the subsea permafrost domain contains ~560 gigatons carbon (GtC) in organic matter and 45 GtC in CH4. Current fluxes of CH4 and CO2 to the water column were estimated at 18 and 38 megatons C yr-1, respectively. Under Representative Concentration Pathway RCP8.5, the subsea permafrost domain could release 43 Gt CO2-equivalent by 2100 and 194 Gt CO2-equivalent by 2300, with ~30% fewer emissions under RCP2.6. All of these estimates had wide ranges of uncertainty, demonstrating a serious knowledge gap but providing initial estimates of the magnitude and timing of the subsea permafrost climate feedback. Experts emphasized that the lack of field data creates high uncertainty regarding carbon stocks and emissions. Additionally, ignoring the hydrochemical links between the subsea and terrestrial permafrost limits our ability to anticipate thresholds in both systems.

Ultimately, for both terrestrial and subsea permafrost, these feedbacks are likely to amplify human-caused warming. However, given that primary emissions from humans are two orders of magnitude higher than the likely range of the permafrost climate feedback, accelerating the decarbonization of the global economy should be the policy focus.

Abbott B W, et al., 2016, Biomass offsets little or none of permafrost carbon release from soils, streams, and wildfire: an expert assessment Environ. Res. Lett. 11 034014.

Abbott B W, et al., 2021, Tundra wildfire triggers sustained lateral nutrient loss in Alaskan Arctic Glob. Change Biol. 27 1408–30.

Lindgren A, et al., 2016, GIS?based Maps and Area Estimates of Northern Hemisphere Permafrost Extent during the Last Glacial Maximum Permafr. Periglac. Process. 27 6–16.

McGuire A D, et al., 2018, Dependence of the evolution of carbon dynamics in the northern permafrost region on the trajectory of climate change Proc. Natl. Acad. Sci. 115 3882–7.

Osterkamp T E and Harrison W D., 1982, Temperature measurements in subsea permafrost off the coast of Alaska 4th Canadian Permafrost Conference pp 238–48.

Sayedi S S, et al., 2020, Subsea permafrost carbon stocks and climate change sensitivity estimated by expert assessment Environ. Res. Lett. 15 124075.

Shakhova N E, et al., 2009, Current state of subsea permafrost on the East Siberian Shelf: Tests of modeling results based on field observations Dokl. Earth Sci. 429 1518–21.

Turetsky M R, et al., 2020, Carbon release through abrupt permafrost thaw Nat. Geosci. 13 138–43.

Evidence for a more extensive Greenland Ice Sheet in southwestern Greenland during the Last Glacial Maximum

Sbarra, Christopher [1]; **Briner**, Jason P. [2]; **Graham**, Brandon [3]; **Thomas**, Elizabeth [4]; **Poinar**, Kristin [5]; **Young**, Nicolás [6]

[2] Presenting Author

[1] University at Buffalo; jbriner@buffalo.edu
[2] University at Buffalo; jbriner@buffalo.edu
[3] University at Buffalo; blgraham@buffalo.edu
[4] University at Buffalo; ekthomas@buffalo.edu
[5] University at Buffalo; kpoinar@buffalo.edu
[6] Lamont-Doherty Earth Observatory; nicolasy@ldeo.columbia.edu

The maximum extent and elevation of the Greenland Ice Sheet (GrIS) in southwestern Greenland during the Last Glacial Maximum (LGM, 26-19.5 ka) is poorly constrained. Yet the size of the GrIS during the LGM helps inform estimates of past ice sheet sensitivity to climate change and provides benchmarks for ice sheet modeling. Reconstructions of LGM ice extents vary between an inner-continental-shelf minimum, a mid-shelf position, and a maximum extent at the shelf break. We use three approaches to resolve LGM ice extent in the Sisimiut sector of southwestern Greenland. First, we explore the likelihood of minimum vs. maximum GrIS reconstructions using existing relative sea level data. We use an empirical relationship between marine limit elevation and distance to LGM terminus established from other Northern Hemisphere Pleistocene ice sheets as context for interpreting marine limit data in southwestern Greenland. Our analysis supports a maximum regional GrIS extent to the shelf break during the LGM. Second, we apply a simple 1D crustal rebound model to simulate relative sea level curves for contrasting ice sheet sizes and compare these simulated curves with existing relative sea level data (Figure 1). The only realistic ice sheet configuration resulting in relative sea level model-data fit suggests that the GrIS terminated at the shelf break during the LGM (Figure 2). Lastly, we constrain the LGM ice sheet thickness using cosmogenic 10Be, 26Al and 14C exposure dating from two summit areas, one at 381 m above sea level at the coast, and another at 798 m asl 32 km inland. Twenty-four cosmogenic radionuclide measurements, combined with results of our first two approaches, reveal that our targeted summits were likely ice-covered during the LGM and became deglaciated at ~11.6 ka. Inventories of in situ 14C in bedrock at one summit point to a small degree of inherited 14C and suggest that the GrIS advanced to its maximum late Pleistocene extent at 17.1 ± 2.5 ka. Our results point to a configuration where the southwestern part of the GrIS reached its maximum LGM extent at the continental shelf break. To celebrate John Andrews' foundational work on glaciation and isostasy, this presentation will focus on the first two approaches highlighted above.

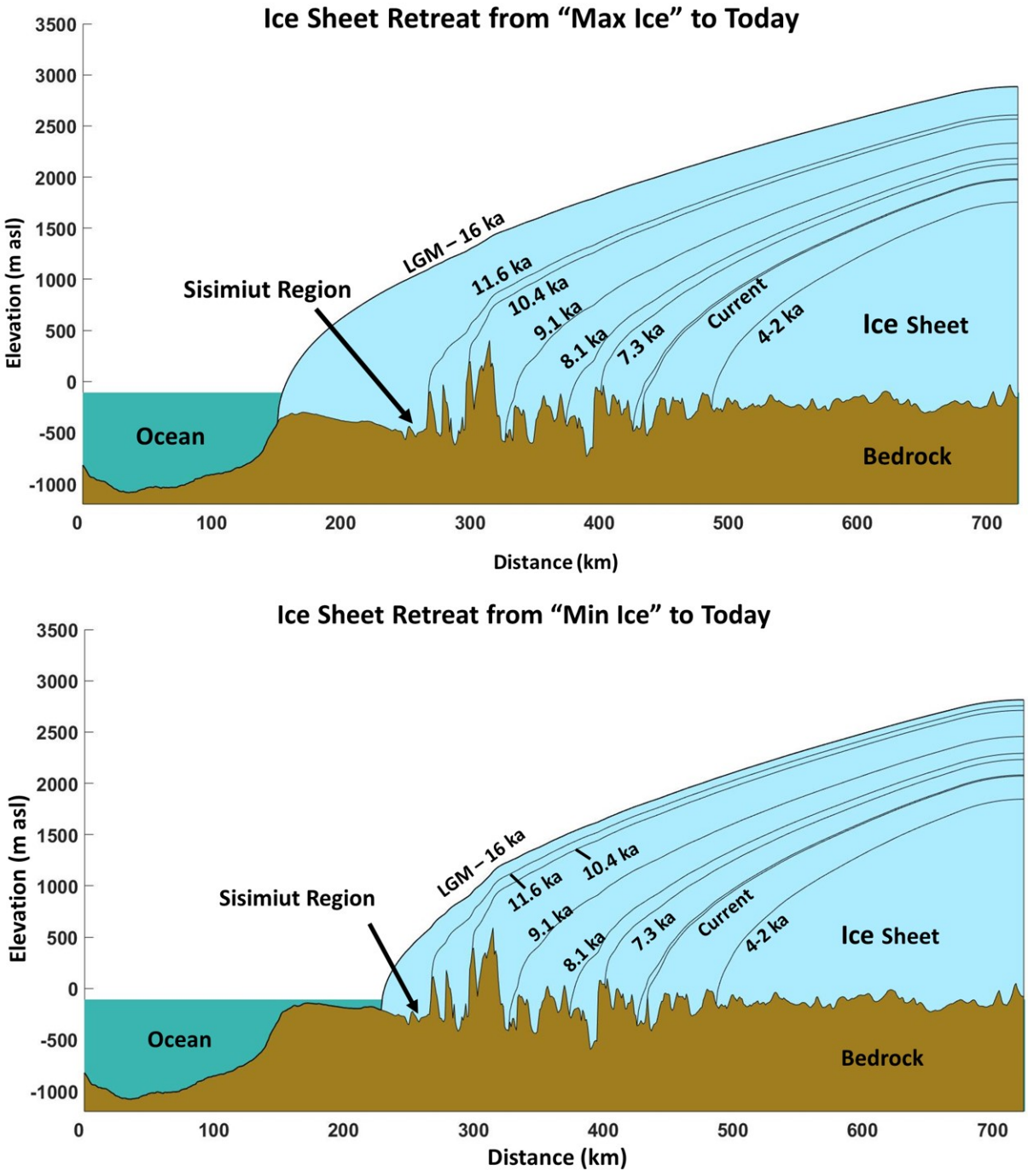

Fig 1. Cross section of crustal rebound model showing "max ice" and "min ice" LGM position and retreat history.

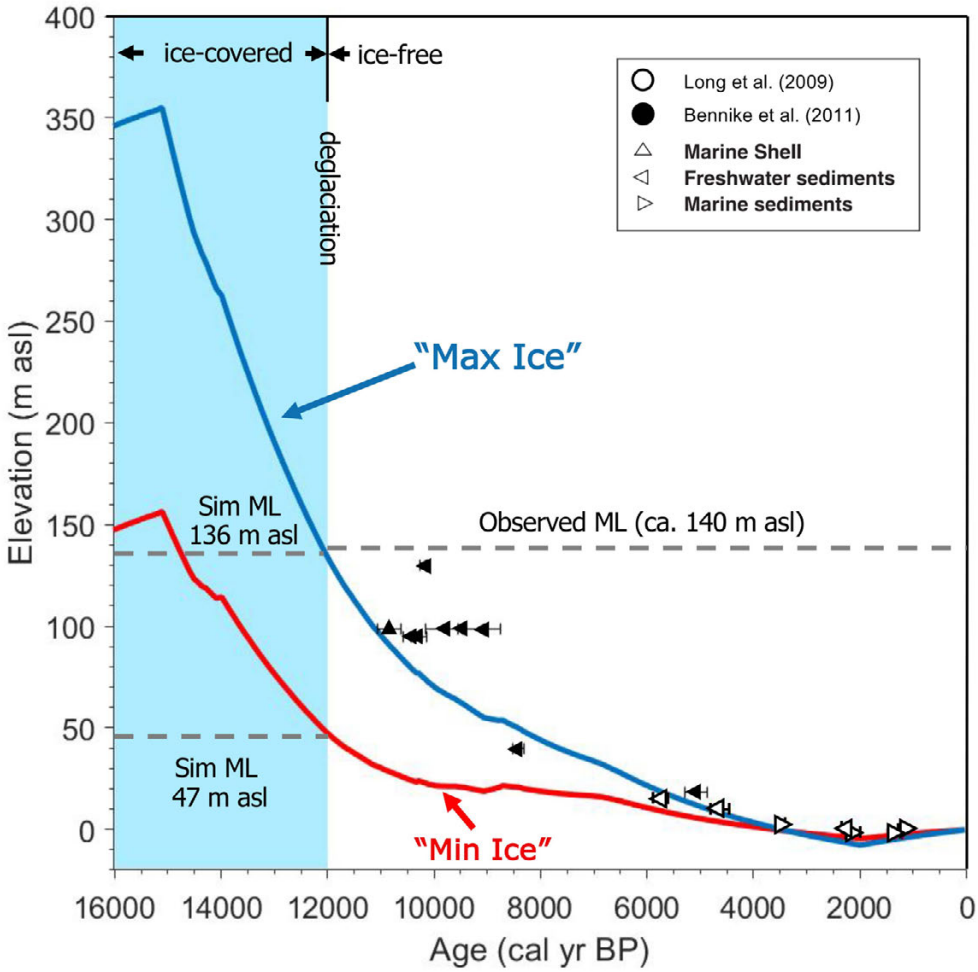

Fig 2. Simulated relative sea level curves for Sisimiut, Greenland, for "max ice" and "min ice" simulations. Independent relative sea level constraints are also shown.

Sedimentary lipid biomarkers combined with novel hyperspectral imaging techniques: A multiproxy Holocene-length sedimentary reconstruction from Lake 578, S Greenland

Schneider, Tobias [1]; **Castañeda**, Isla S. [2]; **Zhao**, Boyang [3]; **Salacup**, Jeffrey M. [4]; **Makri**, Stamatina [5]; **Bradley**, Raymond S. [6]

[1] Department of Geosciences, University of Massachusetts, Amherst; tobiasschnei@umass.edu
[2] Department of Geosciences, University of Massachusetts, Amherst;
[3] Department of Geosciences, University of Massachusetts, Amherst;
[4] Department of Geosciences, University of Massachusetts, Amherst;
[5] Oeschger Centre for Climate Change Research, University of Bern, Switzerland;
[6] Department of Geosciences, University of Massachusetts, Amherst;

Despite a remarkable range of climate reconstructions from ice cores and marine sediments, the de-glaciated "transition zone" between the Greenland ice sheet and the coast is still under-studied. Chronologically well-constrained climate reconstructions from lake sediments can contribute to the understanding of climate variability in these regions and further help elucidate Greenland's past climate variability. Furthermore, little is known about how lake systems in these regions responded to the local climate variability and how they have evolved over the Holocene.

Ice cover extent and duration on lakes can impact their mixing regimes and suppress holomictic events (full turn-over) leading to stratification and causing oxygen-depletion (anoxia) in the hypolimnion. Meromictic conditions further hamper the resuspension and recycling of nutrients deposited in the sediments to the upper (productive) water layers. In combination with reduced light conditions (ice and snow cover) and colder water temperatures this can limit the lacustrine primary productivity during extended ice-covered periods.

Hyperspectral imaging of lake sediments (HSI) is an emerging rapid technique employed to e.g., reconstruct the lake's trophic and anoxic states of the past at high spatio-temporal resolution. The relative absorption band depths measured at ?673 nm wavelength (RABD&sup673; indicative of semiquantitative green chloro-pigment concentrations) and at ?845 nm (RABD&sup845; presence of bacterio-pheophytins) can be used as proxies to semi-quantitatively reconstruct paleo-productivity and oxygen-depletion of the past, respectively.

Here, we present our results of a multiproxy investigation of a Holocene-length sedimentary sequence from Lake 578 (2 m long, obtained in August 2019), a postglacial lake from southern Greenland (61.08°N; 45.61°W, ~170 m a.s.l). Today it is a dimictic freshwater lake (spring-/fall turnovers) with a maximum depth of ~16 m.

Combining non-destructive hyperspectral and μXRF techniques with (destructive) lipid biomarker analyses allowed us to reconstruct Lake's 578 paleo-productivity and anoxia histories, as well as summer mean water temperatures over the Holocene, using branched glycerol dialkyl glycerol tetraethers (brGDGTs) as a paleothermometer.

K-means cluster analysis conducted on the proxies revealed five distinct clusters. The early Holocene sequence in Lake 578 (here ~11k – 9k cal yr BP) is characterized by lithogenic clay rich sediments. The lowest observed productivity in combination with peak values in anoxia-proxies suggest an extensively stratified water column (mero-/amictic conditions). The reconstructed brGDGT summer mean water temperature is the lowest during this period. Interestingly, short-term drops in reconstructed temperature are usually followed by delayed oxygen-depletion. We suggest that, during the early Holocene, Lake 578 was a proglacial lake-system dominated by extended ice cover causing a well-stratified water column.

Thereafter, the lithogenic proportion decreased and the sediments became more enriched in organic material showing that the lacustrine background sedimentation became more important (peak values at ~7.5 – 7k cal yr BP). Indeed, higher temperatures, and a decrease in anoxia-proxies indicate that the lake transformed into a postglacial system with less extensive ice-cover. Furthermore, fine laminations observed at the beginning of this sequence start to fade out. This points towards a better mixed lake system with more pronounced nutrient cycling. The productivity followed the temperature trend, indicating that temperature was the limiting factor during this phase. The period 6k – 3k cal yr BP is characterized by the warmest summer mean water temperatures, a well-mixed water column, and a decrease in productivity. This suggests that the productivity was no longer temperature-limited, but rather nutrient-limited.

After 3k cal yr BP, fine laminations in the sediments indicate a period of reduced holomictic events and hence, more extensive ice-cover, which is in line with a decrease in summer mean water temperature. A strong increase in productivity and anoxia observed at ~1.4 k cal yr BP points to an abrupt enhancement in nutrient-input. We hypothesize that this abrupt event was caused by a lake-level increase that submerged nutrient-rich soils adjacent to the lake (for further details please refer to the presentation of Zhao et al.).

The late Holocene sequence (~1.4k cal yr BP – present) is dominated by two distinct increases in mass accumulation rates between ~1000 – 800 cal yr BP and from ~1900CE to present, coinciding with the Norse settlements, and contemporary land use, respectively. While the productivity was only slightly enhanced during the Norse-period, peak values were observed after ~1960CE.

We provide the first hyperspectral imaging analyses of lake sediments from S Greenland and suggest that its application has great potential to rapidly reconstruct trophic- and anoxia histories of lakes on Greenland. Even though the preliminary chronology is not yet robust enough to pinpoint short-term climate fluctuations (e.g., 9.2k and 8.2k events), the proxy combination provided us with unique insights into the evolution of conditions in Lake 578.

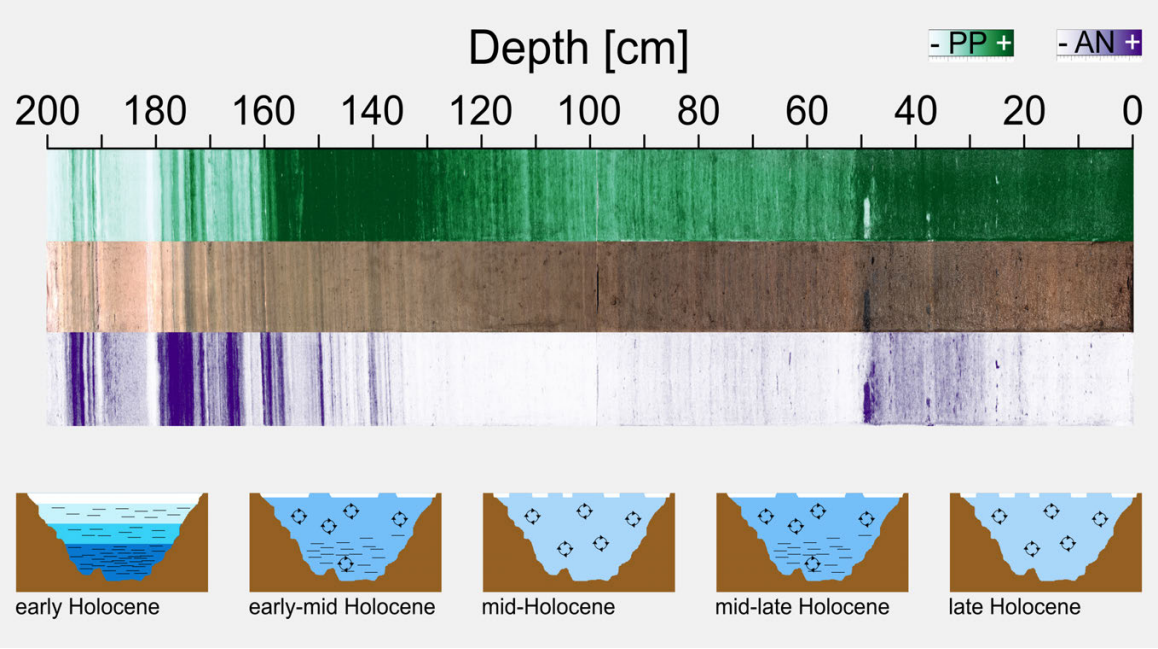

Fig 1. Holocene-length sediment sequence from Lake 578. Top: green-pigment distribution map, middle: true color-photo, bottom: bacterio-pheophytin distribution. 'PP': primary paleo productivity; 'AN': paleo anoxia. The pictograms represent simplified lake-stages over time.

From questions of what and why to why it all matters: Evolving thoughts on the changing Arctic

Serreze, Mark C [1]

[1] CIRES/NSIDC; mark.serreze@colorado.edu

Through what is now a fairly long career as a climate scientist with a special fondness for the Arctic, most of my research has focused on the physical environment and questions of the what and the why. What are the trends in Arctic sea ice extent, and why are we seeing them? Why are the trends bigger in summer than in winter? What changes are we seeing in patterns of Arctic precipitation and temperature and what is causing them? These are among the questions that have driven much of my research. But over the past decade, I, like many others, have been increasing drawn to questions surrounding impacts: why it all matters. What are the impacts of what is now viewed by many as the "New Arctic" on the Arctic terrestrial and marine environments, the peoples of the north and the rest of the world? Why should the rest of the world care about the changing north? In this talk, I'll provide some personal reflections on how my thinking about Arctic change has evolved through the years, and some of the events that have driven that change. What I've realized is that like many others, I am in the middle of a very steep learning curve, made all the steeper by the rapidity of the interconnected changes unfolding in the north.

Creating a database of mountain soil temperature on the subarctic Kola Peninsula

Shtabrovskaya, Irina [1]; **Zenkova**, Irina [2]

[1] Institute of Industrial Ecology Problems of the North Kola Scientific Center of the Russian Academy of Sciences; ishtabrovskaya@mail.ru
[2] Institute of Industrial Ecology Problems of the North Kola Scientific Center of the Russian Academy of Sciences; i.zenkova@ksc.ru

Mountain ecosystems are centers of increased biodiversity due to a combination of environmental conditions such as slope exposure, altitudinal zonation of the soil cover, formation of ecotones and azonal communities, special microclimate, movement of air masses, and the presence of temperature inversions. For the Khibiny massif, such biodiversity was studied almost 100 years ago at the Tietta Mountain Station and repeatedly confirmed by subsequent studies. At the same time, polar mountains and their biota are vulnerable to the influence of natural and anthropogenic factors including climatic changes occurring in high-latitude areas in recent decades, and are indicators of such impacts. In particular, the altitudinal movement of forest boundaries in Khibiny and Subpolar Urals is a response to an increase of average annual air temperatures.

The nature of the temperature distribution in the outer layer is also an indicator that temperature affects the rate of biological, physicochemical, and biochemical processes in the soil, determines the growth and development of living organisms and their vital activity, and ultimately leads to an increase and improvement in soil biota, i.e. soil biodiversity. The greatest fluctuations in temperature are observed in the surface layer of the soil – the organic horizon or litter, the most populated biota. In recent years, studies have been carried out on the temperature regime of mountain soils in the Murmansk region using a new generation of autonomous, programmable "automatic tablets".

In the territory of the Murmansk region the study of the soil temperature was performed in natural forest and cultivated podzolic and peat soils [4,5], both in the Khibiny mountain massif [3] and in the mountains of the Pasvik Nature Reserve [2].

The Khibiny massif is located in the north-west of the European part of Russia - in the Murmansk region (Fig.1), which geographically covers the territory of the Kola Peninsula and part of the mainland. The Khibiny area is estimated at 1300 km2, which is 0.89% of the total area of the Murmansk region, equal to 144.9 thousand km2 [1]. The goal of the research is to study temperature dynamics (daily, seasonal, and year) in mountain soils, taking into account factors of altitudinal zonality of soil and vegetation cover and dependence on slope exposure.

Main tasks:

1. Comparison of litter's temperature parameters in altitude gradient, in the main mountain belts, and with an elevation rise for every 50 m above sea level.
2. Comparison of litter's temperature parameters in mountains ecosystems on a plateau and on slopes of different exposition.

3. Comparison of obtained data on soil temperature with meteorological data and own data on the air temperature.
4. Analysis of the dependence of the mountain soils temperature of organic matter content.
5. Analysis of diversity and distribution of soil invertebrates fauna in dependence on the temperature regime of mountain soils and organic matter content.
6. Comparison of temperature dynamics in the mountain and zonal lowland forest soils.

In recent years: the different modifications of autonomous, compact sensors (loggers) are widely used in field soil researches. The electronic "tablets" for prolongation autonomic registration of temperature and humidity after the programming on a personal computer.

In field research in mountain ecosystems we are using the TR-1, TR-2, and TRV-2 sensors:

- for measurement of air temperature at the altitude of 2 m above ground
- for measurement the temperature on the soil surface in different mountain belts
- for measurement of the soil temperature at a depth of 5 cm in different mountain belts.

The object of the study is the temperature of mountain soils in the thickness of the litter with the help of automatic thermohydrochrons TRV-2 with a maximum measurement range of -25 ... +40 ° C.

The sensors were installed at a depth of 5 cm and programmed to register the temperature every 2 hours (daily dynamics). The daily average, monthly average, and average values for the growing season (July-August) were calculated.

To date, the database contains information about the temperature of 2 mountain ranges (Khibiny Mountains, 67°44 05" N 33°43 34" E, and Pasvik Nature Reserve, 69°04 00" N 29°11 10" E) and foothill plain pine forest (control).

For most of the studied biotopes, the following data were obtained: annual, monthly, summer, and intraday dynamics.

Calculated parameters in the database: average temperature values, minimum and maximum values, amplitude, temperature variability, the sum of positive and negative, the number of days with temperatures above +10, +5 and 0

To date, studies have been carried out for 14 mountain ecosystems and 1 control area.

For the majority of the investigated habitats (of 47) received the temperature data mountain litter (organic horizon) for annual, monthly, and year intraday dynamics for major mountain belts Khibiny – high-mountain desert, tundra, forests tundra, taiga (spruce and pine forest).

All areas on the graph are located near the main mountain-vegetation belts of the Khibiny. A flat northern taiga pine forest present as a control area.

In the control plot with zonal soil type, the average temperatures of litters in the summer season (July - August) are higher in 2016, this is associated with a significantly warmer year ($F > 18.2$ $p = 0.001$).

In the ecosystems of the mountain-taiga belt (221-310 m above sea level), the average monthly temperatures of the litter are the highest in the treeless areas of the intermountain valley as compared to the mountain ones. Anthropogenic areas warm up better since there is a sparseness of the stand, the absence of crowns and moss-dwarf shrub layer, and better heat

absorption by the dark soil surface, colored with ash elements.

In the ecosystems of the mountain-tundra belt (430–800 m above sea level) and in the belt of crooked birch forests, the slope exposure factor has a differentiating effect on differences in average monthly in the warmest month - July (reliability of differences in average monthly July in litters; reliability differences in temperature dynamics; the number of days with effective ? ? +10 º?; the sum of positive temperatures in the litter). The litter of the slopes of the western and southern exposure warms up better.

For the belt of birch crooked forest, the influence of the height above sea level sea (340-460 m above sea level. m.) on the difference in mean monthly temperatures is not obvious.

The differentiating influence on the temperature regime of mountain litter is mainly exerted by 3 factors: "seasonality", "slope exposure", and "altitude zonation".

The seasonality factor is the main factor that determines the change in atmospheric air temperature. This affects the warming of the litter (in spring) and its cooling (in autumn). Thus, the seasonal change in the processes of heat absorption by the litter and its radiation.

Altitudinal zonality determines significant differences in temperatures of the monthly average, minimum and maximum intraday, and average summer temperatures in litters; differences in the dynamics of average daily temperatures, in seasonal variability, in the timing of the transition through the average daily temperature <+5 º? at the end of the growing season (in September). These differences appear for the mountain-forest and mountain-tundra belts throughout the growing season, and they increase from July to September, that is, they are also subject to the influence of the seasonality factor.

The exposure of mountain slopes determines the differences in such parameters of the litter temperature regime as monthly average and maximum temperatures, the number of days with effective ? dayav > +10 and <+10 º?, the sum of positive temperatures in the litter.

However, a significant differentiating effect of this factor was established for the litters of the mountain-tundra and the belt of birch crooked forests only in the warmest month of the growing season - July.

Atlas of the Murmansk region, 1971, Moscow, Research Institute of Geography and Economics, Leningrad State University. A.A. Zhdanova. p.34.

Zenkova, I.V., 2013, Summer temperature dynamics in mountain soils of the Pasvik reserve // Vestnik MSTU. Proceedings of the Murmansk State Technical University, ?.16. ?4. p. 715 – 724.

Zenkova, I.V., 2015, On the characterization of the summer dynamics of litter temperature in the mountains of the Khibiny massif (Murmansk region), Fundamental and applied issues of forest soil science: Proceedings of the VI Russian scientific conference on forest soil science with international participation, Syktyvkar: Komi Scientific Center of the Ural Branch of the Russian Academy of Sciences, p. 85-87.

Kryuchkov, V.V., 1958, Factors Determining the Upper Limits of Vegetation Belts in the Khibiny Mountains, Botanich. Journal, ?.43. ? 6. p. 16.

Yakovlev, B. A., 1961, Climate of the Murmansk region, Murmansk, Murmansk book publishing house, p. 200.

Fig 1. Location of the Khibiny massif

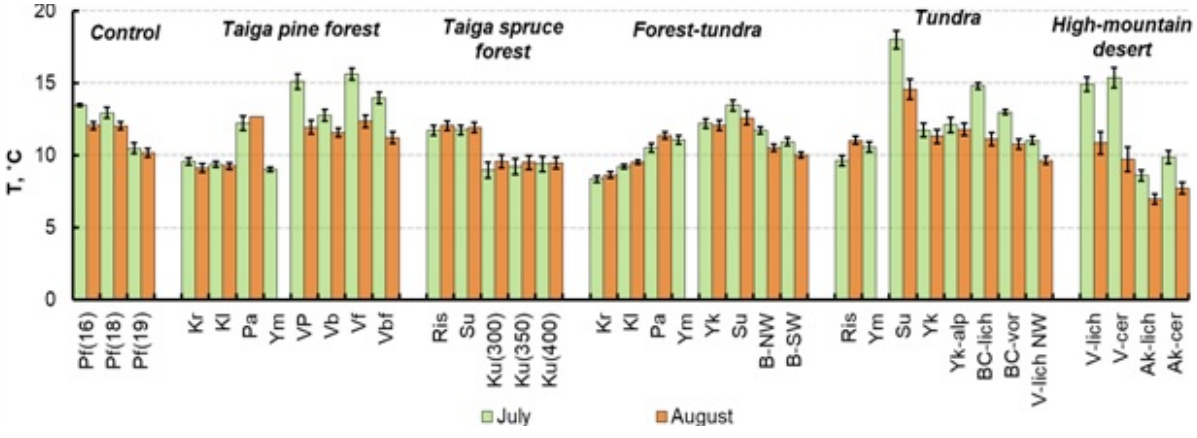

Fig 2. Summer temperature dynamics in 47 mountain sites and 1 zonal studied during 2012-2018

A revised glacial history of the Smoking Hills region, northwestern arctic Canada: evidence for late Pliocene and Quaternary continental Laurentide glaciations and the preservation of old buried glacial ice

Smith, I. Rod [1]; **Evans**, David J.A. [2]; **Gosse**, John C. [3]; **Galloway**, Jennifer M. [4]

[1] Geological Survey of Canada; rod.smith@canada.ca
[2] Durham University; d.j.a.evans@durham.ac.uk
[3] Dalhousie University; John.Gosse@Dal.Ca
[4] Geological Survey of Canada; jennifer.galloway@canada.ca

The Smoking Hills area, in the western Canadian Arctic (~69°15'N; 127°00'W), is a Cretaceous bedrock upland (~380 m asl) that has long been considered to have formed a nunatak during the Late Wisconsinan Laurentide glaciation, encircled by the westward-flowing Amundsen Gulf ice stream and northward flowing ice from the Great Bear Lake divide.

Recent investigations of the glacial history on Banks Island, to the immediate north of Smoking Hills, have demonstrated its inundation by the Late Wisconsinan Laurentide Ice Sheet (England et al., 2009; Lakeman and England, 2013). Stratigraphic sections on Banks Island at Duck Hawk Bluffs, Worth Point, and elsewhere, purported to contain multiple glaciations, interglacials and preglacial fluvial deposits (Vincent, 1983, 1990), have been fundamentally revised, and now indicate perhaps only 2 glaciations (Evans et al., 2014; Vaughan et al., 2014). Of relevance to our Smoking Hills study, these stratigraphic re-assessments also demonstrated widespread glacitectonism, including large rafts of intact, poorly consolidated Cretaceous bedrock, which had not previously been recognized.

In the Smoking Hills in 1968, Rudy Klassen discovered a 57 m high Quaternary section in a small catchment west of the lower Horton River in which he identified a basal sand and gravel deposit, overlain by 3-5 tills containing various inter-till/interglacial deposits. Vincent returned to this section in 1988 and 1991, and described at least 3 tills separated by lacustrine, interglacial, and possible paleosol deposits, and undertook preliminary paleomagnetic measurements that indicated a lower magnetic normal till (? Gauss Chron; 3.04-2.58 Ma), overlain by reversed and then normal magnetic tills (? Matuyama (2.58-0.78 Ma) and Brunhes chrons (0.78-0 Ma), respectively). Duk-Rodkin and Barendregt returned to this site in 2004 and conducted extensive magnetostratigraphic sampling (Barendregt and Duk-Rodkin, 2004; Duk-Rodkin and Barendregt, 2011). They indicated that the basal sand and gravel deposits (what they termed "pre-glacial" fluvial gravels) were reversely magnetized (? Matuyama Chron), and that these were capped by 3 magnetically reversed tills, separated by lacustrine/interglacial deposits, which was then capped by normally magnetized (? Brunhes Chron) interglacial deposits and an uppermost normally magnetized till. They indicated that Canadian Shield erratics were absent from the entire stratigraphy, other than a scattering of

granite boulders on the top of the section. From this, they interpreted that all the underlying tills were the product of a local "Horton Ice Cap" source, and that a continental Laurentide glaciation was only responsible for depositing the uppermost surface lag (age unknown).

In 2018, during 2 weeks of helicopter-supported fieldwork in the Smoking Hills, we studied Klassen's stratigraphic section in detail, and discovered several other notable sections in the area. Detailed sedimentological, structural, lithological, cosmogenic burial dating, and palynological analysis of these sections were undertaken, along with a glacial landsystem approach to mapping and reconstruction of the glacial geomorphology. Based on our results and observations, we have developed a fundamentally different understanding of the glacial history of the region that extends the glacial record back to late Pliocene and records a Late Wisconsinan Laurentide Ice Sheet inundation of the region (Evans et al., accepted).

Numerous observations made by us at Klassen's stratigraphic section change its interpretation. The basal sand and gravel lithofacies contains both faceted and striated clasts, and has a lithological composition that for the most part could not have been derived from the local Cretaceous bedrock catchment. We interpret this basal unit as a glacifluvial deposit, or at least the fluvial reworking of proximal glacial sediments. A reported ice wedge pseudomorph within these sediments (unobserved by us due to slumping; but another example was seen in a different section that we believe to be contemporaneous glacilacustrine sediments) suggests either an earliest glacial, or an oscillating ice margin that subsequently deposited the overlying diamict stratigraphy. A cosmogenic burial age of ~2.9 Ma (Evans et al., accepted) from the lowermost diamict lithofacies places this within the latest Pliocene, roughly coeval (within its standard error) with the most extensive Cordilleran Ice Sheet glaciation recorded in Yukon (2.64 Ma; Hidy et al., 2013).

The diamict sequence overlying the basal glacifluvial gravel is unlike what has been described previously. We recorded three lithofacies comprising massive to laminated, clast-poor diamict (2-10, 16-44, and 47-51 m depth), containing prominent rafts, intraclasts, boudins and stringers of coherent to highly glacitectonised poorly consolidated Cretaceous bedrock (confirmed by palynology and sedimentology). These include two 6 m and 3 m thick rafts of bedrock. Prior studies did not identify any of these, and instead have confused them, we believe, for lacustrine, mudflow, and other deposits (Duk-Rodkin and Barendregt, 2011). Glacitectonism of Cretaceous bedrock, in cases extending up to 20 m depth, was identified by us as being widespread in the field area, and explains some of the overly thick stratigraphic sequences we found. Detail is not provided on what sediments in the Klassen section were sampled by past paleomagnetism studies, but comparisons of photos in Duk-Rodkin and Barendregt (2011), and a tendency for such studies to target fine sediments, leads us to suspect that many of the samples could have been taken from Cretaceous bedrock rafts. We are thus inclined to disregard the published magnetostratigraphy, not least because the reversely magnetized characterization of the lowermost diamict lithofacies contradicts our cosmogenic burial age, which should instead fall within the Gauss Chron normal.

Canadian Shield-derived granitic clasts were observed by us (and also by Vincent) within all

of the diamict deposits at the Klassen section, but not in the basal glacifluvial gravel. This contradicts the previous notion that these deposits were derived from a "Horton Ice Cap", situated north of the Canadian Shield. Instead, it argues for continental Laurentide Ice Sheet sources, and indeed, despite their absence, we do not rule out that the basal glacifluvial gravels could also be produced by the first Laurentide glaciation of the region.

Clast fabrics from the diamict lithofacies record flow generally from the east and southeast, which we relate to glacially streamlined landforms, geomorphology, and ice marginal landform assemblages accordant with past ice flows emanating from Amundsen Gulf and Great Bear Lake sectors of the Laurentide Ice Sheet. The uppermost diamict facies (2-10 m depth) is broadly similar to those underlying it, but exhibits sufficient chemical, sedimentological, and colour variation that we consider it distinct from the underlying stratigraphy, and instead relate it to the last (Wisconsinan) glaciation. In the absence of chronological control, we construct a deglacial landsystem model using surface geomorphology, regional ice flowsets (e.g., Stokes et al., 2006), controlled moraines, and ice marginal erosional and depositional features to illustrate a coherent uncoupling of formerly confluent ice, that inundated the entire landscape, into separate ice lobes retreating eastward into Amundsen Gulf, southeastward towards Great Bear Lake, and southward along the Mackenzie River valley.

One site we discovered along the Anderson River exposes what may be a unique occurrence of buried (pre-last glaciation) glacial ice. A 250 m wide retrogressive thaw slump, exposes an 8 m high headwall of clast-rich, foliated glacier ice, which we presume had stagnated and then became buried by a carapace of insulating sediments. As permafrost aggraded into the site, large vertical ice-wedges formed within the buried glacial ice. Subsequently, the upper extents of these ice wedges were melted, producing a prominent thermal unconformity, and then, or coeval with, they were deformed obliquely downslope, parallel to what we identify as adjacent ice-cored, pitted flutings. Evidence suggests that both the thermal unconformity and deformation of the ice wedges occurred subglacially, as the overriding ice became coupled with the underlying relict glacial ice, forming a glacitectonite shearing interface. The implications of this site are profound for both the historical stability of permafrost conditions and the subglacial dynamics likely to have occurred in areas of northern Canada hosting extensive relict glacier ice, overridden by later glaciations.

The Smoking Hills was found to contain a rich sedimentological record of 2 or more past glaciations, unique for mainland arctic Canada (outside of the Cordillera). Glacial modelling which has relied on past magnetostratigraphies and local ice cap versus continental ice sheet Quaternary glacial histories in this region, require re-examination. We are endeavoring to return to this site to conduct follow up detailed studies of the buried glacier ice. We also will study well preserved and abundant intra- and sub-till wood, peat and other organic macrofossils (including what appears to be a glacial rafted overbank deposit with rooted trees, leaf litter mats and marl), and to conduct OSL and further cosmogenic dating, as a test of our results and to further constrain the basal gravel sequence and other deposits.

Duk-Rodkin, A., Barendregt, R.W., 2011, Stratigraphical record of glacials/interglacials in northwest Canada. In: Ehlers, J., Gibbard, P.L. (eds), Quaternary Glaciations – Extent and Chronology. Developments in Quaternary Science, Vol. 15. Elsevier, Amsterdam, p. 661-698.

Evans, D.J.A., England, J.H., LaFarge, C., Coulthard, R.D., Lakeman, T.R., Vaughan, J.M., 2014, Quaternary geology of the Duck Hawk Bluffs, southwest Banks Island, Arctic Canada: a re-investigation of a critical terrestrial type locality for glacial and interglacial events bordering the Arctic Ocean: Quaternary Science Reviews, v. 91, p. 82-123.

Evans, D.J.A., Smith, I.R., Gosse, J.C., Galloway, J.M., accepted, Glacial landforms and sediments (landsystem) of the Smoking Hills area, Northwest Territories, Canada: Implications for regional Pliocene – Pleistocene Laurentide Ice Sheet dynamics. Quaternary Science Reviews.

Hidy, A.J., Gosse, J.C., Froese, D.G., Bond, J.D., Rood, D.H., 2013, A latest Pliocene age for the earliest and most extensive Cordilleran Ice Sheet in northwestern Canada: Quaternary Science Reviews, v. 61, p. 77-84.

Lakeman, T.R., England, J.H., 2013, Late Wisconsinan glaciation and postglacial relative sea level change on western Banks Island, Canadian Arctic Archipelago: Quaternary Research, v. 80, p. 99-112.

Vincent, J.-S., 1990, Late Tertiary and Early Pleistocene deposits and history of Banks Island, southwestern Canadian Arctic Archipelago: Arctic, v. 43, p. 339-363.

A database for submarine glacial landforms and glacimarine sediments in the High-Arctic

Streuff, Katharina T. [1]; **Ó Cofaigh**, Colm [2]

[1] University of Bremen; kstreuff@marum.de
[2] Durham University; colm.ocofaigh@durham.ac.uk

Paleo-ice sheets have been the focus of research investigations for decades and their reconstruction, especially with regards to past configuration and extent, has become increasingly important to reliably predict the future of our cryosphere. Glacially formed landform-sediment assemblages on the seafloor of Polar continental shelves provide important information in this context, as they record relevant processes, such as ice streaming, glacier advances, or ice front still-stands and oscillations. High-Arctic fjords, where many contemporary glaciers still terminate in tidewater and drain the remainders of larger ice sheets, are of particular interest for a number of reasons: (i) they represent the direct interface between terrestrial, atmospheric, oceanic, and cryospheric processes; (ii) they archive glacial evolution at a high temporal resolution; (iii) their morphology can cause a feedback effect between increased subglacial melt and the internal glaciology of the outlet glacier, thus significantly affecting overall ice sheet mass balance; and (iv) through ongoing ice retreat continuously younger deposits are revealed, which provide a unique opportunity to study the effect of current global warming on contemporary ice masses. Despite these advantages, however, fjords are usually only suitable to study modern and relatively recent depositional processes, while deposits on the mid- and outer continental shelves are more useful to reconstruct large-scale ice dynamics over longer time periods.

Apart from glacier bed morphology, geographic location and presumed associated internal structure of the ice are believed to be factors affecting the glacimarine sedimentary processes and dynamics of glaciers and ice sheets. Accordingly, glaciers in Alaska and southern Chile were suggested to represent the most temperate glacimarine environment with predominantly warm-based glaciers and deposition almost exclusively related to meltwater. Conversely, East Greenland and Antarctica are defined as the significantly colder, Polar glacimarine settings, with a majority of cold-based glaciers much more prone to deposition directly from the ice. Apart from this general classification, however, the internal glacier structure also affects the resulting landform-sediment assemblages. This is especially evident in Svalbard, where many glaciers have been found to undergo somewhat regular cycles of advance and retreat, so-called surges, leading to the formation of characteristic landforms and sedimentary records.

In light of these many variables controlling glacimarine sedimentation and ice dynamics, there is currently a wealth of publications on former ice sheet margin positions, submarine glacial landforms, glacial lithofacies and the glacimarine sedimentary processes observed both on the open continental shelf and in fjords. However, these are often locally constrained and make it difficult to compare glacial deposits across the globe. Furthermore, due to the fact that

data have rarely been collected in a systematic manner, documentations are highly variable in quality. The lack of a coherent terminology for landforms and lithofacies, subjective styles of landform and sediment interpretation, selective presentation of the geomorphological record, and data limitations all resulted in inconsistent, difficult-to-synthesise evidence. It is therefore challenging to fully comprehend the large-scale dynamics of former and contemporary ice sheets despite their relevance for future sea level.

In an effort to facilitate and underpin future research, as well as to improve the quality of forthcoming ice-sheet models, we have created a digital Geographic Information System-based database, which compiles sediments and glacial landforms from High-Arctic fjords and continental shelves in a systematic manner. The database documents evidence of previous glacial activity as visible on the modern seafloor around Svalbard, Greenland, and Alaska, in the Barents and Kara Seas and around Arctic Canada (defined here as north of 66°30' N). It is based on extensive literature research and includes (i) sediment core locations with a description and classification of sampled lithofacies, (ii) radiocarbon dates deemed relevant for constraining the timing of paleo-ice dynamics, and (iii) glacial landforms. The latter include cross-shelf troughs, trough-mouth fans, and grounding-zone wedges, overridden moraines, glacial lineations, drumlins, and crag-and-tails, medial, terminal, recessional and De Geer moraines, debris-flow lobes and glacier-contact fans, crevasse-fill ridges, eskers, and submarine channels. Outlines of bathymetric data used for the description and interpretation of glacial landforms were mapped to give an overview of areas where research has already been conducted. The database is intended as a basis for future modelling of High-Arctic glacier and ice sheet dynamics and, once published, will be freely accessible via download. It will aid researchers in the interpretation of glacial landform-sediment assemblages and the reconstruction of ice dynamics during and since the Last Glacial Maximum. It will further inspire future field work, while also providing a comprehensive bibliography on Arctic glacial geomorphological and sedimentological research.

Honoring John T Andrews: The sediment fill of fjords

Syvitski, Jaia [1]

[1] INSTAAR, University of Colorado; syvitski@colorado.edu

Being the deepest of all nearshore environments (up to 1300 m), fjords can acquire great thicknesses (up to 800 m) of unconsolidated Late Quaternary sediments. Such extreme water depths so close to land, point to the erosive power of glaciers that carved the fjords. Glacial erosion rates depend on several factors, especially ice velocity (<0.1 to >10 km/y), the shear stress at the base of the ice, and substrate properties. Twenty-five percent of world's fjords currently contain marine-terminating or tidewater glaciers.

Sediment fill of fjords is strongly influenced by the magnitude of local sea level. Fjords that deglaciated early (~16 ky) are initially affected by regional isostasy, and then by changes in ocean volume (eustasy). Fjords that deglaciated later (say 5 ky ago) are mostly influenced by isostasy, having largely missed the main eustatic sea level rise of 120 m from about 16 to 7 kyr BP.

Fjord deposits reflect five depositional environments: (1) Ice-contact diamicton associated with grounding line fans, lodgment till and other morainal deposits, deposited at rates up to 100 cm/y; (2) Ice-proximal glacimarine sands and diamicton deposited rapidly (~4–12 cm/y) within a few km from a tidewater ice margin; (3) Ice-distal glacimarine muds, sometimes varved, along with dropstones that record hemipelagic sedimentation (~1–3 cm/y) away from the direct influence of ice front dynamics; (4) Paraglacial gravels, sands and muds deposited (~0.3 – 0.8 cm/y) that record the terrestrial ablation of ice sheets and caps, including the supply sediment along fjord valleys, made available as uplifted marine and fluvial terraces, and as transported by excess discharge of an ablating ice mass; (5) Postglacial sands and muds deposited at rates of ~0.1 – 0.4 cm/y, and gravelly-sandy lags that record modern ocean dynamics, outside of the influence of an ice sheet. Sediment accumulating in fjords during the paraglacial and postglacial phases reflect not only the duration of sediment input, but also the complexities of global versus local sea level rise. Geometry also strongly influences the apparent accumulation rates in fjords.

The sediment volume defining each deposit type depends on the energy supplying the sediment, and the duration of a particular sedimentary environment. With few exceptions, glacial meltwater loads are 10-fold larger than sediment fill rates associated with postglacial loads. For example, of the 80 to 350 m of sediment fill associated with ten Baffin Island fjords, postglacial sediments deposited during the last 6000 years account for <10 m of the sediment columns. Fjord stratigraphic styles include: (1) conformable deposits from hemipelagic sedimentation, (2) onlapping basin fill from decreasing wave or tidal energy with water depth, (3) ponded deposits from sediment gravity flows, (4) deposit wedging from tidal currents, (5) complex stratigraphic patterns associated with both the modern dominant processes, and processes that no longer are present. Fjords with seasonal ice-cover, magnify the seasonality of

deep-basin sediment flux, by limiting the wintertime sediment delivery from rivers, by aeolian transport, and wind-wave resuspension transport.

After 45 years of research on fjords, I claim John T Andrews as my most important mentor and colleague. John and I first sailed into Baffin Fjords in 1982, and later into Greenland fjords in 1993, resulting in many useful papers on fjord sedimentation.

Syvitski JPM, Farrow GE, Atkinson RJA, Moore PG, Andrews JT, 1989. Baffin Island fjord macrobenthos: bottom communities and environmental significance. Arctic 42: 232-247.

Andrews JT, Syvitski JPM, 1994, Sediment fluxes along high latitude glaciated continental margins: Northeast Canada and Eastern Greenland. In: W. Hay (Ed.) Global Sedimentary Geofluxes. National Academy of Sciences Press, Washington, Ch. 7: p. 99-115.

Syvitski JPM, Andrews JT, 1994, Climate change: Numerical modeling of sedimentation and coastal processes, Eastern Canadian Arctic. Arctic & Alpine Research 26(3): 199-212.

Syvitski JPM, Andrews JT, Dowdeswell JA, 1996, Sediment deposition in an iceberg-dominated glacimarine environment, East Greenland: basin fill implications. Global and Planetary Change 12: 251-270.

Andrews JT, Osterman LE, Jennings AE, Syvitski JPM, Miller GH, Weiner N, 1996, Abrupt changes in marine conditions, Sunneshine Fiord, eastern Baffin Island, NWT during the last deglacial transition: Younger Dryas and H-O events. In: JT Andrews, WEN Austin, H Bergsten, AE Jennings (Eds.) Late Quaternary Palaeoceanography of the North Atlantic Margins, Geological Society Spec. Publ. 111: 11-27.

Syvitski JPM, Stein A, Andrews JT, Milliman JD, 2001, Icebergs and the sea floor of the East Greenland (Kangerlussuaq) continental margin. Arctic, Antarctic and Alpine Research 33: 52-61.

The culmination of the last glaciation in the Kenai Peninsula, Alaska based on 10Be ages from Alaska's biggest moraine boulders

Tulenko, Joseph P. [1]; **Ash**, Brendan J. [2]; **Briner**, Jason P. [3]; **Reger**, Richard D. [4]

[1] University at Buffalo, Buffalo, NY 14260; jptulenk@buffalo.edu
[2] University at Buffalo, Buffalo, NY 14260; bash@buffalo.edu
[3] University at Buffalo, Buffalo, NY 14260; jbriner@buffalo.edu
[4] Reger's Geologic Consulting, Soldotna, AK 99669; regerrd80@gmail.com

During the last glaciation of Alaska, referred to as the Naptowne Glaciation, large lobes of ice flowed from the Alaska Range, Talkeetna Mountains and Chugach Mountains coalescing in the lowlands of Cook Inlet where they deposited large, complex landforms. The locally-termed Moosehorn Stade (LGM equivalent) was the earliest and most extensive glacier advance onto the Kenai Peninsula during the Naptowne Glaciation. A prominent terminal moraine trending NE-SW across a section of the northern Kenai Peninsula was deposited at the culmination of the Moosehorn Stade. Giant granitic moraine boulders, thought to be sourced in the western Talkeetna Mountains over 250 km away, are present in the moraine belt. These massive boulders provide an opportunity to use 10Be exposure dating to constrain the timing of terminal moraine emplacement and the culmination of the Moosehorn Stade on the Kenai Peninsula.

We present 10 new 10Be ages from large boulders ranging in height from 2 – 20 m deposited within the mapped limit of the Moosehorn Stade terminal moraine (Fig. 1). Ages range from 22.4 ± 1.2 to 18.2 ± 1.0 ka, excluding one outlier at 47.9 ± 2.0 ka that we suspect was significantly influenced by cosmogenic isotope inheritance or was recycled from a previous glaciation. The average of 9 boulder ages is 20.1 ± 1.4 ka. Radiocarbon ages (n = 3) from barnacle plates deposited in glaciomarine sediments within the limits of the Moosehorn Stade moraine range from 18.6 – 19.5 cal ka BP (2 sigma, DR=0).

These ages support a growing chronologic and stratigraphic framework of glacier advances in Alaska. The culmination of the Moosehorn Stade on the Kenai Peninsula at 20.1 ± 1.4 ka occurred in-step with a majority of alpine glacier histories elsewhere in mainland Alaska (not in SE Alaska). We hypothesize that a relatively early culmination of glaciers across Alaska during Marine Isotope Stage 2 may have been initiated by steadily rising Boreal summer insolation. Further age constraints on post-LGM deposits on the Kenai Peninsula may also elucidate the role of rising eustatic sea level, which barnacle plates deposited in Moosehorn Stade drift suggest may have played a role in modulating deglaciation.

Fig 1. Large granitic boulder deposited within the terminal Moosehorn Stade moraine limit on the Kenai Peninsula

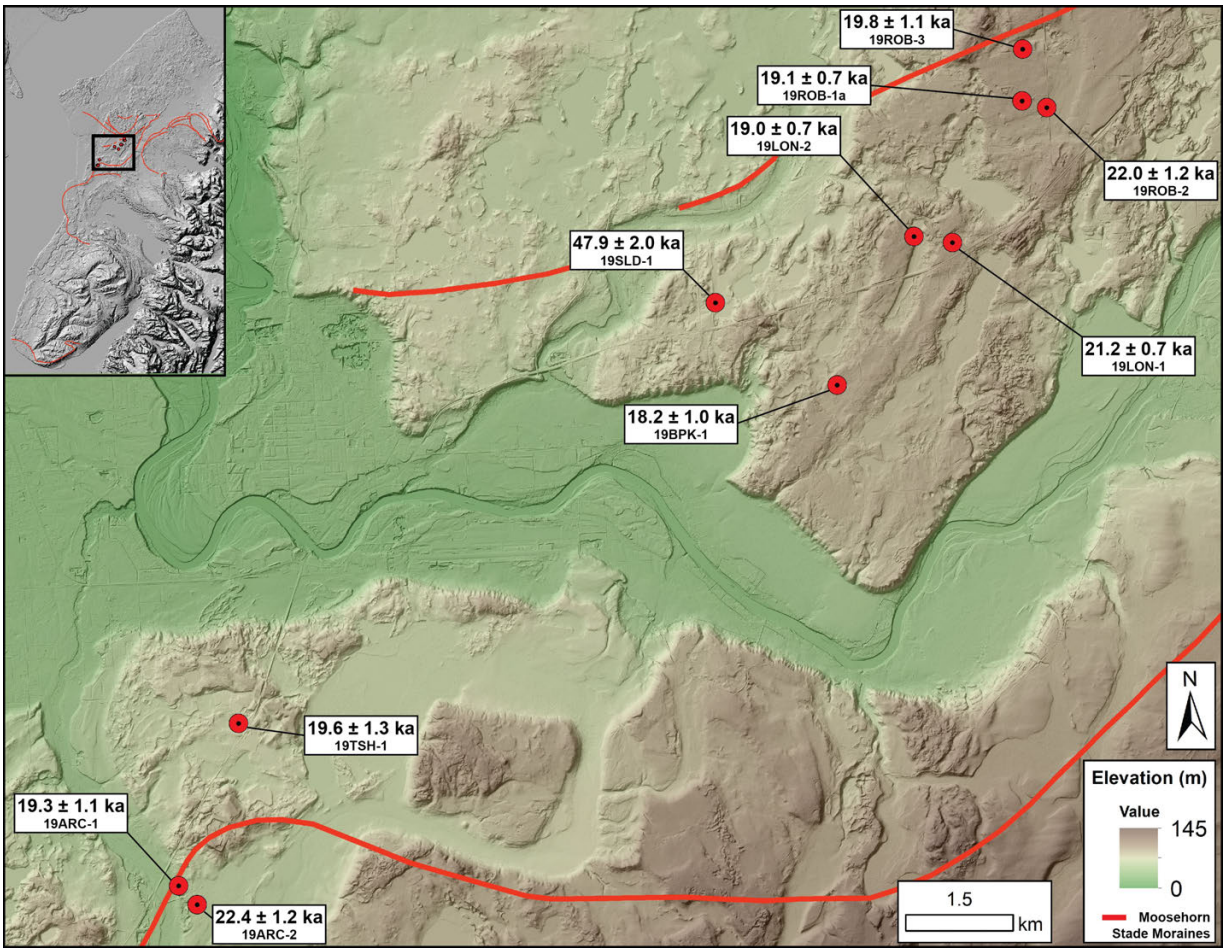

Fig 2. Hillshade map of the area around Soldotna, AK from lidar elevation data made available by the USGS. Each boulder is plotted on the map with its calculated sample 10Be age and analytical uncertainty. Red lines are mapped limits of Moosehorn Stade moraines (same for inset). Inset is of the entire Kenai Peninsula.

The hunt for ice-free areas along the coastal Cordilleran Ice Sheet margin during the LGM continues: No dice in the northern Alexander Archipelago

Walcott, Caleb K. [1]; **Briner**, Jason P. [2]; **Baichtal**, James F. [3]

[1] University at Buffalo; ckwalcot@buffalo.edu
[2] University at Buffalo; jbriner@buffalo.edu
[3] Tongass National Forest; james.baichtal@usda.gov

The late Pleistocene history of the coastal Cordilleran Ice Sheet (CIS) remains relatively unstudied compared to the Laurentide (LIS) and Fennoscandian ice sheets (Dalton et al., 2020; Hughes et al., 2016). Yet accurate reconstructions of CIS extent and timing of ice retreat along the Pacific Coast are essential for a variety of reasons including paleoclimate modeling, assessing meltwater contribution to the North Pacific, and determining the timing and configuration of a coastal human migration route from Beringia into the Americas. This hypothesized "coastal route" relies on the availability of areas that were ice-free throughout the local Last Glacial Maximum (lLGM; 19 – 17 ka; Lesnek et al., 2018) or areas that deglaciated quickly after the lLGM along the coasts of SE Alaska (SEAK) and British Columbia.

We used Be-10 dating of glacial landforms (boulders and sculpted bedrock) to determine when the CIS retreated in the northern Alexander Archipelago, Alaska, and if areas were ice-free throughout the lLGM. Specifically, we targeted areas of the northern Alexander Archipelago that were mapped as ice-free in previous studies (Carrara et al., 2007). Our results show that these hypothesized areas of ice-free land were in fact covered by ice until 15.1 ± 0.9 ka (n = 12 boulders; 1 SD). This work builds off previous studies, and our chronology overlaps (within 1 SD) with their deglaciation date of 16.3 ± 0.8 ka (n = 13 boulders; 1 SD) in the southern Alexander Archipelago (Lesnek et al., 2020; Lesnek et al., 2018). Combined, these data provide a mean deglaciation age of 15.7 ± 1.0 ka (n = 25 boulders; 1 SD) along the coastal Alexander Archipelago., though there may be differences in the timing of deglaciation of different islands.

These results from the northern Alexander Archipelago indicate areas above modern sea-level that were previously-mapped as glacial refugia were covered by ice during the lLGM until ~15.1 ka. Previous ice-sheet reconstructions underestimate the regional maximum CIS extent, as ice likely terminated on the continental shelf. Furthermore, we are now increasingly confident that no areas currently above sea-level were ice-free throughout the lLGM, but it is still unknown whether presently submerged areas on the continental shelf were ice-free.

Carrara, P. E., Ager, T. A., and Baichtal, J. F., 2007, Possible refugia in the Alexander Archipelago of southeastern Alaska during the late Wisconsin glaciation: Canadian Journal of Earth Sciences, v. 44, no. 2, p. 229-244.

Dalton, A. S., Margold, M., Stokes, C. R., Tarasov, L., Dyke, A. S., Adams, R. S., Allard, S., Arends, H. E., Atkinson, N., and Attig, J. W., 2020, An updated radiocarbon-based ice margin chronology for the last deglaciation of the North American Ice Sheet Complex: Quaternary Science Reviews, v. 234, p. 106223.

Hughes, A. L. C., Gyllencreutz, R., Lohne, Ø. S., Mangerud, J., and Svendsen, J. I., 2016, The last Eurasian ice sheets–a chronological database and time?slice reconstruction, DATED?1: Boreas, v. 45, no. 1, p. 1-45.

Lesnek, A. J., Briner, J. P., Baichtal, J. F., and Lyles, A. S., 2020, New constraints on the last deglaciation of the Cordilleran Ice Sheet in coastal Southeast Alaska: Quaternary Research, v. 96, p. 140-160.

Lesnek, A. J., Briner, J. P., Lindqvist, C., Baichtal, J. F., and Heaton, T. H., 2018, Deglaciation of the Pacific coastal corridor directly preceded the human colonization of the Americas: Science Advances, v. 4, no. 5, p. eaar5040.

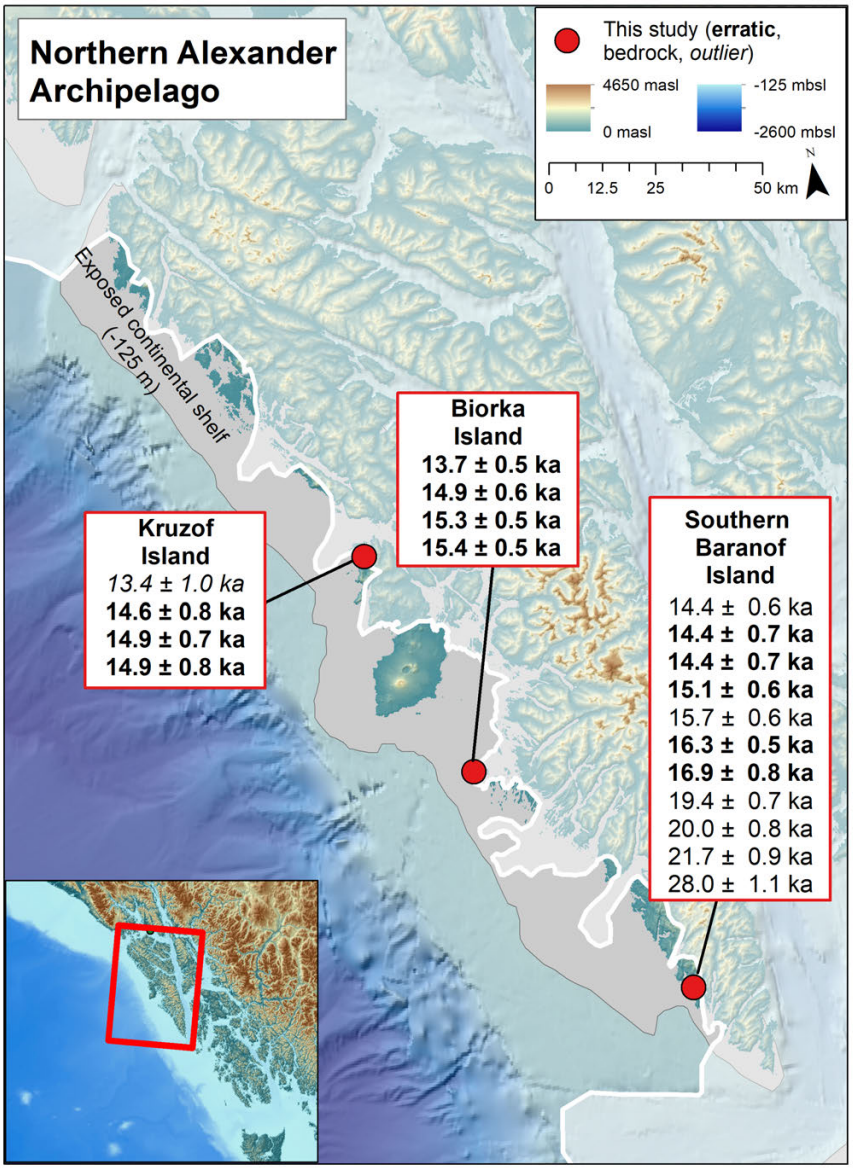

Fig 1. Map of the study sites in the northern Alexander Archipelago, Alaska.

Maximum ice limits after Lesnek et al. (2020).

Extent of exposed continental shelf after Carrara et al. (2007).

Long-term cumulative impacts of a gravel road in an ice-wedge polygon landscape, Prudhoe Bay, Alaska

Walker, Donald A [1]; **Raynolds**, Martha K. [2]; **Kanevskiy**, Mikhail Z. [3]; **Shur**, Yuri [4]; **Romanovsky**, Vladimir E. [5]; **Jones**, Benjamin M. [6]; **Jorgenson**, M.Torre [7]; , et al. [8]

[1] Institute of Arctic Biology, University of Alaska Fairbanks; dawalker@alaska.edu
[2] Institute of Arctic Biology, University of Alaska Fairbanks;
[3] Institute of Northern Engineering, University of Alaska Fairbanks;
[4] Institute of Northern Engineering, University of Alaska Fairbanks;
[5] Geophysical Institute, University of Alaska Fairbanks;
[6] Institute of Northern Engineering, University of Alaska Fairbanks;
[7] Alaska Ecoscience;
[8];

Introduction and methods: How do the combination of Arctic roads and climate change interact to affect adjacent terrain and vegetation in ice-rich permafrost regions? This study was the first ground-based assessment of the long-term cumulative indirect terrain and vegetation impacts that followed the initial construction of an arctic oilfield road in an ice-wedge-polygon landscape. The direct impact is the "footprint" of the original road. The indirect impacts are those that occur following road construction and include the interactions between climate-related changes and infrastructure-related changes.

This study was preceded by studies that documented extensive regional infrastructure- and climate-related landscape changes in the Prudhoe Bay Oilfield (PBO) (Fig. 1), Alaska (e.g., Raynolds et al., 2014) and was prompted the prospect of more roads, seismic trails and transportation corridors being built to fully develop the oil resources of northern Alaska, including in the National Petroleum Reserve-Alaska (NPR-A) and the Arctic National Wildlife Refuge, AK, which was recently opened to development by the U.S. Congress .

Nearly all roads and most of the permanent infrastructure in northern Alaska are built on thick gravel pads, approximately 1.5 m (5 feet) thick. The thick pads are needed to minimize thermokarst and thermal erosion of the permafrost beneath them. The elevated roads, however, also redistribute snow and water, alter the hydrology of adjacent tundra areas, and add large volumes of road dust to adjacent ecosystems.

The landscapes and vegetation adjacent to roads and other forms of infrastructure are also affected by the impacts of climate change. The discovery of recent abrupt widespread geomorphic changes in ice-wedge-polygon landscapes in Northern Alaska (e.g., Liljedahl et al., 2016) has led to more detailed studies of the processes involved in ice-wedge thermokarst, impacts to nutrient cycling, and trace-gas fluxes.

This study further expands this discussion to the long-term cumulative impacts of a heavily travelled road that crosses an ice-wedge polygon landscape in the PBO. Such roads and landscapes are common in the developed areas of the flat coastal plain of northern Alaska. Previous studies have focused on the historical changes within the oilfield, mainly through the application of remote sensing and integrated geoecological and historical change mapping methods (Raynolds et al. 2014). Many indirect cumulative impacts are difficult to assess solely

through the use of remote sensing methods. Recent field data from two sites in the Prudhoe Bay Oilfield (PBO) (e.g., Jorgenson et al. 2015; Kanevskiy et al., 2017; Walker et al. 2015), historical climate data; historical permafrost, landform, soil, and vegetation data (e.g., Walker et al. 1980); an historical aerial photograph record of 42 years between 1949 and 2014 (U.S. Navy: 1949, BP Exploration Alaska 1968–2014), and vegetation-plot data from the 1970s (Walker 1985) were used in the study.

We used ground-based studies and historical data from two sites that are near to each other and to other nearby sites where long-term climate and permafrost data have been collected. The study focused at the Colleen site (CS, Fig. 2) that is adjacent to the most heavily travelled road in the oilfield; the NE (T1) side of road is most seriously impacted by climate change and road dust, and the SW (T2) side is affected by climate change, road dust, and road-related flooding. The Jorgenson site (JS) is relatively unaffected by road-related impacts. We posed two main questions: (1) What were the vegetation and terrain of the of the study sites like prior to oilfield development? (2) How have the cumulative impacts of climate change and the road affected terrain and vegetation at these sites? We examined four scenarios of increasing severity of cumulative impacts (Fig. 3): A. Pre-road (1949–1968); B. Climate change and no road (JS, 1968–present); C. Climate change and road dust (CS, 1968–present); and D. Climate change, road dust, and road-related flooding.

Conclusions and recommendations • Climate-related terrain impacts since the 1970s at the JS and CS were pervasive at both sites and include thicker active layers, large numbers of new thermokarst ponds, increased erosion of the polygon troughs, and greater polygon trough-center microrelief contrasts.

• It is likely that increases in both summer temperatures and precipitation contributed to recent rapid increases in thaw ponds at the JS and CS after approximately 1995.

• Climate-related changes to the vegetation include a likely regional increase in the abundance of dwarf prostrate and erect deciduous willows, and large-scale changes to the distribution of moist, wet, and aquatic vegetation types related to the transformation from low-centered-polygons to transitional and high-centered polygons.

• The large increases in water and aquatic plant communities in polygon troughs require further studies to characterize the plant communities and how they affect the rates of pond succession, trophic structure, food webs, and the degradation and stabilization of ice wedges.

• The road-related impacts included those of heavy road dust, roadside snow drifts, and roadside flooding. The most apparent impact of road dust was the addition of a thick surface soil mineral horizon on top of the original organic surface horizons. This acted to alter polygon morphology near roads. Vegetation impacts from road dust included major reductions in the cover of most plant growth forms and species richness, and the introduction of halophytes near the road probably due to salts used for dust control. The number of species and cover of small forbs, pleurocarpous mosses, and lichens were greatly reduced within 50 m of roads and were apparent well beyond the limits of the 200 m transects in this study.

• Roadside snowdrifts insulate the soils, keeping the tundra relatively warm during winter.

The addition of road dust to the snow promotes early melting snow and pond ice, roadside flooding, warmer soils, and deeper thaw near heavily travelled roads. Snow drifts along infrequently travelled roads and pipelines in more remote areas of the oilfield melt much later.

• The terrain impacts of road-related flooding along CS T2 included complex interactions between the flooded polygon troughs and climate-related erosion of the northern shoreline of Lake Colleen that require further study. The result has been wide deeply eroded thermokarst ponds in polygon troughs near the road that are interconnected to the lake.

• The combined climate-related and infrastructure-related impacts were most pronounced along CS T2, where polygon morphologies were most altered, and the vegetation most changed from pre-road conditions. Longer growing seasons, enhanced productivity, and large increases in water bodies have promoted use by waterfowl near roads that have heavy traffic.

It is difficult, possibly impossible, to build large Arctic oilfields on land without extensive networks of pipelines and roads to connect the many drill sites and facilities. The oil industry now has over a half century of experience with building infrastructure in ice-rich permafrost regions. Major advances in technology have reduced the direct footprint of individual development actions, but there continues to be a need to consider the long-term cumulative indirect impacts of infrastructure and climate change in the construction of new roads and pipelines in areas of ice-rich permafrost.

We recommend that future environmental assessments for new large-scale oil developments in areas with extensive ice-rich permafrost include: (a) consideration of the cumulative indirect impacts of climate change and its interactions with land-use change decisions to assess the full likely area of terrain and vegetation impact; (c) conduct multi-year baseline observations and descriptions of the geoecological and geotechnical conditions during the planning phase that include the details of the distribution and structure of ice-rich permafrost, snow, and vegetation; (d) develop landscape sensitivity maps based on this information to identify the most sensitive areas; (e) use a hierarchical perspective to consider the cumulative consequences of climate change and large-scale land-use actions at plot, landscape, regional, and global scales; (f) develop better methods to decrease the effects of road dust, roadside snow drifts, and flooding; (g) consider avoiding construction altogether in particularly valuable landscapes with highly sensitive ice-rich-permafrost.

Jorgenson, M.T., et al., 2015, Role of ground ice dynamics and ecological feedbacks in recent ice wedge degradation and stabilization. Journal of Geophysical Research: Earth Surface, 120(11), pp. 2280–2297.

Kanevskiy, M., et al., 2017, Degradation and stabilization of ice wedges: Implications for assessing risk of thermokarst in northern Alaska. Geomorphology, 297, pp. 20–42.

Liljedahl, et al., 2016, Pan-Arctic ice-wedge degradation in warming permafrost and its influence on tundra hydrology. Nature Geoscience, 9(4), pp. 312–318.

Raynolds, M.K., et al., 2014, Cumulative geoecological effects of 62 years of infrastructure and climate change in ice-rich permafrost landscapes, Prudhoe Bay Oilfield, Alaska. Global Change Biology, 20(4), pp. 1211–1224.

Walker, D.A., 1985, Vegetation and environmental gradients of the Prudhoe Bay Region, Alaska. CRREL Report 85-14, Hanover, NH: U.S. Army Cold Regions Research and Engineering Laboratory, p. 240.
Walker, D.A., et al., 2015, Infrastructure-Thermokarst-Soil-Vegetation Interactions at Lake Colleen Site A, Prudhoe Bay, Alaska. [online] AGC Data Report, Fairbanks, pp.1–100.
Walker, D.A., et al., 1980, Geobotanical atlas of the Prudhoe Bay region, Alaska. Hanover, NH: Cold Regions Research and Engineering Laboratory, CRREL Report 80-14.

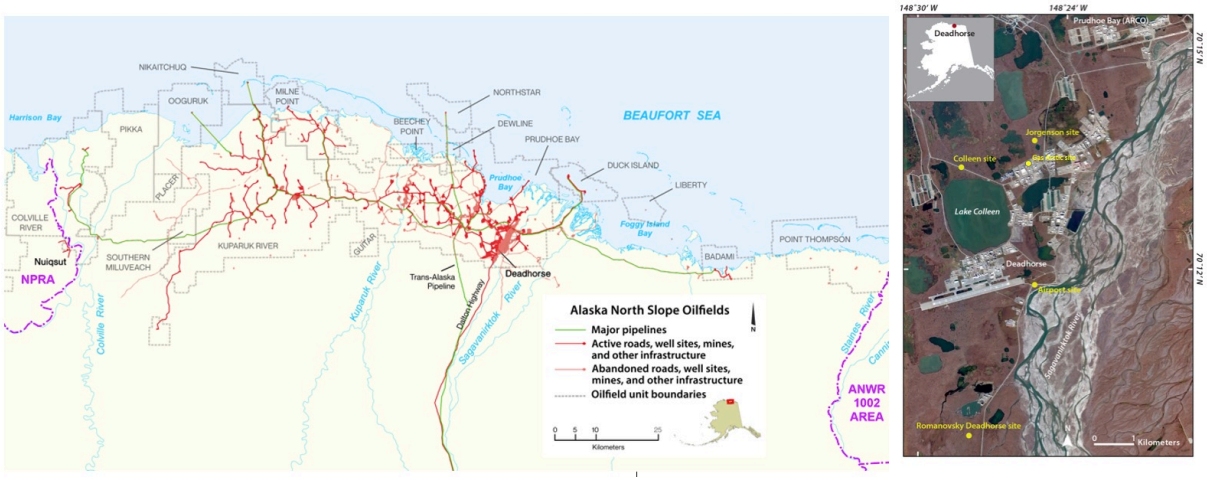

Fig 1. Left: The North Slope oilfields and major infrastructure, 2010. Red lines: gravel roads, airstrips, and construction pads. Green lines: major pipelines. Note the Iñupiat village of Nuiqsut in the National Petroleum Reserve-Alaska (NPRA). Development has expanded into NPRA since 2010. The Trans-Alaska Pipeline System (TAPS) and the James Dalton Highway link the oilfields to Fairbanks, AK. Base map courtesy of BP Exploration-Alaska. Right: Deadhorse, AK region in the eastern portion of the Prudhoe Bay Oilfield. The infrastructure includes two airports, numerous drill sites and support facilities that were constructed on elevated gravel pads designed to protect the permafrost from thawing. Permafrost research has been conducted at the Colleen site, Airport site, Jorgenson site, Gas Arctic site, and the Romanovsky Deadhorse site. The Colleen site is located along a straight section of the Spine Road, 2.9 km north of the Deadhorse airport. Climate data were collected from the Prudhoe (ARCO) station (1969–1985) and Deadhorse station (1986–2019). The image is a false-color infrared image derived from multispectral satellite data. Google Earth, 9/6/2014, ?Maxar Technologies 2020.

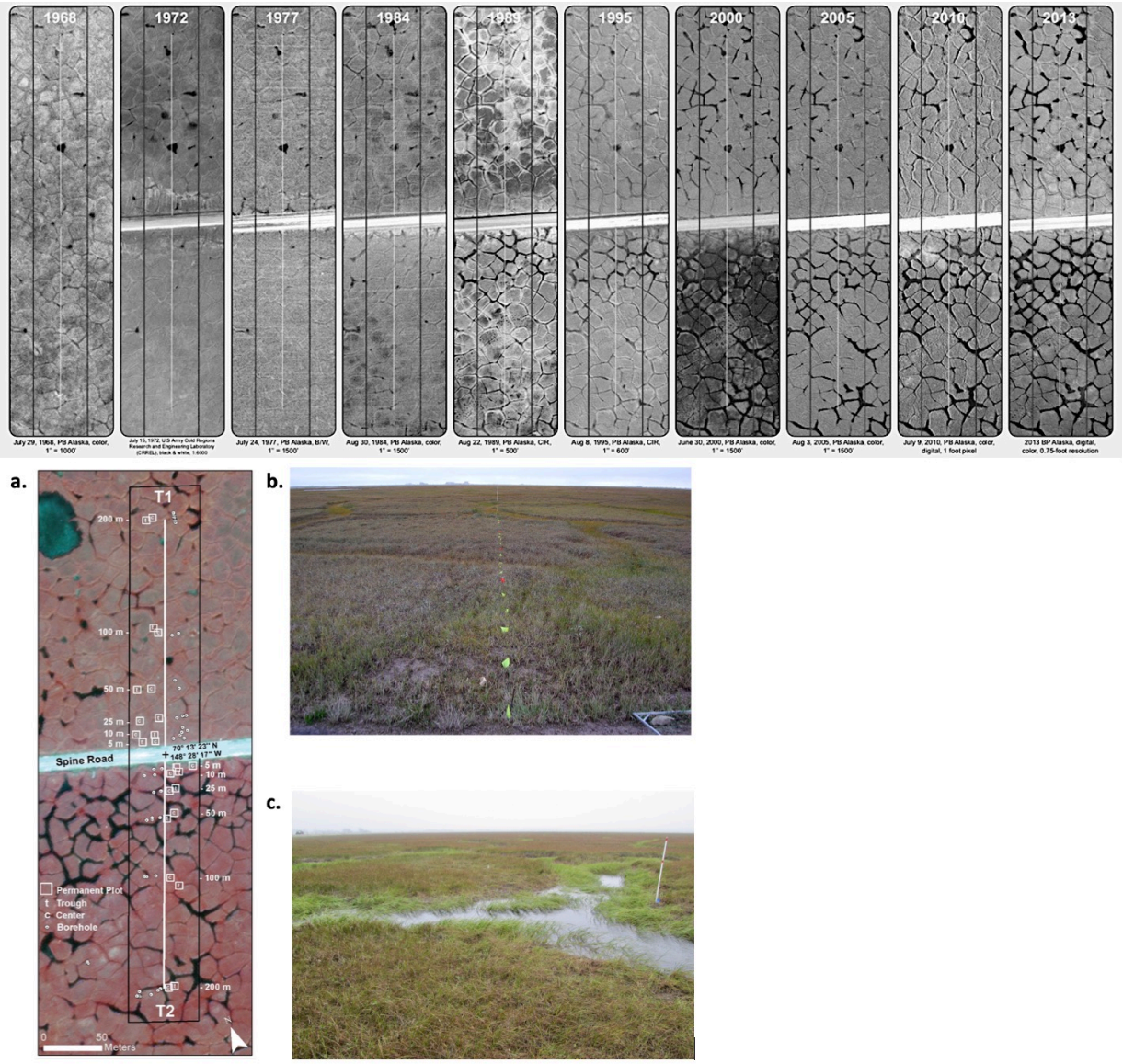

Fig 2. Top: Time series (1968–2013) of changes to ice-wedge polygons at the Colleen Site. The images are a subset of the full record of 42 images between 1949-2014. The 1968 photo was taken before construction of the Spine Road, which is the white band through the center of the 1972–2013 photos. Vertical white lines are the 200-m transects. The black rectangles denote the primary area of analysis along the transects. Aerial photographs: courtesy of the BP Alaska Exploration. Bottom: Transects, plots, and permafrost boreholes at the Colleen site (CS). a. Digital false-color infrared aerial photograph (9 Aug 2010) of the 200-m transects (white lines): T1 (NE side of the road) and T2 (SW side). Paired vegetation plots (open white squares) are located in polygon troughs (t) and centers (c) at approximately 5, 10, 25, 50, 100, and 200 m from the road. Permafrost boreholes (open white circles) are located in troughs and centers at similar distances. b. Ground view in 2014 of Transect T1 on the relatively well-drained side of the road. Pin flags at 1-m intervals are for periodic monitoring of vegetation and environmental factors. Heavy road dust is apparent on this side of the road. c. Transect T2 on the flooded side of the road, where the troughs between polygons are eroded and filled with water. The white 1.5-m stake has iButton® thermistors at 0-, 10-, 25-, 50-, and 100-cm heights. Similar stakes are located at 0 m, 25 m, 50 m, 100 m, and 200 m on both sides of the road.

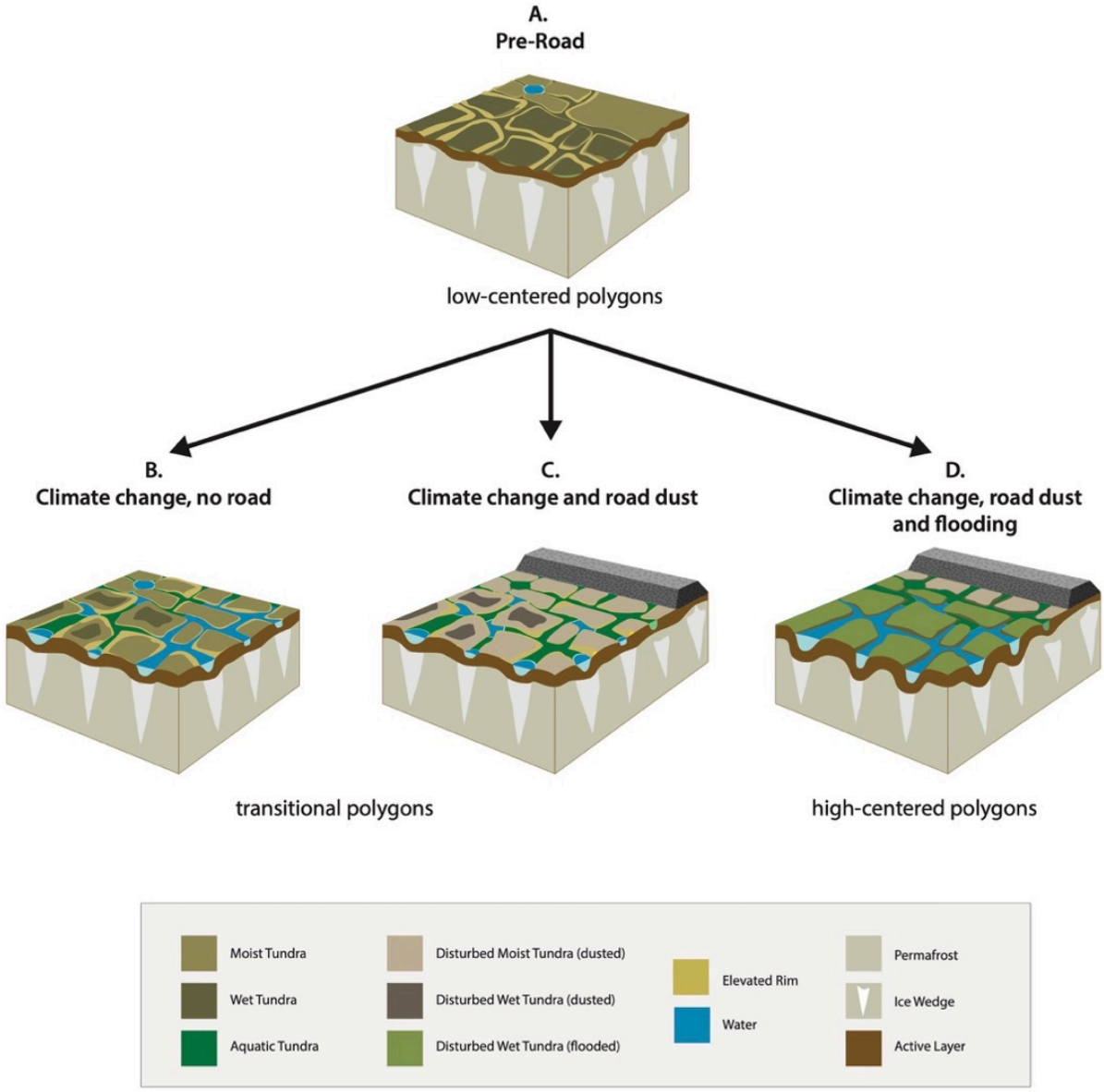

Fig 3. Four scenarios of terrain and vegetation transitions due to climate change and a gravel road. A. Pre-road (1949–1968); interpreted mainly from aerial photographs, geobotanical maps and ground observations by the IBP Tundra Biome in the 1970s; B. Climate change, no road (1969–present), interpreted mainly from information at the JS; C. Climate change and road dust (1969–present), interpreted mainly from CS T1; and D. Climate change, road dust, and flooding (1969–present), interpreted mainly from CS T2.

Thermokarst pond plant communities of Prudhoe Bay, Alaska: Environmental gradients and temperature feedbacks

Watson-Cook, Emily [1]; **Walker**, Donald A. [2]; **Raynolds**, Martha K. [3]; **Breen**, Amy L. [4]

[1] Institute of Arctic Biology, University of Alaska Fairbanks; em.watco@gmail.com
[2] Institute of Arctic Biology, University of Alaska Fairbanks;
[3] Institute of Arctic Biology, University of Alaska Fairbanks;
[4] Institute of Arctic Biology, University of Alaska Fairbanks;

Increases in abundance of thermokarst ponds, which result from ice-wedge degradation and subsequent accumulation of snow and water, have been observed throughout the Arctic (Jorgenson et al. 2006; Schuur et al. 2015). In the Prudhoe Bay region of northern Alaska, ice-wedge degradation is occurring as a result of both climate warming and infrastructure development (Raynolds et al. 2014; Kanevskiy et al. 2017). In some degraded areas, water depth and cover have increased and thermokarst ponds located at the intersection of ice wedges have expanded into surrounding polygon troughs (Walker et al. 2020) (Fig. 1). Recent shifts in water distribution (Liljedahl et al. 2016) are likely to increase the landscape-scale importance of thermokarst ponds in the Prudhoe Bay region.

In the absence of vegetation development, the accumulation of surface water following thaw provides a strong positive feedback that can accelerate the process of ice-wedge degradation (Jorgenson et al. 2015). Vegetation may play an influential role in recovery of degraded permafrost by insulating thawed soil and causing both soil refreezing and aggradation of ground ice (Shur et al. 2011). Through regulation of subsurface temperature, the floating and submerged aquatic vegetation in ponds (Fig. 2) may modulate ecological feedbacks to ice-wedge dynamics. If thermokarst pond vegetation functions in this way, the sediment surface of the pond bottom and underlying ground ice may be insulated to some degree from the radiative heating experienced by surface water in summer.

The aquatic plant communities that characterize thermokarst ponds are of particular interest given their abundance throughout Arctic landscapes, their relative lack of description within existing plant community classification systems, and their potential role in ice-wedge dynamics. In order to make predictions about where and how aquatic vegetation will develop, the factors that drive vegetation characteristics and community composition within thermokarst ponds must be understood. Here, we present a study in-progress that seeks to characterize thermokarst pond plant communities, to determine the factors influencing their species composition, and to evaluate their influence on temperature regulation and subsurface thaw.

To do this, we will examine 30-45 thermokarst ponds at several sites in Prudhoe Bay (Fig. 3) using a combination of plot sampling of vegetation and environmental conditions, temperature monitoring of water and sediment, and aerial site images showing pond development over time. We will use cluster analysis and ordination methods to classify

distinct plant community types and to determine how patterns in species composition vary across environmental gradients. To determine whether vegetation has an effect on within-pond temperature and thaw depth, we will use general linear modeling methods.

This research will be completed as a master's thesis as part of the Navigating the New Arctic: Ice-rich Permafrost Systems (NNA-IRPS) project, which seeks to examine the factors influencing ground ice conditions and landscape evolution in rapidly changing Arctic landscapes. This study will address an existing knowledge gap regarding an increasingly prevalent arctic plant community and its role in ecological feedbacks to ice-wedge degradation, which will allow for predictions to be made about the trajectory of change in Prudhoe Bay and in landscapes throughout the Arctic. Results will reveal connections between vegetation, hydrology, soil, and climate that are relevant to a wide variety of scientific fields involving Arctic landscape change.

Acknowledgements

My committee members, Donald Walker, Amy Breen, Martha Raynolds, and Roger Ruess, all of the University of Alaska Fairbanks, have played an essential role in the development and direction of this project. Other members of the NNA-IRPS project, including Mikail Kanevskiy, Ben Jones, and Anna Liljedahl have provided valuable input that has helped to place this vegetation-focused study in the context of hydrology and permafrost dynamics.

Jorgenson, M.T., et al., 2006, Abrupt increase in permafrost degradation in Arctic Alaska: Journal of Geophysical Research: Earth Surface, v. 120, p. 2280-2297.

Jorgenson, et al., 2015, Role of ground ice dynamics and ecological feedbacks in recent ice wedge degradation and stabilization: Journal of Geophysical Research: Earth Surface, v. 120, p. 2280-2297.

Kanevskiy, M.Z., et al., 2017, Degradation and stabilization of ice wedges: Implications for assessing risk of thermokarst in northern Alaska: Geomorphology, v. 297, p. 20–42.

Liljedahl, A.K., et al., 2016, Pan-Arctic ice-wedge degradation in warming permafrost and its influence on tundra hydrology: Nature Geoscience, v. 9(4), p. 312-318.

Raynolds, M.K., et al., 2014, Cumulative geoecological effects of 62 years of infrastructure and climate change in ice-rich permafrost landscapes, Prudhoe Bay Oilfield, Alaska: Global Change Biology, v. 20, p. 1211–1224.

Schuur, E.A.G., et al., 2015, Climate change and the permafrost carbon feedback: Nature, v. 520(7546), p. 171-179.

Shur, Y., 2011, Permafrost, In: V.P. Singh, P. Singh, and U.K. Haritashya (Eds.), Encyclopedia of Snow, Ice and Glaciers, Dordrecht, Netherlands: Springer, p. 841-848.

Walker et al., 2020, Long-term environmental and vegetation effects of a road and climate change in an ice-wedge polygon landscape, Prudhoe Bay Oilfield, Alaska: Manuscript in preparation.

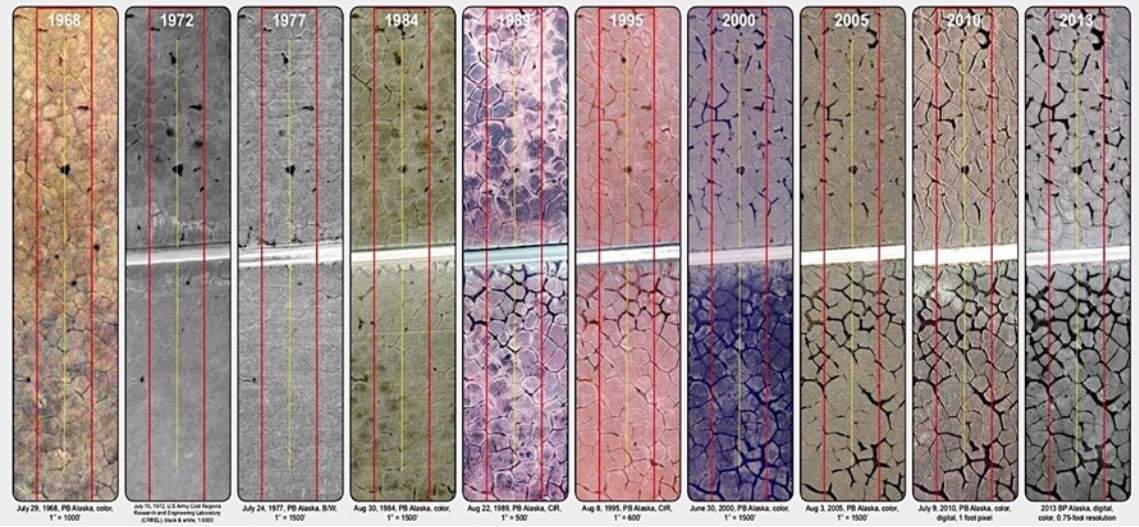

Fig 1. Time series (1968-2013) showing landscape change along two 200m transects intersecting the Spine Road near Lake Colleen in Prudhoe Bay, AK. Expansion of water-filled polygon troughs is evident, particularly along southern transect. Image from Walker et al. (2020). Aerial photos from BP Alaska Exploration.

Fig 2. Image of a thermokarst pond near Prudhoe Bay, AK. Growth of emergent aquatic forbs (Hippurus vulgaris) and submerged mosses (Calliergon giganteum and Scorpidium scorpiodes) is visible, along with distant oilfield infrastructure.

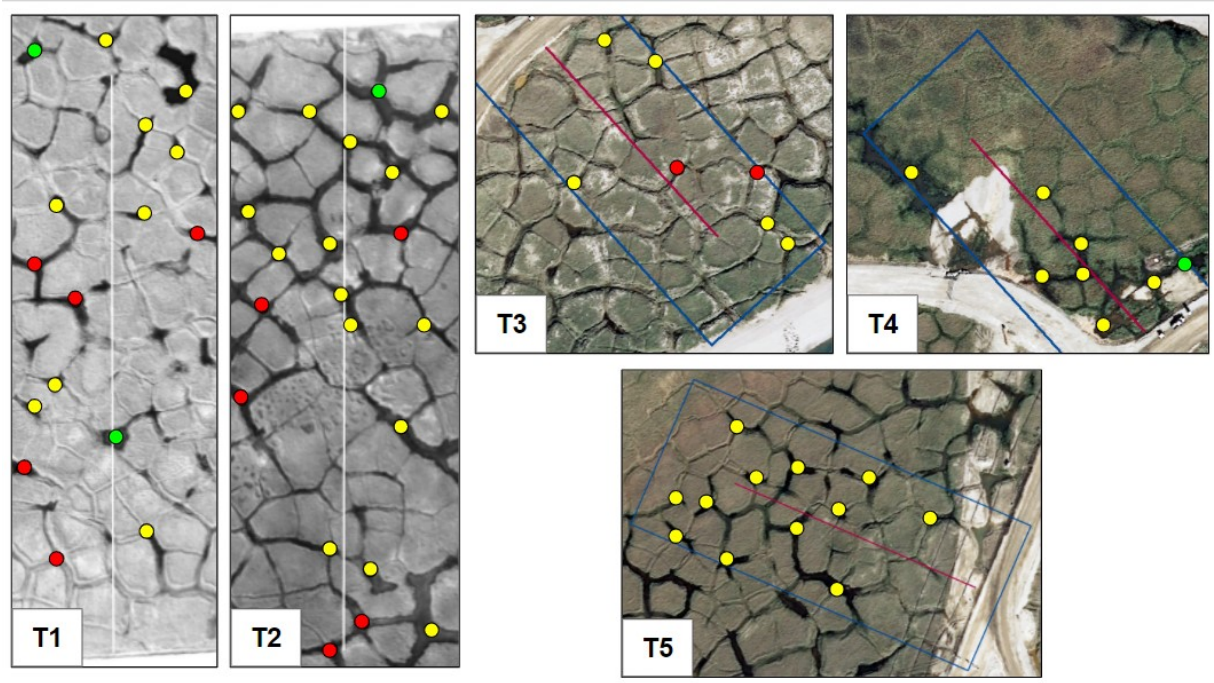

Fig 3. Preliminary selections of possible sampling locations along five transects at Prudhoe Bay, AK. Points represent possible sampling locations and point colors represent broad pond age categories for reference: green (pre-1968), yellow (1969-2000), red (2001-2018). Photos from BP Alaska Exploration.

Late Holocene temperature and hydroclimate reconstruction from southern Greenland: evidence from biomarkers in lake sediments

Zhao, Boyang [1]; **Castañeda**, Isla S. [2]; **Bradley**, Raymond S. [3]; **Salacup**, Jeff M. [4]; **Schneider**, Tobias [5]

[1] University of Massachusetts Amherst; boyangzhao@geo.umass.edu
[2] University of Massachusetts Amherst;
[3] University of Massachusetts Amherst;
[4] University of Massachusetts Amherst;
[5] University of Massachusetts Amherst;

Southern Greenland was colonized by Norse settlers from 985 AD until the early 15th century when they abruptly left (McGovern, 2014). Despite being a topic of many studies, reasons for the abandonment of the Norse Eastern Settlement have been controversial and debated for a long time. As some previous investigations have suggested, the demise of Norse settlement could have resulted from multiple issues, including climate change, management failure, economic collapse, or social stratification (Dugmore et al., 2012; McGovern, 2014). To test whether climate change contributed to settlement abandonment, we collected a short sediment core from Lake 578 (61°5' N, 45°37' W) in southern Greenland, a site that contains Norse ruins within the lake catchment, and constructed an age model based on ^{210}Pb and ^{137}Cs activity (upper sediments) and terrestrial macrofossils ^{14}C dating. Further, we employed branched glycerol dialkyl glycerol tetraethers (brGDGTs) in lake sediments to generate a summer water temperature record, based on a site-specific calibration (Zhao et al., 2021), and measured sedimentary leaf wax hydrogen isotopes to reconstruct relative humidity changes (ΔRH) using a dual-biomarker approach model (Rach et al., 2017). Our temperature reconstruction shows a general agreement with other local records from sites across the Eastern Settlement, indicating an overall prominent cooling trend in the past ~1700 years, which coincides with a decrease in summer insolation at 61°N. Importantly, there is no evidence of an unusually abrupt temperature drop around the time when Norse settlements were abandoned. Our reconstructed ΔRH indicates a persistent wet interval from 580–950 AD, prior to the arrival of the Norse. After ~950 AD, reconstructed ΔRH depicts a long-term drying trend until the 16th century, becoming relatively stable thereafter. This drying trend is concurrent with a change in the Norse diet from one based on terrestrial animals to one that relied on sea mammals (Arneborg et al., 1999; McGovern and Palsdóttir, 2006). A drier environment would have significantly reduced grass production, which was the critical food source for their livestock and essential for over-wintering. Collectively, we conclude that increasingly dry conditions likely played a more important role in driving the demise of the Eastern Settlement rather than minor changes in temperature. Overall, our organic biomarker investigation of Lake 578 demonstrates the potential of using brGDGTs to generate high-resolution temperature records from Arctic lakes and leaf wax hydrogen isotopes to reconstruct local hydrological conditions.

Arneborg, J., Heinemeier, J., Lynnerup, N., Nielsen, H.L., Rud, N., 1999. Change of diet of the greenland vikings determined from stable carbon isotope analysis and "c dating of their bones. Radiocarbon 41, 157–168.
Dugmore, A.J., McGovern, T.H., Vésteinsson, O., Arneborg, J., Streeter, R., Keller, C., 2012. Cultural adaptation, compounding vulnerabilities and conjunctures in Norse Greenland. Proceedings of the National Academy of Sciences of the United States of America 109, 3658–3663.
McGovern, T.H., 2014. Management for extinction in Norse Greenland, in: The Anthropology of Climate Change: An Historical Reader. pp. 131–150.
McGovern, T.H., Palsdóttir, A., 2006. Preliminary Report of a Medieval Norse Archaeofauna from Brattahlið North Farm (KNK 2629), Qassiarsuk, Greenland. National Geographic 1–22.
Rach, O., Kahmen, A., Brauer, A., Sachse, D., 2017. A dual-biomarker approach for quantification of changes in relative humidity from sedimentary lipid D/H ratios. Climate of the Past 13, 741–757.
Zhao, B., Castañeda, I.S., Bradley, R.S., Salacup, J.M., de Wet, G.A., Daniels, W.C., Schneider, T., 2021. Development of an in situ branched GDGT calibration in Lake 578, southern Greenland. Organic Geochemistry 152, 104168.

Mapping ice flow velocity using an interactive, cloud-based feature tracking workflow

Zheng, Whyjay [1]; **Grigsby**, Shane [2]; **Sapienza**, Facundo [3]; **Taylor**, Jonathan [4]; **Snow**, Tasha [5]; **Pérez**, Fernando [6]; **Siegfried**, Matthew R [7]

[1] University of California, Berkeley; whyjz@berkeley.edu
[2] University of Maryland / NASA Goddard Space Flight Center; grigsby@mines.edu
[3] University of California, Berkeley; fsapienza@berkeley.edu
[4] Stanford University; jonathan.taylor@stanford.edu
[5] Colorado School of Mines; tasha.snow@colorado.edu
[6] University of California, Berkeley; fernando.perez@berkeley.edu
[7] Colorado School of Mines; siegfried@mines.edu

Observations of ice flow velocity provide a key component for modeling glacier dynamics and mass balance (e.g., Collao-Barrios et al., 2018). Studies also use these measurements as a proxy of glacier change due to climate, ocean, or bed conditions (e.g., Khazendar et al., 2019). While field campaigns may provide precise velocity data for selected glacier sites, deriving velocity from satellite data is usually the only way to obtain velocity for many remote glaciers. The feature tracking technique (also known as pixel tracking, offset tracking, or template matching) is one of the most commonly used methods for deriving ice flow velocity from remote sensing data. This technique computes the cross-correlation between two images of the same glacier acquired at different times and measures glacier motion from offset of the surface features, such as crevasses (e.g., Strozzi et al., 2002).

Despite being cost-effective for mapping ice flow velocity, running a feature tracking workflow is not easy. This is because: (1) Searching for good data can be time-consuming. Users have to define a list of search criteria (e.g., spatial coverage, temporal coverage, maximum cloud cover, orbital tracks) and perform a query on a particular data distribution system. It is usually necessary to change the search criteria multiple times depending on the query results. For data stored on different distribution systems, the learning curve for this step can become even steeper. (2) Fetching and storing the data can be challenging because the source images often come in a large size. For example, a Landsat 8 image pair takes ~1 Gb of disk space, not including the feature tracking results. To calculate the temporal variation of ice flow velocity, one might need 100-1000 Gb of storage for each glacier. (3) There is no standardized routine or workflow for performing feature tracking (e.g., Heid and Kääb, 2012). Multiple cross-correlation kernels, pre- and post-processes, and software packages (e.g., autoRIFT, CARST, ImGRAFT, vmap, and GIV) exist. Still, a detailed intercomparison of recent feature tracking tools has not been conducted. As such, the relative strengths and weaknesses of the different software packages are challenging to evaluate. Selection of a particular workflow and parameter set is often arbitrary and does not guarantee the best results. (4) To date, there have been some online repositories that directly distribute glacier velocity data, such as the NASA ITS_LIVE project (Gardner et al., 2019). While this serves as an essential contribution to many studies, there are still limitations to these readily available

datasets. For example, the feature tracking kernel and the workflow are fixed and are applied to certain source data sets. Users can't use the same workflow on the other datasets or test a different workflow on the same data sets. Besides, the data repository may not be updated with real-time satellite acquisitions. Users have to either wait for new releases or perform feature tracking themselves.

Here we present a Jupyter notebook-based interface that deploys the entire feature tracking workflow from searching the data to visualizing the results. The workflow builds up from these key modular steps: (1) query data, (2) retrieve data and aggregate them to the memory, (3) select feature tracking kernel and parameters, (4) filter data for feature enhancement, (5) perform feature tracking, (6) mask outliers and interpolate results if needed, and (7) visualize and save results. For the first two steps, we develop a library called GeoStacks and use it with the other tools from the Jupyter ecosystem, such as Jupyter-widgets and Geopandas. Steps 3 to 6 are typically included in a feature tracking package, and we implement corresponding algorithms from the CARST software (Cryosphere And Remote Sensing Toolkit; Zheng et al., 2021) in this demo example. CARST will parallelize the image correlation kernel and achieve fast processing time. Each step is fully customizable and extensible, which will help researchers explore new data, compare different algorithms, and validate their results. We use ipyleaflet and Jupyter-widgets and provide an entirely interactive control panel, allowing users to quickly select desired input data and run the feature tracking processes.

In our demo notebook, we query data over Jakobshavn Isbræ, a large outlet glacier of the Greenland Ice Sheet with a history of seasonal flow speed variation (Khazendar et al., 2019; Figure 1). Users can choose to explore the ITS_LIVE velocity dataset or the Landsat 8 imagery and perform feature tracking for the latter. As mentioned above, the feature tracking kernel and all related filters, masks, and interpolation processes are from CARST, but users can easily replace any of them or the entire package with their algorithms or a different feature tracking package (e.g., autoRIFT; Lei et al., 2021). The modules used by this demo notebook, including the GeoStacks and CARST packages, are open-source software and welcome community contributions. The demo notebook represents a way to integrate the entire feature tracking application. Users can also access the same modular content from the tools we use and adopt them in their own projects. Future integration of this work into a numerical glacier model (such as the Open Global Glacier Model, Maussion et al., 2019) or a web-based feature tracking service is also possible.

This work is part of the Jupyter meets the Earth project, supported by the NSF EarthCube program (awards 1928406 & 1928374). The demo notebook is available on Github: https://github.com/whyjz/EZ-FeatureTrack.

Collao-Barrios, G., et al., 2018, Ice flow modelling to constrain the surface mass balance and ice discharge of San Rafael Glacier, Northern Patagonia Icefield. Journal of Glaciology, 64(246), 568–582. doi.org/10.1017/jog.2018.46
Gardner, A. S., et al., 2019, ITS_LIVE Regional Glacier and Ice Sheet Surface Velocities. Data Archived at NSIDC.
Heid, T., & Kääb, A., 2012, Evaluation of existing image matching methods for deriving glacier surface displacements globally from optical satellite imagery. Remote Sensing of Environment, 118, 339–355. doi.org/10.1016/j.rse.2011.11.024
Khazendar, A., et al., 2019, Interruption of two decades of Jakobshavn Isbrae acceleration and thinning as regional ocean cools. Nature Geoscience, 12(4), 277–283. doi.org/10.1038/s41561-019-0329-3
Lei, Y., et al., 2021, Autonomous Repeat Image Feature Tracking (autoRIFT) and Its Application for Tracking Ice Displacement. Remote Sensing, 13(4), 749. doi.org/10.3390/rs13040749
Maussion, F., et al., 2019, The Open Global Glacier Model (OGGM) v1.1. Geoscientific Model Development, 12(3), 909–931. doi.org/10.5194/gmd-12-909-2019
Strozzi, T., et al., 2002, Glacier motion estimation using SAR offset-tracking procedures. IEEE Transactions on Geoscience and Remote Sensing, 40(11), 2384–2391. doi.org/10.1109/TGRS.2002.805079
Zheng, W., et al., 2021, Cryosphere And Remote Sensing Toolkit (CARST) v2.0.0a1. Zenodo. doi.org/10.5281/zenodo.4592619

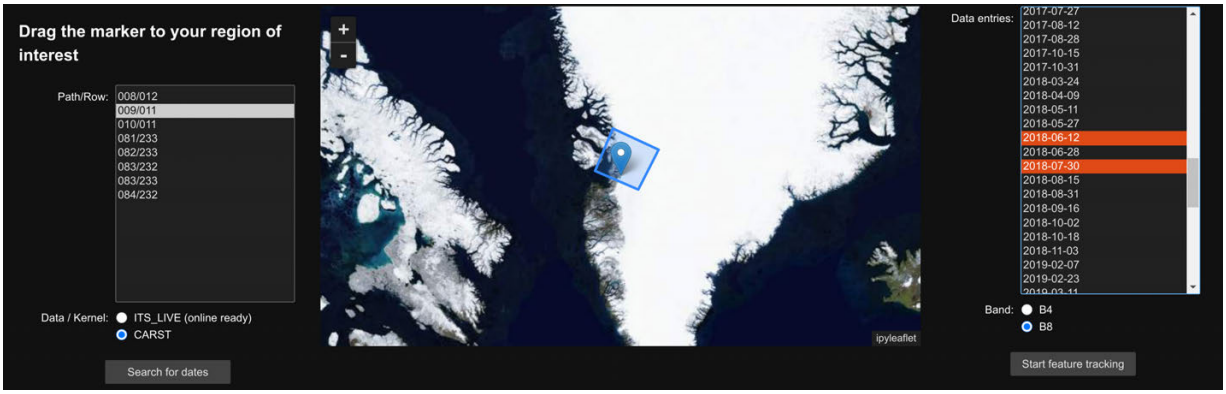

Fig 1. Jupyter notebook-based graphical interface allows users to explore data, select input and run feature tracking algorithms without much hassle.

Registrants

Ackerman, Hannah
University of Ottawa

Anderson, Lesleigh
U.S. Geological Survey

Andersson, Carin
NORCE Norwegian Research Centre

Andresen, Camilla
Geological Survey of Denmark and Greenland

Andrews, John
University of Colorado Boulder

Aradóttir, Nína
University of Iceland

Arazny, Andrzej
Nicolaus Copernicus University in Torun

Ardenghi, Nicolò
CU Boulder - INSTAAR

Axford, Yarrow
Northwestern University

Ball, Matthew
Durham University

Bhiry, Najat
Université Laval Département de géographie

Bischof, Hannah
University of Edinburgh

Bradley, Raymond
University of Massachusetts, Amherst

Brigham-Grette, Julie
Dept of Geosciences UMass Amherst

Briner, Jason
University at Buffalo

Brown, Jerry
retired

Caine, Nel
INSTAAR

Caissie, Beth
USGS

Carlson, Brandee
University of Colorado

Caro, Tristan
CU Boulder

Castañeda, Isla
University of Massachusetts Amherst

Cluett, Allison
University at Buffalo

Coulthard, Roy
MacEwan University

Crump, Sarah
University of California Santa Cruz

Daniels, William
University of Massachusetts Amherst

Davis, Thom
Bentley University

Detlef, Henrieka
Aarhus University

Dixon, john
University of Arkansas

Edgerton, Briana
Syracuse University

Elias, Scott
Univ of Colorado

Francus, Pierre
INRS-ETE (Québec City, Canada)

Furze, Mark
UNIS - The University Centre in Svalbard

Geirsdóttir, Áslaug
University of Iceland

Gorbey, Devon
University at Buffalo

Gustafson, Michaela
Boise State University

Hall-Bowman, Jenifer
INSTAAR

Harning, David
University of Colorado Boulder

Henderson, Michael
The Peregrine Fund

Hoffecker, John
University of Colorado at Boulder

Hollister, Kayla
University at Buffalo

Hughes, Anna
University of Macnhester

Jackson, Rebecca
Geological Survey of Denmark and Greenland

Jenkins, Chris
INSTAAR CU Boulder

Jennings, Anne
INSTAAR

Jensen, Britta
University of Alberta

Kaplan, Mike
Lamont-Doherty Earth Observatory

Kelleher, Robert
CU Boulder

Kelley, Sam
University College Dublin

Kindstedt, Ingalise
University of Maine

King, Leslie
Royal Roads University

Kopf, Sebastian
University of Colorado Boulder

Lapointe, Francois
University of Massachusetts

Larocca, Laura
Northwestern University

Larsen, Nicolaj
University of Copenhagen

Lehman, Scott
INSTAAR

Lenetsky, Jed
National Snow and Ice Data Center

Leonard, Eric
Colorado College

Lepore, Walter
Royal Roads University

Lesnek, Alia
University of New Hampshire

Licciardi, Joseph
University of New Hampshire

Licht, Kathy
Indiana University Purdue University Indianapolis

Lindberg, Kurt
University at Buffalo

Löf, Annette
Swedish University of Agricultural Sciences (SLU)

Lovell, Katie
University at Buffalo

Lysså, Astrid
Geological Survey of Norway

Mahar, Isabelle
Barnard College

Mastro, Halley
Gettysburg College

McFarlin, Jamie
University of Colorado Boulder

McLean, Erin
Arctic Data Center

Melnick, Niki
Gettysburg College

Mette, Madelyn
USGS

Miles, Martin
NORCE and INSTAAR Univ. Colorado, Boulder

Miller, Gifford
University of Colorado

Musselman, Keith
INSTAAR, CU Boulder

Nash, Bailey
U.S. Geological Survey

Ogilvie, Astrid
INSTAAR

OMeara, Katie
MICA

Otto-Bliesner, Bette
National Center for Atmospheric Research

Overeem, Irina
University of Colorado

Pearce, Christof
Aarhus University

Pendleton, Simon
Woods Hole Oceanographic Institution

Pierce, Ethan
University of Colorado Boulder

Poinar, Kristin
University at Buffalo

Polyak, Leonid
Ohio State University

Potapova, Olga
The Mammoth Site of Hot Springs, SD, Inc.

Power, Matthew
Curtin University

Prince, Karlee
University at Buffalo

Principato, Sarah
Gettysburg College

Przybylak, Rajmund
Nicolaus Copernicus University, Poland

Raberg, Jonathan
University of Colorado, Boulder and INSTAAR

Raynolds, Martha
University of Alaska Fairbanks

Retelle, Mike
Bates College

Riddell-Young, Benjamin
Oregon State University

Roy, Austin
University of Texas at El Paso

Sampson, Jenna
freelance

Schneider, Tobias
Department of Geosciences, UMass Amherst

Seidenkrantz, Marit-Solveig
Aarhus University

Sejrup, Hans Petter
University of Bergen

Shtabrovskaya, Irina
Federal Research Centre "Kola Sciense Centre of th

Smith, Rod
Geological Survey of Canada

Soleymani, Armina
University of Waterloo

Søndergaard, Anne Sofie
ETH, Zürich

Streuff, Katharina
University of Bremen, Germany

Thaarup, Cecilie
UNIS

Thomas, Elizabeth
Dept of Geology, University at Buffalo

Tiessen, Tamara
Royal Roads University

Tulenko, Joseph
University at Buffalo

van der Wal, Rene
Swedish University of Agricultural Sciences (SLU)

Vanderwilt, Mia
UC Boulder

Vermassen, Flor
Stockholm university

Vogt, Christoph
Geosciences/MARUM University of Bremen

Wagner, Katrin
Goethe-University Frankfurt am Main

Walcott, Caleb
University at Buffalo

Walker, Donald "Skip"
University of Alaska Fairbanks

Wangner, David
GEOMAR, Kiel

Watson-Cook, Emily
University of Alaska Fairbanks

Weaver, Ron
retired - CU Boulder CIRES/NSIDC

Werner, Al
Mount Holyoke College

West, Gabriel
Stockholm University

Zhao, Boyang
University of Massachusetts Amherst

Zheng, Whyjay
UC Berkeley